

PHOTOPLETHYSMOGRAPHY FOR DETERMINING MAJOR AIRWAY
RESISTANCE CHANGES AND FOR DETECTING FLUID LOSS IN BLOOD
DONORS AND RENAL HEMODIALYSIS PATIENTS

By

BRIAN SCOTT FUEHRLEIN

A DISSERTATION PRESENTED TO THE GRADUATE SCHOOL
OF THE UNIVERSITY OF FLORIDA IN PARTIAL FULFILLMENT
OF THE REQUIREMENTS FOR THE DEGREE OF
DOCTOR OF PHILOSOPHY

UNIVERSITY OF FLORIDA

2006

Copyright 2006

by

Brian Scott Fuehrlein

To my wife, Dianna: I attribute my achievements to your love, support, and caring. This would not have been possible without you.

ACKNOWLEDGMENTS

First I would like to thank my parents for affording me every opportunity to achieve. I did not always make the right decisions in life, but through it all they believed that I would succeed even when I did not believe it myself. I thank the rest of my family for their support and caring. I wish that my grandfathers were alive to witness my achievements. I see more and more of both of them in me every day. I also thank my dog, T-Bone for making me look forward to coming home from work every day. Where's the light?

I thank Richard Melker for becoming my mentor many years before I began pursuing my PhD. He is the reason I became a Doctor and that is something I will carry with me the rest of my life. I thank my supervisory committee (Hans van Oostrom, Neil Euliano, Charles Wood, and Chris Batich) for their guidance and support. I thank the departments of Biomedical Engineering and Anesthesiology. I thank the staff of the renal hemodialysis clinic (especially Ed Ross and Tracy Hollen). I thank the staff of the LifeSouth Community Blood Center. I thank George Worley of Beta Biomed Services for giving me valuable real-world experience and practical advice. I thank Convergent Engineering for providing software and technical expertise, and Novamatrix for providing equipment. I thank Mark Gold for providing so many opportunities to enhance my training. I thank Lou Ritz for every now and then allowing me to win in racquetball. I thank Steve Bonett for sharing an office with me for many years and listening to my rants. I hope I can do 20 stadiums when I am 48 years old. I thank all of my friends of

the medical school class of 2005 for constantly reminding me that I have yet to complete the third year of medical school. I thank Matthew Warren for completing everything before me and then instructing me on how to do it. Finally, I thank the members of the 2006 National Championship Florida Gator Men's Basketball team for all of the excitement. It was something I will never forget.

TABLE OF CONTENTS

	<u>page</u>
ACKNOWLEDGMENTS	iv
LIST OF TABLES	ix
LIST OF FIGURES	xii
ABSTRACT	xix
CHAPTER	
1 BACKGROUND	1
Pulse Oximetry	1
Theory of Pulse Oximetry	1
History of Pulse Oximetry	4
Reasons for Errors in Pulse Oximetry	7
Photoplethysmography	8
Fundamentals of Photoplethysmography	8
Photoplethysmograph Processing	9
Uses of the Photoplethysmograph	10
Arterial mechanics	10
Respiratory rate	11
Pulsus paradoxus	14
Blood volume	14
Patent Review	16
2 INTRODUCTION	20
Novel Pulse Oximeter Prototypes	20
Literature Review	20
Novel Probe Designs	21
Pulse Oximeter Data Acquisition Viewer	22
Pilot Operating Room Study	23
Secondary Findings	24
Arrhythmias	25
Ventilator effect	26
Cardiac bypass	27
Blood pressure cuff	27

	Limitations	27
	Updated Signal Separation Algorithm.....	28
	Secondary Findings from the Operating Room Study Revisited.....	29
	Nasal Alar Probe.....	30
	Additional Studies	31
3	BROAD CLINICAL GOALS	45
	Clinical Goal 1	45
	Clinical Populations.....	45
	Asthma	45
	Obstructive sleep apnea syndromes	48
	Changes Caused By Respiration	51
	Pilot Data.....	51
	Exploratory pilot study.....	51
	Ventilator and volunteer resistance study	52
	Mathematically characterizing the resistance.....	54
	Clinical Goal 2	55
	Rationale.....	56
	Blood Donors.....	57
	Renal Hemodialysis.....	58
4	EXPERIMENTAL DESIGN AND METHODS.....	64
	Methods	64
	Blood Donors.....	65
	Hemodialysis Patients	67
	Photoplethysmograph Processing and Novel Variables.....	68
	Signal Processing Algorithm.....	68
	Separating Breath Data.....	70
	Hypotheses.....	72
	Hypotheses – Clinical Goal 1	72
	Hypotheses – Clinical Goal 2	72
	Justification.....	73
	Justification for Hypotheses 1 and 2	73
	Justification Hypotheses 3, 4, and 5	74
5	STATISTICAL ANALYSIS AND RESULTS	81
	Data Filtering.....	81
	Multiple Breaths	81
	Cardiac Arrhythmias	82
	Artifact.....	83
	Unattainable Photoplethysmograph.....	83
	Demographics	84
	Statistical Analysis.....	84
	Hypothesis 1	84

Hypothesis 2	87
Hypothesis 3	89
Hypothesis 4	90
Hypothesis 5	91
Discussion of Statistical Results	92
Hypotheses 1 and 2	93
Hypothesis 3	95
Hypotheses 4 and 5	99
Regression Analysis	100
6 CLINICAL SIGNIFICANCE AND INDIVIDUAL SUBJECT ANALYSIS	139
Statistical and Clinical Significance	139
Individual Analysis	140
Hypothesis 1	140
Hypothesis 2	143
Hypothesis 3	144
Hypotheses 4 and 5	148
7 CONCLUSIONS	162
Summary of Conclusions	162
Clinical Relevance and Future Studies	163
Clinical Goal 1	163
Clinical Goal 2	168
LIST OF REFERENCES	172
BIOGRAPHICAL SKETCH	182

LIST OF TABLES

<u>Table</u>	<u>page</u>
3-1. Estimated pressure drop across the ET tubes based on Poiseuille's Law.	61
3-2. Calculated, simulated, and measured intrathoracic pressure changes	62
5-1. Demographic information for the blood donors.....	101
5-2. Demographic information for the HD patients.....	102
5-3. Test for normality in the LFC Swings of the blood donors.....	102
5-4. Test for normality in the LFC Swings of the HD patients.....	103
5-5. Friedman's test results for the LFC Swings of the blood donors.....	103
5-6. Friedman's test results for the LFC Swings of the HD patients.....	104
5-7. Wilcoxon Signed-Rank results across the three resistance levels for the LFC Swings for the blood donors.....	104
5-8. Wilcoxon Signed-Rank results across the three resistance levels for the LFC Swings for the HD patients.	104
5-9. R ² values of LFC Swings compared to estimated intrathoracic pressure for blood donors.....	104
5-10. R ² values of LFC Swings compared to estimated intrathoracic pressure for HD patients.	105
5-11. Wilcoxon Signed-Rank results for the LFC Swings of the blood donors before and after blood loss.	105
5-12. Wilcoxon Signed-Rank results for the LFC Swings of the HD patients before and after HD.....	105
5-13. Test for normality for the PCC MagDiff of the blood donors.....	105
5-14. Test for normality for the PCC MagDiff of the HD patients.....	105

5-15. Wilcoxon Signed-Rank results for the PCC MagDiff of the blood donors and HD patients.....	106
5-16. Test for normality for the PCC MagMean of the blood donors.	106
5-17. Test for normality for the PCC MagMean of the HD patients.	106
5-18. Wilcoxon Signed-Rank results for the PCC MagMean of the blood donors and HD patients.....	106
5-19. Friedman’s test results for the respiratory flow rates of the blood donors.	107
5-20. Wilcoxon Signed-Rank results for the respiratory flow rates of the blood donors.	107
5-21. Friedman’s test results for the respiratory volume of the blood donors.	107
5-22. Wilcoxon Signed-Rank results for the respiratory volume of the blood donors. ...	108
5-23. Friedman’s test results for the respiratory flow rates of the HD patients.	108
5-24. Wilcoxon Signed-Rank results for the respiratory flow rates of the HD patients. .	108
5-25. Friedman’s test results for the respiratory volume of the HD patients.....	109
5-26. Wilcoxon Signed-Rank results for respiratory volume of the HD patients.....	109
5-27. Wilcoxon Signed-Rank results for the respiratory flow rates and volumes of the blood donors before and after blood loss.	109
5-28. Wilcoxon Signed-Rank results for the respiratory flow rates and volumes of the HD patients before and after HD.....	109
5-29. Wilcoxon Signed-Rank results of the pulse rate and blood pressure of the blood donors before and after blood loss.	110
5-30. Wilcoxon Signed-Rank results of the pulse rate and blood pressure of the HD patients before and after HD.	110
5-31. Wilcoxon Signed-Rank results for the LFC Swings of the blood donors comparing breaths 1 and 2 to subsequent breaths in the alar.	110
5-32. Wilcoxon Signed-Rank results for the LFC Swings of the blood donors comparing breaths 1 and 2 to subsequent breaths in the finger.....	110
5-33. Wilcoxon Signed-Rank results for the LFC Swings of the HD patients comparing breaths 1 and 2 to subsequent breaths in the alar.	110
5-34. Wilcoxon Signed-Rank results for the LFC Swings of the HD patients comparing breaths 1 and 2 to subsequent breaths in the finger.....	111

5-35. Wilcoxon Signed-Rank results for the LFC Swings of the blood donors comparing breaths 1 and 2 before and after blood loss.....	111
5-36. Wilcoxon Signed-Rank results for the LFC Swings of the HD patients comparing breaths 1 and 2 before and after HD.	111
6-1. The R^2 values for the regression analysis between estimated intrathoracic pressure changes and alar LFC Swings for the blood donors.	153
6-2. The R^2 values for the regression analysis between estimated intrathoracic pressure changes and alar LFC Swings for the HD patients.	153
6-3. Multiple variable regression analysis for the alar LFC Swings during high resistance for the HD patients.	153
6-4. Multiple variable linear regression analysis for the alar PCC MagDiff for the blood donors.	154
6-5. Multiple variable linear regression analysis for the alar PCC MagMean for the blood donors.	154

LIST OF FIGURES

<u>Figure</u>	<u>page</u>
1-1. A Graphic representation of the LFC and PCC from a typical finger probe.....	18
1-2. A typical display of a processed pulse oximeter waveform.	19
2-1. Novel pulse oximeter probes manufactured by Beta Biomed Services (Rowlett, TX)..	35
2-2. Variance of SpO ₂ from SaO ₂ as hypoxic conditions increased, as measured by the cheek probe.....	35
2-3. Variance of SpO ₂ from SaO ₂ as hypoxic conditions increased, as measured by the nasal septum probe.	36
2-4. The Pulse Oximetry Data Acquisition Viewer software.	36
2-5. A 30 min pulse rate tracing of an operating room pilot study subject, showing arrhythmias.....	37
2-6. A 30 sec PCC tracing of the PPG of an operating room pilot study subject, showing arrhythmias.	37
2-7. A 30 sec PCC tracing of the PPG of an operating room pilot study subject, showing the effect of the ventilator.....	37
2-8. A 30 min oxygen saturation trend of an operating room pilot study subject, showing how the cheek probe resumed functionality 5 min sooner than the finger probe following cardiac bypass.	38
2-9. A 30 sec PCC tracing of the PPG of an operating room pilot study subject, showing the effect of a blood pressure cuff.	38
2-10. The unprocessed PPG data of an operating room subject with the peaks and troughs identified discretely.	38
2-11. The PCC of the PPG from the cheek of an operating room pilot study subject, showing periodic reduction in amplitude corresponding to blood flow.....	38
2-12. The PCC of the PPG from the nasal septum of an operating room pilot study subject, showing periodic reduction in amplitude corresponding to blood flow.	39

2-13. The PCC of the PPG from the nasal septum of an operating room pilot study subject, showing changes in blood flow over time.	39
2-14. The LFC of the PPG from the nasal septum of an operating room pilot study subject, showing changes in baseline venous blood over time.	39
2-15. The LFC of the PPG from the nasal septum of an operating room pilot study subject, showing increased fluctuations over time.	39
2-16. The PCC of the PPG from the finger of an operating room pilot study subject, showing the periodic effect of a blood pressure cuff.	40
2-17. The LFC of the PPG from the finger of an operating room pilot study subject, showing the periodic effect of a blood pressure cuff.	40
2-18. The PCC of the PPG from the nasal septum of an operating room pilot study subject, showing the effect of the ventilator.	40
2-19. The nasal alar probe design, based on the cheek probe design.	40
2-20. The PCC of the PPG from the finger of a healthy volunteer, showing the effect of a blood pressure cuff over time.	41
2-21. The LFC of the PPG from the finger of a healthy volunteer, showing the effect of a blood pressure cuff over time.	41
2-22. The PCC of the PPG from the finger of a healthy volunteer, showing the effect of brachial artery occlusion.	41
2-23. The LFC of the PPG from the finger of a healthy volunteer, showing the effect of brachial artery occlusion.	41
2-24. The PCC of the PPG from the finger of a healthy volunteer, showing the effect of a Valsalva maneuver.	42
2-25. The LFC of the PPG from the finger of a healthy volunteer, showing the effect of a Valsalva maneuver.	42
2-26. The PCC and LFC of the PPG from the finger of a healthy volunteer, showing the effect of position of the hand with respect to the heart.	42
2-27. The PCC of the PPG from the finger of a healthy volunteer, showing the effect of Mueller and Valsalva maneuvers.	43
2-28. The LFC of the PPG from the finger of a healthy volunteer, showing the effect of Mueller and Valsalva maneuvers.	43
2-29. The PCC of the PPG from the alar of a healthy volunteer, showing the effect of breathing through various endotracheal tubes.	43

2-30. The LFC of the PPG from the alar of a healthy volunteer, showing the effect of breathing through various endotracheal tubes.....	44
2-31. The LFC of the PPG from the alar of a healthy volunteer, showing the effect of spontaneous respiration.....	44
3-1. Average simulated intrapleural pressure changes per breath	62
3-2. Measured esophageal pressure changes per breath in healthy volunteers.....	63
3-3. Intrathoracic pressure changes per breath, simulated and measured.....	63
4-1. A spectral analysis, where the x-axis corresponds to the frequency in Hz and the y-axis corresponds to power and is a log scale.	77
4-2. A low-pass filter.....	77
4-3. A high-pass filter.....	78
4-4. The unprocessed PPG recorded from the nasal alar of a blood donor subject.....	78
4-5. The LFC of the PPG recorded from the nasal alar of a blood donor subject.....	78
4-6. The PCC of the PPG recorded from the nasal alar of a blood donor subject.....	78
4-7. The respiratory flow data, where the x-axis represents time and the y-axis represents flow rate.....	79
4-8. The LFC of the PPG with respiratory flow.....	79
4-9. The PCC of the PPG plotted with respiratory flow.....	79
4-10. The PCC for the duration of one breath.....	80
4-11. The unprocessed PPG demonstrating the exaggerated affect of respiration on the LFC, hiding the PCC.....	80
5-1. Respiratory flow data showing the elimination of one breath.....	111
5-2. The PCC for the duration of one breath, showing an arrhythmia.....	112
5-3. The unprocessed PPG with respiratory flow data, showing the result of motion artifact.....	112
5-4. The alar LFC Swings for the blood donors, before and after blood loss.....	112
5-5. The finger LFC Swings for the blood donors, before and after blood loss.....	113
5-6. The alar LFC Swings for the HD patients, before and after HD.....	113

5-7. The finger LFC Swings for the HD patients, before and after HD.	114
5-8. Estimated intrathoracic pressure change per breath vs alar LFC Swings in blood donors, before blood loss.	114
5-9. Estimated intrathoracic pressure change per breath vs alar LFC Swings in blood donors, after blood loss.	115
5-10. Estimated intrathoracic pressure change per breath vs finger LFC Swings in blood donors, before blood loss.	115
5-11. Estimated intrathoracic pressure change per breath vs finger LFC Swings in blood donors, after blood loss.	116
5-12. Estimated intrathoracic pressure change per breath vs alar LFC Swings in HD patients, before HD.	116
5-13. Estimated intrathoracic pressure change per breath vs alar LFC Swings in HD patients, after HD.	117
5-14. Estimated intrathoracic pressure change per breath vs finger LFC Swings in HD patients, before HD.	117
5-15. Estimated intrathoracic pressure change per breath vs finger LFC Swings in HD patients, after HD.	118
5-16. The alar LFC Swings of the blood donors, before and after blood loss.	118
5-17. The finger LFC Swings of the blood donors, before and after blood loss.	119
5-18. The alar LFC Swings of the HD patients, before and after HD.	119
5-19. The finger LFC Swings of the HD patients, before and after HD.	120
5-20. The alar and finger PCC MagDiff in blood donors, before and after blood loss. ...	120
5-21. The alar and finger PCC MagDiff in HD patients, before and after HD.	121
5-22. The alar and finger PCC MagMean in blood donors, before and after blood loss. ...	121
5-23. The alar and finger PCC MagMean in HD patients, before and after HD.	122
5-24. The peak inspiratory flow rates in the blood donors, before and after blood loss. ...	122
5-25. The peak expiratory flow rates in the blood donors, before and after blood loss. ...	123
5-26. The respiratory volumes in the blood donors, before and after blood loss.	123
5-27. The peak inspiratory flow rates in the HD patients, before and after HD.	124

5-28. The peak expiratory flow rates in the HD patients, before and after HD.....	124
5-29. The respiratory volumes in the HD patients, before and after HD.....	125
5-30. The peak inspiratory flow rates of the blood donors for all three levels of respiratory resistance.....	125
5-31. The peak expiratory flow rates of the blood donors for all three levels of respiratory resistance.....	126
5-32. The respiratory volumes of the blood donors for all three levels of respiratory resistance.	126
5-33. The peak inspiratory flow rates of the HD patients for all three levels of respiratory resistance.....	127
5-34. The peak expiratory flow rates of the HD patients for all three levels of respiratory resistance.....	127
5-35. The respiratory volume of the HD patients for all three levels of respiratory resistance.	128
5-36. The pulse rate of the blood donors for all three levels of resistance.	128
5-37. The seated blood pressure of the blood donors for all three levels of resistance. ...	129
5-38. The pulse rate of the HD patients for all three levels of resistance.	129
5-39. The seated blood pressure of the HD patients for all three levels of resistance.	130
5-40. A comparison between the alar LFC Swings from the first two breaths and subsequent breaths in the blood donors, before and after blood loss.....	130
5-41. A comparison between the finger LFC Swings from the first two breaths and subsequent breaths in the blood donors, before and after blood loss.....	131
5-42. A comparison between the alar LFC Swings from the first two breaths and subsequent breaths in the HD patients, before and after HD.	131
5-43. A comparison between the finger LFC Swings from the first two breaths and subsequent breaths in the HD patients, before and after HD.	132
5-44. The alar LFC Swings from the first two breaths of the blood donors, before and after blood loss.	132
5-45. The finger LFC Swings from the first two breaths of the blood donors, before and after blood loss.	133

5-46. The alar LFC Swings from the first two breaths of the HD patients, before and after HD.	133
5-47. The finger LFC Swings from the first two breaths of the HD patients, before and after HD.	134
5-48. Ultrafiltrate removed vs alar LFC Swings in the HD patients for the high resistance level.	134
5-49. Ultrafiltrate removed vs alar LFC Swings in the HD patients for the medium resistance level.	135
5-50. Ultrafiltrate removed vs alar LFC Swings in the HD patients for the low resistance level.	135
5-51. Ultrafiltrate removed as a percent of body weight vs alar LFC Swings in the HD patients for the high resistance level.	136
5-52. Ultrafiltrate removed as a percent of body weight vs alar LFC Swings in the HD patients for the medium resistance level.	136
5-53. Ultrafiltrate removed as a percent of body weight vs alar LFC Swings in the HD patients for the low resistance level.	137
5-54. Estimated blood volume vs alar PCC MagDiff in the blood donors for the low resistance level.	137
5-55. Estimated blood volume vs alar PCC MagMean in the blood donors for the low resistance level.	138
6-1. The alar LFC Swings for all three resistance levels for the first ten blood donors, before blood loss.	155
6-2. The unexpected alar LFC Swings for all three resistance levels for the blood donors, both before and after blood loss.	155
6-3. The unexpected alar LFC Swings for all three resistance levels for the HD patients, both before and after HD.	156
6-4. The peak inspiratory flow rates for all three levels of resistance for the blood donors, before blood loss.	156
6-5. Estimated intrathoracic pressure changes per breath vs alar LFC Swings in blood donor subject 1, after blood loss.	157
6-6. The alar LFC Swings for the HD patients, both before and after HD.	157
6-7. Fluid removed as a percent of body weight in the HD patients.	158

6-8. The alar PCC MagDiff for the blood donors, both before and after blood loss.	158
6-9. The alar PCC MagMean for the blood donors, both before and after blood loss...	159
6-10. The peak inspiratory flow rate for the blood donors, both before and after blood loss.....	159
6-11. The total respiratory volume for the blood donors, both before and after blood loss.....	160
6-12. The approximate percentage of red blood cells removed in the blood donors.....	160
6-13. The pulse rate of the blood donors, both before and after blood loss.....	161
6-14. The alar LFC Swings for the blood donors, both before and after blood loss.....	161

Abstract of Dissertation Presented to the Graduate School
of the University of Florida in Partial Fulfillment of the
Requirements for the Degree of Doctor of Philosophy

PHOTOPLETHYSMOGRAPHY FOR DETERMINING MAJOR AIRWAY
RESISTANCE CHANGES AND FOR DETECTING FLUID LOSS IN BLOOD
DONORS AND RENAL HEMODIALYSIS PATIENTS

By

Brian Scott Fuehrlein

August 2006

Chair: Richard Melker
Major Department: Biomedical Engineering

There is currently no gold standard for noninvasive monitoring of respiratory airway resistance or fluid volume status. The photoplethysmograph (PPG) is a noninvasive optical method that can be used to monitor hemodynamic parameters and has been shown to correlate with respiratory rate.

The PPG was recorded from the finger and nasal alar of 40 subjects: 20 volunteer blood donors and 20 hemodialysis (HD) patients. Before and after donation/HD, each subject performed resistance breathing maneuvers through three different endotracheal tubes. A standard Butterworth filter was used to separate the PPG into a low frequency component (LFC) and pulsatile cardiac component (PCC). A novel LFC measure was compared across the three resistance levels. Three novel measures—one involving the LFC and two involving the PCC—were compared before and after donation/HD.

Statistical differences were found across all three levels of resistance, indicating that the PPG may be useful in detecting major changes in airway resistance. Statistical

differences were found in the PCC variables in the blood donor subjects after blood loss, and in the LFC variables in the dialysis subjects after fluid loss. These results indicate that the PPG may be useful in detecting fluid loss and also in differentiating between whole blood and ultrafiltrate loss. Patients with asthma and obstructive sleep apnea should be studied to test the clinical application of the PPG for detecting changes in airway resistance. Critically ill subjects should be studied to test the clinical application of the PPG for monitoring fluid status.

CHAPTER 1 BACKGROUND

Pulse Oximetry

Pulse oximetry is a standard of care in anesthesia and is found in many operating rooms in the country. It is also used in doctors' offices, by emergency paramedic personnel, and in intensive care units. It is simple to use and noninvasive.

Theory of Pulse Oximetry

Hemoglobin (Hb) is the oxygen-transporting molecule in our blood. It contains two pairs of globin peptide chains: alpha and beta. Each of these chains is able to combine with a heme group. Each heme group is composed of one atom of iron combined with a protophyrin molecule, and is able to combine reversibly with one molecule of oxygen (Perutz 1969). The shape of the Hb changes with the binding of oxygen and is the basis for the change in the optical absorption spectrum detected by the spectrophotometric methods of pulse oximeters (Middleton and Henry 2000).

Spectrophotometry is based on the Beer-Lambert law, which relates the fraction of radiant energy absorbed by the tested substance to the concentration and amount of the substance. It states that the concentration can be determined as a mathematical function of the light transmitted through the solution (Middleton and Henry 2000).

The Beer-Lambert law is a combination of Beer's law and Lambert's law. Beer's law states that the intensity of a transmitted light decreases exponentially as the concentration of the substance increases, and can be expressed as $A = \ln (I_0 / I)$ (Equation 1-1). Lambert's law says the intensity of transmitted light decreases

exponentially as the distance traveled through the substance increases, and can be expressed as $A = \epsilon * L * C$ (Equation 1-2). Where A is absorbance, ϵ is the molar absorptivity (or molar extinction coefficient), L is the path length, and C is the concentration of the compound in the solution. These laws can be combined and expressed as $\ln(I_0/I) = \epsilon * L * C$ (Equation 1-3). This is the fundamental basis by which pulse oximeters calculate oxygen saturation.

Two wavelengths of light are emitted from a light emitting diode (LED). A red wavelength (~660 nm) and infrared (IR) wavelength (~900 nm) are used. The isobestic point is the point at which the two different Hbs absorb the two wavelengths of light to the same extent. This occurs at 805 nm. The red and IR wavelengths were chosen because they fall approximately equidistant from the isobestic point. Absorbance of oxygenated hemoglobin (HbO_2) at the red wavelengths is less than that of Hb, hence HbO_2 is more transparent to red light than Hb (Middleton and Henry 2000). The reverse is seen in the IR spectrum, but to a lesser extent. Thus, comparison of absorbencies at different wavelengths allows estimation of the relative concentrations of HbO_2 and Hb (i.e., saturation)—the basis of pulse oximetry. At wavelengths shorter than 600 nm, melanin causes a greater degree of absorption; therefore blue, green, and yellow light are not useful. At wavelengths longer than 1300 nm, absorption is excessive due to the presence of water in the tissues (Middleton and Henry 2000).

The pulse oximeter probe consists of an LED mounted perpendicular to a semiconductor photodiode (PD). An LED is a low-cost, mass-produced light source. A separate LED is used for each wavelength. They are monochromatic, easy to manufacture, and can be rapidly switched on and off. Major disadvantages associated

with LEDs include variations in the central wavelength of different diodes of the same type. This variability can be as much as ± 15 nm from the central wavelength. This range can be significant, particularly in the red range, as the absorption spectra change rapidly over a short distance. The LEDs alternate flashing the red, IR, and no light many times per second, depending on the main power frequency. The purpose of the dark period is to detect ambient light, which can then be subtracted from the detected red and IR. This minimizes interference caused by external light. A single PD is used to detect the light from both the red and IR LEDs. This PD is usually made from silicone, which uses the semiconductor property of altering its electrical performance when exposed to outside energy. It has a wide dynamic output range. Finally, the cable carrying the signals from the probe to the oximeter unit must be shielded from electromagnetic radiation. This is accomplished by including a flexible conductive braid in the covering of the cable (Middleton and Henry 2000).

Pulse oximetry relies on the pulsatile nature of blood flow for its calculations. The pulsatile absorbance between the light source and the PD is caused by arterial blood. The pulse oximeter calculates the absorbance at each wavelength in the pulsatile component and divides this by the corresponding nonpulsatile component to obtain a pulse-added value. This value is independent of both the incident light intensity and the distance. It then calculates the ratio (R) of these pulse-added absorbances at the different wavelengths. This is then empirically related to saturation (Grace 1994). This can be stated as $R = (AC_{\text{red}} / DC_{\text{red}}) / (AC_{\text{ir}} / DC_{\text{ir}})$ (Equation 1-4). This R is then calibrated against a “co-oximeter”. This instrument uses small samples of heparinized blood hemolyzed by ultrasound. This blood then has up to 17 wavelengths of light transmitted

through it. Using known oxygen concentrations from healthy volunteers, the pulse oximeter is calibrated. This limits the accuracy of the device to oxygenation values attainable from the healthy volunteers during calibration, and is the source of error in hypoxic states (Jubran 1999).

History of Pulse Oximetry

Stokes (1864) reported that the colored substance in blood carries oxygen. This was followed by Hoppe-Seyler (1864) who first crystallized this substance and coined the term “haemoglobin.” Additionally, it was shown that the pattern of light absorption changes when shaken with air (Hoppe-Seyler 1864).

Hertzman (1937a) described using photoelectric plethysmography of fingers and toes as a dynamic analysis of the peripheral circulation. The device consisted of a beam of light directed from an ordinary automobile headlight bulb on the finger or toe placed above a shielded photoelectric cell of the photo-emissive type, purchased from the radio trade. Photoelectric oscillations with variations in the blood content of the digit were recorded by a string of galvanometer or suitable oscillograph after amplification. Movements of the arm must not be transmitted to the finger, and a comfortable saddle or sling is necessary to secure the arm to achieve the desired muscle relaxation, which affects finger volume. This method was also used over the nasal septum and the values were compared.

Millikan et al. (1941) first coined the term “oximeter” and described a method for the continuous measurement of arterial saturation. A small unit placed over the shell of the ear contained a lamp; two color filters; and two barrier-type, light-sensitive cells, with which the transmission of either green or red light is measured. The green reading depends on the amount of total Hb there is between the lamp and the photocell, and is

used to measure the degree of vasodilation, or “blood thickness” in the ear. This enables one to choose the correct direct-reading calibration scale for estimating arterial oxygen saturation, as measured in the red reading. This method has an accuracy of 5% in the top half of its range and 8% in the bottom half. Goldie (1942) developed a device for continuous indication of oxygen saturation of circulating blood in man.

This led Wood and Geraei (1949) to improve on these devices and develop a method for photoelectric determination of arterial oxygen saturation. Prior instruments were required to be preset to known arterial saturation values and could not be conveniently used in patients who had arterial hypoxia, nor could they be used for the actual determination of arterial oxygen saturation. The older devices could only be used for qualitative changes in saturation. As a result of these shortcomings, Wood and Geraei (1949) developed a device that could measure, and follow continuously, the absolute value of arterial oxygen saturation from a pickup unit attached to the pinna of the human ear. This new design consisted of a photoelectric earpiece that allows simultaneous measurement of the transmission of red and near-IR light through either the normal heat-flushed ear or the bloodless ear. Then by calculation, the light transmission of the blood alone in these spectral regions can be determined, and in turn the percentage of oxygen saturation of this blood content can be derived. This device was used in clinical physiologic laboratories but its use did not spread.

Oximetry research then went dormant until 1972 when Aoyagi (2003) began his work. His group wanted to build on the theories and success of the Wood oximeter. They created a dye densitometry method. Two wavelengths of light were used. The ratio of the two optical densities was calculated to obtain a dye curve. This curve was

expected to correspond to dye concentrations in blood. During this series of experiments that importance of the pulsatile variations was first reported. After investigating the effect of this pulsatile component using mathematical analysis of the Beer-Lambert law, it was concluded that calculating the ratio of two optical densities compensates for the pulsations. At this point, Aoyagi concluded if the optical density of the pulsating portion is measured at two appropriate wavelengths and the ratio of the optical densities is obtained, the result must be equivalent to Wood's ratio. Aoyagi also concluded that the arterial blood is selectively measured, and the venous blood does not affect the measurement. Therefore, the probe site is not restricted to the ear. Finally, the reference for optical density calculation is set for each pulse. Therefore, an accidental shift of probe location introduces a short artifact and quick return to normal measurements.

Aoyagi continued working on oximeters until 1975. By 1975 he had developed a technique very similar to modern-day pulse oximeters. Two wavelengths of light (630 nm and 900 nm) were chosen. From the transmitted light intensity data, the pulsation amplitude (AC) and the total intensity (DC) were obtained, and the ratio (AC/DC) was calculated. This ratio was obtained at both wavelengths of light to create a ratio of ratios that corresponded to SaO₂.

In 1980, Minolta developed OXIMET using two optical fibers and precision optics. They adopted the finger as the probe site and proved that pulse oximetry was accurate (Aoyagi 2003). Nellcor followed this in 1983 with development of the N-100. This was a convenient pulse oximeter that used high-performance LEDs, a highly sensitive and accurate PD, and a microcomputer. These technological advances led to the widespread clinical use of pulse oximeters in the 1980s.

As pulse oximeters continue to improve, active research is being conducted (Aoyagi 2003) in several key areas. Current research is focused on accuracy, optimum alarm level setting, response time to desaturation, and motion artifact.

Reasons for Errors in Pulse Oximetry

In low perfusion states, saturation readings are intermittent or unavailable. This is caused by the calibration of the devices using healthy adult volunteers. Therefore, the accuracy is decreased at low saturation levels. Unfortunately, low saturation levels are when the pulse oximeters are extremely useful.

The calculation of oxygenation is a moving average of user-preset length. The problem of a delayed response time for pulse oximeters to detect desaturations can be partially overcome by reducing the averaging setting to the shortest duration: usually two seconds (Grace 1994). This is seldom done clinically, however, as it increases the likelihood of artifact and false alarms. To overcome the problem of delayed response time, it is necessary to develop processing algorithms sensitive enough to detect changes quickly, while allowing for artifact rejection and avoiding false alarms.

Trivedi et al. (1997) explored the effects of various common sources of error on several pulse oximeter models. In phase 1, a 150 watt Sylvania operating room light was shone on pulse oximeter probes at a distance of 4 ft. Errors were defined as a heart rate of more than 5% difference from electrocardiograph (ECG) and a SpO₂ greater than 4% from the SaO₂ measured value. Inability of the pulse oximeter to obtain a reading was also defined as an error. Error rates in phase 1 were as high as 63% for heart rate and 57% for saturation. In phase 2 of the study a motion generator was designed to generate a standardized up-and-down 2 hz and 4 hz motion of a subject's hand with oximeter probes attached. The amplitude of this motion was approximately 4 in. All tested pulse

oximeters showed clinically significant error rates in saturation in both 2 hz and 4 hz movements. Error rates were low in the 2 hz motion for heart rate calculations, however all devices failed at 4 hertz motion. Others have also reported on the errors and false alarms associated with movement artifact (Reich et al. 1996, Moller et al. 1993, Runciman et al. 1993, Lawless 1994). Other sources of error include darkly pigmented skin (Jubran 1999), nail polish, finger and/or toe burns, and inaccessibility of the extremities.

A study was designed by van Oostrom and Melker (2004) to compare the accuracy of nonproprietary probes designed for use with a variety of pulse oximeters with that of their corresponding proprietary probes. A controlled signal was used to simulate apneas. Statistical significance was not found in most of the comparisons but in some instances the proprietary probes were closer to arterial oxygen than the nonproprietary probes. Whether or not the manufacturer of the probe is the same as the manufacturer of the pulse oximeter may have importance.

Photoplethysmography

Fundamentals of Photoplethysmography

There are two main frequencies of variation in the value of light hitting the PD, and both are affected by absorption of the light by blood and various tissues. The low frequency component (LFC), or nonpulsatile component, represents the baseline amount of light hitting the PD. This value is affected by the total path traveled by the light. Skin, bone, cartilage, adipose, blood, and so on—all absorb light, and this relatively constant path results in a baseline amount of light hitting the PD. This baseline amount fluctuates at a lower frequency than the heart rate. Since the biological tissues in the path of the light are constant, with the exception of venous and arterial blood, the changes in the

LFC component correspond to changes in baseline blood volume in the path of the light. Most of this baseline blood resides in the venous system.

The pulsatile cardiac component (PCC) corresponds to changes in the arterial blood volume with each heartbeat. The magnitude of the change of the PCC with each heartbeat is related to stroke volume, and the area under the curve of each heartbeat is related to the volume of blood entering the vascular bed with each beat (Murray and Foster 1996). The PCC therefore represents flow into a vascular bed, while the LFC represents changes in venous volume (Figure 1-1).

The typical pulse oximeter displays a processed waveform (Figure 1-2). Since the raw data collected by the device corresponds to light hitting the PD (which is inversely related to blood volume), the waveform must be inverted to resemble an arterial pressure waveform. If the photoplethysmograph (PPG) was shown as raw data and not inverted, Point A would represent increasing light hitting the PD (corresponding to a decrease in blood volume), and Point B would correspond to the point of maximum light hitting the PD, or the point of least blood in the vascular bed being monitored. Steepness of the flow of inflow Phase A may indicate ventricular contraction, and the amplitude of the phase may be used to indicate stroke volume (Murray and Foster 1996). The vertical position of the dicrotic notch can be used to indicate vasomotor tone. Under most circumstances the notch descends to the baseline during increasing vasodilation, and climbs toward the apex with vasoconstriction (Murray and Foster 1996).

Photoplethysmograph Processing

Before the advent of powerful personal computers, many researchers printed the PPG waveform and measured various parameters with a ruler. More recent efforts involve elaborate mathematical and signal processing models. Battacharya et al. (2001)

used a novel concept aimed at detecting the dominant nonsinusoidal period and extracting the associated periodic component. This detection and extraction was performed with a moving window to accommodate the variations of the physiological oscillations. They also characterized the system with a nonlinear dynamical system.

Goldman et al. (2000) published a detailed description of their signal extraction for error reduction. Massimo signal extraction technology used a new conceptual model of light absorption for pulse oximetry and used discrete saturation transforms to isolate individual saturation components in the optical pathway. Johansson (2003) processed the PPG signal with a 16th-order bandpass Bessel filter and a 5th-order bandpass Butterworth filter. A neural network analysis was performed. Nilsson et al. (2003) used three separate methods for evaluating the PPG (called the blood volume pulse) for changes caused by exercise. First they derived a single parameter from the distribution found in the average histogram of the time-aligned beats. Their second approach analyzed the ratio observed between the first harmonic and higher harmonics in the signal. The third approach evaluated the dicrotic notch depth directly from the PPG waveform.

Uses of the Photoplethysmograph

Arterial mechanics

Kato et al. (1999) constructed a mathematical model of the fingertip arterial wall from the relationship between the PPG wave and arterial pressure. The PPG and pressure at the ipsilateral radial artery were monitored simultaneously. Different mathematical models were tested to fit the data. The best model was then applied to data obtained during administration of vasoactive drugs in anesthetized patients. The vasoactive agents produced changes in the model parameters implying mechanical alterations in the arterial

wall. The authors concluded that a four-element, two-compartment model can be applied to the PPG to determine peripheral vascular wall mechanics.

Chowienczyk et al. (1999) sought to determine whether a simple index of pressure wave reflection may be derived from the digital volume pulse (DVP) and used to examine endothelium dependent vasodilatation in patients with type II diabetes mellitus. They focused on the relative height of the inflection point separating the systolic and diastolic components of the DVP. By administering various drugs and monitoring the DVP, they were able to conclude that PPG assessment of the DVP may provide a useful method to examine vascular reactivity.

Millasseau et al. (2002) concluded that contour analysis of the DVP provides a simple, reproducible, noninvasive measure of large artery stiffness. Millasseau et al. (2003) concluded that indices of pressure wave reflection and large artery stiffness can be used as an index of vascular aging. Bortollo et al. (2000) determined that the second derivative of the PPG and the pulse wave velocity can both be used to evaluate vascular aging in hypertensives.

The use of the PPG as an indicator of various vascular functions is an active area of research. If the PPG can provide a noninvasive window into the functioning of the vascular system this would provide a major medical advancement.

Respiratory rate

Changes in intrathoracic pressure during the respiratory cycle displace venous blood, affecting the LFC. These changes also affect cardiac return, changing the amplitude of the PCC. During spontaneous breathing, subatmospheric pressure during inspiration draws air and blood together into the lungs: blood is drawn from the vena cava into the right heart and pulmonary vascular bed. A minor decrease in peripheral

venous pressure (PVP) ensues. Soon thereafter the expiratory pressure normalizes the system. During positive pressure ventilation, the inspiration is drawn by positive pressure, which raises intrathoracic pressure and reduces venous return to the right heart. Simultaneously, and very briefly, blood forced from the low-pressure pulmonary vascular bed increases return to the left heart and stroke volume (Pinsky and Summer 1983). This is followed by a decrease in cardiac output as venous return into the central circulation drops off. The extent of the fluctuations caused by positive pressure ventilation depend on the state of filling of the peripheral vascular bed, the intrathoracic pressure changes, peripheral vasoconstrictor activity, and central blood volume (Murray and Foster 1996). Since positive pressure ventilation often accompanies general anesthesia, which causes vasodilation and damped vasomotor response, respiratory fluctuations are emphasized. It was also discovered that early hypovolemia may be reflected in an exaggerated respiratory wave before other more classic signs of decreased urine output, tachycardia or hypotension (Murray and Foster 1996).

Nilsson et al. (2000) extracted the cardiac and respiratory related components, applied a mathematical algorithm, and developed a new PPG device for monitoring heart rate and respiratory rate simultaneously. Sixteen patients undergoing routine operations received general anesthesia. Continuous PPG measurements were made for 60 min in each patient. The signal was amplified, the LFC was eliminated, and various analyses were performed. They concluded that the PPG has the potential for respiratory rate monitoring.

Nilsson et al. (2003) looked at the physiologic basis for the changes in the LFC, which they termed respiratory induced intensity variations (RIIV). They hypothesized

that the filling of peripheral veins is a major mechanism behind the RIIV signal. In the study, 16 adult volunteers had a cannula inserted for the measurement of PVP. The PVP and RIIV amplitudes changed significantly with tidal volume and respiratory rate and with thoraco-abdominal separation. These signals were significantly greater in predominantly thoracic respiration than in natural respiration. They concluded that a correlation exists in the amplitudes of the RIIV in the PPG and the respiratory variations in PVP ($p < .01$). This correlation could be a co-variance and not an explanatory factor.

Leonard et al. (2003 and 2004) sought to determine if analysis of the PPG by wavelet transforms could determine respiratory rate at an earlier stage than a drop in saturation. They concluded that baseline respiratory rate was easily identified from a pulse oximeter PPG using wavelet transforms. Foo and Wilson (2005) estimated the breathing interval (BI) in children using the PPG. The BI was extracted from the PPG using a two-stage signal processing technique termed zero-phase digital filtering. They concluded that the BI obtained from the PPG was significantly related to that estimated by a calibrated air pressure transducer during tidal breathing in the absence of motion artifact ($p < .05$). Nilsson et al. (2005) concluded that respiration can be monitored by the PPG with high sensitivity and specificity regardless of anesthesia and ventilatory mode. Reflectance PPG was measured at the forearm on awake spontaneously breathing patients, anesthetized spontaneously breathing patients and anesthetized ventilated patients.

Leonard et al. (2006) continued their work by developing a fully automated algorithm for the determination of respiratory rate from the PPG. The PPG was recorded

from 12 spontaneously breathing, healthy adult volunteers. The automated algorithm used wavelet analysis techniques with two novel secondary transforms.

Pulsus paradoxus

Pulsus paradoxus (PP) is the inspiratory decrease in systolic blood pressure, which is proportional to changes in intrathoracic pressure during inspiration and expiration (Frey and Butt 1998). It is increased in asthma, upper airway obstruction, cardiac tamponade, myocardial decompensation and hypovolemia (Miro and Pinsky 1992, Heitmiller and Wetzel 1996, Pfenninger 1985, Morgan et al. 1969). Butt and Frey (1998) sought to correlate the respiratory variations of the PPG to PP. They defined the respiratory dependent changes of the PPG as the difference between the highest value of the upper peak of the wave and the lowest value in the upper peak of the wave. In 62 nonintubated children, the PPG wave, arterial blood pressure, breathing cycle and ECG were recorded. They concluded that pulse oximetry is a rapid, noninvasive method for objectively estimating the degree of PP.

Hartert et al. (1999) studied 26 patients with obstructive airway disease. They described the characteristic alterations in the pulse oximetry tracings that occur in the presence of pulsus paradoxus and auto positive end expiratory pressure. The pulse oximetry tracings were evaluated for respiratory waveform variation, measured in millimeters from the PPG printout. The respiratory tracing was derived by connecting the AC component minimums.

Blood volume

The changes in systolic pressure with respiration, as shown by arterial pressure waveforms, are referred to as systolic pressure variation (SPV). This variability with positive pressure ventilation is useful in estimating various conditions (Perel et al. 1987,

Pizov et al. 1988, Coriat et al. 1994, Rooke et al. 1995). Perel et al. (1987) quantified the SPV during graded hemorrhage in ventilated dogs and compared its reliability relative to other hemodynamic parameters. They concluded that the difference between systolic pressure at end-expiration and the lowest value during the respiratory cycle (dDown) correlated to the degree of hemorrhage. It also correlated with the cardiac output and the pulmonary capillary wedge pressure. Thus, SPV and its dDown component are accurate indicators of hypovolemia in ventilated dogs subjected to hemorrhage. Rooke et al. (1995) also concluded that SPV and the dDown appear to follow shifts in intravascular volume in relatively healthy, mechanically ventilated humans under isoflourane anesthesia.

Building on this principle, Partridge (1987) attempted to use pulse oximetry as a noninvasive method to assess intravascular volume status. Data was collected from 12 patients, ranging in age from 29 to 80 years, undergoing general anesthesia. The patients were monitored with intraarterial and central venous or pulmonary artery catheters. Printouts were made of the PPG waveform over a two breath cycle. They measured mean intraarterial blood pressure, mean central venous pressure (CVP) at end expiration in mm Hg, SPV, CVP variation, and pulse waveform variation. The study showed that the PPG correlated with the SPV ($r = .61$), which was previously shown to be a sensitive indicator of hypovolemia.

Shamir et al. (1999) investigated ventilation induced changes in the PPG after removing and reinfusing 10% estimated blood volume in 12 anesthetized patients. The plethysmographic SPV was measured as the vertical distance between maximal and minimal peaks of waveforms during the ventilatory cycle and expressed as a percentage

of the amplitude of the PPG signal during apnea. This was measured during five consecutive mechanical breaths before apnea and the mean value was obtained for analysis. The 10% loss of estimated blood volume resulted in increased heart rate without changes in mean arterial pressure. Both the PPG waveform changes and the SPV from the arterial blood pressure tracing increased significantly after blood withdrawal ($p < .01$). The changes in the PPG correlated with the changes in the SPV. After volume replacement, heart rate decreased while arterial pressure remained unchanged. There were no significant changes in the PPG waveform or the SPV with volume replacement.

Patent Review

United States Patent number 3,334,065 by Al-Ali et al. (2001) discussed an improved stereo pulse oximeter providing simultaneous, noninvasive oxygen status and PPG measurements at both single and multiple sites. It measures both arterial and venous oxygen saturation with a corresponding PPG. Its main advantage is the detection and management of persistent pulmonary hypertension in neonates, patent ductus arteriosus, and aortic coarctation.

United States Patent number 6,616,613 by Goodman (2003) discussed a health monitoring and biofeedback system made of a PPG sensor, a processing device, and a web site server for determining, displaying and analyzing various cardiovascular parameters. The PPG was recorded specifically for the purpose of measuring the systolic wave pulse and the systolic reflected wave pulse present within the DVP signal. The PPG was processed in a variety of ways including first, second, third and fourth order derivatives and a 6 to 20 Hz filter. The mean volume pulse amplitude and the area under the contour during the duration of the DVP pulse were analyzed. The PPG measures were a fraction of the overall measures used in the monitoring system.

United States Patent number 6,709,402 by Dekker (2004) claimed the use of the PPG to monitor secondary physiological processes, such as respiratory rate and heart rate. He discussed the “DC component,” which generally corresponds to the attenuation related to the nonpulsatile volume of the perfused tissue. He also discussed the “AC component,” which corresponds to the heart rate. Additionally, the signal separation of the DC and AC components was discussed. The DC component varies over a low frequency and small amplitude and this variation is attributable to changes in the monitored tissue caused by other physiologic processes.

The International Patent Application number WO 2004/080300 by Shelley et al. (2004) discussed a method of assessing blood volume using photoelectric plethysmography. The method analyzed the cardiovascular waveform—representing the systolic pressure upon the cardiac signal—and compared it to the per heartbeat minimums of the cardiovascular waveform—representing the diastolic pressure upon the cardiac signal. The analyzing step included applying harmonic analysis to the cardiovascular waveform, extracting a frequency signal created by ventilation, and applying the extracted frequency signal in determining blood volume of the subject.

United States Patent number 6,898,452 by Al-Ali et al. (2005) discussed additional uses for stereo pulse oximeters. Stereo pulse oximeters simultaneously measure both arterial and venous oxygen saturation at specific sites, and generate a corresponding PPG waveform. Additionally, they compute the corresponding arterial minus venous oxygen saturation, which is advantageous for oxygen therapy management. The PPG is recorded at two different sites and analyzed for phase differences and damping.

United States Patent Application 20060058691 (Kiani 2006) discussed a hypovolemia monitor by utilizing a PPG signal. A measurement of the respiration-induced variation was made. The measurement was normalized and converted into a hypovolemia parameter. An audible or visual indication of hypovolemia was provided.

International Patent number WO2006/037184 (Oates and Martin 2006) discussed a method and apparatus for noninvasive monitoring of respiratory parameters in sleep disordered breathing. They described the analysis of both the alternating current (AC) amplitude and offset. The AC amplitude is most indicative of vascular compliance and is best analyzed from a PPG derived from a finger. They describe how the offset varies with respiratory effort. They also describe the relationship between the PPG baseline and pulsus paradoxus.

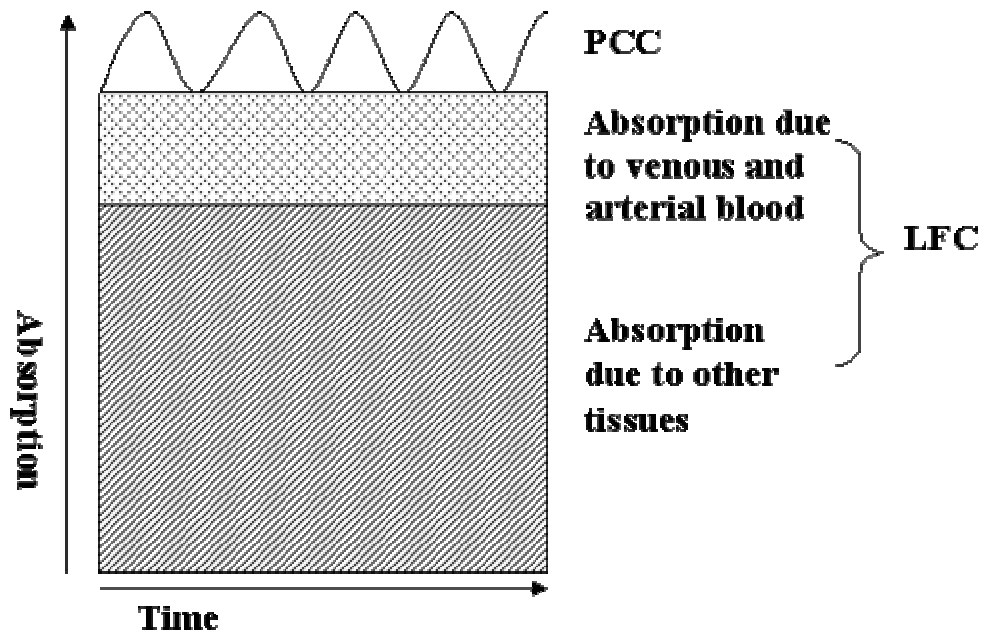


Figure 1-1. A Graphic representation of the LFC and PCC from a typical finger probe. The PCC is typically less than 5% of the total signal acquired.

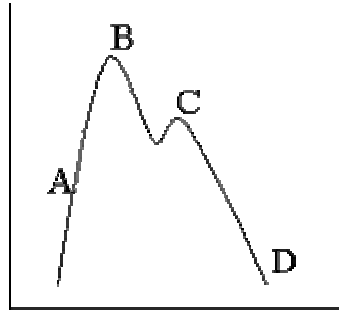


Figure 1-2. A typical display of a processed pulse oximeter waveform. A) the rate of maximum volume increase, B) the point of maximum volume, C) the dicrotic notch, and D) the minimal basal volume.

CHAPTER 2 INTRODUCTION

Novel Pulse Oximeter Prototypes

Literature Review

The nasal septum was explored as a possible monitoring site in 1937 (Hertzman 1937b). Groveman et al. (1966) also explored the nasal septum and believed that it represents a constant picture of the internal carotid circulation and reflects cerebral flow. Cucchiara and Messick (1981) showed that plethysmography from the nasal septum failed to estimate cerebral blood flow during carotid occlusion. In 1991 the nasal septum was explored during hypothermia (Ezri et al. 1991). Fourteen patients were monitored every 20 min during major abdominal procedures. The nasal septum probe was superior to the finger probe in detecting a pulse during hypothermia. The authors concluded that monitoring at the nasal septum was more reliable than monitoring at the finger in hypothermic patients. They acknowledged several limitations, including use during nasal intubation, in patients with extremely small nostrils, or the presence of a nasogastric tube.

Buccal probes were evaluated as an alternative. They were prepared by taping a malleable metal bar securely over the back of a disposable Nellcor finger probe and bending the metal bar and probe around the corner of a patient's mouth (O'Leary et al. 1992). It was determined that buccal SpO₂ was greater than finger SpO₂ and agreed more closely with SaO₂. The authors concluded that buccal pulse oximetry is a viable alternative to the finger. Limitations included longer preparation time, difficult placement, and possible dislodgement during airway maneuvers.

Awad et al. (2006) demonstrated that the ear plethysmographic waveform is relatively immune to vasoconstriction. They also determined that the PPG width has a good correlation to cardiac output. They concluded that the ear is more suitable for monitoring hemodynamic changes than the finger.

Novel Probe Designs

A significant number of subjects can not be adequately monitored using the fingers and other peripheral sites. We developed pulse oximeter probes specifically for monitoring saturation and pulse rate from central sites: the cheek and nasal septum. The prototype probes (Figure 2-1) were adapted for use with Novamatrix 520A pulse oximeters.

The nasal septum has strong promise as a pulse oximeter monitoring site. Kiesselbach's Plexus is the area in the anteroinferior part of the nasal septum. It is supplied by the sphenopalatine, greater palatine, superior labial and anterior ethmoid arteries (Grovesman 1966). These vessels originate from both the internal and external carotid arteries and are the most frequent cause of epistaxis. The anastomotic blood supply from both branches of the common carotid artery allows for a unique look at blood flow to the head and brain. The strength of the photoplethysmograph (PPG) signal from the nasal septum is strong enough to force the use of physical filters over the light emitting diodes (LED) to prevent PD saturation.

To test the accuracy of the novel nasal septum and cheek probes, a desaturation study was conducted in the hypoxia research laboratory at the University of California San Francisco. A Perkin Elmer Model 1100 medical gas analyzer, Radiometer Model OSM-3 hemoximeter, Radiometer Model ABL-5 blood gas machine and Nellcor Model N200 pulse oximeter were used in the analysis. Six males and six females were

desaturated to a SaO₂ of 65%. The variation in saturation readings for the cheek probe (Figure 2-2) and nasal septum probe (Figure 2-3) was consistently less than $\pm 3\%$ and the root mean square (RMS) error within one standard deviation of all data points was approximately two.

While the SpO₂ readings in the testing laboratory were accurate, the clinical utility of the probes needed to be addressed. A 30 patient study was designed to evaluate the clinical utility of these novel pulse oximeter probes. This study required the development of software that allowed for collection of pulse oximetry data.

Pulse Oximeter Data Acquisition Viewer

Pulse Oximetry Data Acquisition Viewer (PODAV) was developed by Convergent Engineering (Gainesville, FL). It simultaneously communicates with three pulse oximeters. It interfaces with the serial output port of the Novametrix Oxypleth 520A and uses the Novametrix proprietary Venus data logging protocol. It collects pulse rate, SpO₂ and the PPG. The PPG waveform is sampled at 100 Hz from the infrared (IR) LED, and the SpO₂ and pulse rate are sampled once per second. The Venus protocol also provides access to the LED power of the transmitter. The LED power is a normalized value that varies between zero and 254. The PODAV software stores all data in Microsoft Access database files for analysis. While recording the data, users can also record time-stamped notes for future reference and enter patient information.

In PODAV, the PPG is displayed based on the data collected from the IR channel of the pulse oximeter. Since the data collected in PODAV represents values of light hitting the photodiode (PD), processing is required to display the real-time PPG in a user-friendly format. To display the pulsatile cardiac component (PCC) of the PPG, a simple algorithm was used to remove the baseline low frequency component (LFC). Depending

on the pulse oximeter collection site, data values are in the range of hundreds of thousands of arbitrary light units while the PCC fluctuations are in the range of thousands, resulting in a small signal to noise ratio. Many pulse oximeter manufacturers use complex, proprietary algorithms to boost signal strength and eliminate this problem. The PODAV software continuously calculates a 10 sec moving average of the data. This value is continually subtracted from the baseline data. This new data is plotted and centered at zero and represents the PCC. The subtracted value is displayed in the software as “DC Gain” (Figure 2-4), and represents the LFC.

The PCC is displayed (Figure 2-4) for three pulse oximeter probes. The PODAV software interface shows the oxygen saturation for up to three probes for the previous 20 min, the pulse rate, and the LED power. The LED power is automatically adjusted by the pulse oximeter so the light hitting the PD falls within a desired range. The septum is a thin piece of cartilage and requires less light to penetrate it, hence the LED power required to power the pulse oximeter usually very low. The LED power of a finger probe is always 254, the highest value. The DC gain is continuously updated and subtracted from the raw data to obtain the PCC. Additionally, the pulse rate can be graphed for the previous 20 min (similar to saturation). Finally, patient information can be entered and notes can be taken at any time during the case.

Pilot Operating Room Study

After the development of PODAV, the operating room pilot clinical utility testing study of the two novel pulse oximeter probes was conducted. Thirty adult subjects undergoing surgery at a university medical hospital were recruited. Of the 30 subjects, 15 were male and 15 were female. They ranged in age from 21 to 80 years. Subjects undergoing head or neck surgery or a procedure where the nasal septum or cheek probes

would interfere with the surgical field were excluded. The anesthetic technique used was at the discretion of the anesthesiologist. The study was approved by the Western IRB. Subjects were paid for their participation.

On the day of surgery, a novel nasal septum pulse oximeter probe, a novel cheek pulse oximeter probe and a standard finger pulse oximeter probe were all placed on the subject. The finger probe was placed on a finger adjacent to the routine finger probe used by the anesthesiologist. The three experimental probes were connected to Novamatrix Oxypleth pulse oximeters. The data was ported to PODAV, running on a laptop computer, and recorded continuously throughout the surgery. The saturation averaging was set to 2 sec. The age, height, weight, gender, and surgical procedure were recorded for each subject. Additional data including blood gas results and intermittent blood pressure readings were recorded during the procedure. A minimum of 45 min of data was collected for each subject.

The study concluded that the oxygen saturation and pulse readings of the nasal septum and cheek probes did not differ from the gold standard finger probe. Additionally, it was concluded that the ease of access to the face by the anesthesiologist offered an advantage over the traditional finger probe.

Secondary Findings

The moving average algorithm eliminated the LFC and displayed the PCC in a user friendly form. By nature, a moving average does not eliminate relatively fast changes. The more stable the LFC was, the more easily it was eliminated. The nature of the algorithm provided valuable insight.

Arrhythmias

Arrhythmias were detectable using the PPG. Arrhythmias create sharp fluctuations in the pulse rate. Since the pulse rate is calculated by the timing of the individual heartbeats, it is affected by arrhythmias. During a premature ventricular contraction (PVC) a premature heartbeat is followed by a delayed beat. This variation in the timing of the heartbeats causes the pulse rate to change rapidly. If the pulse rate calculation averaging is set to the longest duration, the slight delay in the heart rate caused by the arrhythmias is not sufficient to affect the calculation. Since most clinicians set the averaging to the longest duration, this information is usually not available.

A pulse tracing for a 30 min period is shown (Figure 2-5). Until the 9:36 mark the pulse rate was relatively stable. At approximately 9:36, high frequency fluctuations began. This marked the beginning of period of very frequent cardiac arrhythmias (Figure 2-6).

There are three examples of arrhythmias in the 30 sec window (Figure 2-6). The exact cause and nature of the arrhythmias was not known as an electrocardiograph (ECG) was not being simultaneously recorded. Premature beats occur at a faster rate than the normal heart rate, resulting in a sharp increase in the heart rate while the subsequent delayed beat results in a decrease in heart rate. These changes occur for only these two beats and the pulse quickly resumes its previous rate. Arrhythmias affected eight of the 30 patients in the study. Further studies should be conducted to determine the type of arrhythmias detectable with PPG. Preliminary observations suggest that arrhythmia detection can very easily be built into existing pulse oximeters by using the PPG with simple processing algorithms.

Ventilator effect

During positive pressure ventilation the intrathoracic pressure increases, reducing venous return to the right heart. Simultaneously, and very briefly, blood forced from the low-pressure pulmonary vascular bed increases return to the left heart and stroke volume (Pinsky and Summer 1983). This is followed by a decrease in cardiac output as venous return into the central circulation drops off. The extent of the fluctuations caused by positive pressure ventilation depend on the state of filling of the peripheral vascular bed, the intrathoracic pressure changes, peripheral vasoconstrictor activity, and central blood volume (Murray and Foster 1996). Since positive pressure ventilation often accompanies general anesthesia, which causes vasodilation and damped vasomotor response, respiratory fluctuations are emphasized. It has also been discovered that early hypovolemia may be reflected in an exaggerated respiratory wave before other more classic signs of decreased urine output, tachycardia or hypotension.

Several of the subjects in the operating room study were under anesthesia for greater than 3 h, and in some cases the ventilator effect on the PPG was magnified. In some cases the effects were large enough to not be removed with the 10 sec moving average algorithm, resulting in low frequency baseline fluctuations of the PCC component of the PPG.

The ventilator effect on the PCC from the nasal septum was easily identifiable (Figure 2-7). The moving average algorithm was serendipitous in that it removed enough LFC to allow for a user friendly display centered at zero yet did not remove too much to eliminate interesting fluctuations. An ideal separator of PCC and LFC would always keep the PCC centered at zero, regardless of ventilator effect. The ventilator effect on the

PPG—particularly how it is magnified in the nasal septum and cheek probes—is the cornerstone of many subsequent studies, updated software, and newer probe designs.

Cardiac bypass

Two of the 20 cases required a cardiac bypass pump. During bypass, the lack of pulsations prevented the pulse oximeter from calculating oxygen saturation. The nasal septum, cheek and finger probes were equally ineffective. In one of the cardiac bypass surgery cases, the cheek probe detected a pulse significantly earlier than the other two probes when the pump was turned off and the heart began pumping. This resulted in an oxygen saturation reading 5 min earlier than the nasal septum and finger pulse oximeter probes. The oxygen saturation trends of the cheek and finger pulse oximeter probes are shown (Figure 2-8).

Blood pressure cuff

In one subject, the noninvasive blood pressure cuff was placed on the same arm as the finger pulse oximeter probe. The PCC component of the PPG from a finger pulse oximeter probe is displayed using the 10 sec moving average algorithm (Figure 2-9). It shows the effects of a blood pressure cuff on the PCC. The blood pressure cuff inflates to a pressure greater than systolic pressure and blood flow to the finger ceases. As the cuff deflates, the magnitude of the PCC slowly returns to its baseline level.

Limitations

To avoid injury, the nasal septum probe does not contact the septum. For this reason, it is extremely susceptible to movement artifact. The pilot study was performed during general anesthesia and the subjects were motionless. Due to artifact caused by movement, the nasal septum probe requires redesign to be used in awake subjects.

Light interference errors occurred in the nasal septum several times. This error was attributed to the lack of septum contact with the PD resulting in exposure to ambient light. In subjects with a thin septum, the PD was saturated, rendering the probe useless. Physical filters were placed over the PD to absorb some of the light allowing the probes to function normally. In darkly pigmented subjects, or those with a thick septum, the filters created low signal strength errors as too much light was being absorbed. Ideally, there would be a range of nasal septum probe designs to be used on different patient populations.

The position of the cheek probe varied the saturation reading in one case. The saturation reading rose after slight positional adjustment. It is possible that the beard of the subject caused the interference.

Updated Signal Separation Algorithm

These interesting findings, coupled with the utility of PCC and LFC extraction, prompted the need for an improved algorithm for signal separation. MatLab was used and an algorithm was created to facilitate this analysis. First, the peaks and troughs of the signal were identified discretely. They were identified at the expected heart rate, estimated by Fourier or autocorrelation analysis. Finding the midpoints between peaks and troughs were then calculated. The LFC was extracted as the interpolated (and possibly smoothed, or splined) line that connects these midpoints. The PCC was extracted as the raw signal minus the LFC.

The algorithm was applied to unprocessed data and further interesting findings were obtained from the pilot OR study. The unprocessed PPG obtained from the nasal septum is shown (Figure 2-10). The scale on the left corresponds to 320,000 to 330,000 arbitrary light intensity units obtained directly from the PD. The high frequency

fluctuations correspond to the heart rate. These heart rate induced changes are very small relative to the overall amount of light hitting the PD. In this case, the baseline light hitting the PD is around 320,000 while the magnitude of change from the heart beating is approximately 3,000. The lower frequency changes represent the ventilator effect. When the ventilator fires, there is an increase in intrathoracic pressure leading to a reduction of venous return to the heart. This blood becomes temporarily pooled in tissue beds distal to the heart. This results in an increase in absorbance and decrease in light hitting the PD. Each time the ventilator fires the PPG shifts downward. Using raw data and applying the algorithm described, the PCC and LFC were plotted separately.

Secondary Findings from the Operating Room Study Revisited

The amplitude of the PCC of the PPG is an indicator of stroke volume (Murray and Foster 1996) and may be a surrogate marker for blood flow. When analyzing the PCC for trends, it is often helpful to plot the PCC during several hours.

The PCC from the cheek probe and nasal septum probe of the same patient over the course of nearly 2 h is shown (Figures 2-11 and 2-12). The baseline LFC changes have been removed from the PCC. Periodically, blood flow to the cheek and nasal septum diminished. The causes of the local changes in blood flow are unclear but independent probes demonstrating the same phenomena at the same time indicate a true physiologic change occurred.

The PCC and LFC from the nasal septum from the same 10 min period from the same subject are shown (Figures 2-13 and 2-14). The PCC shows an increase in blood flow near the beginning of this 10 min period evidenced by the increase in amplitude. Simultaneously, there was a decrease in the LFC. This patient experienced a local increase in blood flow to the head illustrated by the increase in PCC, and an increase in

local venous blood volume evidenced by the drop in LFC. The slightly different lines depicting the LFC represent slightly different smoothing algorithms used for display.

In several cases, the amplitude of the LFC fluctuations, corresponding to the ventilator firing, changed throughout the case. This coincides with previous observations of increased ventilator effect on the PPG. The LFC from the nasal septum probe over a 20 min period is shown (Figure 2-15). The sharp fluctuations represent the LFC changes corresponding to the ventilator firing. The amplitude of these changes increased toward the end of this case. This shows the exaggerated effect of the ventilator on the LFC.

The PCC and LFC from the finger pulse oximeter of the subject with the blood pressure cuff are shown (Figures 2-16 and 2-17). The reduction of the PCC seven times corresponds to the blood pressure cuff inflation. The LFC decreases with each inflation. This decrease corresponds to an increase in absorption due to the pooled peripheral venous blood, which accumulates in the hand while the cuff is inflated. The higher frequency low magnitude fluctuations in the LFC correspond to the ventilator rate. Additionally, there is a slight decrease in PCC magnitude in between the second and third cuff firing simultaneous to a slight increase in overall LFC. This case illustrates just a few of the potential applications of the PCC and LFC of the PPG and the ability to detect a variety of physiologic events. The effect of the ventilator can be seen in the PCC as well. When the troughs of the PCC were aligned with the zero axis, the respiratory effect on cardiac output is seen on a beat-to-beat basis (Figure 2-18).

Nasal Alar Probe

To reduce motion artifact while preserving the signal to noise ratio and physiologic sensitivity, a spin-off of the nasal septum probe was designed. The nasal alar is fed by the same branches of the internal and external carotid arteries as the nasal septum. Since

the alar is protected by a layer of epidermis, it allows for a probe that can apply slight pressure, which reduces movement artifact and light interference. A nasal alar probe was designed (Figure 2-19). Similar to the nasal septum probe, this alar probe is able to obtain readings from branches of both the internal and external carotids. The major drawbacks of the nasal septum probe previously discussed were reduced or eliminated.

Additional Studies

The PCC is mainly affected by arterial blood, while the LFC is mainly affected by venous blood. The PCC and LFC from a finger probe in a healthy volunteer over 20 min are shown (Figures 2-20 and 2-21). A blood pressure cuff was inflated at a rate of 5 mmHg per minute until the pressure in the cuff exceeded systolic pressure. The PCC amplitude gradually decreased. This corresponded to a gradual decrease in flow to the finger with increasing cuff pressure. Finally, once systolic pressure was exceeded the flow to the finger fell to zero indicated by the flat PCC. Meanwhile, the LFC continued to drop as blood was trapped in the arm.

The PCC and LFC from the finger probe from a volunteer are shown (Figure 2-22 and 2-24). In this case the brachial artery was occluded by direct pressure while allowing venous blood to continue to drain from the arm. The PCC immediately fell to zero as there was no pulsatile flow to the finger. The LFC, however, rose, as more light hit the PD as venous blood was allowed to drain from the arm while no arterial blood entered. This simple series of experiments using a finger probe on a volunteer clearly showed the need to look at both the PCC and LFC when attempting to understand what is happening physiologically.

The PCC and LFC from a finger probe are shown (Figures 2-23 and 2-24). In this experiment a Valsalva maneuver was performed. A Valsalva maneuver involves bearing

down against a closed glottis. This increases intrathoracic pressure, impeding venous return, causing a pooling of venous blood in the periphery. The lack of venous return causes a reduction in cardiac output. The amplitude of the PCC dropped immediately after the onset of the Valsalva (arrow of Figure 2-24). Simultaneously, the LFC also fell rapidly as there was a pooling of blood in the periphery reducing the amount of light hitting the PD (Figure 2-25). Initially there was a one beat increase in the PCC at the onset of the Valsalva maneuver. The heart was squeezed, forcing additional blood out with the initial beat. This is the basis for antigravity induced loss of consciousness Valsalva training in military pilots. Holding the Valsalva for longer than a few seconds, however, reduces cardiac output.

In the following study, the effect of hand position relative to the heart on the PPG derived from a finger probe was explored using Valsalva maneuvers. The PCC and LFC (Figure 2-26) were derived from the finger probe of a volunteer subject. The probe was held at heart level for phase 1 of the study. During the phase 2 the subject had his hand raised above heart level. Finally, in phase 3 the probe was below heart level. During each phase, a Valsalva maneuver was performed. The PCC and LFC at heart level were at a baseline and the effect of the Valsalva was as previously described. When the arm was raised above the head, the PCC increased dramatically, and the LFC also increased. The reasons for the increase in the PCC amplitude were not clear. One hypothesis is that an intact sympathetic nervous system may cause a local increase in blood flow while the hand is above the head. This local increase overcomes gravity and causes an increase in flow. This could be the foundation for a future study in people with known autonomic dysfunction. A second hypothesis relates to venous congestion creating impedance

surrounding the arteries. When the hand was raised above the head, the venous blood drained from the arm increasing the LFC. This allowed for the small vessels in the hand to expand at a larger rate as there was less impedance surrounding them. The opposite was apparent in phase 3. With the arm below the heart, venous congestion in the arm caused a decrease in LFC, and this local impedance also caused the drop in PCC amplitude.

To fully understand the effect of spontaneous breathing on the PCC and LFC, a study was conducted involving several breathing maneuvers. The PCC and LFC were recorded from the nasal alar of a volunteer (Figures 2-27 and 2-28). Mueller and Valsalva maneuvers were both conducted. Mueller maneuvers involve a forced inspiration against a closed glottis. The Mueller maneuvers had little effect on the PCC but increased the LFC. During a Mueller maneuver there is a sharp decrease in the intrathoracic pressure associated with a strong forced inspiration. This decrease in intrathoracic pressure draws blood into the thorax decreasing the amount of pooled venous blood in the periphery. This reduction in peripheral venous blood resulted in more light hitting the PD and an increase in the LFC.

Mueller and Valsalva maneuvers represent the maximum intrathoracic pressure changes associated with spontaneous breathing. A follow-up study involved a volunteer, monitored with an alar probe, breathing through endotracheal (ET) tubes with decreasing diameters. These ET tubes represent increasing resistance. The PCC and LFC from a nasal alar probe in a healthy volunteer instructed to inhale and exhale through a series of ET tubes with decreasing diameters are shown (Figures 2-29 and 2-30). The duration through each ET tube was approximately 1 min followed by 1 min of no resistance.

Breathing through resistance magnifies the effects of spontaneous breathing. During inspiration though resistance it is necessary to create a large negative pressure. This enhances venous return. Upon exhalation it is necessary to create a large positive pressure, which dampens venous return. These effects increase with increasing resistance as the intrathoracic pressure changes become more pronounced. The LFC amplitude increased as a direct reflection of the movement of the venous blood in the periphery (periphery is anywhere distal to the heart). Also, as the diameters of the ET tubes decreased, and resistance increased, the PCC reflected this. This represents changes in the cardiac output through the breathing cycle. On inspiration, cardiac output increased due to enhanced venous return while during expiration cardiac output fell due to decreased venous return. As the intrathoracic pressure swings increased this effect was exaggerated.

The upstroke of the swings (Figure 2-31) corresponds to increasing light hitting the PD. This represents decreasing pooled peripheral blood. This occurs during inspiration as pooled blood is being forced into the thorax created by the negative pressure. The downstroke represents decreasing light hitting the PD. This occurs when pooled peripheral blood is increasing during forced expiration. The trough represents the point of least light hitting the PD corresponding to the maximum pooling of blood with each respiratory cycle. Since venous blood flow is affected by intrathoracic pressure swings, and this affect is enhanced by adding resistance to the breathing, the PPG is the ideal way to monitor these changes.

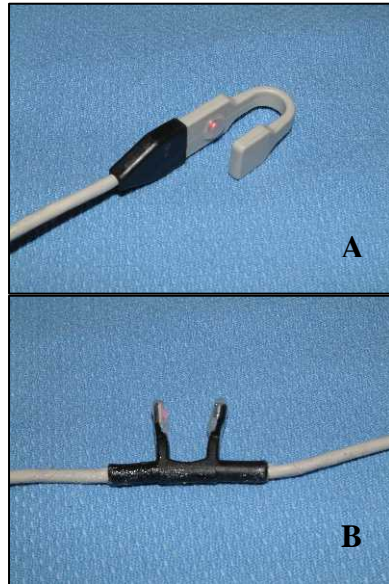


Figure 2-1. Novel pulse oximeter probes manufactured by Beta Biomed Services (Rowlett, TX). A) Cheek, B) Nasal septum.

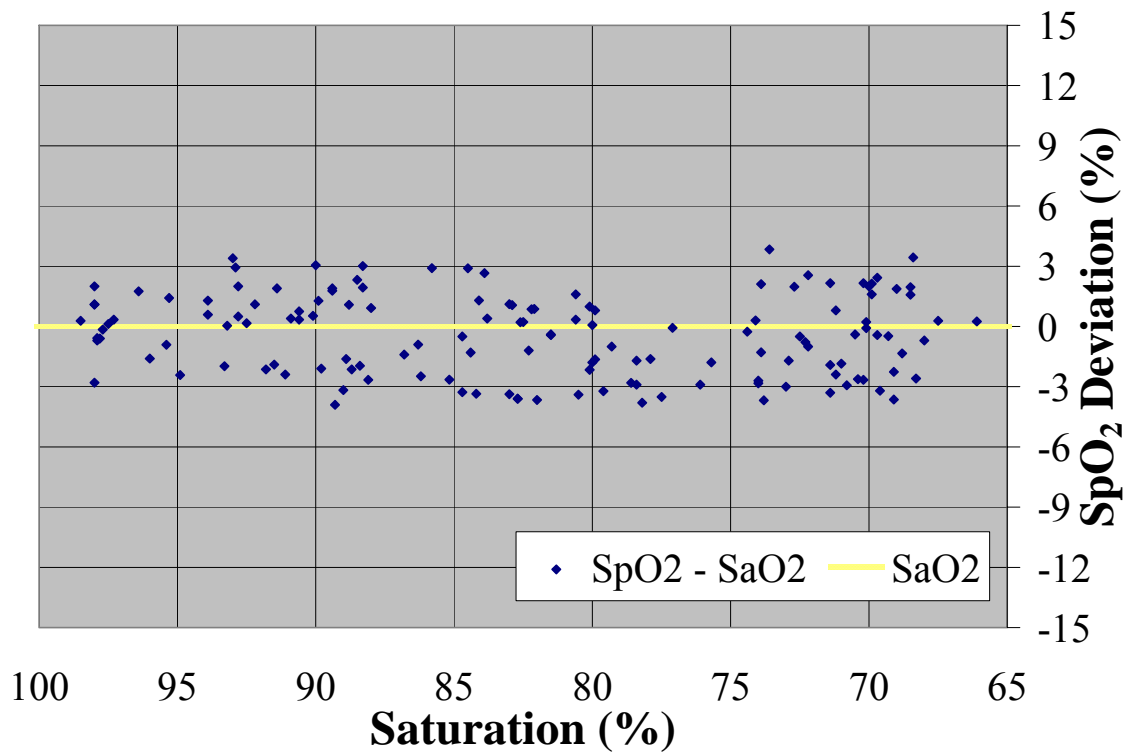


Figure 2-2. Variance of SpO₂ from SaO₂ as hypoxic conditions increased, as measured by the cheek probe.

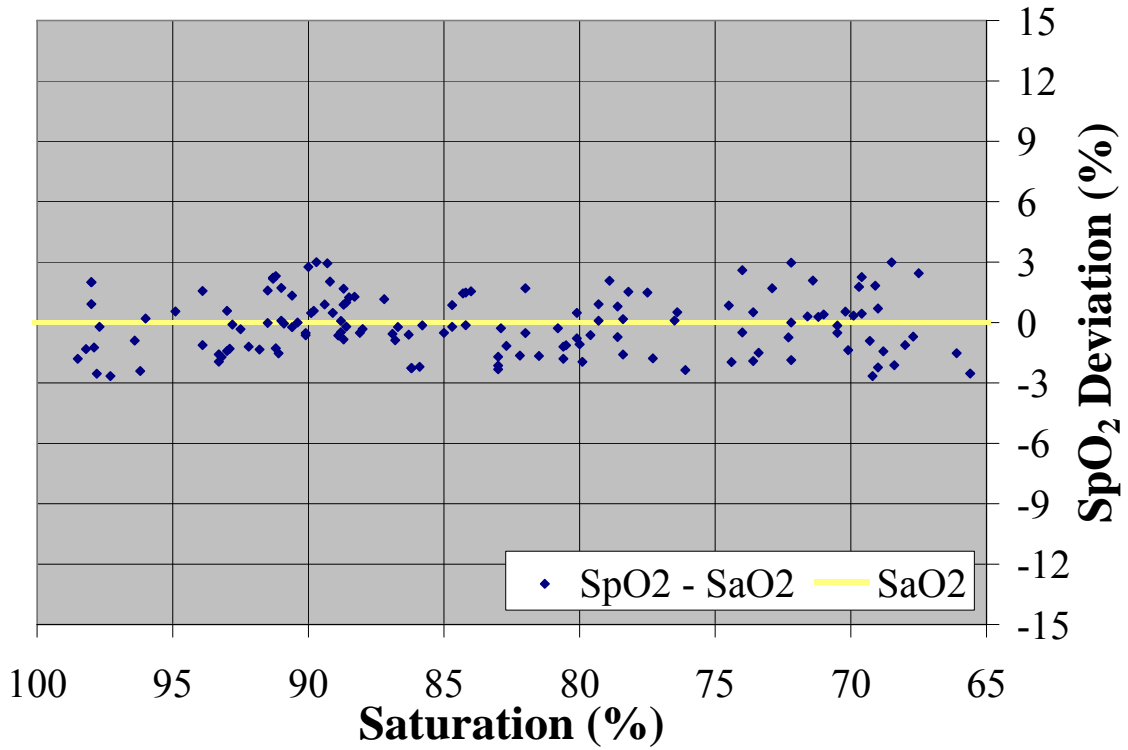


Figure 2-3. Variance of SpO₂ from SaO₂ as hypoxic conditions increased, as measured by the nasal septum probe.

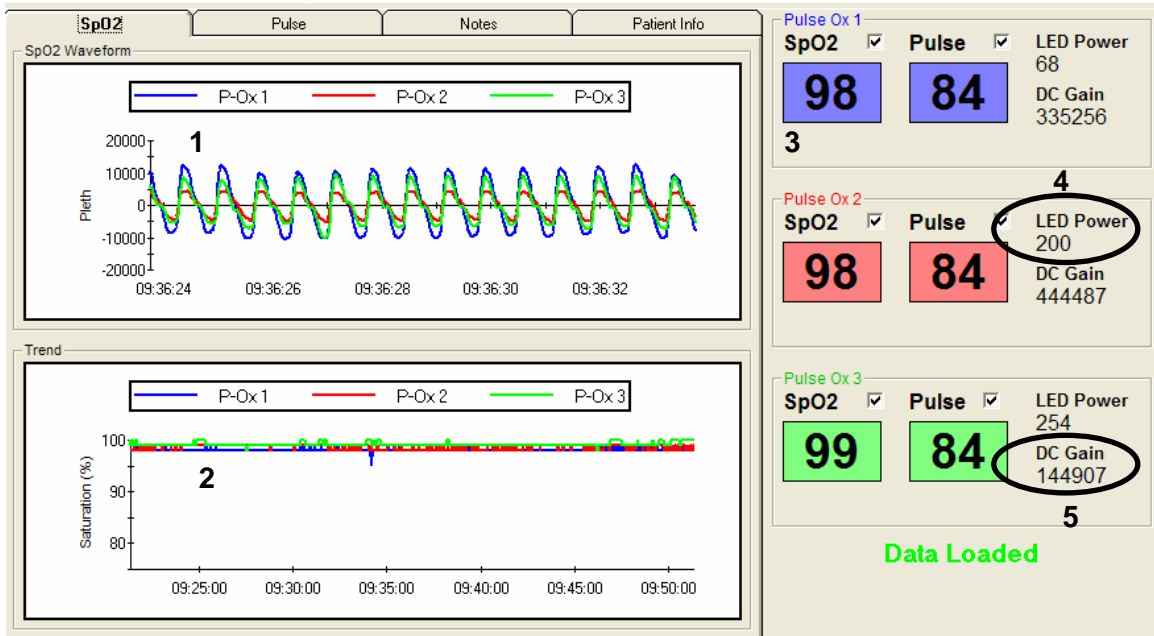


Figure 2-4. The Pulse Oximetry Data Acquisition Viewer software. 1) The PCC, 2) The 30 min saturation tracing, 3) Oxygen saturation and pulse rate, 4) LED power, 5) DC gain.

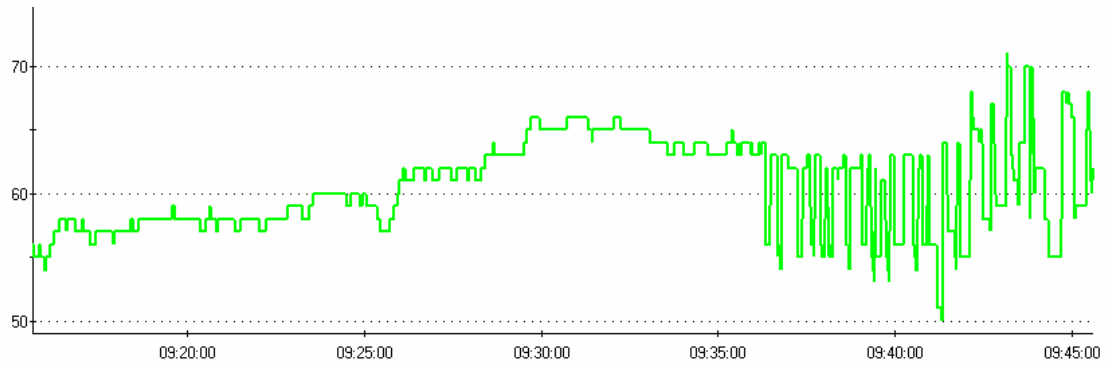


Figure 2-5. A 30 min pulse rate tracing of an operating room pilot study subject, showing arrhythmias.

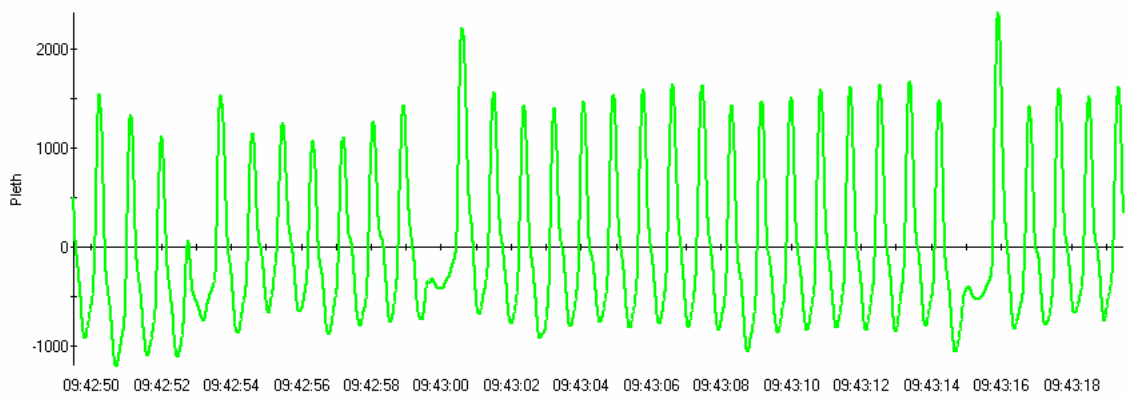


Figure 2-6. A 30 sec PCC tracing of the PPG of an operating room pilot study subject, showing arrhythmias.

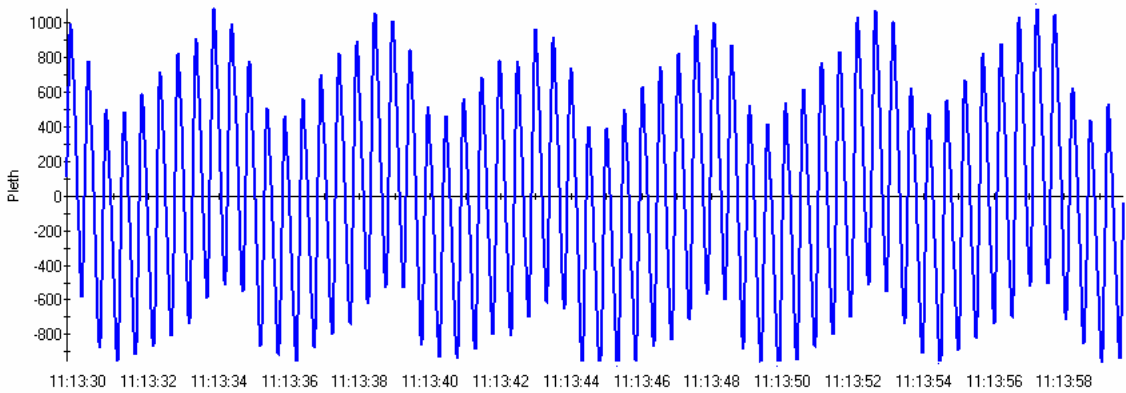


Figure 2-7. A 30 sec PCC tracing of the PPG of an operating room pilot study subject, showing the effect of the ventilator.

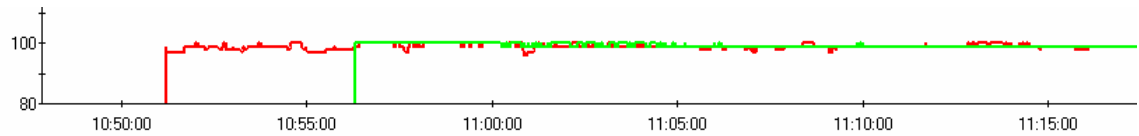


Figure 2-8. A 30 min oxygen saturation trend of an operating room pilot study subject, showing how the cheek probe resumed functionality 5 min sooner than the finger probe following cardiac bypass.

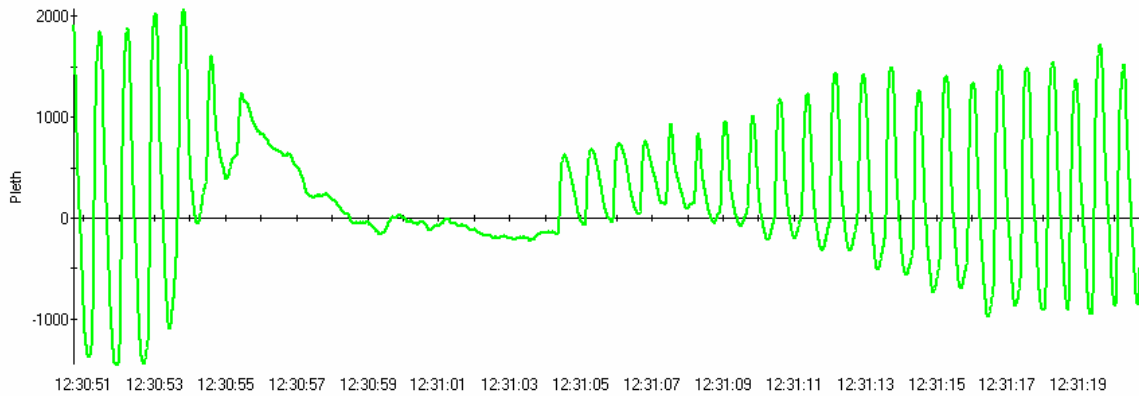


Figure 2-9. A 30 sec PCC tracing of the PPG of an operating room pilot study subject, showing the effect of a blood pressure cuff.

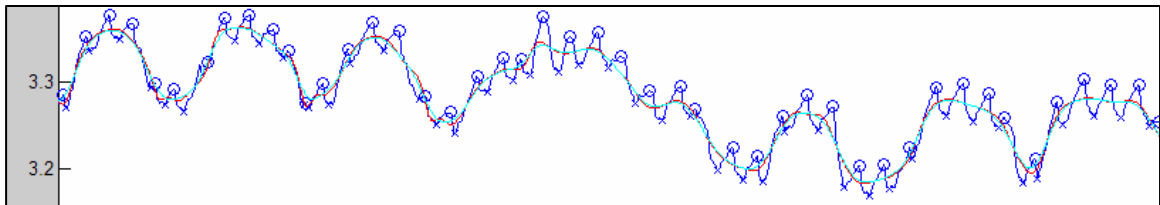


Figure 2-10. The unprocessed PPG data of an operating room subject with the peaks and troughs identified discretely.

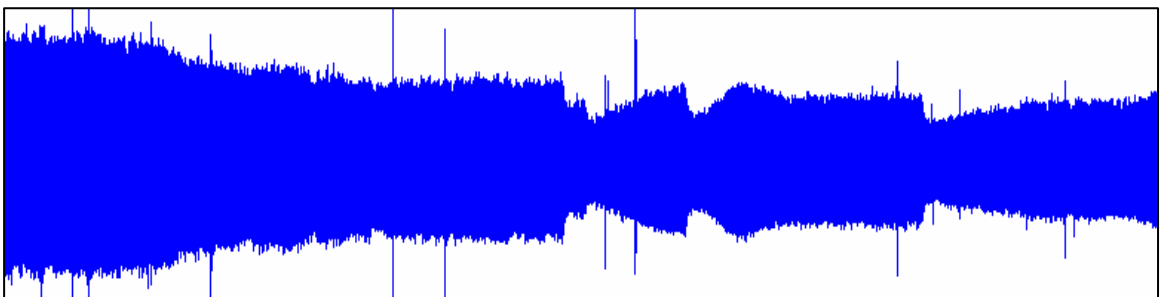


Figure 2-11. The PCC of the PPG from the cheek of an operating room pilot study subject, showing periodic reduction in amplitude corresponding to blood flow.

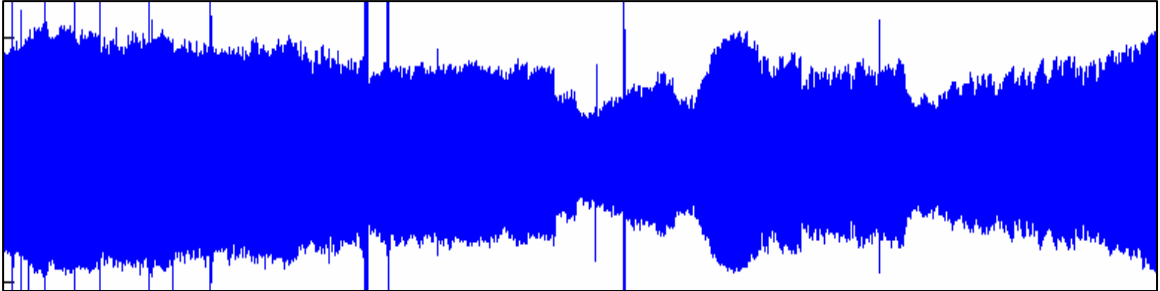


Figure 2-12. The PCC of the PPG from the nasal septum of an operating room pilot study subject, showing periodic reduction in amplitude corresponding to blood flow.

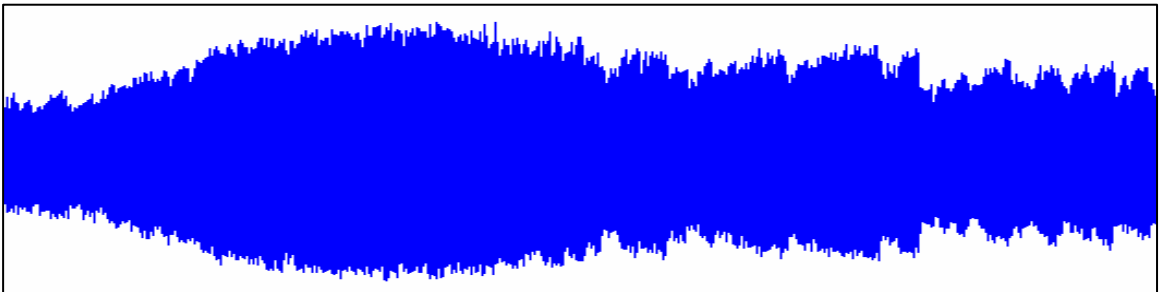


Figure 2-13. The PCC of the PPG from the nasal septum of an operating room pilot study subject, showing changes in blood flow over time.

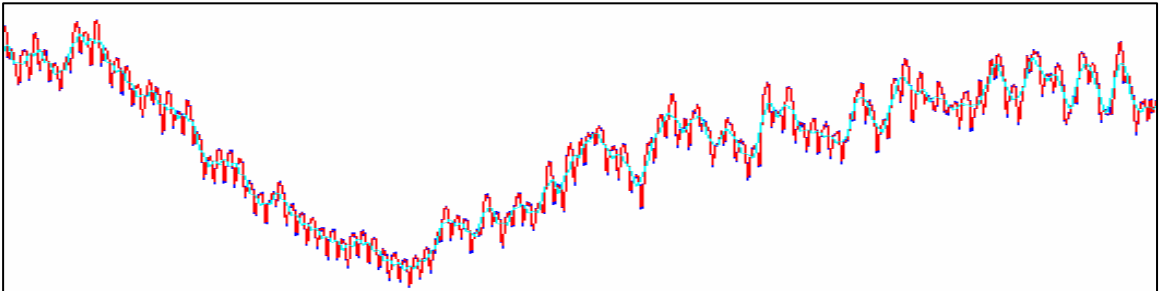


Figure 2-14. The LFC of the PPG from the nasal septum of an operating room pilot study subject, showing changes in baseline venous blood over time.

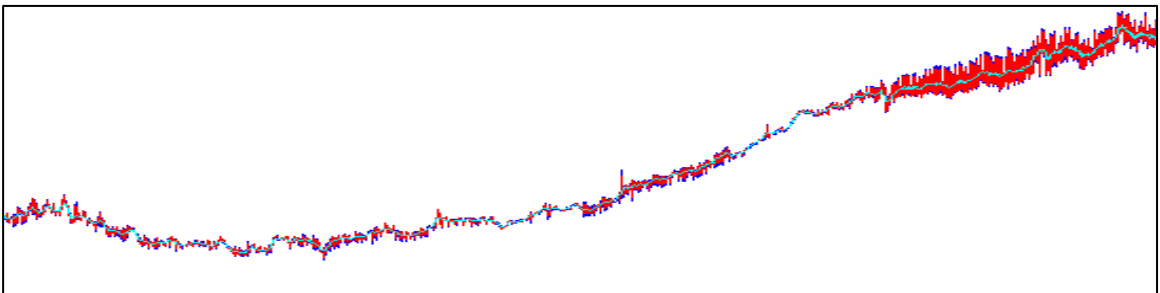


Figure 2-15. The LFC of the PPG from the nasal septum of an operating room pilot study subject, showing increased fluctuations over time.

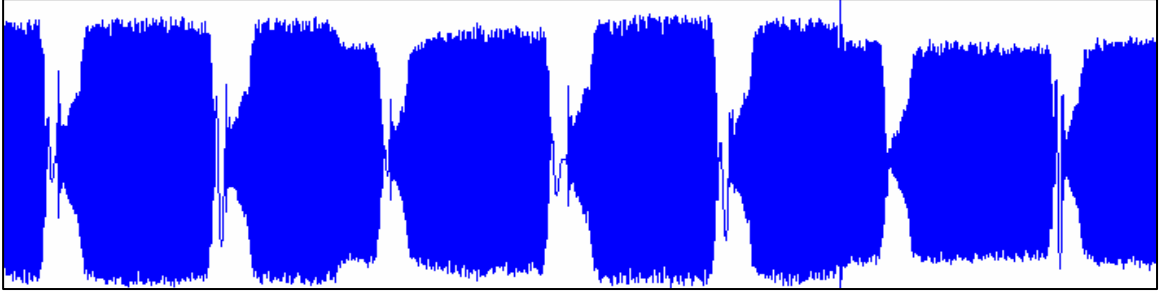


Figure 2-16. The PCC of the PPG from the finger of an operating room pilot study subject, showing the periodic effect of a blood pressure cuff.

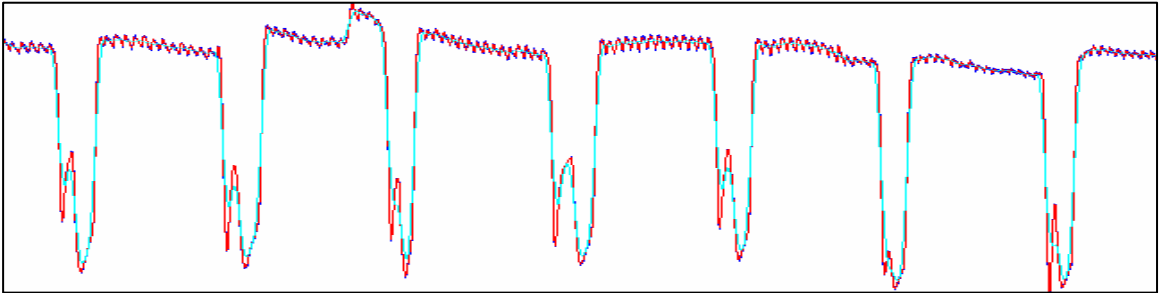


Figure 2-17. The LFC of the PPG from the finger of an operating room pilot study subject, showing the periodic effect of a blood pressure cuff.

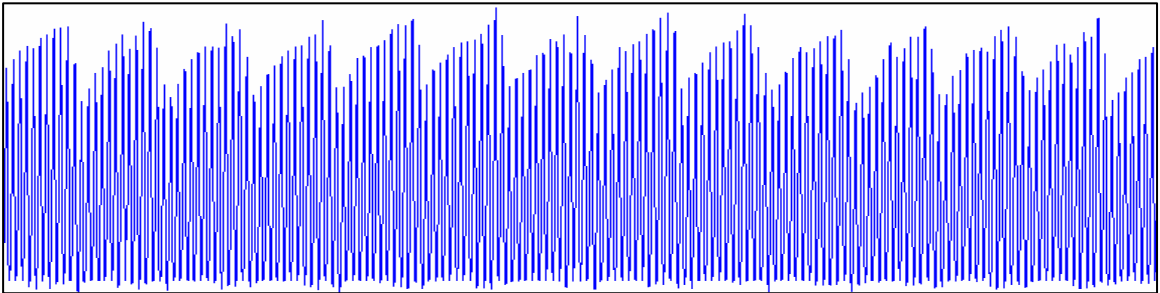


Figure 2-18. The PCC of the PPG from the nasal septum of an operating room pilot study subject, showing the effect of the ventilator.



Figure 2-19. The nasal alar probe design, based on the cheek probe design.

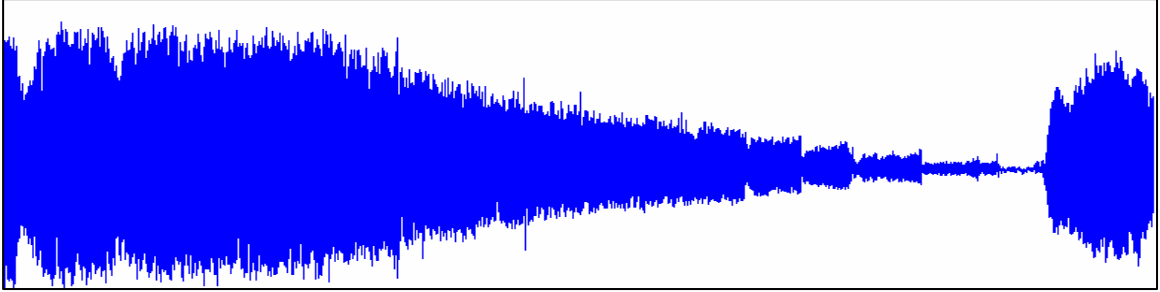


Figure 2-20. The PCC of the PPG from the finger of a healthy volunteer, showing the effect of a blood pressure cuff over time.

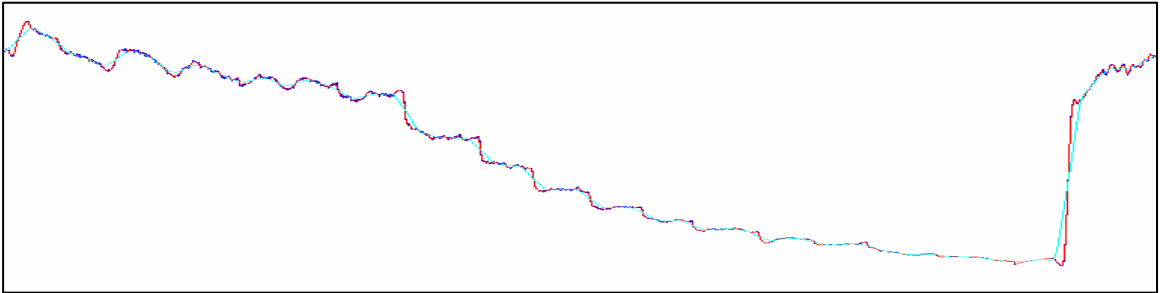


Figure 2-21. The LFC of the PPG from the finger of a healthy volunteer, showing the effect of a blood pressure cuff over time.

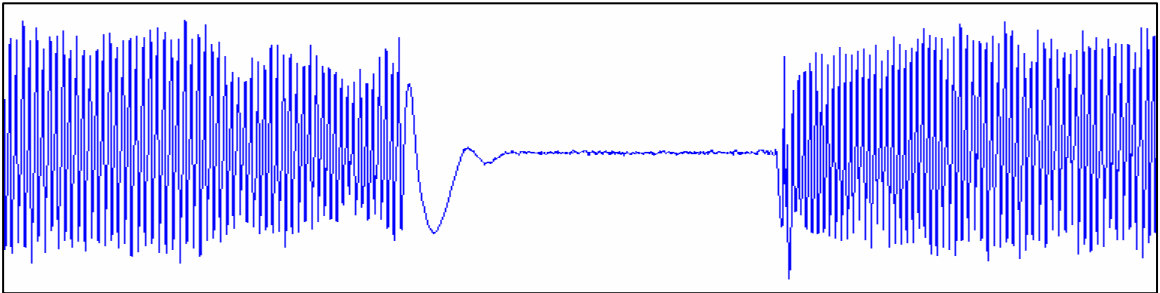


Figure 2-22. The PCC of the PPG from the finger of a healthy volunteer, showing the effect of brachial artery occlusion.

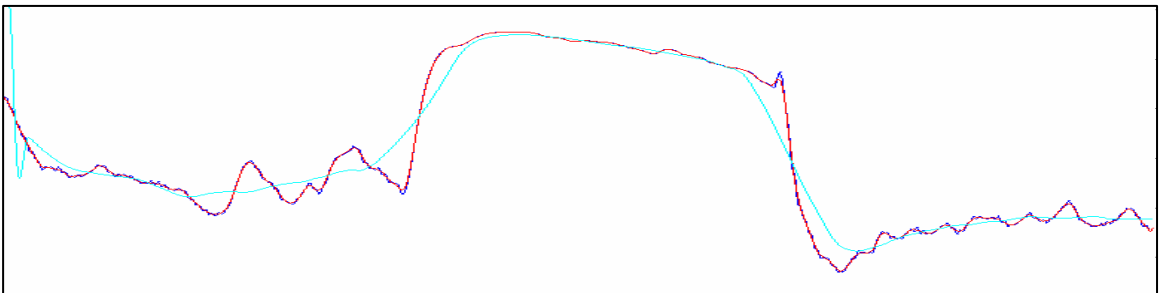


Figure 2-23. The LFC of the PPG from the finger of a healthy volunteer, showing the effect of brachial artery occlusion.

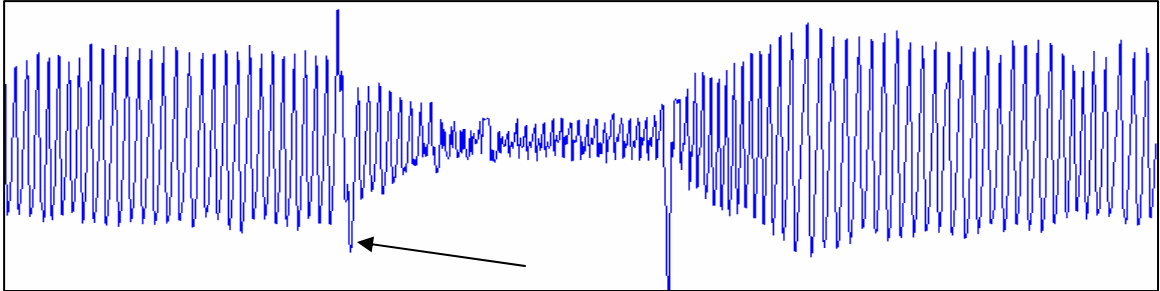


Figure 2-24. The PCC of the PPG from the finger of a healthy volunteer, showing the effect of a Valsalva maneuver (arrow).

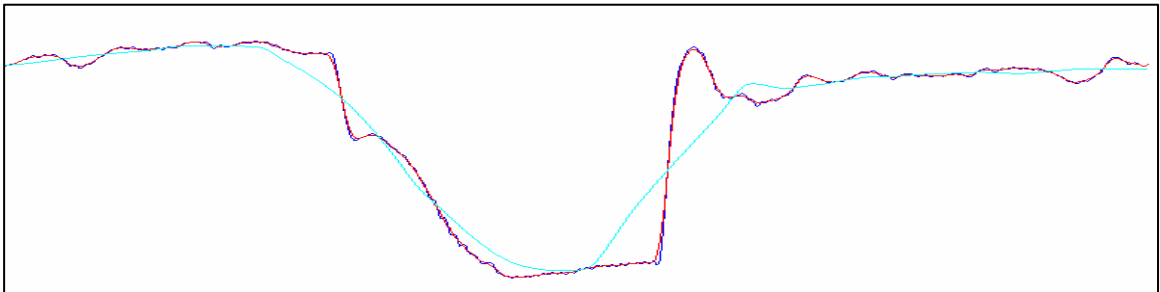


Figure 2-25. The LFC of the PPG from the finger of a healthy volunteer, showing the effect of a Valsalva maneuver.

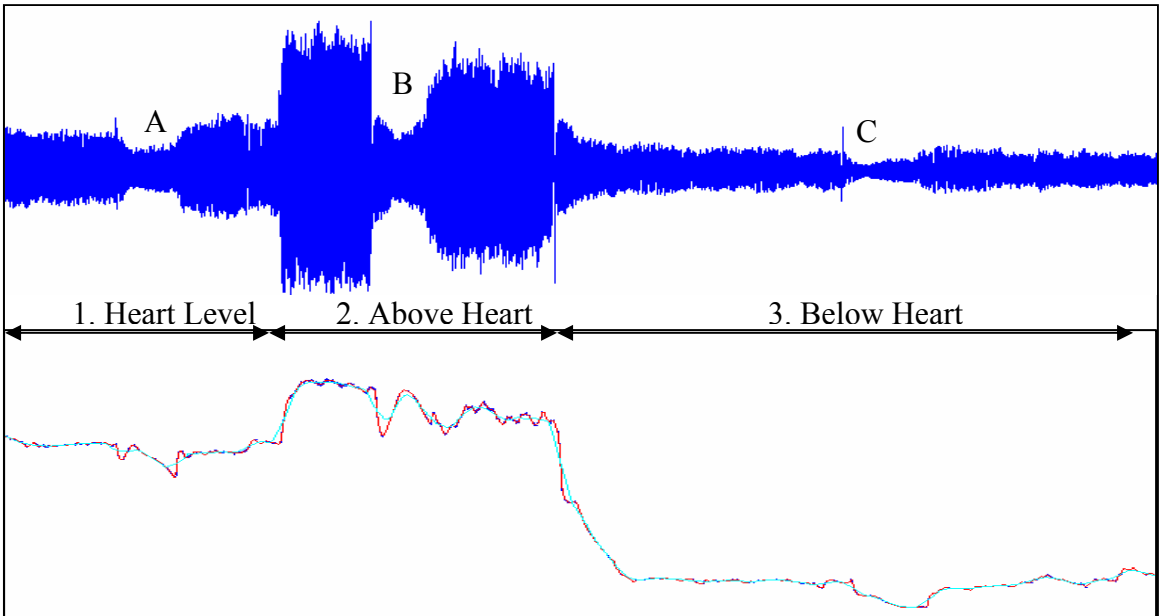


Figure 2-26. The PCC and LFC of the PPG from the finger of a healthy volunteer, showing the effect of position of the hand with respect to the heart. A) Valsalva maneuver, B) Valsalva maneuver, C) Valsalva maneuver.

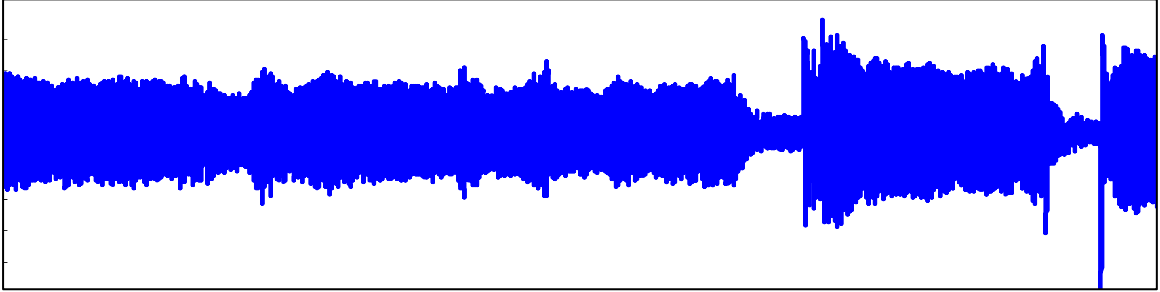


Figure 2-27. The PCC of the PPG from the finger of a healthy volunteer, showing the effect of Mueller and Valsalva maneuvers.

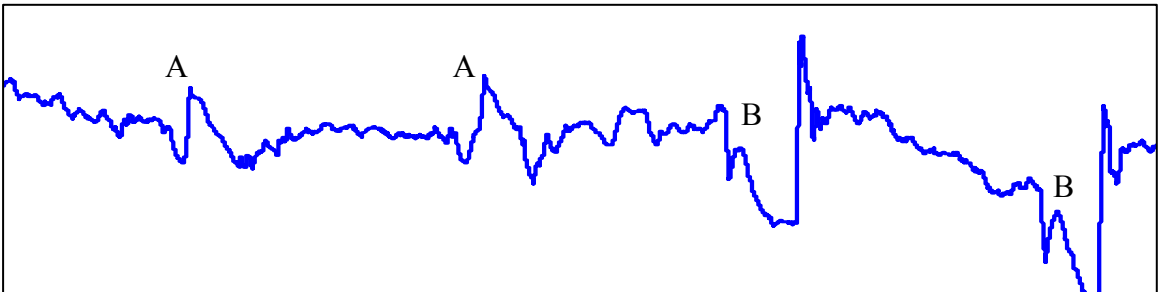


Figure 2-28. The LFC of the PPG from the finger of a healthy volunteer, showing the effect of Mueller and Valsalva maneuvers. A) Mueller maneuver, B) Valsalva maneuver.

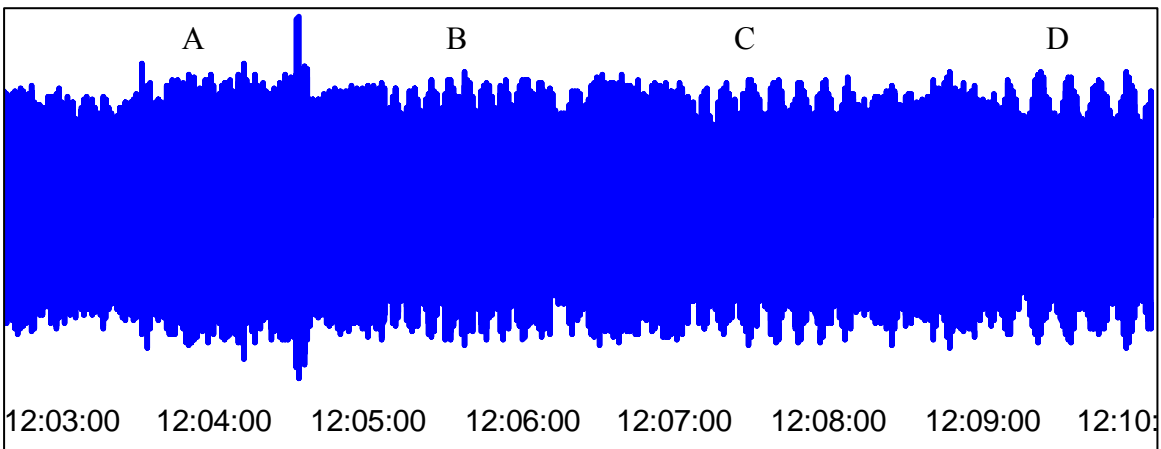


Figure 2-29. The PCC of the PPG from the alar of a healthy volunteer, showing the effect of breathing through various endotracheal tubes. A) 5.5 mm, B) 5.0 mm, C) 4.5 mm, D) 4.0 mm.

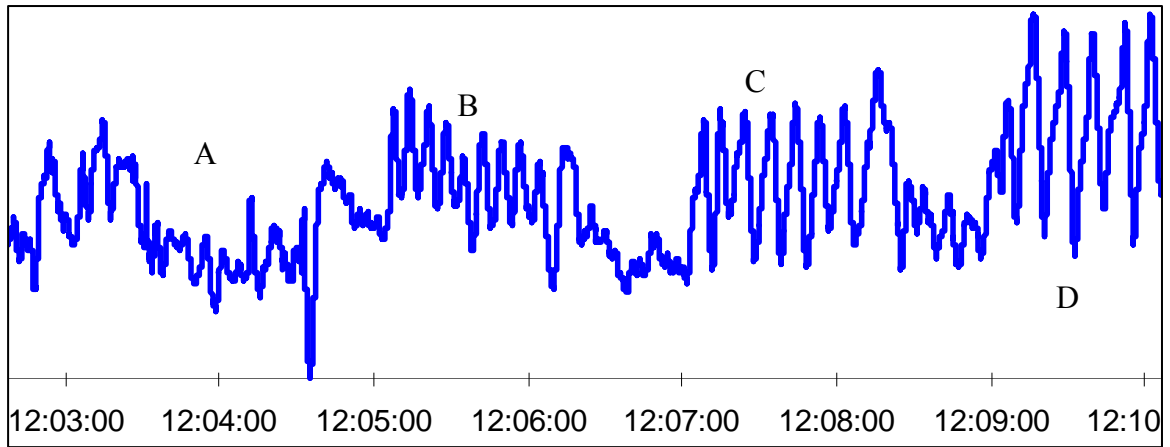


Figure 2-30. The LFC of the PPG from the alar of a healthy volunteer, showing the effect of breathing through various endotracheal tubes. A) 5.5 mm, B) 5.0 mm, C) 4.5 mm, D) 4.0 mm.

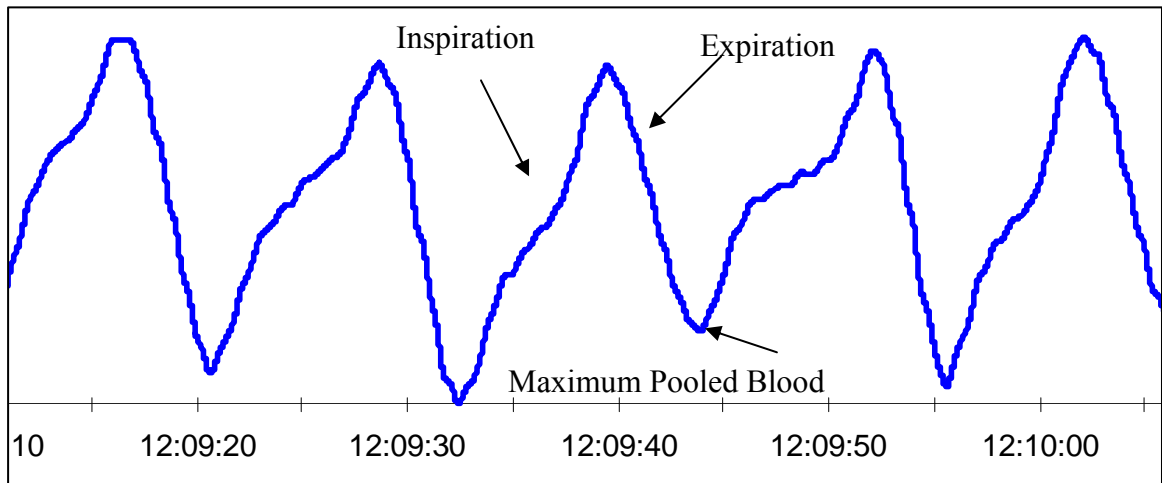


Figure 2-31. The LFC of the PPG from the alar of a healthy volunteer, showing the effect of spontaneous respiration.

CHAPTER 3 BROAD CLINICAL GOALS

Clinical Goal 1

The first clinical goal is to use the photoplethysmograph (PPG) to detect changes in airway resistance. Disorders that increase airway resistance include asthma, obstructive sleep apnea (OSA), chronic bronchitis, cystic fibrosis and chronic obstructive pulmonary disease. Other disorders, such as acute respiratory distress syndrome and pneumonia, increase work of breathing by reducing lung compliance. These disorders necessitate large negative and positive intrathoracic pressures to move air in and out of the lungs, either due to increasing airway resistance or decreasing lung compliance. Large intrathoracic pressure changes, both negative during inspiration and positive during exhalation, affect cardiac return and cardiac output. These changes may be detectable using the PPG. The first broad clinical goal is to show that the PPG can be used to detect changes in airway resistance. Clinical uses include, but are not limited to, noninvasive diagnosis of severity of asthma and detecting OSA, and estimating its severity.

Clinical Populations

Asthma

Asthma is a chronic inflammatory disease of the airways affecting 14 to 15 million people in the United States and is the most common chronic disease of childhood. People with asthma collectively have more than 100 million days of restricted activity and 470,000 hospitalizations annually. Each year more than 5000 people die from asthma (NAEPP 1997).

In 1991 the National Asthma Education and Prevention Program (NAEPP) published four recommendations for the management and treatment of asthma including the use of objective measures of lung function to assess the severity of asthma and to monitor the course of therapy (NAEPP 1991). The current standard of care for the monitoring of asthma includes monitoring signs and symptoms, monitoring pulmonary function with spirometry and peak flow measurements, monitoring quality of life and functional status, monitoring asthma history, monitoring pharmacotherapy, and monitoring patient-provider communication and patient satisfaction (NAEPP 1997). Specific evaluations for asthma severity include physical examinations by a health care provider, spirometry and patient self-assessment (NAEPP 1997).

Spirometry measures the maximal volume of air forcibly exhaled from the point of maximal inhalation (FVC) and the volume of air exhaled during the first second of the FVC (FEV_1). The degree of airway obstruction is indicated by a reduced FEV_1 and FEV_1/FVC values relative to reference values (NAEPP 1997). There is no standard for direct measurement of airway resistance. The ability to noninvasively measure airway resistance for the monitoring of asthma severity could have broad clinical implications.

The interrupter technique for measuring airway resistance (R_{int}) was first introduced by Von Neergaard and Wirz (1927) but has only been commercially available for the last five years (Hadjikoumi et al. 2003). It is a rapid, noninvasive, and convenient method for measuring airway resistance. During transient interruption of airflow (100 msec) alveolar pressure equilibrates rapidly with pressure at the mouth (Von Neergaard and Wirz 1927). The alveolar pressure is derived from the measurement of mouth pressure immediately following occlusion. If flow is measured immediately before

occlusion, then airway resistance can be calculated by dividing the pressure by the flow (Hadjikoumi et al. 2003).

The interrupter technique is primarily used for children too young for accurate spirometry measures and is not without flaws. There is no standard way to measure pressure change during valve closure. In patients requiring a longer time to gain equilibrium, the end occlusion might underestimate the pressure change measured at the mouth and therefore the calculated airway resistance (Kooi et al. 2005). It is also important to firmly support the cheeks and mouth floor of the subject. Unsupported cheeks lead to significantly lower R_{int} values. In many children, a facemask instead of a mouthpiece could simplify the measurements but many children are not accepting of a facemask (Kooi et al. 2005). The interrupter method is an active area of research for noninvasive resistance measurements in children.

Determining respiratory resistance by forced oscillation (R_{fo}) is a noninvasive, effort-independent technique that can be obtained at the bedside in children as young as 3 years old (Dubois et al. 1956a, Dubois et al. 1956b, Cogswell 1973, Solymar et al. 1989, Duiverman et al. 1985). The technique was proven valid, with strong correlations between respiratory resistance measured by R_{fo} and whole body plethysmography (Fichter et al. 1989, Barleban et al. 1990, Simm 1989). It was also proven feasible in children older than 3 years old, both stable and acutely ill (Ducharme and Davis 1997, Cogswell 1973). It was also evaluated as a reproducible and responsive measure of asthma severity, and appears to be an attractive alternative for evaluating children who are too young or too sick for spirometry (Ducharme and Davis 1998).

Pagani et al. (2003) evaluated pulse transit time (PTT) as a measure of inspiratory effort in children. The PTT is the time it takes the pulse wave to travel between two arterial sites (normally heart to finger). The speed at which the pulse wave travels is indirectly proportional to the PTT. The authors found a good correlation between the induced inspiratory effort and the amplitude of PTT variations and concluded that PTT should be a method for quantifying changes in inspiratory effort due to augmented upper airway resistance in awake children.

Officer et al. (1998) compared four least squares regression algorithms for determining pulmonary resistance and dynamic elastance in subjects with emphysema, normal subjects, and subjects with asthma; before and after bronchoconstriction. The four methods gave comparable results in normal and asthmatic subjects and differed slightly in the emphysema subjects.

Identification of new noninvasive measures of airway resistance for determining asthma severity is an active area of research. Asthma severity is dictated by airway resistance, which is proportional to the intrathoracic pressure changes with respiration. If the PPG derived noninvasively from a pulse oximeter can reliably measure intrathoracic pressure changes it may also be an indicator of airway resistance and hence asthma severity.

Obstructive sleep apnea syndromes

There are several forms of sleep-disordered breathing. One major group is the obstructive sleep apnea syndromes; including primary snoring, upper airway resistance syndrome (UARS) and OSA (Collop 2005). A narrowing or complete obstruction of the upper airway is a commonality among these disorders.

Snoring is a respiratory noise generated from the upper airway during sleep that may occur during inspiration or expiration. Primary snoring occurs regularly and usually does not result in significant daytime impairment although some studies have shown snorers may have an increased risk of cardiovascular disease (Hoffstein 1996, Hu et al. 2000). A decrease in tone of the upper airway muscles results in constriction of the oropharynx and results in snoring. There is no standard measure of snoring and it is often quantified using a microphone and sound meter (Collop 2005).

In 1993 the term UARS was first used by Guilleminault et al. (1993) to describe a group of patients with excessive daytime somnolence. Extensive monitoring utilizing an esophageal pressure catheter revealed repetitive instances of increasingly negative intrathoracic pressure associated with upper airway flow limitation. These events culminated in arousal and return of intrathoracic pressure and upper airway flow to normal. These respiratory effort measurements are important in detecting obstructed breathing events, however esophageal catheters are invasive and not practical for standard polysomnography (Collop 2005). A noninvasive, simpler method to accurately measure respiratory effort by measuring intrathoracic pressure changes would make diagnosis of UARS more practical.

Obstructive sleep apnea is a repetitive, partial or complete obstruction of the upper airway during sleep and is the most severe of the obstructive sleep apnea syndromes. Its prevalence is approximately 5% (Young et al. 2002) and is more common in males. Its severity is commonly determined by the apnea-hypoxia index (AHI) frequency. The AHI is computed by (apneas + hypopneas / total hours of sleep). The level of severity is arbitrary as there is little data on the relationship between AHI and

morbidity and mortality as AHI alone fails to take into account the severity of oxygen desaturation or the amount of sleep disruption (Collop 2005). A more accurate indicator of OSA severity is needed.

Since intrathoracic pressure measurements correlate with the degree of upper airway obstruction, researchers are evaluating ways to measure this pressure during sleep. Patil et al. (2004) developed and validated a simplified approach to analyze the pressure-flow relationship in sleeping subjects. They concluded that the analytic approach has the potential for standardizing and simplifying the ascertainment of the critical pressure for studies examining the effect of therapeutic devices and agents on upper airway collapsibility during sleep.

Haba-Rubio et al. (2005) evaluated the use of the pulse wave amplitude (PWA) derived from the PPG of a standard finger pulse oximeter for evaluating sleep fragmentation. Several respiratory events were analyzed, including apnea, hypopnea and upper airway resistance episodes. The PWA changes were significantly greater than heart rate changes during these events. The authors concluded that the PWA obtained from a simple pulse oximeter might be a valuable method to evaluate sleep fragmentation in breathing disorders.

The gold standard for diagnosing OSA remains the attended, overnight level I polysomnogram (Pang and Terris 2006). Unfortunately, limited resources, including limited number of recording beds, high cost, long waiting lists, and labor requirements prevent diagnosis in a large portion of the population. Screening questionnaires and devices have also been developed. The ideal screening device should be cheap, readily

accessible, easily used with minimal instructions, have no risks or side effects to the patient and be safe and accurate.

Obstructive sleep apnea syndromes increase airway resistance and subsequently intrathoracic pressure. The PPG derived noninvasively from a pulse oximeter may offer a simple, easy to use indicator of severity and diagnosis of these syndromes.

Changes Caused By Respiration

During spontaneous breathing, subatmospheric pressure during inspiration draws air and blood into the lungs: blood is drawn from the vena cava into the right heart and then into the expanding pulmonary vascular bed. Simultaneously, left ventricular output briefly decreases for one or two heartbeats as blood accumulates in the pulmonary circuit. Thereafter, expiratory pressure improves flow to the left heart, increasing stroke volume, peripheral pulse flow, pulse amplitude and peripheral venous pressure (Murray and Foster 1996). These changes are predicated upon intrathoracic pressure changes and are magnified when intrathoracic pressure changes increase, as with added respiratory resistance.

Pilot Data

Exploratory pilot study

To determine the practical range of resistance breathing, healthy volunteers were recruited to breathe through a series of decreasing diameter endotracheal (ET) tubes. The study was designed to determine the flow rates and volumes achievable through various levels of resistance by healthy volunteers. A breathing circuit was connected to a Non-Invasive Cardiac Output (NICO), (Novamatrix) to monitor inspiratory and expiratory flow rates and respiratory volume. Based on the data collected and feedback from the subjects, it was determined that peak inspiratory and expiratory flow rates of 40 L/min

with a total breath volume of 1.5 L was ideal through a broad range of resistance levels. The smallest diameter ET tube used was 3.5 mm, creating the largest resistance. Through this ET tube, flow rates of greater than 40 L/min were not attainable with healthy volunteers. The largest diameter ET tube used was 7.5 mm, creating the lowest level of resistance. Through this ET tube a flow rate of 40L/min was reported as of similar difficulty to breathing through no resistance, thus minimally affecting intrathoracic pressure. Increasing the flow rate through the 7.5mm ET tube would increase the intrathoracic pressure changes, however the flow rate should remain constant and rates higher than 40L/min were not attainable through the highest resistance.

Ventilator and volunteer resistance study

To estimate the intrathoracic pressure changes associated with breathing through a variety of resistors at constant flow rates and volumes, the following two-part experiment was conducted. In the first part of the study, a Puritan Bennett 7200 Series Ventilatory System was used to simulate breathing and a Michigan Instruments Inc. Model 1600 Dual Adult Training Test Lung was used to simulate the lungs (Katz, et al. 1988, Banner et al. 1993). Endotracheal tubes of length 7-11 cm with diameters 3.5 mm, 4.0 mm, 4.5 mm, 5.0 mm, 5.5 mm, 6.0 mm, 6.5 mm, 7.0 mm and 7.5 mm were connected to the breathing circuit and tested. Respiratory flow rates and volumes were measured using a NICO and collected using proprietary software developed by Convergent Engineering. Pressure was measured at the lung inlet, simulating intrapleural pressure and collected using the same software.

First, the 3.5 mm diameter ET tube was inserted into the breathing circuit. The ventilator was set to achieve a peak inspiratory flow rate of 40 L/min to a volume of 1.5 L. The test lung exhales passively with a force determined by a user set compliance level

and is unable to simulate forced exhalation. The compliance was set to .10 L/cmH₂O to simulate a healthy volunteer. This compliance was not enough to force the exhalation through the resistor at 40 L/min. To maintain normal compliance while simulating forced exhalation a brass weight was placed on the lung platform during exhalation only. The weight was placed in a position appropriate to force the exhalation at a flow rate of 40 L/min. Once the ventilator settings were appropriate and the position of the weight was determined the experiment began. Ten mechanical breaths were recorded at a volume of 1.5 L through the 3.5 mm diameter ET tube at peak inspiratory and expiratory flow rates of 40 L/min. Peak minimum pressure during inspiration was approximately -50 cmH₂O and peak positive pressure on expiration was approximately 40 cmH₂O.

This experiment was repeated with each ET tube between 3.5 mm and 7.5 mm. The ventilator settings and position of the brass weight were modified to maintain the 40 L/min flow rate and 1.5 L volume per breath. Through the 5.0 mm ET tube, the brass weight was no longer necessary to achieve the expiratory flow rate of 40 L/min, indicating that the normal elastic recoil of the simulated healthy lung was sufficient. As the tube diameter exceeded 5.0 mm the expiratory flow rates began exceeding 40 L/min. It was not possible to simulate a deliberate decrease in expiratory force and the machine was simply allowed to recoil passively. Flow rates up to 80 L/min were recorded through the largest ET tubes but the affect on positive pressure was negligible.

The average simulated intrapleural pressure change per breath, created by the nine ET tubes are shown (Figure 3-1). Ten breaths were recorded for each level of resistance. Y-Error bars in the graph represent \pm standard error of measure (SEM) and are barely visible due to the consistency of the ventilator and lack of variability between breaths.

Next, informed consent was obtained on two healthy volunteers for an institutional review board approved study. Subject one was a 47 year-old male in good health. Subject two was a 38 year-old male in good health. Each subject swallowed an esophageal balloon; used to measure esophageal pressure, an estimate of intrathoracic pressure. Placement of the balloon in the esophagus was verified using occlusion tests. Subjects were coached to breathe at inspiratory and expiratory flow rates of 40 L/min at a volume of 1.5 L through the same ET tubes discussed previously. Once proficient, ten breaths were recorded through the 3.5mm ET tube at flow rates of 40 L/min at a volume of 1.5 L. These data, along with the esophageal pressure, were collected. The study was repeated for each ET tube between 3.5 mm and 7.5 mm.

The average esophageal pressure changes per breath created by the nine levels of resistance is shown (Figure 3-2). Ten breaths were collected for each resistance level. Y-Error bars represent \pm SEM. The intrathoracic pressure changes per breath for each of the nine ET tubes—both simulated using the ventilator and test lung apparatus, and measured from the two volunteers—are shown (Figure 3-3). Intrathoracic pressure is estimated as intrapleural pressure from the test lung and as esophageal pressure from the two volunteers.

Mathematically characterizing the resistance

The resistance created by a tube of known radius and length can be calculated using Poiseuille's Law, $R = 8\eta L/\pi r^4$ (Equation 3-1). Where η is the viscosity of the fluid moving through the tube, L is the length of the tube and r is the inner radius of the tube. Based on this formula, the estimated pressure drop across each ET tube was estimated (Table 3-1). Poiseuille's Law assumes laminar flow. Since the calculated pressure drop is significantly different from the measured pressure drop (Figure 3-3) it was necessary to

determine if the flow was laminar. For this, the Reynold's number calculation, based on $R = \rho v d / \eta$ (Equation 3-2) was used. Where R is Reynold's number (unitless), ρ is the fluid density, v is the fluid velocity, d is the tube diameter and η is the fluid viscosity. This calculation resulted in a Reynold's number of 17429. If Reynold's number is > 2000 flow is considered turbulent and Poiseuille's law does not apply.

Guttmann et al. (2000) experimentally determined the flow-pressure relationship through various ET tubes. They derived $P = K_1 F + K_2 F^2$ (Equation 3-3) where P equals the pressure drop across the tube, K_1 and K_2 are experimentally derived constants, and F is flow. The expected pressure changes caused by inspiring and expiring through various ET tubes in cmH₂O at a flow rate of 40 L/min are shown (Table 3-2). These values were consistent with previous results.

Resistance created by ET tubes of varying diameters has been characterized and the intrathoracic pressure changes they cause have been estimated using a ventilator and validated using a healthy volunteer. The agreement with Equation 3-3 validates the pressure change results. Equation 3-3 will be used to estimate intrathoracic pressure changes in subsequent analyses.

Clinical Goal 2

Clinical goal 2 is to use the PPG to detect fluid loss. The current gold standard for monitoring volume status in critically ill patients is measuring pulmonary artery occlusion pressure, or in its absence, central venous pressure through an invasive catheter. Nonspecific measures include heart rate, blood pressure and urine production. To explore the feasibility of using the PPG to detect changes in fluid volume, two patient populations who lose a measurable amount of fluid were explored. Blood donors lose a measurable amount of whole blood while hemodialysis (HD) subjects lose a measurable

amount of ultrafiltrate, while retaining red blood cells. Studying blood donors and HD patients may provide an important first step in determining the feasibility of the PPG for estimating fluid loss.

Rationale

Many studies have explored the value of the difference between systolic pressure at end-expiration and the lowest value during the respiratory cycle (dDown) as an indicator of hypovolemia. This requires an invasive catheter to continuously monitor arterial blood pressure. Very few studies, however, have investigated the use of the PPG as an indicator of volume status even though it is noninvasive and used routinely.

Partridge (1987) sought to prove a relationship between changes in the PPG and the dDown of arterial pressure. Monitoring the plethysmographic waveform of the pulse oximeter should indicate instantaneous blood volume changes in the tissue between the light emitter and sensor. Twelve patients were studied and a relationship was found between the PPG and systolic blood pressure variations (SPV). It was concluded that the PPG could be used to detect hypovolemia based on the established relationship between SPV and volume status. While this study is a good foundation, several limitations were present. First, only a finger pulse oximeter probe was used. Second, data was not collected continuously. Instead, once per hour, three seconds of data was sampled and printed. Pulse waveform variation was defined as the maximum variation in the waveform peaks during positive pressure ventilation as measured on the printout. The printouts reflected a PPG after processing by the Nelcor unit.

Shamir et al. (1999) removed then reinfused 10% blood volume in 12 patients while monitoring the PPG. It was concluded that the PPG is a good indicator of mild hypovolemia. The first major limitation of this study was the use of a finger probe only.

Secondly, a paper printout of a processed waveform was used and was only obtained for five consecutive mechanical breaths, one time following blood removal. While these studies were able to show a relationship between the PPG and volume status, the state of technology greatly limited their ability to collect data and monitor alternate sites.

Blood Donors

Blood donors must be healthy, at least 17 years old, weigh at least 110 pounds and not have donated blood in the past 56 days. “Healthy” means feeling well and able to perform daily activities. If chronic conditions such as diabetes or hypertension exist, healthy also means that these conditions are being treated and are under control.

According to the American Red Cross, each of the following will disqualify donors for varying lengths of time: acupuncture treatment where the sterility of the needles can not be verified, body temperatures greater than 99°, autoimmune diseases, certain cancers such as leukemia and lymphoma, clotting disorders, Creutzfeldt-Jakob disease, hemochromatosis, hemoglobin below 12.5 g/dL, hematocrit below 38%, hepatitis caused by a virus, HIV/AIDS, active infections, malaria or recent travel to an area prevalent in malaria, pregnancy, syphilis, gonorrhea, sickle cell disease, and recent tattoos. In general, medications do not disqualify donors.

Before donation, blood pressure, pulse rate and temperature are taken. During the donation approximately 500 ccs of blood is removed over a 10 min period. Most people experience no effects though some get an upset stomach, feel faint or dizzy and can have a local hematoma at the puncture site. It is rare for a person to faint, suffer nerve damage or have muscle spasms.

During volunteer blood donation a fixed amount of blood is lost in a measurable amount of time. This represents an ideal opportunity to study the effects of blood loss.

Total pre-donation blood volume can be estimated using Allen's formula (Allen et al. 1956), $BV_{\text{men}} = 0.417 * H^3 + 0.0450 * W - 0.030$ (Equation 3-4) and $BV_{\text{women}} = 0.414 * H^3 + 0.0328 * W - .030$ (Equation 3-5). Where H is the height in meters and W is the weight in kilograms.

Renal Hemodialysis

End stage renal disease (ESRD) can only be treated with renal transplant or renal HD. Hemodialysis is an important life sustaining treatment for ESRD. A patient on HD will spend approximately 4 h undergoing treatment, three days per week.

Before treatment, the accumulated volume load is mainly located in the interstitial space and must be removed. Plasma water removal by ultrafiltration (UF) increases oncotic pressure in the blood and decreases hydrostatic pressure in the venous system. This enhances the vessel refilling from the interstitial space. The refilling rate depends on several factors (Basile 2001) including individual state of hydration, vessel permeability, and protein balance. Refilling usually proceeds slower than UF and only partially compensates for fluid loss. As a result, intravascular water content progressively decreases (Donauer and Bohler 2003). In addition to the refilling of vessels, several other factors contribute to intradialytic intravascular volume changes including autonomic function (Kersh et al. 1974, Lilley et al. 1976, Daul et al. 1987, Converse et al. 1992, Esforzado et al. 1997, Stojceva-Taneva et al. 1991), impaired venous compliance (Rouby et al. 1978, Kooman et al. 1992) and heat accumulation during the treatment (Maggiore et al. 1981, Jost et al. 1993, Van der Sande et al. 2001).

Since the main goal of HD therapy is to remove the excess fluid that has accumulated during the interdialytic period, intradialytic hypotension (IDH) remains one of the most common, and serious complications of HD (Daugirdas 2001). The initial

cause of IDH is intravascular hypovolemia (Leunissen et al. 2000). Considering the number of elderly, cardiovascular-compromised patients on HD is increasing, it is likely that IDH will remain a serious concern. The etiology and management of IDH has become an increasingly complex issue (Sherman 2002). Patients vary markedly in their hemodynamic tolerance to fluid removal indicating that IDH has many underlying causes. If patients fail to support blood pressure with adequate vasoconstriction and increased heart rate as a response to hypovolemia they will experience IDH.

The venous system maintains cardiac output and blood pressure during HD since most of the blood volume is contained in the venous system. With hypovolemia, arteriolar resistance increases, which increases systemic blood pressure; not only by increasing total peripheral resistance, but also by decreasing pressure in the highly compliant venous bed. This decrease in pressure favors passive venous recoil, resulting in translocation of blood to the central vessels and maintains cardiac filling. The effectiveness of this mechanism may vary greatly in HD patients (Sherman 2002). In addition, venous constriction promotes cardiac return and increases blood pressure.

The first prerequisite of a hemodynamically stable HD treatment is the correct definition of dry weight. Dry weight is the body weight during normal urine production. During HD the weight should be brought down to the correct dry weight. If a large amount of fluid is withdrawn after the patient has reached the dry weight, no physiologic mechanism or technical device will prevent hypotension (Donauer and Bohler 2003). Unfortunately, dry weight estimation is one of the most difficult tasks in the management of HD patients and results in frequent reevaluations throughout the year. Even with correct dry weight assumptions, IDH continues to occur.

To reduce the incidence of IDH, relative blood volume (RBV) measurements have been developed. These measurements are based on the optical reflection method (Leunissen et al. 2000) and monitor changes in hematocrit or total protein content in whole blood via ultrasonically measured blood velocity (Koomans et al. 1984). The rationale is that the red cell mass (or protein content) should remain constant while ultrafiltration removes fluid from the intravascular space, making the change in blood volume inversely proportional to the change in hematocrit (or plasma proteins). This technique was shown to correlate well with those determined by albumin concentration (Leypoldt et al. 1995). Data supports the use of blood volume monitoring in chronic HD patients as a tool both in preventing IHD and in identifying patients with volume overload (Mitra et al. 2002, Tonelli et al. 2002, Krepel et al. 2000) showed that changes in the RBV showed considerable intra and inter-individual variability that could not be explained by differences in UF volume. They concluded that the RBV is not necessarily a good indicator of IDH.

Other tools are available for the assessment of volume status including biochemical markers, inferior vena cava diameter and bioimpedance (Ishibe and Peixoto 2004). Even if a perfect measure of RBV did exist, studies have shown that measurements of stroke volume, cardiac output and total peripheral resistance are also very important indicators of IDH. Wallin et al. (2003) showed that immediately after HD, central blood volume was reduced in parallel with reductions in plasma volume, stroke volume, cardiac output, systolic blood pressure and serum atrial natriuretic peptide (ANP). Two hours after HD, central blood volume had recovered while plasma volume, stroke volume, systolic blood pressure and serum ANP remained low. Boon et al. (2004)

determined that during HD, patients responding to a blood volume reduction with a blood pressure decrease differ in their stroke volumes from patients with a stable blood pressure. Hence, changes in blood volume alone do not predict blood pressure response to HD.

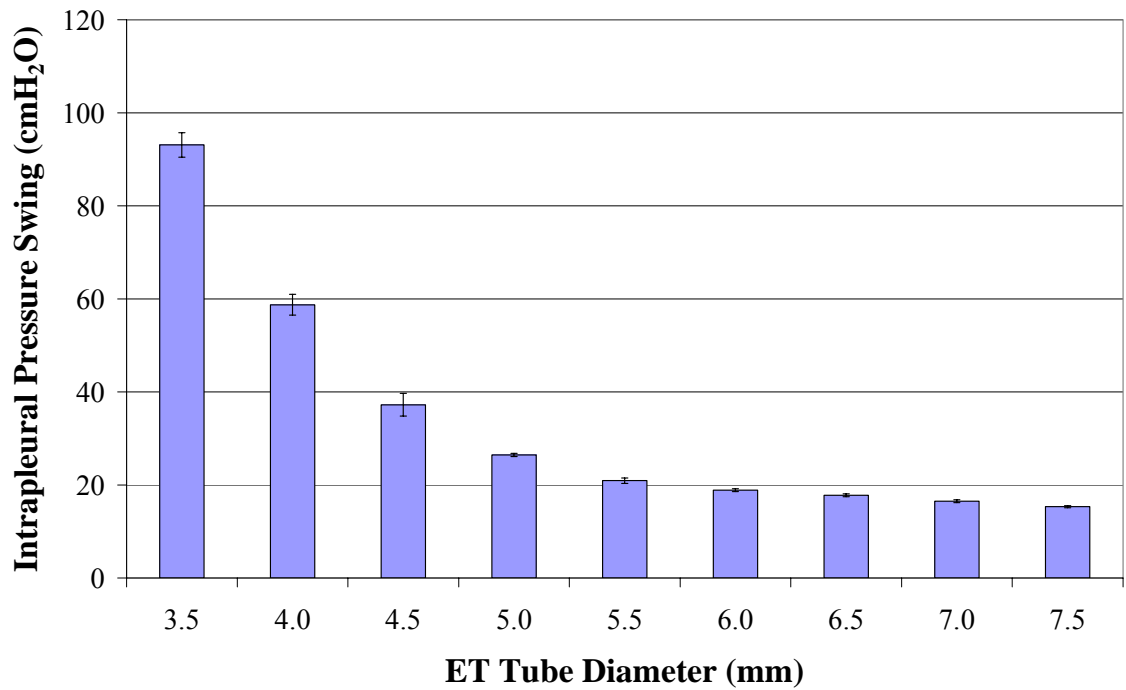
In summary, the most optimum system would be to develop an algorithm on the basis of all of the above mentioned factors that could be manipulated to regulate the target blood volume in concert with the vascular reactivity target to control blood pressure. Such an integrated system is the technical answer to the problem of IDH in the cardiac compromised patients (Leunissen 2000). While a broad clinical goal is to use the PPG for volume loss estimation in critically ill subjects, HD subjects may also benefit from a device able to detect IDH. The PPG was shown to correlate with blood volume status, can be used to determine vascular wall mechanics and is related to stroke volume yet no research has been done to correlate PPG with fluid loss in renal HD patients.

Table 3-1. Estimated pressure drop across the ET tubes based on Poiseuille's Law.

mm	length (m)	Resistance (kg/m ⁴ s)	Pressure Drop (Pa)	Pressure Drop (cmH ₂ O)
3.5	0.102	496540	333	3.39
4.0	0.102	291063	195	1.98
4.5	0.111	198744	133	1.35
5.0	0.073	85689	57	0.58
5.5	0.076	61071	41	0.41
6.0	0.073	41324	28	0.28
6.5	0.076	31307	21	0.21
7.0	0.076	23275	16	0.15
7.5	0.083	19134	13	0.13

Table 3-2. Calculated, simulated, and measured intrathoracic pressure changes

mm	Simulated				Measured			
	Equation 3-3		Ventilator		Subject 1		Subject 2	
	Insp	Exp	Insp	Exp	Insp	Exp	Insp	Exp
3.5	42.13	46.26	-48.98	44.11	-54.53	39.86	-58.28	45.67
4.0	26.94	28.45	-27.80	30.93	-37.35	18.95	-39.28	23.08
4.5	16.68	17.17	-17.78	19.44	-26.78	16.80	-28.56	13.47
5.0	13.35	12.32	-11.39	15.06	-18.64	4.36	-18.81	5.31
5.5	8.14	9.25	-6.64	14.28	-15.75	1.39	-13.09	2.62
6.0	5.89	6.49	-5.28	13.58	-11.97	3.03	-10.89	1.05
6.5	4.49	4.69	-4.44	13.33	-10.92	2.81	-8.78	1.08
7.0	na	na	-3.92	12.58	-10.05	2.33	-8.14	0.75
7.5	na	na	-3.61	11.72	-10.14	1.39	-8.53	-0.78

Figure 3-1. Average simulated intrapleural pressure changes per breath. Y-error bars represent \pm SEM.

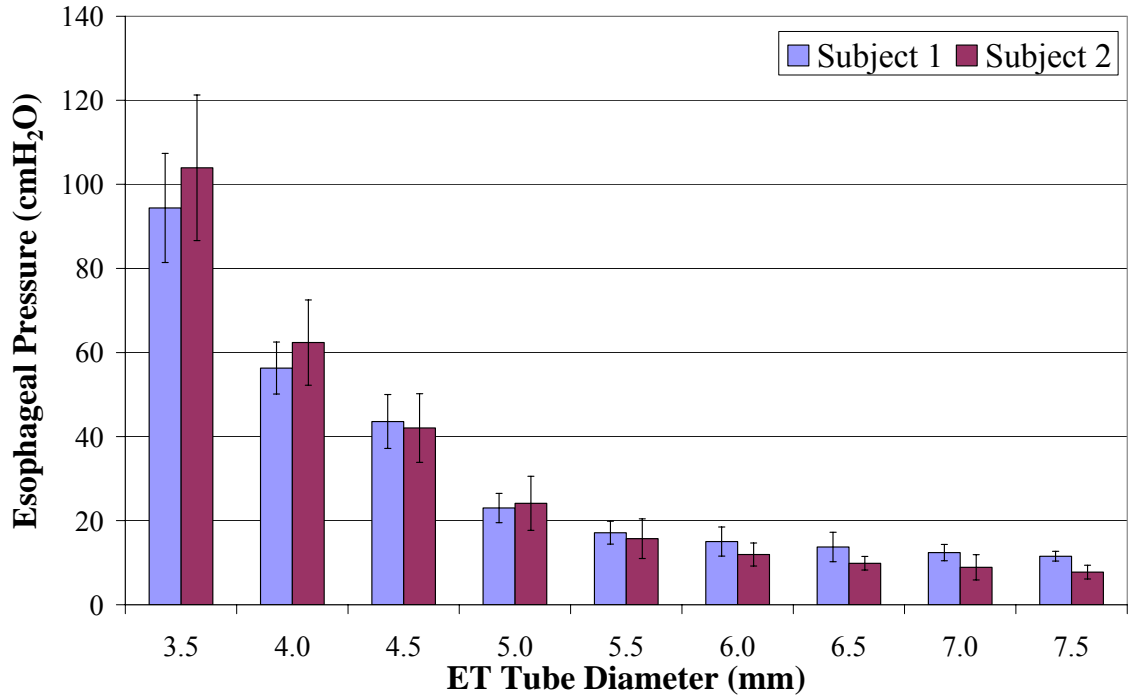


Figure 3-2. Measured esophageal pressure changes per breath in healthy volunteers. Y-error bars represent \pm SEM.

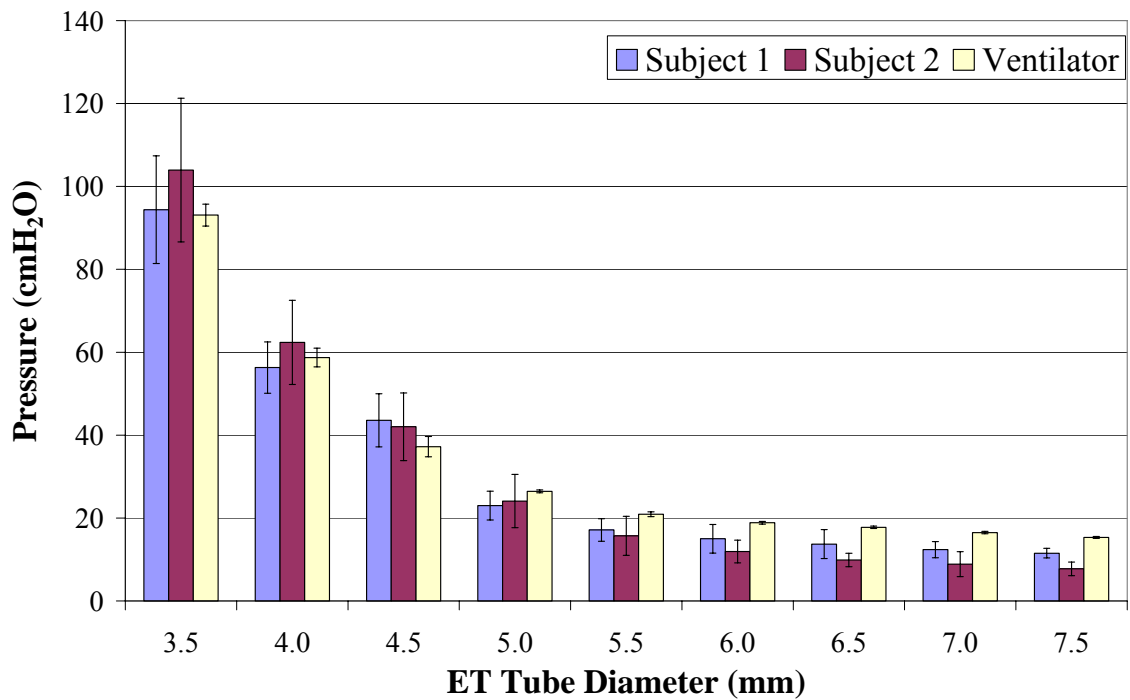


Figure 3-3. Intrathoracic pressure changes per breath, simulated and measured. Y-error bars represent \pm SEM.

CHAPTER 4 EXPERIMENTAL DESIGN AND METHODS

Methods

The low frequency component (LFC) is an indicator of venous blood volume and varies with respiration. The LFC is impacted by a loss in blood volume hence the variable “LFC Swings”, defined below, is an outcome variable. Additionally, stroke volume is affected by a loss of blood volume and the pulsatile cardiac component (PCC) is an indicator of stroke volume (Murray and Foster 1996), hence the “PCC MagDiff” and “PCC MagMean”, as described below, are the second and third outcome variables.

All variables were measured on a breath-by-breath basis. Each breath was defined by the respiratory flow data, as defined below. Multiple breaths through the same level of resistance reflect repeated measures, and were averaged for comparison purposes.

The first broad clinical goal is to use the photoplethysmograph (PPG) to noninvasively detect changes in airway resistance. To demonstrate this, three levels of resistance were chosen. It was previously described (Chapter 3) that volunteers could breathe to a volume of 1.5 L at a flow rate of 40 L/sec through endotracheal (ET) tubes as small as 3.5 mm in diameter. The mean intrathoracic pressure changes per breath—as estimated by esophageal pressure—created by different ET tubes, were presented (Table 3-2).

The 3.5 mm, 4.0 mm and 5.5 mm ET tubes were selected based upon their affect on intrathoracic pressure. When subjects breathed at a flow rate of 40 L/min to 1.5 L

through these three ET tubes, the intrathoracic pressure changes per breath were approximately 100 cmH₂O, 60 cmH₂O and 20 cmH₂O, respectively. From this point on, the 3.5 mm ET tube is referred to as “high resistance”, the 4.0 mm ET tube is referred to as “medium resistance” and the 5.5 mm ET tube is referred to as “low resistance”.

The second clinical goal is to use the PPG to noninvasively detect fluid loss. As previously described (Chapter 3), it was determined that blood donors and hemodialysis (HD) patients represent ideal patient populations to test this clinical goal.

Blood Donors

Twenty blood donors were recruited on the day of donation and informed consents obtained. Inclusion and exclusion criteria were identical to that for blood donation. Before donation, subjects reported height, weight, age and sex. Seated blood pressure was measured.

Two pulse oximeter probes were placed on the subject before donation. One was placed on the opposite finger of the donation arm and one placed on the nasal alar. These probes were connected to Novamatrix Oxypleth 520A pulse oximeters and data was collected continuously and ported through the pulse oximetry data acquisition viewer (PODAV) software to a laptop computer. Subjects were provided a mouthpiece for breathing, connected to a CO₂SMO (Novamatrix). The CO₂SMO measures air flow and volume during respirations. These measurements were made by flow sensors creating a pressure drop, which is transmitted to a differential pressure transducer calibrated to relate this pressure drop to flow.

Before donation, subjects performed the breathing study outlined below. The parameters of the breathing study were selected based upon the results of the pilot data previously described (Chapter 3). The high, medium and low resistance ET tubes were

used to create resistance. The order that the subjects breathed through the resistors was randomized. Subjects breathed at peak inspiratory and expiratory flow rates of 40 L/min to a volume of 1.5 L per breath. The pulse oximetry data acquisition viewer (PODAV) software includes a real-time graph of both volume and flow and was used as feedback to train the subjects to breathe consistently. The breathing study was performed in the following phases:

- **Phase 1:** Breathing through ET tube 1 for approximately 10 breaths.
- **Phase 2:** Baseline breathing with no resistance for approximately 30 sec.
- **Phase 3:** Breathing through ET tube 2 for approximately 10 breaths.
- **Phase 4:** Baseline breathing with no resistance for approximately 30 sec.
- **Phase 5:** Breathing through ET tube 3 for approximately 10 breaths.

During the breathing study, the saturation, pulse rate, and PPG were recorded continuously from the two pulse oximeter probes. The respiratory flow rates and volumes were recorded using the CO₂SMO. The subjects were coached to breathe at 40 L/min to a volume of 1.5 L.

Upon completion of the breathing study, the mouthpiece was removed and the blood donation began. The two pulse oximeter probes were left in place during donation, and pulse rate, saturation and PPG were monitored. The respiratory flows and volumes were not collected during blood donation as this required the mouthpiece, and was not practical during blood donation. When the donation was complete, the breathing study was repeated. The order was again randomized. When the second breathing study was completed, the pulse oximeter probes were removed and data collection ceased. Seated

blood pressure was once again measured. Orthostatic blood pressure was also measured in several subjects. Subjects were paid for participation in the study.

Hemodialysis Patients

Twenty subjects undergoing renal HD were recruited and informed consents obtained. There were no specific inclusion or exclusion criteria, other than the HD physician recommending subjects based upon their state of health and physical ability. Before HD, subjects reported height, weight, age, and sex. Seated blood pressure was measured. The past medical history was obtained for each subject.

Two pulse oximeter probes were placed on the subject before HD. One was placed on a finger and the other was placed on the nasal alar. These probes were connected to Novamatrix Oxypleth 520A pulse oximeters and data was collected continuously and ported through PODAV to a laptop computer. Collected data included oxygen saturation, pulse rate, PPG, and respiratory flow and volume. Patients were provided a mouthpiece for breathing, connected to a CO₂SMO.

Before HD, subjects performed the breathing study outlined below. The parameters of the breathing study were selected based upon the results of the pilot data previously described (Chapter 3). The high, medium and low resistance ET tubes were used to create resistance. The order that the subjects breathed through the resistors was randomized. Subjects breathed at peak inspiratory and expiratory flow rates of 40 L/min to a volume of 1.5 L per breath. The study was performed in the following phases:

- **Phase 1:** Breathing through ET tube 1 for at least 10 breaths.
- **Phase 2:** Baseline breathing with no resistance for approximately 30 sec.
- **Phase 3:** Breathing through ET tube 2 for at least 10 breaths.

- **Phase 4:** Baseline breathing with no resistance for approximately 30 sec.
- **Phase 5:** Breathing through ET tube 3 for at least 10 breaths.

Upon completion of the breathing study, the mouthpiece was removed. The two pulse oximeter probes were left in place during HD, and pulse rate, saturation and PPG were continuously monitored. The respiratory flows and volumes were not collected during HD as this required the mouthpiece and was not practical during HD.

Upon completion of HD, the breathing study was repeated. The order of the resistance levels was randomized. Total volume of ultrafiltrate removed was recorded. Blood pressure was measured at the conclusion of HD and orthostatic blood pressure was measured in several of the patients. The pulse oximeter probes were then removed and the study was completed. Subjects were paid for participation in the study.

The HD subjects performed two breathing studies, the first representing before HD and the second representing after HD. In some cases the first breathing study occurred just after the start of HD and in some cases the after HD breathing study occurred just before the end of HD. Additionally, HD time varies between subjects as there were under 3 h between the breathing studies in some subjects and over 4 h in other subjects.

Photoplethysmograph Processing and Novel Variables

Signal Processing Algorithm

The unprocessed PPG for the duration of each breathing study was isolated for each patient. The beginning and end of each breathing study was determined by the flow data measured by the CO₂SMO. For each breathing study, each level of resistance was separated from the unprocessed data. For each blood donor and HD patient, there were six unprocessed data sets—three resistance levels for each of two breathing studies.

A spectral analysis was then applied to each individual data set to identify the frequencies present (Figure 4-1). The original data was sampled at 100 hz, providing two frequency peaks. The first peak occurred at approximately .2 Hz, or 12 beats per minute. This corresponds to the respiratory rate. The second peak, located at approximately 1.5 Hz, or 90 beats per minute, corresponds to the heart rate.

The spectral analysis is estimated using Welch's averaged periodogram method. Welch's method splits a data set into smaller data sets and calculates the modified periodogram of each set. The modified periodogram is calculated by applying a window function to the time-domain data, computing the discrete Fourier transform, and then computing the magnitude square of the result. The frequency domain coefficients arising from calculating the modified periodograms are averaged over the frequency components of each data set to reduce the variance. Due to the windowing, the Welch method provides a smoothed periodogram estimate (Welch 1967).

To separate the two frequencies, a cutoff frequency was selected based on the spectral analysis of the data set. A standard Butterworth filter was then applied to the unprocessed data using a cutoff frequency of .8 Hz and a filter kernel (M) of 5. The filter kernel represents roll off and is inversely proportional to the width of the transition band. A larger M results in a more accurate signal separation and is necessary when the frequencies are very close together in the spectrum. A large M also requires a longer compute time. The Butterworth filter was used as both a high-pass and low-pass filter.

Low-pass and high-pass filters are presented (Figures 4-2 and 4-3). The stopband frequencies are blocked while the passband frequencies pass. An ideal filter has a

perfectly vertical transition zone (very large M). The width of the transition zone and magnitude of M are dictated by the frequencies of interest.

The signal separation is shown (Figures 4-4 to 4-6). The two frequencies in the unprocessed PPG signal are apparent (Figure 4-4). The low-pass filter removed all frequencies greater than the cutoff frequency resulting in the LFC (Figure 4-5). The high-pass filter removed all frequencies lower than the cutoff frequency resulting in the PCC (Figure 4-6). While the cutoff frequency for each data set for each patient may have differed slightly, an M of 5 was used for all subjects.

Separating Breath Data

Once the LFC and PCC for each level of resistance for each of the two breathing studies were separated, each individual breath was defined. The breaths were defined using the flow data (Figure 4-7). The upward slope corresponds to inspiration—with the peak representing peak inspiratory flow—while the downward slope represents exhalation—with the trough representing peak expiratory flow. The breaths were defined as the period of time from the peak of the inspiratory flow to the following peak.

The respiratory flow data, with peaks identified, was plotted with the LCF (Figure 4-8). The flow curve immediately before the third indicated peak briefly goes flat. The CO₂SMO automatically purges the pressure sensor line every 2, 5, or 10 min depending on system conditions. The timing of the second breath was affected. This had a very minor affect on the calculations presented below.

The first outcome variable is the LFC Swing. It is defined as the maximum LFC value minus the minimum LFC value during the duration of one breath. Breath one corresponds to the maximum LFC value minus the minimum LFC value between respiratory flow peaks one and two. This analysis was performed for all breaths, for each

level of resistance, for both breathing studies, for the alar, and finger PPG, for each of the subjects.

The second and third outcome variables were based on the PCC of the PPG. They are the “PCC MagDiff” and “PCC MagMean.” The PCC for each individual breath was plotted (Figure 4-9). Approximately eight heartbeats occurred during the duration of this breath. The PCC for one of these breaths was plotted (4-10). First, the amplitude of each heartbeat was calculated. The amplitude of heartbeat one corresponds to the value at peak one minus the value at trough one. Heartbeat two is the value at peak two minus the value at trough two. This was repeated for each heartbeat during each breath. Once the PCC amplitude for each heartbeat was calculated, the outcome variables were computed. The PCC MagDiff is the difference between the largest amplitude minus the smallest amplitude for the each breath. This represents the stroke volume fluctuation during the respiratory cycle. The PCC MagDiff was computed for each breath, for only the low level of resistance, for each breathing study, for the alar and finger, for each subject. The PCC MagMean is the average of all heartbeat amplitudes in a breath adjusted for heart rate. The adjustment is the number of heartbeats (represented by the number of peaks) divided by the duration of time for that breath. This factor is then multiplied to the mean of the amplitudes. The PCC MagMean represents the average cardiac output (CO) per breath. This variable is calculated for each breath, for only the low level of resistance, for each breathing study, for the alar and finger, for each subject.

As the airway resistance increased, large intrathoracic pressure changes were needed to drive flow through the small ET tube. The large intrathoracic pressure changes created very large baseline low frequency swings in the PPG—the basis for the LFC

measurement described above. These large baseline changes can be several orders of magnitude larger than the PCC and distort the PCC frequency (Figure 4-11). For this reason, the PCC variables were only computed for the low level of resistance.

In summary, there were three outcome variables measured from the PPG. The LFC Swing was measured for each breath, for each of the three levels of resistance. The LFC Swing represents the shifting of venous blood with respiration. The second outcome variable was the PCC MagDiff, which represents stroke volume variability per respiration. It was measured for each breath, but only for the low level of resistance. The final outcome variable is the PCC MagMean, which represents the average CO per respiratory cycle. It was measured for each breath, but also only for the low level of resistance.

Hypotheses

Hypotheses – Clinical Goal 1

- **Hypothesis 1:** The LFC Swings for the high level of resistance will be greater than the LFC Swings for the medium and low levels of resistance, and the LFC Swings for the medium will be greater than the low level of resistance, independent of fluid state, and PPG monitoring site.
- **Hypothesis 2:** The LFC Swings will correlate with intrathoracic pressure change per breath as estimated by Equation 3-3 (Guttmann 2000), independent of fluid state, and PPG monitoring site.

Hypotheses – Clinical Goal 2

- **Hypothesis 3:** The LFC Swings for breathing study one (before fluid loss) will be less than the LFC swings for breathing study two (after fluid loss), for each level of resistance, independent of monitoring site.
- **Hypothesis 4:** The PCC MagDiff for breathing study one (before fluid loss) will be greater than the PCC MagDiff for breathing study two (after fluid loss), independent of monitoring site.

- **Hypothesis 5:** The PCC MagMean for breathing study one (before fluid loss) will be greater than the PCC MagMean for breathing study two (after fluid loss), independent of monitoring site.

Justification

Justification for Hypotheses 1 and 2

An unprocessed PPG contains two main frequencies, and both are affected by absorption of the light by blood and other tissues. The LFC represents the baseline amount of light hitting the photodiode (PD). This value is affected by the path traveled by the light. Skin, bone, cartilage, adipose, and blood absorb light and it is this relatively constant path that results in a baseline amount of light hitting the PD. This baseline amount fluctuates at a frequency that corresponds to changes in venous blood caused by ventilation—both mechanical and spontaneous. Since the biological tissues in the path of the light are constant, with the exception of venous and arterial blood, the changes in the LFC component correspond to changes in the venous blood volume in the path of the light.

During spontaneous breathing, subatmospheric pressure draws air and blood into the lungs: blood is drawn from the vena cava into the right heart and then into the expanding pulmonary vascular bed. Simultaneously, left ventricular output briefly decreases for one or two heartbeats as blood accumulates in the pulmonary circuit. Thereafter, expiratory pressure improves flow to the left heart, increasing stroke volume, peripheral pulse flow, pulse amplitude and peripheral venous pressure (Murray and Foster 1996). These changes are predicated upon intrathoracic pressure changes, and are magnified when intrathoracic pressure changes increase, as with added respiratory resistance.

Nilsson et al. (2003) looked at the physiologic basis for the changes in the LFC, which they termed respiratory induced intensity variations (RIIV). They hypothesized that the filling of peripheral veins is a major mechanism behind the RIIV signal. In the study, 16 adult volunteers had a cannula inserted for the measurement of peripheral venous pressure (PVP). The PVP and RIIV amplitudes changed significantly with tidal volume and respiratory rate, and with thoraco-abdominal separation. These signals were significantly greater in predominantly thoracic respiration than in natural respiration. They concluded that a correlation exists in the amplitudes of the respiratory induced intensity variations in the PPG and the respiratory variations in peripheral venous pressure.

Frey and Butt (1998) concluded that pulse oximetry is a rapid, noninvasive method for the objective estimation of the degree of pulsus paradoxus. Pulsus paradoxus is increased in asthma, upper airway obstruction, cardiac tamponade, myocardial decompensation and hypovolemia (Miro and Pinsky 1992, Heitmiller and Wetzel 1996, Pfenninger 1985, Morgan et al. 1969). They defined the respiratory dependent changes of the PPG as the difference between the highest value of the upper peak of the wave and the lowest value in the upper peak of the wave.

It is well documented that the LFC of the PPG corresponds to respiratory rate and is caused by fluctuations in intrathoracic pressure. It should follow that as respiratory resistance increases, the change in the LFC per breath (LFC Swing) should also increase. These changes should correlate with intrathoracic pressure changes.

Justification Hypotheses 3, 4, and 5

It was documented that the extent of the fluctuations of the LFC caused by positive pressure ventilation depends on central blood volume (Murray and Foster 1996). It has

also been discovered that early hypovolemia may be reflected in an exaggerated respiratory wave before other more classic signs of decreased urine output, tachycardia or hypotension.

Several researchers have attempted to relate fluid loss to changes in the PPG. Perel et al. (1987) aimed to quantify the systolic pressure variation (SPV) during graded hemorrhage in ventilated dogs, and to compare its reliability relative to other hemodynamic factors. They concluded that the difference between systolic pressure at end-expiration and the lowest value during the respiratory cycle (dDown) correlated to the degree of hemorrhage, CO, and the pulmonary capillary wedge pressure. Rooke et al. (1995) also concluded that SPV and the dDown appear to follow shifts in intravascular volume in relatively healthy, mechanically ventilated humans under isoflourane anesthesia. Partridge (1987) found a significant correlation between the PPG and SPV. Shamir et al. (1999) found both the PPG waveform changes and the SPV from the arterial blood pressure tracing increased significantly after blood withdrawal. The changes in the PPG correlated with the changes in the SPV.

Based upon the results of these researchers, the PPG and more specifically, the LFC of the PPG, can potentially be used to monitor fluid loss. LFC amplitude changes with respiration have been reported and the physiology is understood (Murray and Foster 1996). Additionally, they have been shown to correlate with hypovolemia (Partridge 1987, Shamir et al. 1999). Therefore, it is expected that the LFC Swings will be exaggerated by hypovolemia.

The PCC corresponds to changes in arterial blood volume in the vascular bed with each heartbeat. The PCC was shown to correlate with stroke volume (SV) (Murray and

Foster 1996), which is affected by circulating volume status. A smaller volume of total blood should correspond to a smaller stroke volume and hence reduce the PCC MagMean.

Inspiratory impedance threshold devices (ITD) have been the subject of many experiments as they increase SV and venous return without causing hemodilution (Convertino et al. 2004). These devices have been shown to decrease intrathoracic pressure with each inspiration, which increases preload and venous return to the heart (Lurie et al. 2000a, Lurie et al. 2000b, Lurie et al. 2002a, Lurie et al. 2002b). This increases SV and CO and raises blood pressure. Inspiratory impedance threshold device training imposes no additional resistance during expiration, keeping the SV and CO elevated throughout the duration of treatment. It is suspected that increasing expiratory resistance, in addition to inspiratory resistance, will elevate intrathoracic pressure temporarily impeding venous return and lowering SV and CO. Thus, with added inspiratory and expiratory resistance, SV should show increased variability with each respiration. Since stroke volume and CO decrease with fluid loss it is suspected that this variability will be blunted. As a result, the PCC MagDiff, which represents the stroke volume variability per respiratory cycle, should decrease with fluid loss.

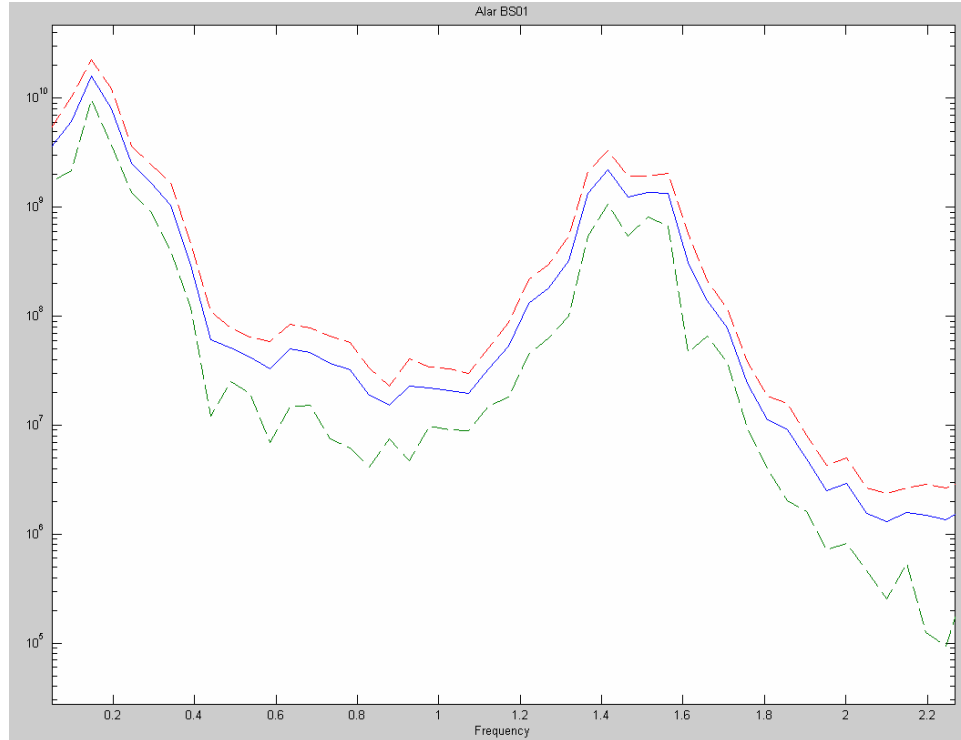


Figure 4-1. A spectral analysis, where the x-axis corresponds to the frequency in Hz and the y-axis corresponds to power and is a log scale.

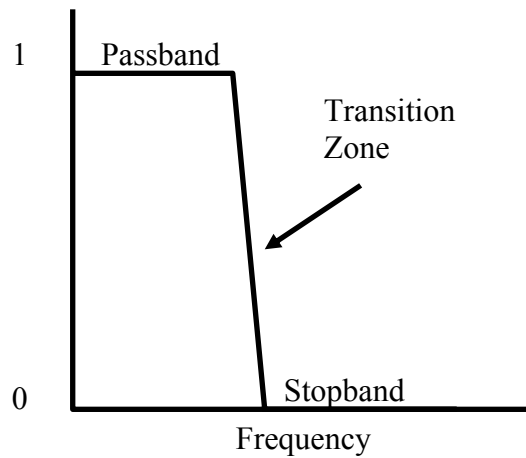


Figure 4-2. A low-pass filter. The width of the transition zone is determined by the magnitude of M .

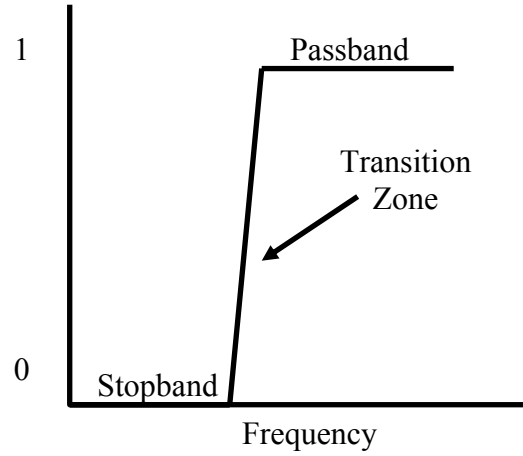


Figure 4-3. A high-pass filter. The width of the transition zone is determined by the magnitude of M .

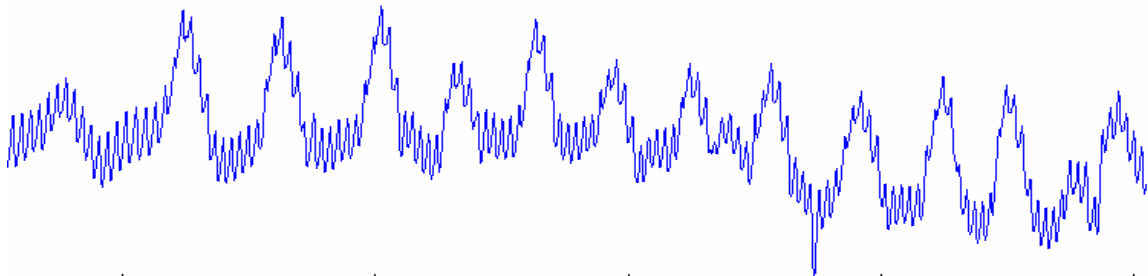


Figure 4-4. The unprocessed PPG recorded from the nasal alar of a blood donor subject.

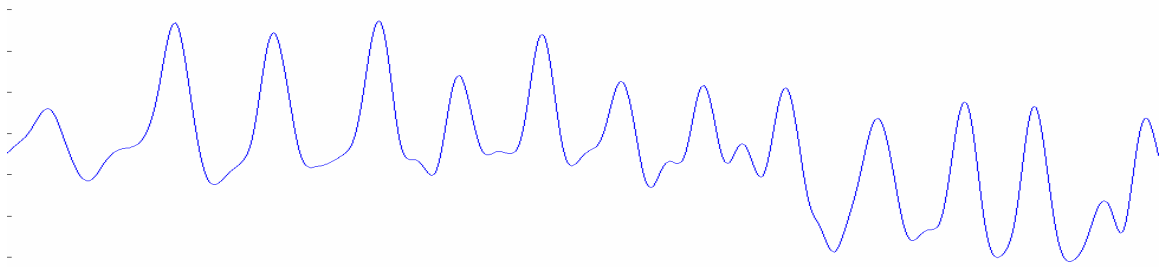


Figure 4-5. The LFC of the PPG recorded from the nasal alar of a blood donor subject.

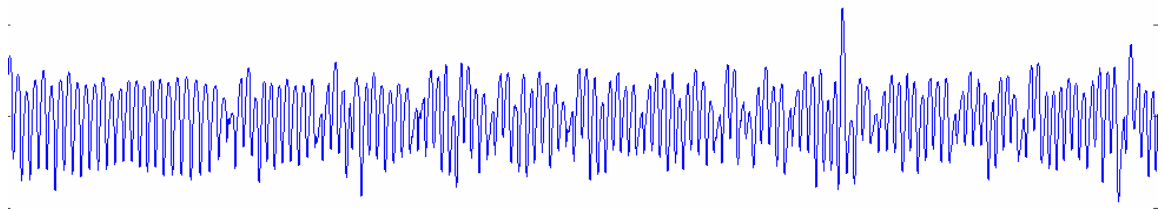


Figure 4-6. The PCC of the PPG recorded from the nasal alar of a blood donor subject.

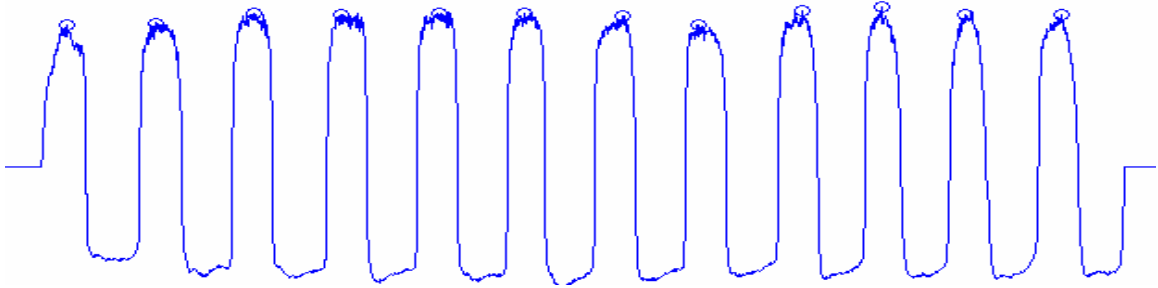


Figure 4-7. The respiratory flow data, where the x-axis represents time and the y-axis represents flow rate. The peak inspiratory flow rates for each breath are indicated (o).

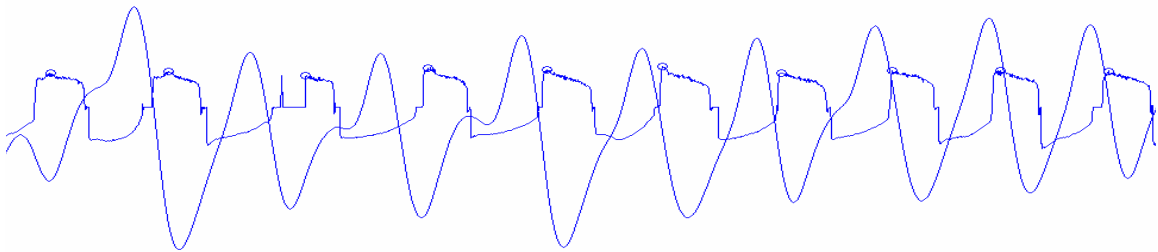


Figure 4-8. The LFC of the PPG with respiratory flow. The flow has identified peaks (o) and the LFC does not. The x-axis scale is time. The y-axis was adjusted to fit both plots and does not indicate that the amplitude of the flow is equal to the amplitude of the LFC.

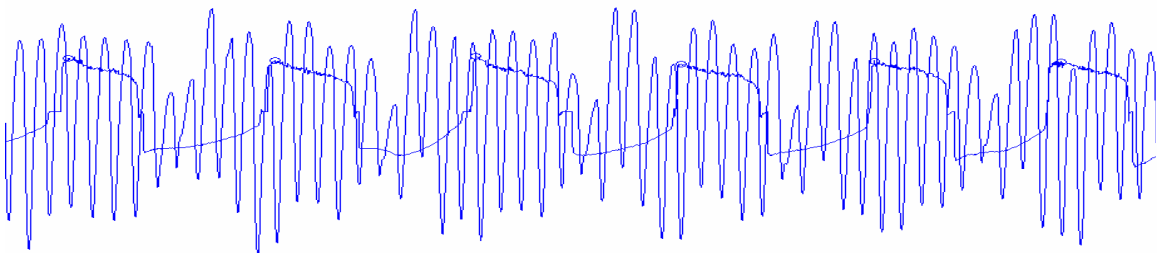


Figure 4-9. The PCC of the PPG plotted with respiratory flow. The high frequency tracing represents the PCC. Approximately six breaths are shown. The x-axis scale is time. The y-axis was adjusted to fit both tracings and is arbitrary.

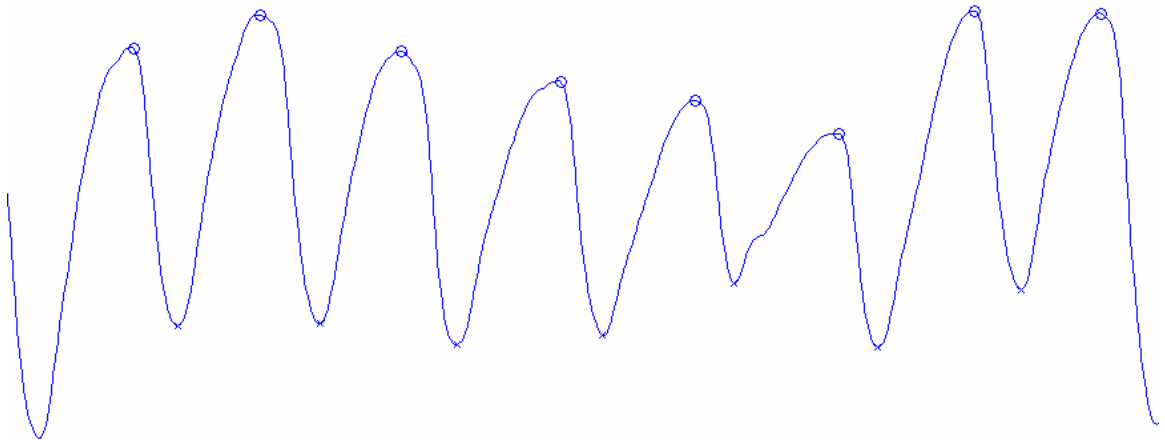


Figure 4-10. The PCC for the duration of one breath. The peaks (o) and troughs (x) are shown. The x-axis represents time and the y-axis represents the amplitude of the PCC in light units.

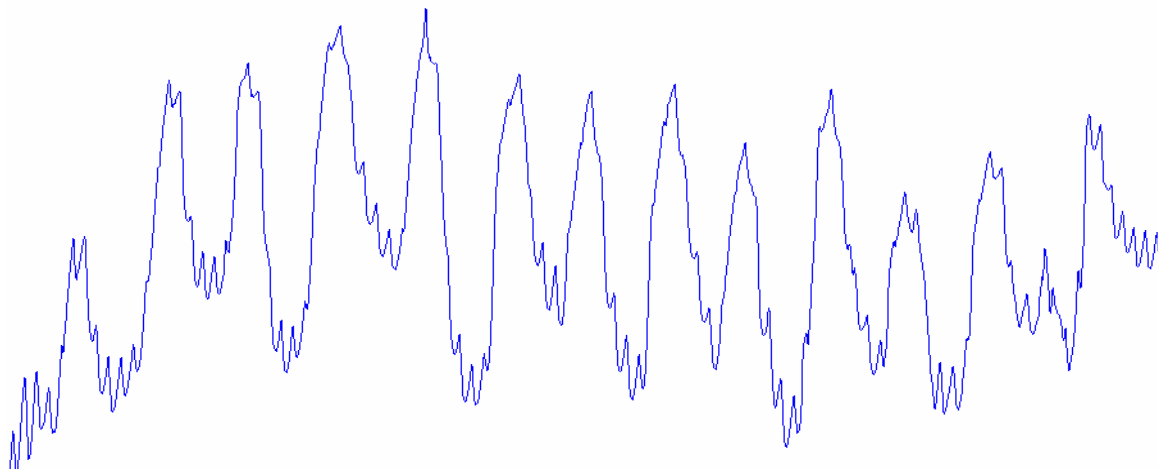


Figure 4-11. The unprocessed PPG demonstrating the exaggerated affect of respiration on the LFC, hiding the PCC.

CHAPTER 5 STATISTICAL ANALYSIS AND RESULTS

Statistical significance indicates the level of certainty that differences in the sampled populations are real. The likelihood that the differences are not true is represented by P. Statistical significance in no way indicates clinical utility.

Data Filtering

All outcome variables were measured on a breath-to-breath basis. Each breathing study consisted of three levels of resistance, of approximately ten breaths each. The ten breaths within each level of resistance, for each breathing study, represent repeated measures. These values were averaged together, resulting in one data point, for each variable, for each level of resistance. Averaging these repeated measures reduces the likelihood of aberrant data. Before averaging the data and performing the statistical analysis, each individual data point was observed for artifact or other obvious sources of error.

Multiple Breaths

Respiratory flows and volumes were measured using a CO₂SMO. The CO₂SMO periodically purges its pressure sensor, temporarily eliminating the ability to record measurements. This may either cause a minor delay in the timing of the individual breaths (Figure 4-8) or it may eliminate an entire breath from the data set (Figure 5-1). When the data from at least one breath was eliminated, all outcome variables measured during that breath were discarded.

There were approximately ten breaths of data recorded for each of the three levels of resistance, both before and after blood donation or hemodialysis (HD). This was approximately 60 breaths of data from each of the 20 blood donors and each of the 20 HD patients, or 1200 individual breaths from each population. There were 13 instances of eliminated breaths in the blood donor subjects and nine occurrences in the HD patients. If these breaths occurred during the low level of resistance, the low frequency component (LFC) Swing, pulsatile cardiac component (PCC) MagDiff and PCC MagMean variables were eliminated for that breath. If these breaths occurred during the medium or high level of resistance, only the LFC Swing variable was discarded as this was the only variable measured. Since the data points were averaged together, the effect of the elimination of one data point was minimal, thus reinforcing the reason for the repeated nature of the measurements.

Cardiac Arrhythmias

The PCC MagDiff and PCC MagMean variable calculations are dependent upon accurately calculating the amplitude of each individual heart beat through the duration of each individual breath. Cardiac arrhythmias, such as premature ventricular contractions, affect the stroke volume and the amplitude of the PCC (Figure 5-2). A premature beat occurred immediately following the fifth heart beat. This premature beat was followed by a larger amplitude, delayed beat. The PCC MagDiff represents the difference between the smallest and largest heart beats was therefore affected. The PCC MagMean, which represents the average value of these amplitudes, was also affected.

Neither the blood donor subjects nor the HD patients were monitored with an electrocardiograph, rendering it impossible to diagnose the occurrence and type of cardiac arrhythmias. All PCC variable calculations corresponding to breaths containing a

suspected cardiac arrhythmia were eliminated. Since the PCC variables were only calculated for the low level of resistance, the PCC of the medium and high levels of resistance were not evaluated for arrhythmias. Individual occurrences of suspected arrhythmias occurred in four blood donors and five HD patients.

Artifact

The nature of pulse oximetry monitoring, coupled with the fact that the blood donor and HD patients were awake and alert, caused movement artifact during data collection. In addition to movement artifact, the photodiode (PD) occasionally experienced ambient light interference. All variables were evaluated for these sources of artifact.

The unprocessed photoplethysmograph (PPG), plotted with respiratory flow, is shown (Figure 5-3). During the ninth breath there was a sharp spike in the unprocessed PPG data. This spike is not consistent with the data surrounding it and appears nonphysiologic. The cause of such artifact was related to movement of the subject. All individual breath data containing artifact were eliminated.

Overall, less than 5% of the total data were eliminated due to the reasons presented above. By reproducibly eliminating the data points representing possible sources of calculation error, the reliability of the averages of the remaining data points increased.

Unattainable Photoplethysmograph

In one blood donor subject and two HD patients, a PPG was unattainable from the finger. The HD patients each reported a history of poor peripheral circulation and an inability of a finger pulse oximeter to function. The blood donor subject was a 21 year-old female and the inability to acquire a reliable PPG tracing from the finger was surprising. The inability of a finger pulse oximeter probe to function in three out of 40

total subjects reinforces the need for alternative site pulse oximeter monitoring, even for routine use.

Demographics

The blood donor subjects ranged in age from 19 to 65 years of age. There were seven males and 13 females (Table 5-1). The dialysis patients ranged in age from 26 to 80 years of age and there were ten males and ten females (Table 5-2).

Statistical Analysis

Upon completion of the outcome variable filtering, the data points were averaged. The averaging of the repeated measures resulted in one outcome data point for each variable, for each level of resistance, for each breathing study, for the alar and the finger, for each subject. All analyses occurred separately for the blood donor data and the HD data and at no time were these two data sets combined. All analysis occurred separately for the data collected from the alar and finger and at no time were these data sets combined.

Hypothesis 1

Hypothesis 1 states that the LFC Swings for the high level of resistance are greater than the LFC Swings for the medium and low levels of resistance and the LFC Swings for the medium are greater than the LFC Swings for the low level of resistance, independent of fluid state, and PPG monitoring site.

All LFC Swing outcome measures were separated by resistance level, donation state and monitoring site. The following data sets were compared:

- **Blood donor alar LFC Swings before donation:** high vs medium vs low resistance.
- **Blood donor alar LFC Swings after donation:** high vs medium vs low resistance.

- **Blood donor finger LFC Swings before donation:** high vs medium vs low resistance.
- **Blood donor finger LFC Swings after donation:** high vs medium vs low resistance.
- **Hemodialysis alar LFC Swings before donation:** high vs medium vs low resistance.
- **Hemodialysis alar LFC Swings after donation:** high vs medium vs low resistance.
- **Hemodialysis finger LFC Swings before donation:** high vs medium vs low resistance.
- **Hemodialysis finger LFC Swings after donation:** high vs medium vs low resistance.

Since there was one LFC Swing data point for each resistance level, the sample sizes corresponded to the number of subjects. For the blood donor subjects N=20 for the alar and N=19 for the finger. For the HD patients N=20 for the alar and N=18 for the finger. The reduced sample size for the finger was due to the inability to acquire a finger PPG signal in the three subjects.

To determine the appropriate statistical tests to run, it was first necessary to determine if the data sets were normally distributed. A Kolmogorov-Smirnov (KS) test for normality with Lilliefors significance correction was applied to the data. The KS test is used to determine whether a sample of data comes from a specific distribution (Chakravarti et al. 1967). When testing for normality, minor corrections are made by applying the Lilliefors correction. The Lilliefors test is used to test the null hypothesis that the data come from a normally distributed population (Lilliefors 1967).

The results are presented (Tables 5-3 and 5-4). Of the 24 individual data sets, only four were significantly normal. Since most of the data sets were not normally distributed and $N \leq 20$ for all data sets, nonparametric tests were used for the statistical tests.

For each of the eight analyses, three data sets were compared. The data in each of the three sets were paired. The Friedman's test is the nonparametric equivalent of a one-way ANOVA. The Friedman's test tests the null hypothesis that k related variables come from the same population. For each case, the k variables are ranked from 1 to k . The test statistic is based on these ranks (SPSS 2005).

The results are shown for the blood donors and HD patients (Tables 5-5 and 5-6). The mean ranks, coupled with the significance level of each test, indicates that in all eight analyses there are significant differences between the three resistance levels with high > medium > low.

To determine where specific differences exist, a post-hoc analysis comparing the individual data sets was performed. The Wilcoxon signed-rank test is a nonparametric alternative to the paired Student's t -test for the case of two related samples or repeated measurements of a single sample. The test is named for Frank Wilcoxon, who proposed this, and the rank-sum test for two independent samples (Wilcoxon 1945).

The results are shown for the Wilcoxon signed-rank test for the blood donor and HD patients (Tables 5-7 and 5-8). To determine which outcome variables differ, each level of resistance was compared to the other levels of resistance. The four parts of each of the two tables represent the eight analyses described above. Within each of these analyses there were three individual analyses performed using the Wilcoxon signed-rank

test. All analyses showed significance with the exception of the medium vs high level of resistance in the HD patients from the alar, before fluid loss.

Hypothesis 1 states that differences exist between the low, medium and high levels of resistance. This was proven to be true. Graphical representations of the results are shown (Figures 5-4 to 5-7).

Hypothesis 2

Hypothesis 2 states that the LFC Swings will correlate with the intrathoracic pressure changes per breath, as estimated by Equation 3-3, independent of fluid state and PPG monitoring site. Equation 3-3 estimates pressure drop across endotracheal (ET) tubes and correlated well with the measured results previously discussed (Chapter 3). To estimate the intrathoracic pressure change using this equation, the inspiratory and expiratory flow rates were used and the two constants (K_1 and K_2) were based upon the diameter of the ET tubes. The estimated intrathoracic pressure change per breath was then calculated for each subject. For each resistance level, all breaths were averaged, as previously described.

For each subject there was a single LFC Swing value for each level of resistance before and after fluid loss for the alar and finger. There was also a corresponding estimated intrathoracic pressure change. A regression analysis was performed to explore the relationship between these values. The following data sets were compared:

- Estimated intrathoracic pressure changes and alar LFC Swings through all resistance levels for the blood donor subjects, before donation.
- Estimated intrathoracic pressure changes and alar LFC Swings through all resistance levels for the blood donor subjects, after donation.
- Estimated intrathoracic pressure changes and finger LFC Swings through all resistance levels for the blood donor subjects, before donation.

- Estimated intrathoracic pressure changes and finger LFC Swings through all resistance levels for the blood donor subjects, after donation.
- Estimated intrathoracic pressure changes and alar LFC Swings through all resistance levels for the HD patients, before HD.
- Estimated intrathoracic pressure changes and alar LFC Swings through all resistance levels for the HD patients, after HD.
- Estimated intrathoracic pressure changes and finger LFC Swings through all resistance levels for the HD patients, before HD.
- Estimated intrathoracic pressure changes and finger LFC Swings through all resistance levels for the HD patients, after HD.

Linear and second order regression analyses were performed to determine a relationship between the LFC Swings and estimated intrathoracic pressure changes and the results are shown (Tables 5-9 and 5-10). Graphical representations of these values are also shown (Figures 5-8 through 5-15). The R^2 values for the linear and second order analyses were virtually identical. In the blood donors and HD patients there were no significant relationships between the LFC Swings and the estimated intrathoracic pressure changes in any comparisons. This lack of relationship was caused primarily by the inter-subject variability and presence of outliers.

Hypothesis 2 states that there is a relationship between the LFC Swings and the estimated intrathoracic pressure changes. Due to inter-subject variability and outliers, no statistically significant relationship was found. Chapter six explores this relationship on a subject to subject basis eliminating the effect of inter-subject variability.

Hypothesis 3

Hypothesis 3 states that the LFC Swings for breathing study one (before fluid loss) are less than the LFC swings for breathing study two (after fluid loss) for each level of resistance, independent of monitoring site.

The LFC Swing data before fluid loss was compared to the LFC Swing data after fluid loss for the following:

- Blood donor subjects, alar, high level of resistance.
- Blood donor subjects, alar, medium level of resistance.
- Blood donor subjects, alar, low level of resistance.
- Blood donor subjects, finger, high level of resistance.
- Blood donor subjects, finger, medium level of resistance.
- Blood donor subjects, finger, low level of resistance.
- Hemodialysis patients, alar, high level of resistance.
- Hemodialysis patients, alar, medium level of resistance.
- Hemodialysis patients, alar, low level of resistance.
- Hemodialysis patients, finger, high level of resistance.
- Hemodialysis patients, finger, medium level of resistance.
- Hemodialysis patients, finger, low level of resistance.

The 12 individual hypothesis 3 comparisons were each an individually paired, before and after analysis. The fundamental statistical test for this type of comparison is the paired Student's t-test. As previously discussed, however, the LFC Swing data was not normally distributed. The Wilcoxon signed-rank test is the nonparametric alternative to the paired Student's t-test for the case of two related samples, and was used.

The results of the 12 individual comparisons are shown (Tables 5-11 and 5-12 and Figures 5-16 to 5-19). In the blood donor subjects, none of the comparisons were significantly different; however, the LFC Swings from the low resistance level from the finger had a p-value of .059 indicating a trend towards significance. In contrast, the HD patients all had $P < .2$ with half of them being $< .05$ or statistically significant.

Hypothesis 3 states that the LFC Swings before fluid loss are smaller than the LFC swings after fluid loss, for each level of resistance, independent of monitoring site. Of the six comparisons, three significantly differed and the other three trended towards significance. For the blood donor subjects, none of the comparisons showed significant differences.

Hypothesis 4

Hypothesis 4 states that the PCC MagDiff for breathing study 1 (before fluid loss) is greater than PCC MagDiff for breathing study 2 (after fluid loss), independent of monitoring site. The PCC MagDiff data before fluid loss was compared to the PCC MagDiff data after fluid loss for the following:

- Blood donor subjects, alar, low level of resistance.
- Blood donor subjects, finger, low level of resistance.
- Hemodialysis patients, alar, low level of resistance.
- Hemodialysis patients, finger, low level of resistance.

The four individual hypothesis 4 comparisons were each an individually paired, before and after analysis. To determine the appropriate statistical test, each data set was first tested for normality. As previously described, a KS test with Lilliefors correction was used.

The results of the KS normality test with Lilliefors significance correction for the PCC MagDiff are shown (Tables 5-13 and 5-14). Since not all of the PCC MagDiff data was normally distributed and the sample sizes were small, a Wilcoxon signed-rank test, the nonparametric alternative to the paired Student's t-test, was used.

The difference between the before and after blood donation alar PCC MagDiff was statistically significant (Table 5-15 and Figures 5-20 and 5-21). The same comparison in the HD patients was not significantly different. Neither the blood donors nor the HD patients were significantly different in the finger PCC MagDiff.

Hypothesis 4 states that the PCC MagDiff before fluid loss is greater than PCC MagDiff after fluid loss, independent of monitoring site. This was true for the blood donor subjects measured from the alar and was not true of the other comparisons.

Hypothesis 5

Hypothesis 5 states that the PCC MagMean for breathing study one (before fluid loss) is larger than the PCC MagMean for breathing study two (after fluid loss), independent of monitoring site.

The PCC MagMean before fluid loss was compared to the PCC MagMean data after fluid loss for the following:

- Blood donor subjects, alar, low level of resistance.
- Blood donor subjects, finger, low level of resistance.
- Hemodialysis patients, alar, low level of resistance.
- Hemodialysis patients, finger, low level of resistance.

The four individual hypothesis 5 comparisons were each an individually paired, before and after analysis. To determine the appropriate statistical test, each data set was

first tested for normality. As previously described, a KS test with Lilliefors correction was used.

The results of the KS normality test with Lilliefors significance correction for the PCC MagMean are shown (Tables 5-16 and 5-17). Since only one of the eight data sets were found to not be normally distributed and since the sample size for all data sets was small (either 18 or 20), a nonparametric test was used for the comparison. A Wilcoxon signed-rank test, the nonparametric alternative to the paired Student's t-test was used.

The difference between the before and after blood donation alar PCC MagDiff was statistically significant (Table 5-18 and Figures 5-22 and 5-23). Additionally, the change was consistent with that of the PCC MagDiff. The difference in the finger PCC MagMean of the HD patients was also statistically different. The same comparison in the blood donor subjects was not.

Hypothesis 5 states that the PCC MagMean before fluid loss is larger than the PCC MagMean after fluid loss, independent of monitoring site. This was true for the blood donor subjects measured from the alar and the HD patients measured from the finger. It was not true of the other comparisons.

In summary, hypothesis 1 was supported while hypothesis 2 was not. Hypothesis 3 was supported in the HD patients while Hypotheses 4 and 5 were supported in the blood donor subjects from the alar. The fact that the HD patients show differences in the LFC Swings while the blood donors subjects show differences in the PCC variables has important clinical and theoretical implications.

Discussion of Statistical Results

The blood donors and HD patients represent two distinctly different populations. Although a medical history was not performed, in general, the blood donor subjects were

in good health. The blood donation screening procedure does not exclude all chronic medical conditions but the subjects must be in general good health and be feeling well the day of donation. On the other hand, the HD patients generally have a long and complicated medical history and were taking an average of nearly ten medications. Additionally, the blood donor subjects lose whole blood, including red blood cells, while HD patients lose ultrafiltrate, not including red blood cells.

Hypotheses 1 and 2

Hypotheses 1 and 2 from clinical goal 1 were analyzed separately for a relatively healthy population (blood donors) and a relatively unhealthy population (HD patients). Additionally, the analysis was performed separately before and after fluid loss. As a result, hypotheses 1 and 2 were tested for a total of four populations: a euvoletic, relatively healthy population; a relatively healthy population with minor whole blood loss; a fluid loaded relatively unhealthy population; and a euvoletic, relatively unhealthy population.

All four of these populations, showed statistical differences across the three levels of resistance. This indicates that the LFC could potentially be used to distinguish major airway resistance differences in a variety of patient populations.

Hypothesis 2 explored the relationship between the LFC Swings and the estimated changes in intrathoracic pressure. The intrathoracic pressure changes per breath used in this analysis were estimated using an experimentally derived equation (Equation 3-3). The equation only uses inspiratory and expiratory flow rates to predict the pressure drop across ET tubes and does not account for intrinsic pressure changes in each individual.

In addition to the possible inaccuracy of Equation 3-3, the level of variation in the LFC Swings between subjects was high. The inability to account for actual variability in intrathoracic pressure changes coupled with the high inter-subject variability of the LFC Swings resulted in a nonsignificant relationship between the LFC Swings and estimated intrathoracic pressure.

The differences in the LFC Swings as shown in hypothesis 1 are caused by the intrathoracic pressure changes created by the added respiratory resistance. Inspiratory and expiratory flow rates and total respiratory volume contribute to the intrathoracic pressure change per breath. The inspiratory and expiratory flow rates and the respiratory volumes were analyzed for differences between resistance levels, since this would affect intrathoracic pressure, and could possibly confound the LFC Swing resistance data comparison. The statistical analysis that has been previously described was used and the results are presented (Tables 5-19 to 5-26 and Figures 5-24 to 5-29).

The peak inspiratory and expiratory flow rates differed significantly across all levels of resistance. They were greater in the low level of resistance than medium and greater in medium than high. Although the subjects were coached to breathe in and out at constant flow rates though all resistance levels, the flow rates increased as resistance decreased. Only one peak inspiratory comparison had a $P > .05$ and it was .07. The respiratory volume data in the blood donors and HD patients did not differ consistently. The high level of resistance was less than the other two levels before HD. Otherwise, no differences in the volumes were present.

Respiratory flow rate is directly related to the intrathoracic pressure change, which affects the LFC. Since the flow rates differed across the three resistance levels this

potentially confounded the LFC results. With all resistance levels being equal, the subjects with the greatest peak inspiratory and expiratory flow rates would be expected to have the greatest change in intrathoracic pressure and hence the largest LFC Swings. The results of hypothesis 1 indicate that the subjects breathing through the high resistance level had the greatest LFC Swings. These are the same subjects with the smallest peak inspiratory and expiratory flow rates. The difference in intrathoracic pressure caused by the difference in the flow rates does not override the difference caused by the added resistance. It did, however, possibly reduce the difference in the LFC Swings of the three resistance levels. Had the peak flow rates been identical, the differences found in the LFC Swings across the three resistance levels may have been even larger.

Since it is not feasible to guarantee that all subjects will have the ability to breathe to exact flow rates and volumes, this shortcoming can never truly be overcome. Since the foundation of the LFC Swings is the intrathoracic pressure, and the added resistance is only a means to increase intrathoracic pressure changes, future studies should monitor similar groups of patients with esophageal balloons, which provide an estimate of intrathoracic pressure. The variability of peak flow rates would not be as important since the actual intrathoracic pressure changes caused by the resistance levels, flows and volume would be known.

Hypothesis 3

The comparisons in clinical goal 2 were based upon the fluid state of the subjects. Blood donors lose whole blood while HD patients lose ultrafiltrate and retain red blood cells. In both patient populations, the clinical goal 2 comparisons were before and after fluid loss.

Hypothesis 3 analyzed the LFC Swings for changes related to fluid loss. The three individual resistance levels were analyzed separately. Differences in the LFC Swings of the HD patients were either significant or trending toward significance whereas no differences were found in the blood donors subjects.

Respiratory flow rates and volumes were compared before and after fluid loss for the blood donor and HD patients. The statistical methods previously described were used. The results are presented (Tables 5-27 and 5-28 and Figures 5-30 to 5-35). No differences were found in peak inspiratory flow, peak expiratory flow or respiratory volume in either blood donors or HD patients. The differences in the alar LFC Swings of the HD patients before and after HD were therefore not caused by variation in peak inspiratory flow, peak expiratory flow or respiratory volume. Additionally, there were no before and after blood loss differences found in the LFC Swings of the blood donor subjects. This lack of difference was not affected by differences in these respiratory parameters.

Hypothesis 3 states that the LFC Swings increased after fluid loss. It was assumed that enough fluid would be lost during HD or blood donation to cause this change. Other expected changes that would occur with fluid loss include increased heart rate and decreased blood pressure. Pulse rate and seated blood pressure were analyzed for differences before and after fluid loss in the blood donor and HD patients. The results are presented (Tables 5-29 and 5-30 and Figures 5-36 to 5-39).

Consistent with the LFC Swing differences, the pulse rate and blood pressure did not differ in the blood donor subjects before and after blood donation. In the HD

patients, however, the pulse rate at all resistance levels increased significantly after fluid loss and the systolic and diastolic blood pressure both decreased significantly.

The LFC Swing results, coupled with the pulse and blood pressure results, indicate that the overall physiologic effect of the fluid loss in HD is greater than in blood donation. The total blood lost in blood donation does not cause an increase in pulse rate or a decrease in blood pressure. It is therefore not surprising that there were no changes in the LFC Swings.

Hemodialysis patients, on the other hand, lose enough fluid to have a statistically significant increase in pulse rate and decrease in blood pressure. These physiologic compensatory mechanisms indicate that the fluid lost is physiologically significant. The LFC Swings either increased significantly or trended toward significance in the alar and finger of the HD patients.

These data indicate that compensatory physiologic mechanisms must be present for the LFC Swings to significantly increase. It is suspected that the overall effect of the blood loss resulting from blood donation is too small to influence the LFC Swings. An interesting follow-up study could remove enough whole blood from volunteer donors to cause compensatory mechanisms, indicating that the blood loss is physiologically significant. If the LFC Swings significantly increase, this would support this theory.

In many of the subjects, the effects of the resistance breathing on the LFC was greater in the first two breaths than subsequent breaths. To explore this relationship, the first two breaths for each subject were separated from subsequent breaths and averaged separately. First, the mean of breaths one and two were compared to the mean of the subsequent breaths. This analysis was performed for the alar and finger, before and after

fluid loss, in the blood donor and HD patients. The results are presented (Tables 5-31 to 5-34 and Figures 5-40 to 5-43).

In the blood donor subjects there were six instances of the difference between the mean of the first two breaths being significantly different from the mean of subsequent breaths. This occurred three times in the HD patients with a fourth $P=.053$. In all ten cases the mean of the first two breaths was greater than the mean of the subsequent breaths.

When resistance is initially added to a breathing circuit, the LFC responds with large changes. After two breaths, the magnitude of the LFC Swings stabilizes to a slightly lower level than the magnitude of the first two breaths. Considering not all analyses were significantly different, more research should be conducted to fully understand the physiologic significance of the initial shifting of the venous blood and how this differs from the stabilized changes.

A follow-up analysis explored the differences between the first two breaths before and after fluid loss. The results of the before and after fluid loss analysis of the first two breath LFC Swing data are presented (Tables 5-35 and 5-36 and Figures 5-44 to 5-47).

No difference were found in the LFC Swings of the blood donors when all breaths were combined, however when looking at the first two breaths only, differences were found in the high level of resistance. The LFC Swings of the first two breaths after blood loss were significantly greater than before blood loss. It is possible that the LFC Swings of the first two breaths may be a more sensitive indicator of blood loss than other more traditional measures, such as pulse rate and blood pressure.

In HD patients, the LFC Swings in the first two breaths were significantly greater in the after HD compared to before HD in the medium and low levels of resistance. Since the average of all breaths was also significant or trending towards significance, the first two breaths may not provide any additional information in the HD patient population, probably because the fluid loss is physiologically significant. It is suspected that initial LFC Swings caused by the first two breaths may be a sensitive indicator of minor blood loss whereas in the case of more significant fluid loss, all LFC Swings can be used.

Hypotheses 4 and 5

Hypotheses 4 and 5 explored the effects of fluid loss on the PCC. In blood donor subjects, the alar PCC MagDiff and alar PCC MagMean both decreased after blood donation whereas in HD patients there were no differences. This is in contrast to the LFC Swings, which increased in HD patients and not blood donors.

The absorbance of red and infrared light in pulse oximetry mainly occurs as hemoglobin passes by the PD. The PPG is a graphical representation of the absorbance of infrared light. In blood donation, red blood cells, and hence hemoglobin, are removed. Even though the blood loss has minor physiologic consequences, the PCC MagDiff and PCC MagMean both decreased significantly. This is logical considering red blood cells are lost and light absorption decreases. While the decrease in PCC variables indicates a decrease in stroke volume and cardiac output it may simply reflect the decrease in absolute amount of hemoglobin absorbing infrared light. The fact that HD patients lose a physiologically significant amount of fluid while experiencing no change in the PCC variables support this theory.

To date, no studies have explored the differences between losing whole blood and clear fluid. The PPG may be used to detect physiologic changes with fluid loss but may also be used to detect changes in hemoglobin concentration. As with blood loss during donation, the physiologic consequences are insignificant yet detectable by a decrease in the PCC measures.

Regression Analysis

The LFC Swings significantly increased after fluid loss in HD and the PCC variables significantly decreased after blood donation. To determine if the magnitude of fluid loss affects the magnitude of these variables, a regression analysis was performed.

First, the difference between the LFC Swings before and after HD was calculated for each level of resistance. The total fluid removed in each HD patient was noted. A regression analysis was performed to determine a relationship between the volume of fluid removed and the magnitude of the LFC Swing change following this fluid loss. The regression analysis plots along with R^2 values for the linear and second order analysis are presented (Figures 5-48 to 5-50).

No relationship was found between total fluid removed and the magnitude of the change in the LFC Swings in HD patients. The total amount of fluid removed was then divided by total body weight to give an estimation of the relative amount of fluid removed. A follow-up regression analysis was then performed to determine if changes in the LFC Swings correlated with an estimation of relative fluid loss. These results are presented (Figures 5-51 to 5-53). Similarly, no relationship was found between the magnitude of LFC Swing change and the fluid removed as a percent of total body weight.

A similar relationship was explored for the blood donors. First, the total blood volume in the blood donor subjects was estimated using Equations 3-4 and 3-5. The PCC

MagDiff and PCC MagMean differences were calculated as before blood loss minus after blood loss. The results of this regression analysis are presented (Figures 5-54 and 5-55). Since all but two of the blood donors lost the same amount of blood, calculating the percent blood loss would not add additional information.

Whole blood loss in a population of blood donors causes significant changes in the PCC measures while fluid loss in a population of HD patients causes significant changes in the LFC measures. Inter-subject variability prohibits these measures from accurately estimating the degree of fluid loss in these populations.

Table 5-1. Demographic information for the blood donors.

	Height (cm)	Weight (kg)	Sex	Age
P01	183	81.8	M	60
P02	165	107.7	F	40
P03	160	60.5	F	21
P04	157	50.0	F	27
P05	178	81.8	M	35
P06	157	59.1	F	55
P07	178	71.8	F	26
P08	178	95.5	M	34
P09	201	104.5	M	32
P10	170	75.0	M	48
P11	175	86.4	F	31
P12	178	67.7	F	33
P13	165	84.1	F	33
P14	183	84.1	M	54
P15	183	84.1	M	65
P16	165	68.2	F	20
P17	175	66.4	F	21
P18	152	63.6	F	19
P19	168	85.5	F	21
P20	157	59.1	F	20

Table 5-2. Demographic information for the HD patients.

	Height (cm)	Weight (kg)	Sex	Age
P01	175	72.5	M	52
P02	193	110.0	M	50
P03	173	78.5	F	61
P04	168	129.5	F	45
P05	160	56.0	F	26
P06	188	131.4	M	54
P07	168	73.0	M	80
P08	165	82.6	F	49
P09	168	91.3	F	36
P10	180	91.7	F	56
P11	170	136.0	F	29
P12	170	72.2	M	44
P13	180	86.4	M	58
P14	196	130.1	M	54
P15	160	80.8	F	36
P16	188	83.9	M	62
P17	188	94.1	M	38
P18	160	60.6	F	57
P19	175	83.0	F	40
P20	170	62.3	M	44

Table 5-3. Test for normality in the LFC Swings of the blood donors.

Tests of Normality Blood Donors			
Kolmogorov-Smirnov(a)			
	Statistic	df	Sig.
Alar high before	0.19	20	0.049
Alar high after	0.29	20	0.000
Alar medium before	0.16	20	0.2*
Alar medium after	0.17	20	0.137
Alar low before	0.17	20	0.114
Alar low after	0.29	20	0.000
Finger high before	0.14	19	0.2*
Finger high after	0.19	19	0.083
Finger medium before	0.25	19	0.002
Finger medium after	0.17	19	0.141
Finger low before	0.16	19	0.2*
Finger low after	0.24	19	0.004

* Lower bound of the true significance.
(a) Lilliefors Significance Correction

Table 5-4. Test for normality in the LFC Swings of the HD patients.

Tests of Normality HD patients			
Kolmogorov-Smirnov(a)			
	Statistic	df	Sig.
Alar high before	0.30	20	0.000
Alar high after	0.16	20	0.171
Alar medium before	0.29	20	0.000
Alar medium after	0.20	20	0.029
Alar low before	0.28	20	0.000
Alar low after	0.30	20	0.000
Finger high before	0.21	18	0.028
Finger high after	0.21	18	0.030
Finger medium before	0.14	18	0.2*
Finger medium after	0.18	18	0.149
Finger low before	0.25	18	0.003
Finger low after	0.25	18	0.004

* Lower bound of the true significance.
(a) Lilliefors Significance Correction

Table 5-5. Friedman's test results for the LFC Swings of the blood donors.

	Mean Rank		Mean Rank		Mean Rank		Mean Rank
Alar high before	2.85	Alar high after	2.85	Finger high before	2.74	Finger high after	2.79
Alar med before	1.90	Alar med after	2.05	Finger med before	2.05	Finger med after	2.16
Alar low before	1.25	Alar low after	1.10	Finger low before	1.21	Finger low after	1.05
Test Statistics							
N	20	N	20	N	19	N	19
Chi-Square	25.9	Chi-Square	30.7	Chi-Square	22.21	Chi-Square	29.37
df	2	df	2	df	2	df	2
Sig.	2.38E-06	Sig.	2.16E-07	Sig.	1.50E-05	Sig.	4.19E-07

Table 5-6. Friedman's test results for the LFC Swings of the HD patients.

	Mean Rank		Mean Rank		Mean Rank		Mean Rank
Alar high before	2.65	Alar high after	2.75	Finger high before	2.81	Finger high after	2.83
Alar med before	2.35	Alar med after	2.15	Finger med before	2.00	Finger med after	2.11
Alar low before	1	Alar low after	1.1	Finger low before	1.19	Finger low after	1.06
Test Statistics							
N	20	N	20	N	18	N	18
Chi-Square	30.9	Chi-Square	27.9	Chi-Square	23.69	Chi-Square	28.78
df	2	df	2	df	2	df	2
Sig.	1.95E-07	Sig.	8.74E-07	Sig.	7.2E-06	Sig.	5.64E-07

Table 5-7. Wilcoxon Signed-Rank results across the three resistance levels for the LFC Swings for the blood donors.

	Before			After		
	Alar med	Alar low	Alar low	Alar med	Alar low	Alar low
	vs	vs	vs	vs	vs	vs
	Alar high	Alar med	Alar high	Alar high	Alar med	Alar high
Sig.	0.0010	0.0012	0.0001	0.0008	0.0003	0.0001
	Before			After		
	Finger med	Finger low	Finger low	Finger med	Finger low	Finger low
	vs	vs	vs	vs	vs	vs
	Finger high	Finger med	Finger high	Finger high	Finger med	Finger high
Sig.	0.0100	0.0025	0.0002	0.0048	0.0004	0.0001

Table 5-8. Wilcoxon Signed-Rank results across the three resistance levels for the LFC Swings for the HD patients.

	Before			After		
	Alar med	Alar low	Alar low	Alar med	Alar low	Alar low
	vs	vs	vs	vs	vs	vs
	Alar high	Alar med	Alar high	Alar high	Alar med	Alar high
Sig.	0.0620	0.0001	0.0001	0.0111	0.0004	0.0009
	Before			After		
	Finger med	Finger low	Finger low	Finger med	Finger low	Finger low
	vs	vs	vs	vs	vs	vs
	Finger high	Finger med	Finger high	Finger high	Finger med	Finger high
Sig.	0.0012	0.0014	0.0004	0.0123	0.0003	0.0002

Table 5-9. R² values of LFC Swings compared to estimated intrathoracic pressure for blood donors.

	Alar before	Alar after	Finger before	Finger after
Linear	0.2902	0.3449	0.1984	0.3005
Second Order	0.3018	0.415	0.2593	0.3132

Table 5-10. R² values of LFC Swings compared to estimated intrathoracic pressure for HD patients.

	Alar before	Alar after	Finger before	Finger after
Linear	0.0318	0.0128	0.1529	0.2803
Second Order	0.1227	0.2308	0.162	0.2172

Table 5-11. Wilcoxon Signed-Rank results for the LFC Swings of the blood donors before and after blood loss.

	Alar			Finger		
	High after	Med after	Low after	High after	Med after	Low after
	vs	vs	vs	vs	vs	vs
	High before	Med before	Low before	High before	Med before	Low before
Sig.	0.823	0.502	0.911	0.717	0.629	0.059

Table 5-12. Wilcoxon Signed-Rank results for the LFC Swings of the HD patients before and after HD.

	Alar			Finger		
	High after	Med after	Low after	High after	Med after	Low after
	vs	vs	vs	vs	vs	vs
	High before	Med before	Low before	High before	Med before	Low before
Sig.	0.108	0.028	0.126	0.145	0.020	0.043

Table 5-13. Test for normality for the PCC MagDiff of the blood donors.

Tests of Normality Blood Donors			
Kolmogorov-Smirnov(a)			
	Statistic	df	Sig.
Alar low before	0.14	20	0.2*
Alar low after	0.29	20	0.000
Finger low before	0.16	19	0.2*
Finger low after	0.15	19	0.2*

* Lower bound of the true significance.
(a) Lilliefors Significance Correction

Table 5-14. Test for normality for the PCC MagDiff of the HD patients.

Tests of Normality HD patients			
Kolmogorov-Smirnov(a)			
	Statistic	df	Sig.
Alar low before	0.21	20	0.018
Alar low after	0.26	20	0.001
Finger low before	0.42	18	0.000
Finger low after	0.31	18	0.000

* Lower bound of the true significance.
(a) Lilliefors Significance Correction

Table 5-15. Wilcoxon Signed-Rank results for the PCC MagDiff of the blood donors and HD patients

	Blood Donor		HD	
	Alar	Finger	Alar	Finger
	Low before	Low before	Low before	Low before
	vs	vs	vs	vs
	Low after	Low after	Low after	Low after
Sig.	0.017	0.643	0.970	0.286

Table 5-16. Test for normality for the PCC MagMean of the blood donors.

Tests of Normality Blood Donors				
Kolmogorov-Smirnov(a)				
	Statistic	df	Sig.	
Alar low before	0.19	20	0.054	
Alar low after	0.19	20	0.052	
Finger low before	0.27	19	0.001	
Finger low after	0.16	19	0.188	
* Lower bound of the true significance.				
(a) Lilliefors Significance Correction				

Table 5-17. Test for normality for the PCC MagMean of the HD patients.

Tests of Normality HD patients				
Kolmogorov-Smirnov(a)				
	Statistic	df	Sig.	
Alar low before	0.22	20	0.016	
Alar low after	0.20	20	0.039	
Finger low before	0.12	18	0.2*	
Finger low after	0.24	18	0.006	
* Lower bound of the true significance.				
(a) Lilliefors Significance Correction				

Table 5-18. Wilcoxon Signed-Rank results for the PCC MagMean of the blood donors and HD patients.

	Blood Donor		HD	
	Alar	Finger	Alar	Finger
	Low before	Low before	Low before	Low before
	vs	vs	vs	vs
	Low after	Low after	Low after	Low after
Sig.	0.028	0.968	0.852	0.010

Table 5-19. Friedman's test results for the respiratory flow rates of the blood donors.

	Mean Rank		Mean Rank		Mean Rank		Mean Rank
Insp high before	1.18	Insp high after	1.05	Exp high before	1.43	Exp high after	1.43
Insp med before	1.95	Insp med after	2.08	Exp med before	1.75	Exp med after	1.88
Insp low before	2.88	Insp low after	2.88	Exp low before	2.83	Exp low after	2.70
Test Statistics							
N	20	N	20	N	20	N	20
Chi-Square	29.72	Chi-Square	34.78	Chi-Square	22.31	Chi-Square	18.33
df	2	df	2	df	2	df	2
Sig.	3.52E-07	Sig.	2.80E-08	Sig.	1.43E-05	Sig.	1.05E-04

Table 5-20. Wilcoxon Signed-Rank results for the respiratory flow rates of the blood donors.

	Before			After		
	Insp med vs Insp high	Insp low vs Insp med	Insp low vs Insp high	Insp med vs Insp high	Insp low vs Insp med	Insp low vs Insp high
Sig.	0.0009	0.0002	0.0001	0.0002	0.0003	0.0001
	Before			After		
	Exp med vs Exp high	Exp low vs Exp med	Exp low vs Exp high	Exp med vs Exp high	Exp low vs Exp med	Exp low vs Exp high
Sig.	0.0732	0.0001	0.0003	0.0102	0.0007	0.0002

Table 5-21. Friedman's test results for the respiratory volume of the blood donors.

	Mean Rank		Mean Rank
High before	1.58	High after	1.88
Med before	2.05	Med after	2.13
Low before	2.38	Low after	2.00
Test Statistics			
N	20	N	20
Chi-Square	6.82	Chi-Square	0.64
df	2	df	2
Sig.	0.033	Sig.	0.726

Table 5-22. Wilcoxon Signed-Rank results for the respiratory volume of the blood donors.

	Pre			Post		
	Vol med	Vol low	Vol low	Vol med	Vol low	Vol low
	vs	vs	vs	vs	vs	vs
	Vol high	Vol med	Vol high	Vol high	Vol med	Vol high
Sig.	0.052	0.365	0.046	0.108	0.658	0.171

Table 5-23. Friedman's test results for the respiratory flow rates of the HD patients.

	Mean Rank		Mean Rank		Mean Rank		Mean Rank
Insp high before	1.025	Insp high after	1	Exp high before	1.025	Exp high after	1
Insp med before	2.05	Insp med after	2	Exp med before	1.975	Exp med after	2
Insp low before	2.925	Insp low after	3	Exp low before	3	Exp low after	3
Test Statistics							
N	20	N	20	N	20	N	20
Chi-Square	37.10	Chi-Square	40.00	Chi-Square	39.52	Chi-Square	40.00
df	2	df	2	df	2	df	2
Sig.	8.78E-09	Sig.	2.06E-09	Sig.	2.62E-09	Sig.	2.06E-09

Table 5-24. Wilcoxon Signed-Rank results for the respiratory flow rates of the HD patients.

	Before			After		
	Insp med	Insp low	Insp low	Insp med	Insp low	Insp low
	vs	vs	vs	vs	vs	vs
	Insp high	Insp med	Insp high	Insp high	Insp med	Insp high
Sig.	1.28E-04	2.45E-04	8.79E-05	8.43E-05	8.72E-05	8.72E-05
	Before			After		
	Exp med	Exp low	Exp low	Exp med	Exp low	Exp low
	vs	vs	vs	vs	vs	vs
	Exp high	Exp med	Exp high	Exp high	Exp med	Exp high
Sig.	1.24E-04	8.79E-05	8.75E-05	8.23E-05	8.76E-05	8.68E-05

Table 5-25. Friedman's test results for the respiratory volume of the HD patients.

	Mean Rank		Mean Rank	
High before	1.3		High after	1.725
Med before	2.35		Med after	2.175
Low before	2.35		Low after	2.100
Test Statistics				
N	20		N	20
Chi-Square	15.08		Chi-Square	2.35
df	2		df	2
Sig.	0.001		Sig.	0.308

Table 5-26. Wilcoxon Signed-Rank results for respiratory volume of the HD patients.

	Before			After		
	Vol med	Vol low	Vol low	Vol med	Vol low	Vol low
	vs	vs	vs	vs	vs	vs
	Vol high	Vol med	Vol high	Vol high	Vol med	Vol high
Sig.	0.001	0.879	0.001	0.024	0.641	0.048

Table 5-27. Wilcoxon Signed-Rank results for the respiratory flow rates and volumes of the blood donors before and after blood loss.

	Inspiration			Expiration			Respiratory Volume		
	High	Med	Low	High	Med	Low	High	Med	Low
	before	before	before	before	before	before	before	before	before
	vs	vs	vs	vs	vs	vs	vs	vs	vs
	High	Med	Low	High	Med	Low	High	Med	Low
	after	after	after	after	after	after	after	after	after
Sig.	0.504	0.952	0.150	0.482	0.584	0.599	0.731	0.421	0.155

Table 5-28. Wilcoxon Signed-Rank results for the respiratory flow rates and volumes of the HD patients before and after HD.

	Inspiration			Expiration			Respiratory Volume		
	High	Med	Low	High	Med	Low	High	Med	Low
	before	before	before	before	before	before	before	before	before
	vs	vs	vs	vs	vs	vs	vs	vs	vs
	High	Med	Low	High	Med	Low	High	Med	Low
	after	after	after	after	after	after	after	after	after
Sig.	0.585	0.925	0.409	0.159	0.795	0.952	0.145	0.601	0.380

Table 5-29. Wilcoxon Signed-Rank results of the pulse rate and blood pressure of the blood donors before and after blood loss.

	Pulse			Blood Pressure	
	High before	Med before	Low before	Sys before	Dia before
	vs	vs	vs	vs	vs
	High after	Med after	Low after	Sys after	Dia after
Sig.	0.965	0.060	0.515	0.075	0.169

Table 5-30. Wilcoxon Signed-Rank results of the pulse rate and blood pressure of the HD patients before and after HD.

	Pulse			Blood Pressure	
	High before	Med before	Low before	Sys before	Dia before
	vs	vs	vs	vs	vs
	High after	Med after	Low after	Sys after	Dia after
Sig.	0.007	0.008	0.005	0.000	0.009

Table 5-31. Wilcoxon Signed-Rank results for the LFC Swings of the blood donors comparing breaths 1 and 2 to subsequent breaths in the alar.

	Before			After		
	High	Medium	Low	High	Medium	Low
Breath	1 and 2					
	vs	vs	vs	vs	vs	vs
Breath	> 2	> 2	> 2	> 2	> 2	> 2
Sig.	0.100	0.717	0.033	0.023	0.823	0.023

Table 5-32. Wilcoxon Signed-Rank results for the LFC Swings of the blood donors comparing breaths 1 and 2 to subsequent breaths in the finger.

	Before			After		
	High	Medium	High	Medium	High	Medium
Breath	1 and 2					
	vs	vs	vs	vs	vs	vs
Breath	> 2	> 2	> 2	> 2	> 2	> 2
Sig.	0.658	0.133	0.002	0.005	0.091	0.004

Table 5-33. Wilcoxon Signed-Rank results for the LFC Swings of the HD patients comparing breaths 1 and 2 to subsequent breaths in the alar.

	Before			After		
	High	Medium	High	Medium	High	Medium
Breath	1 and 2					
	vs	vs	vs	vs	vs	vs
Breath	> 2	> 2	> 2	> 2	> 2	> 2
Sig.	0.433	0.028	0.014	0.355	0.191	0.455

Table 5-34. Wilcoxon Signed-Rank results for the LFC Swings of the HD patients comparing breaths 1 and 2 to subsequent breaths in the finger.

	Before			After		
	High	Medium	High	Medium	High	Medium
Breath	1 and 2					
	vs	vs	vs	vs	vs	vs
Breath	> 2	> 2	> 2	> 2	> 2	> 2
Sig.	0.811	0.586	0.349	0.811	0.053	0.008

Table 5-35. Wilcoxon Signed-Rank results for the LFC Swings of the blood donors comparing breaths 1 and 2 before and after blood loss.

	Alar			Finger		
	High before	Med before	Low before	High before	Med before	Low before
	vs	vs	vs	vs	vs	vs
	High after	Med after	Low after	High after	Med after	Low after
Sig.	0.011	0.520	0.881	0.099	0.913	0.117

Table 5-36. Wilcoxon Signed-Rank results for the LFC Swings of the HD patients comparing breaths 1 and 2 before and after HD.

	Alar			Finger		
	High before	Med before	Low before	High before	Med before	Low before
	vs	vs	vs	vs	vs	vs
	High after	Med after	Low after	High after	Med after	Low after
Sig.	0.212	0.351	0.247	0.199	0.031	0.002

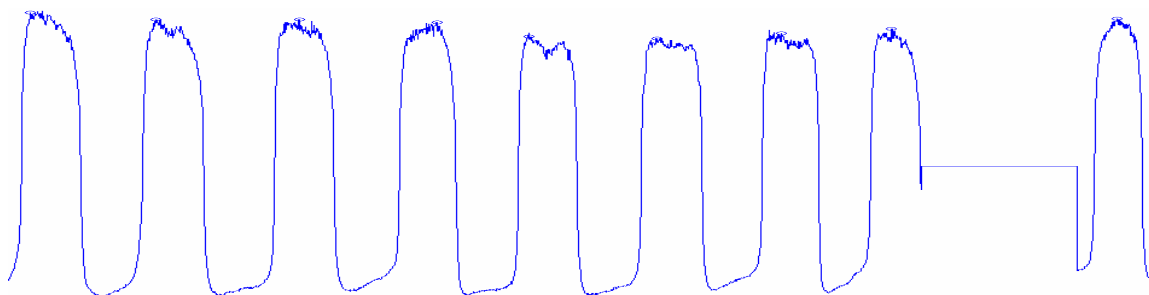


Figure 5-1. Respiratory flow data showing the elimination of one breath. The peak inspiratory flow rates are marked (o).

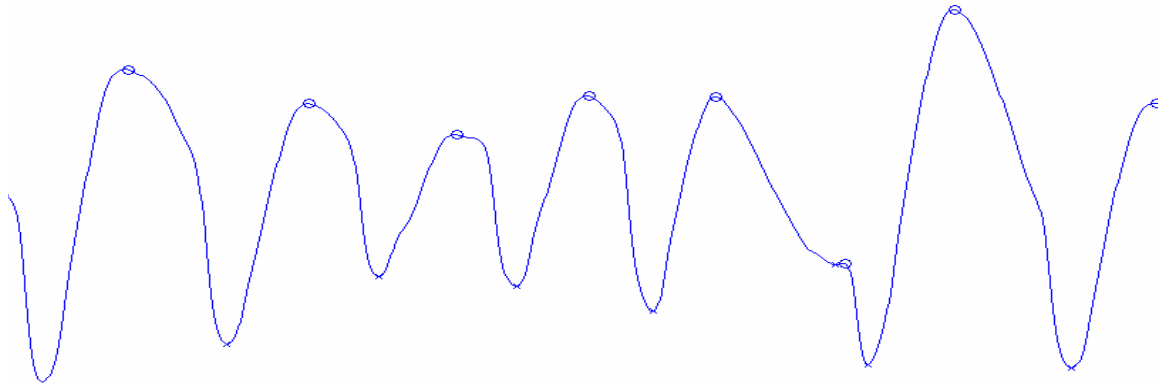


Figure 5-2. The PCC for the duration of one breath, showing an arrhythmia.

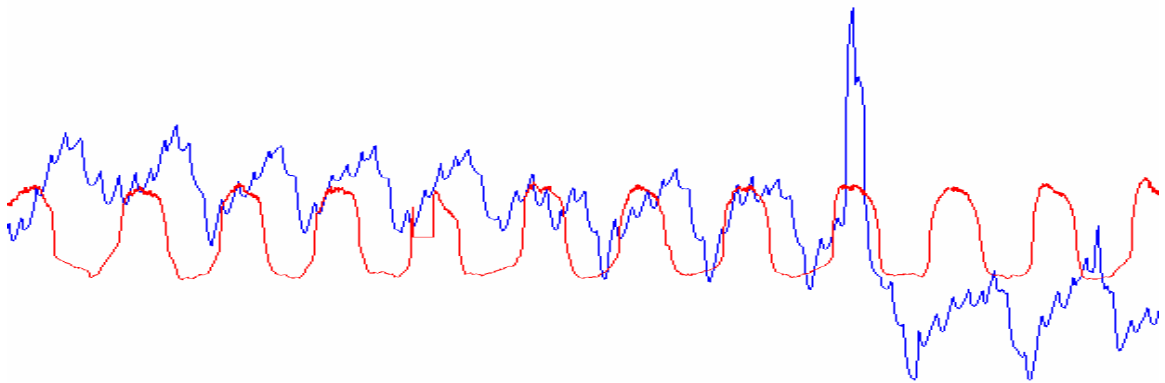


Figure 5-3. The unprocessed PPG with respiratory flow data, showing the result of motion artifact.

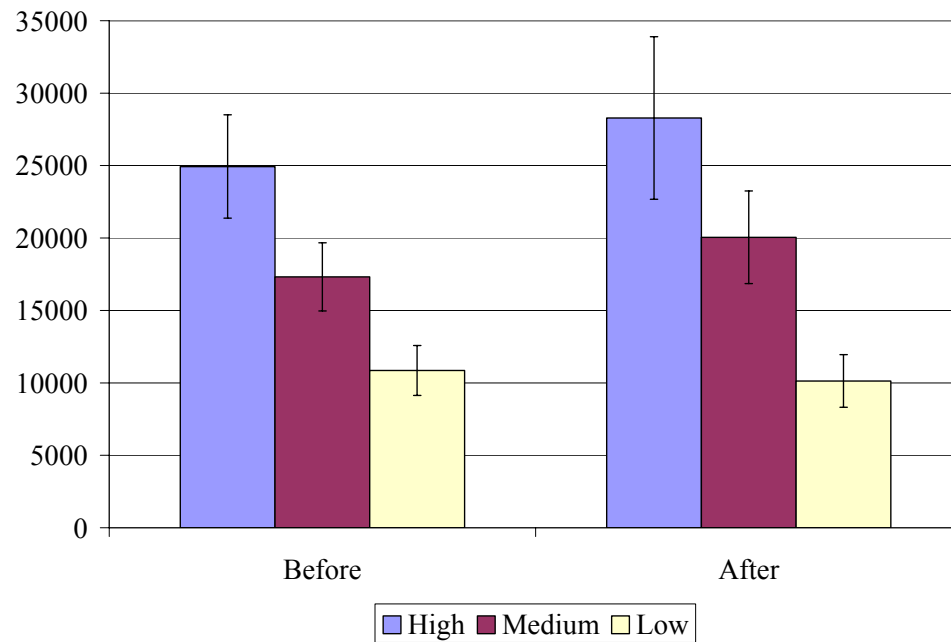


Figure 5-4. The alar LFC Swings for the blood donors, before and after blood loss.

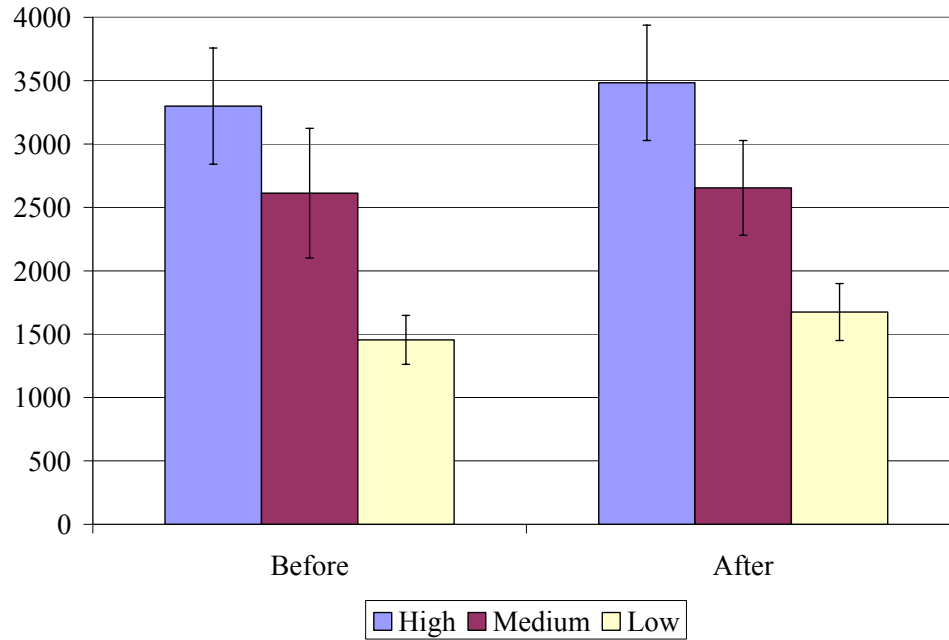


Figure 5-5. The finger LFC Swings for the blood donors, before and after blood loss.

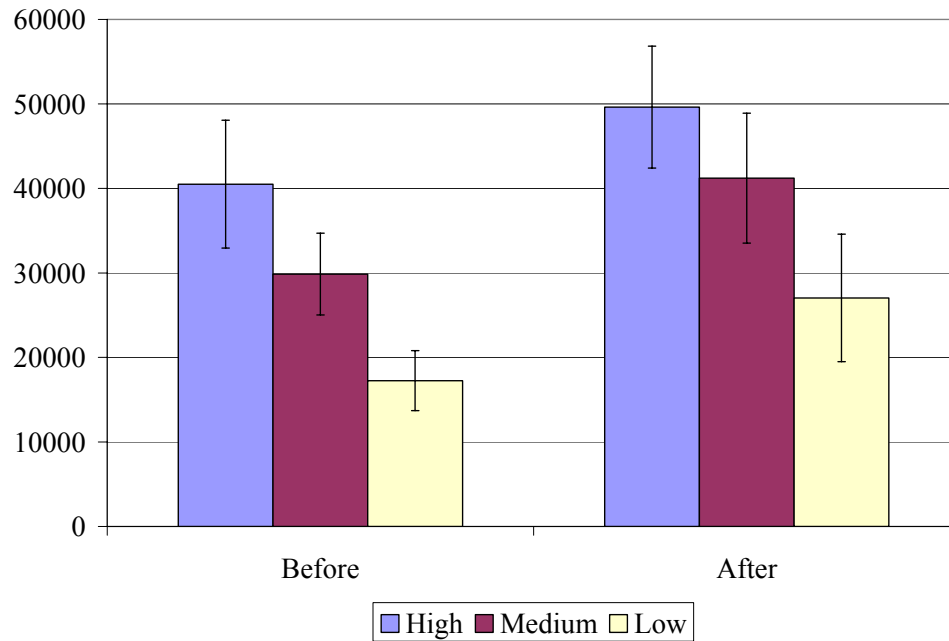


Figure 5-6. The alar LFC Swings for the HD patients, before and after HD.

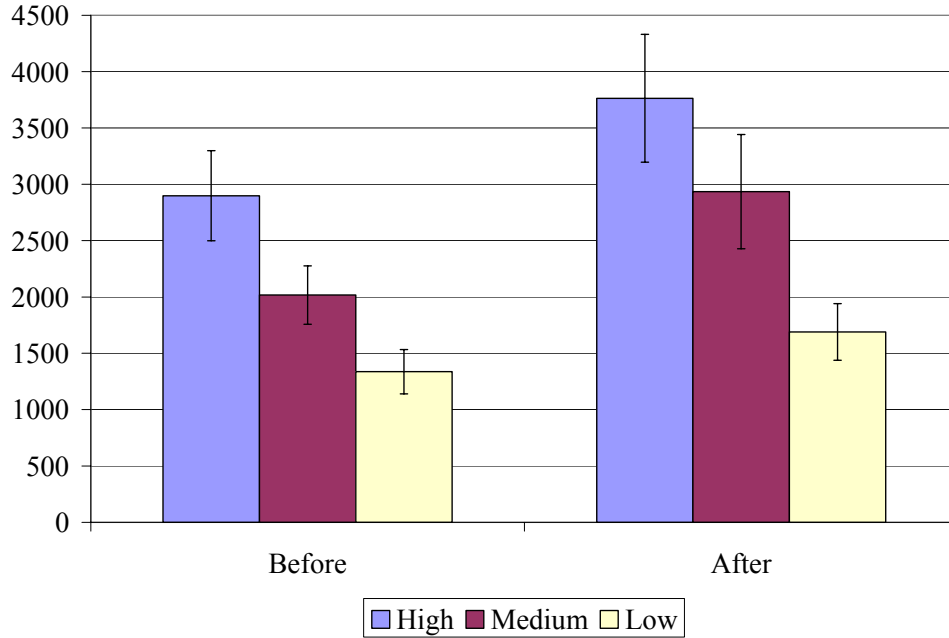


Figure 5-7. The finger LFC Swings for the HD patients, before and after HD.

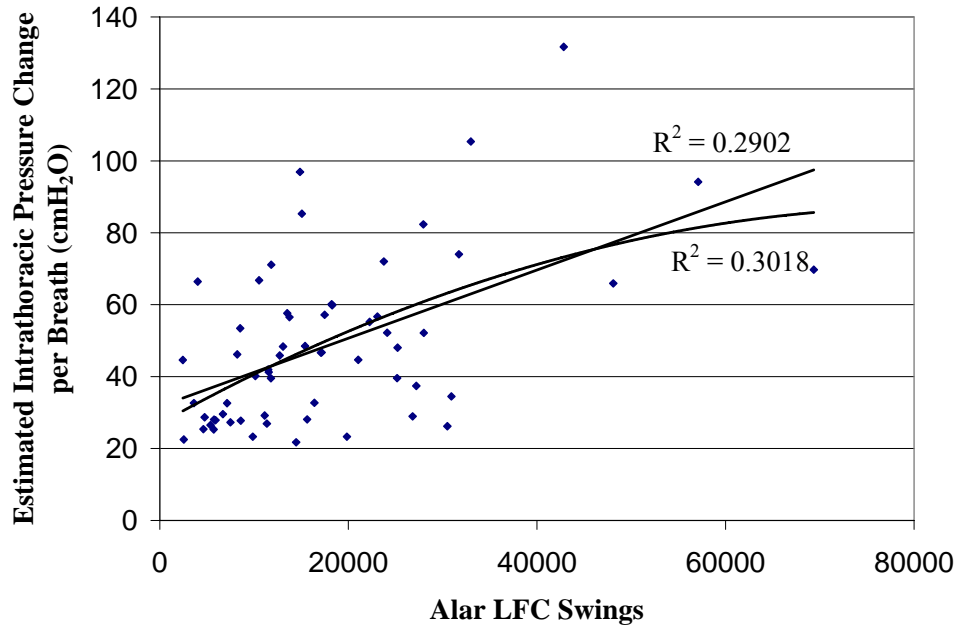


Figure 5-8. Estimated intrathoracic pressure change per breath vs alar LFC Swings in blood donors, before blood loss.

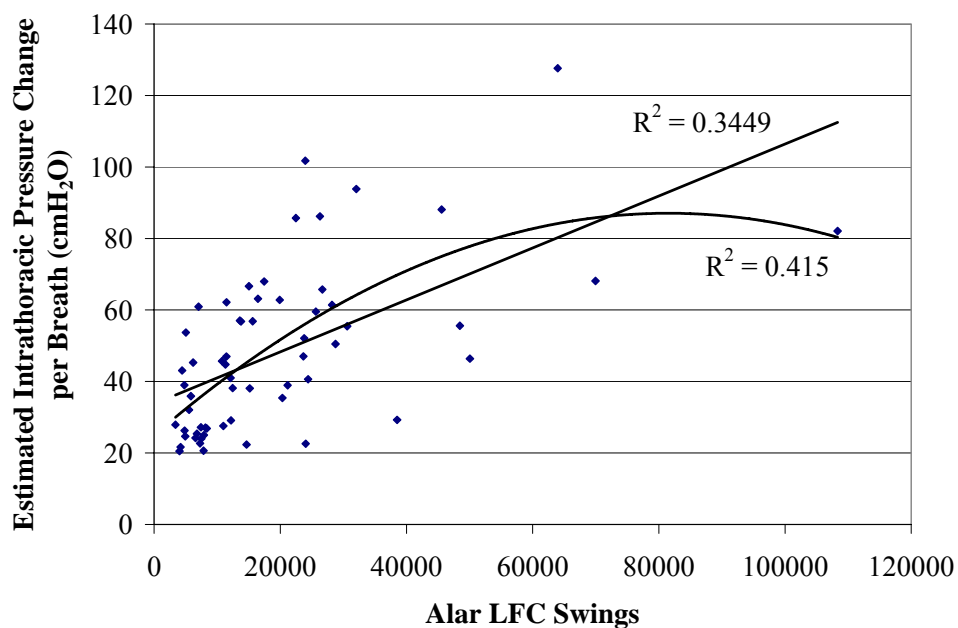


Figure 5-9. Estimated intrathoracic pressure change per breath vs alar LFC Swings in blood donors, after blood loss.

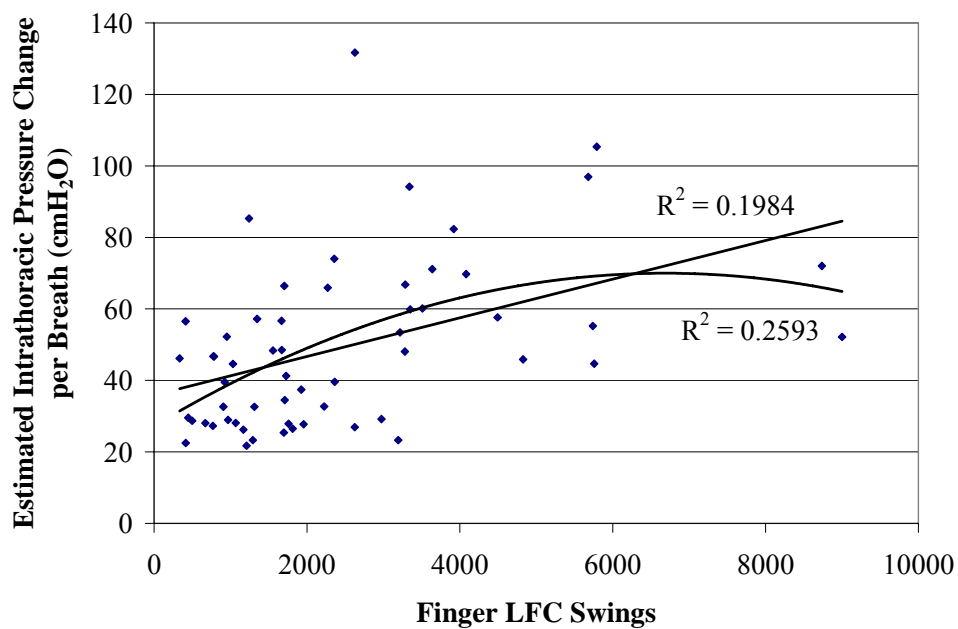


Figure 5-10. Estimated intrathoracic pressure change per breath vs finger LFC Swings in blood donors, before blood loss.

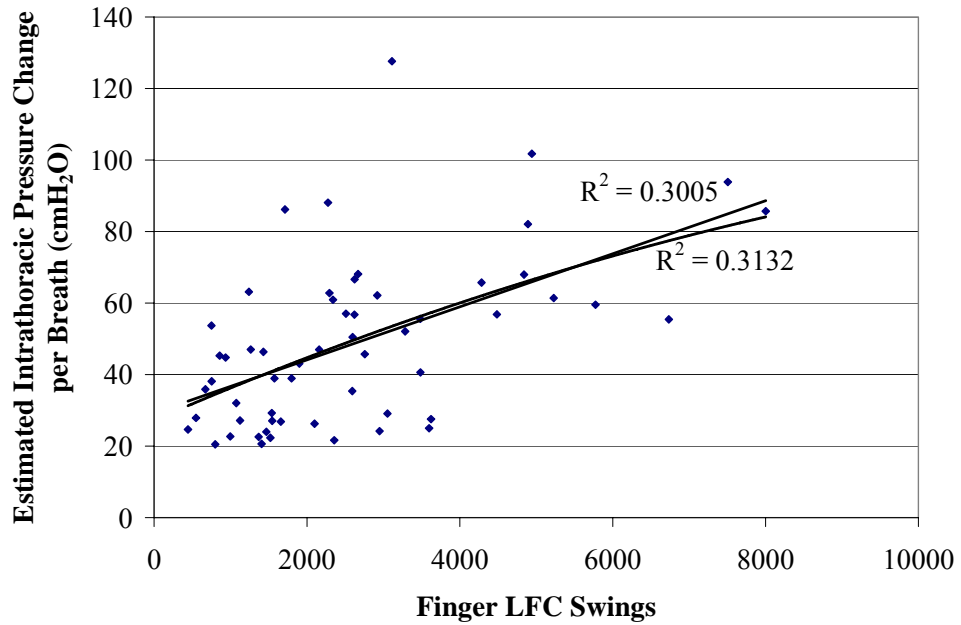


Figure 5-11. Estimated intrathoracic pressure change per breath vs finger LFC Swings in blood donors, after blood loss.

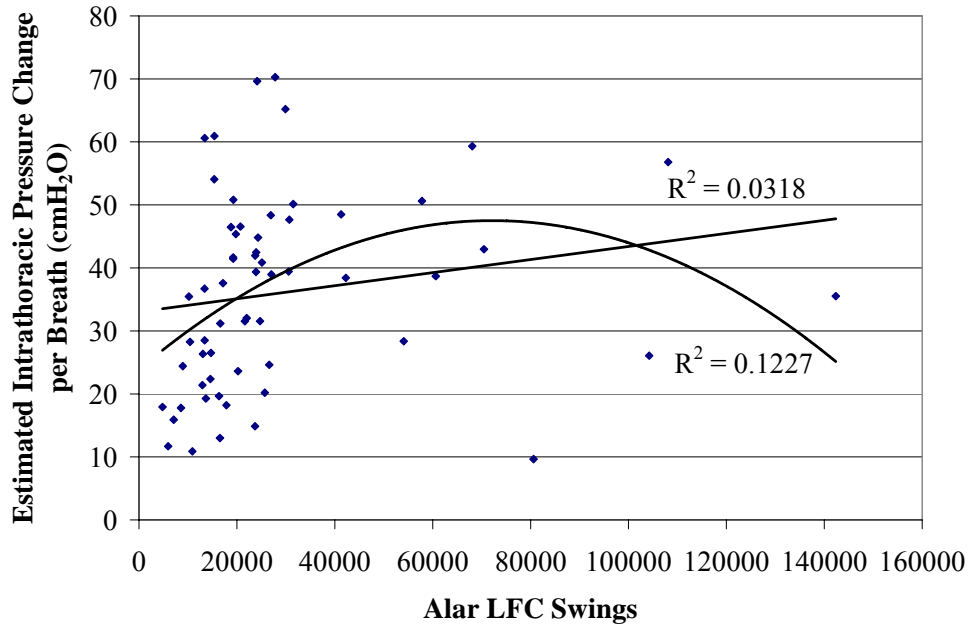


Figure 5-12. Estimated intrathoracic pressure change per breath vs alar LFC Swings in HD patients, before HD.

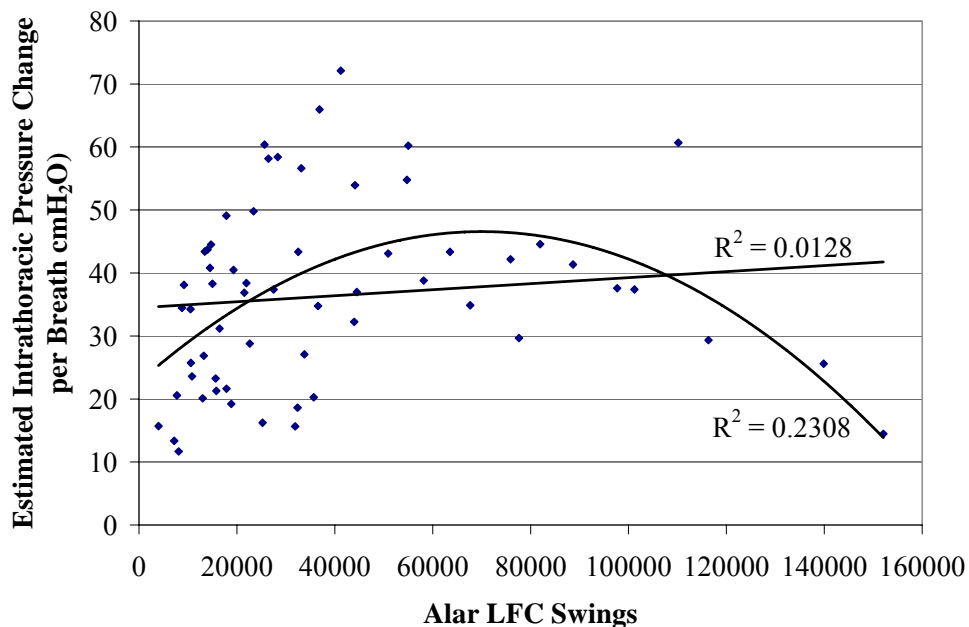


Figure 5-13. Estimated intrathoracic pressure change per breath vs alar LFC Swings in HD patients, after HD

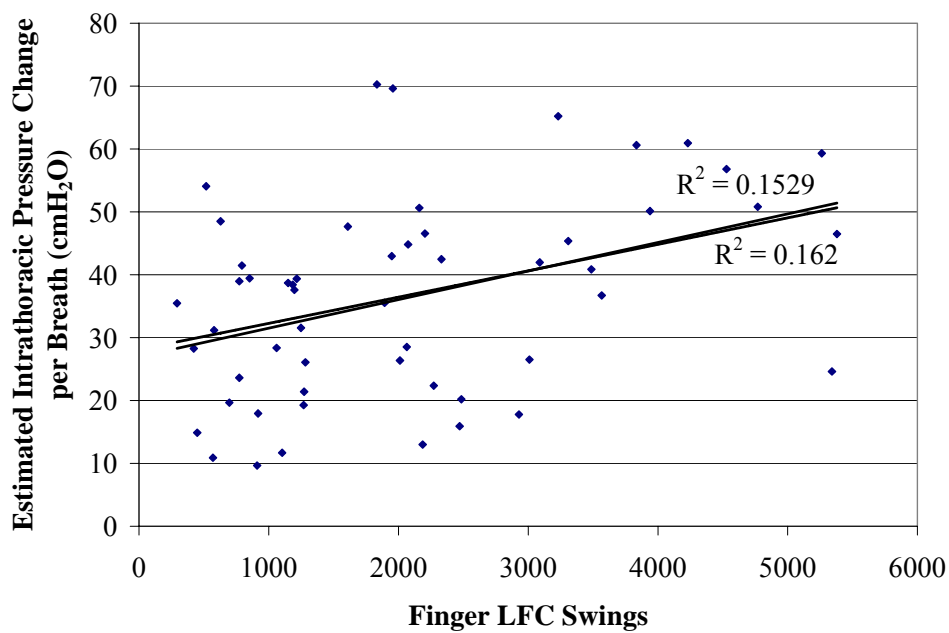


Figure 5-14. Estimated intrathoracic pressure change per breath vs finger LFC Swings in HD patients, before HD.

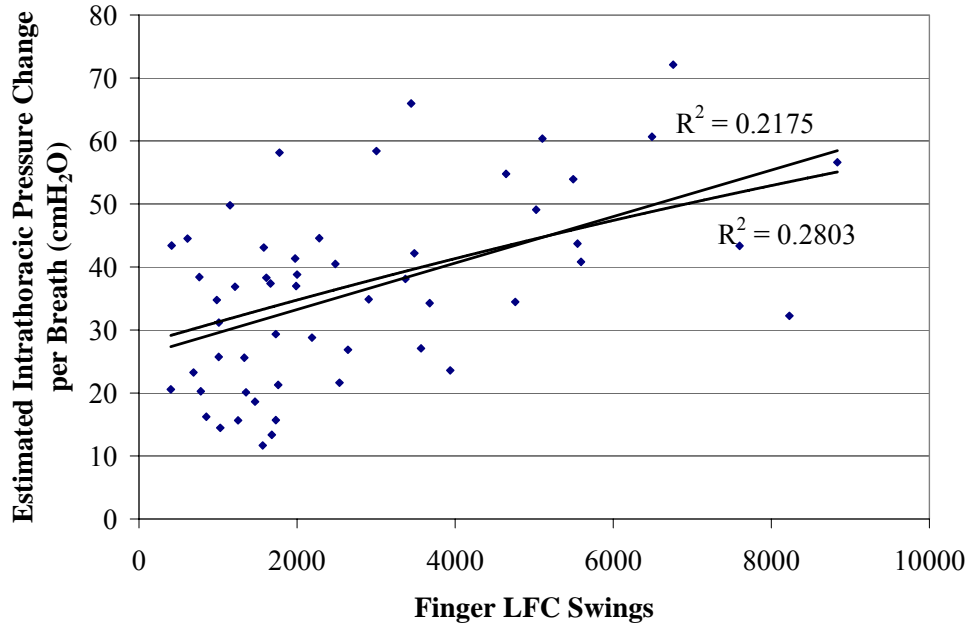


Figure 5-15. Estimated intrathoracic pressure change per breath vs finger LFC Swings in HD patients, after HD.

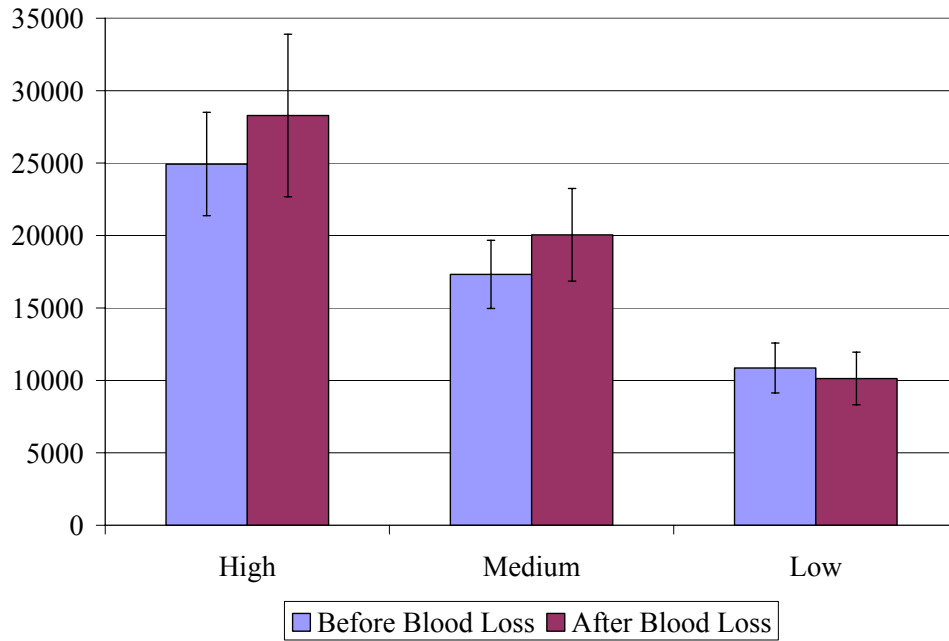


Figure 5-16. The alar LFC Swings of the blood donors, before and after blood loss.

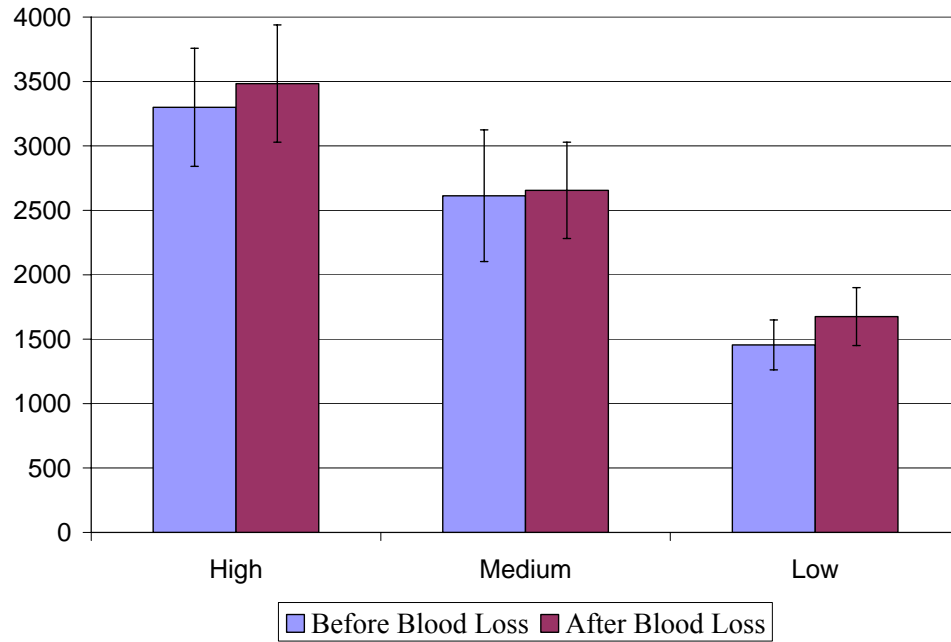


Figure 5-17. The finger LFC Swings of the blood donors, before and after blood loss.

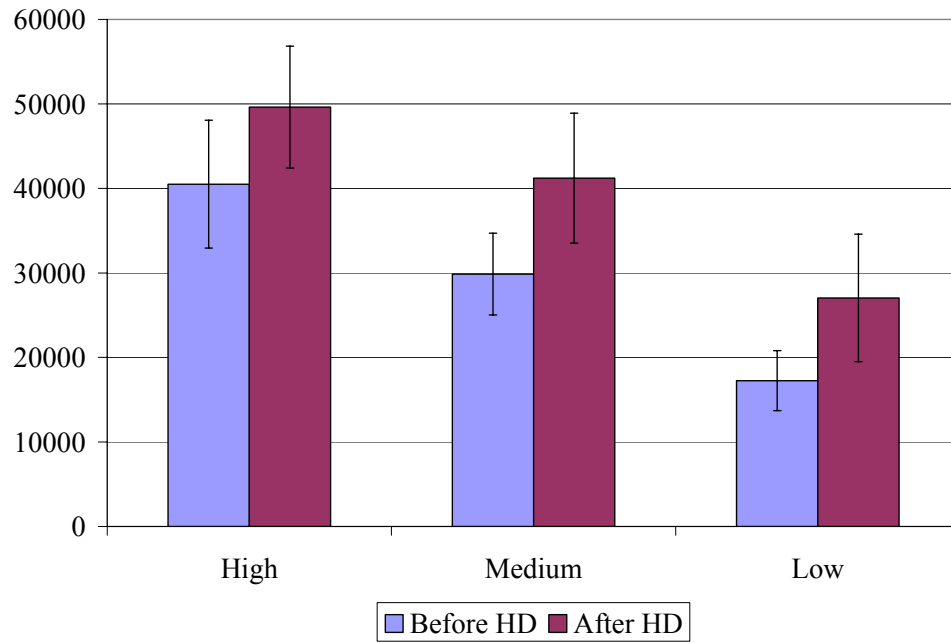


Figure 5-18. The alar LFC Swings of the HD patients, before and after HD.

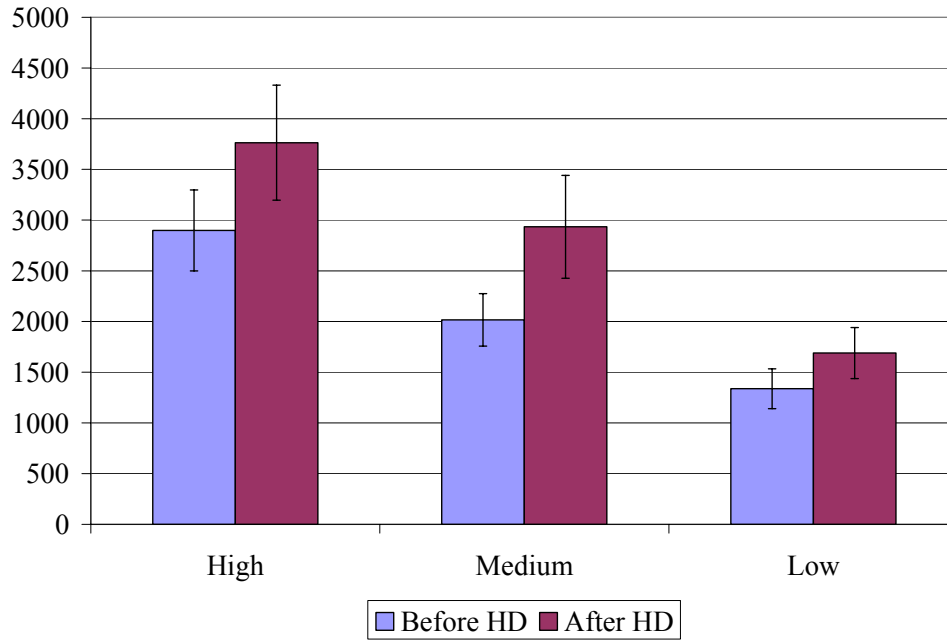


Figure 5-19. The finger LFC Swings of the HD patients, before and after HD.

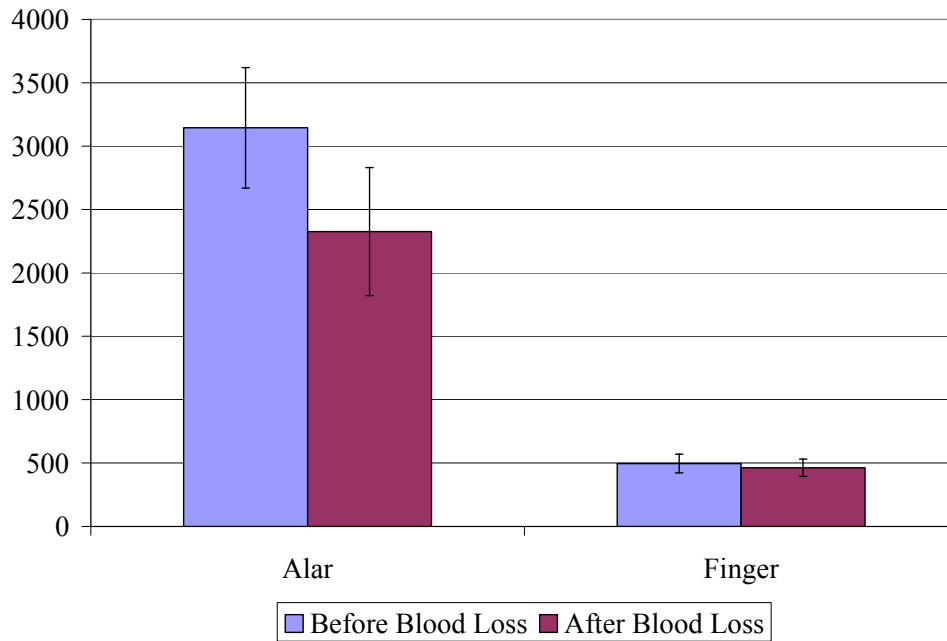


Figure 5-20. The alar and finger PCC MagDiff in blood donors, before and after blood loss.

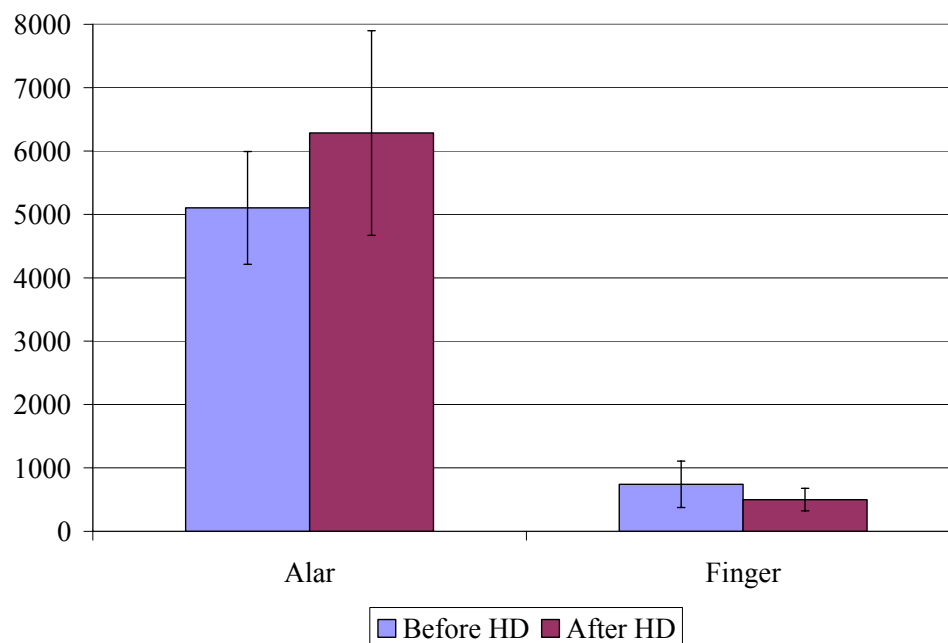


Figure 5-21. The alar and finger PCC MagDiff in HD patients, before and after HD.

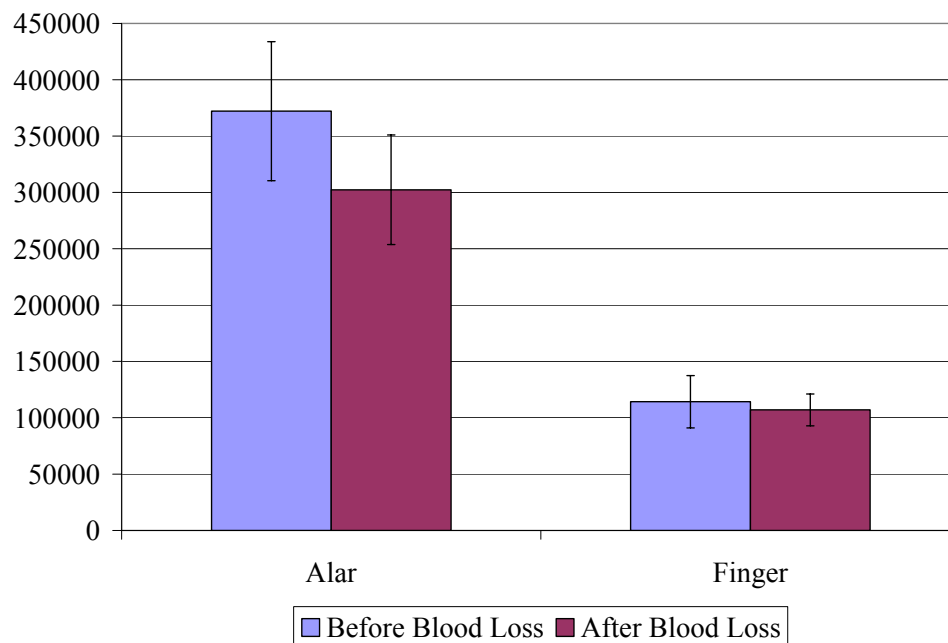


Figure 5-22. The alar and finger PCC MagMean in blood donors, before and after blood loss.

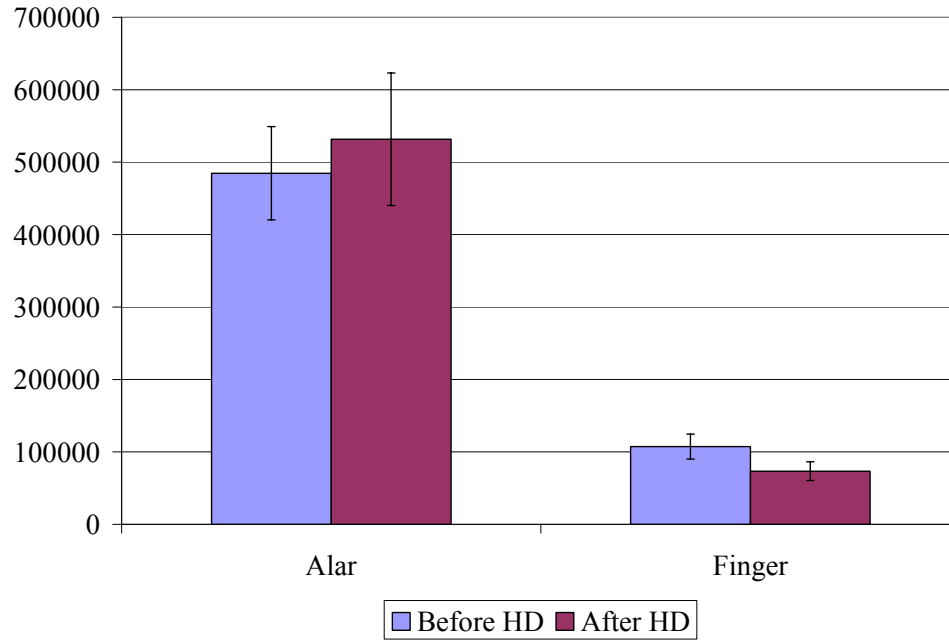


Figure 5-23. The alar and finger PCC MagMean in HD patients, before and after HD.

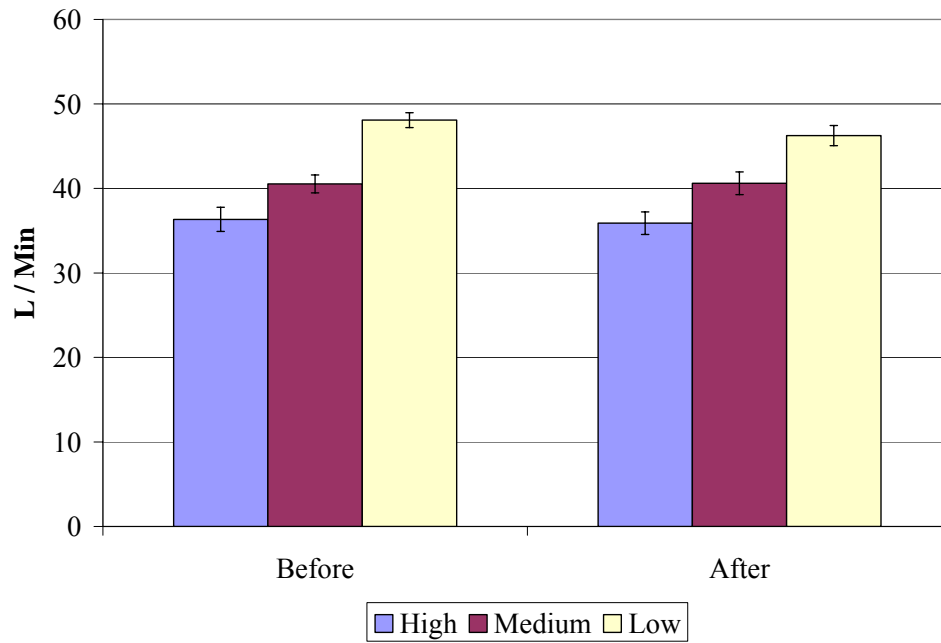


Figure 5-24. The peak inspiratory flow rates in the blood donors, before and after blood loss.

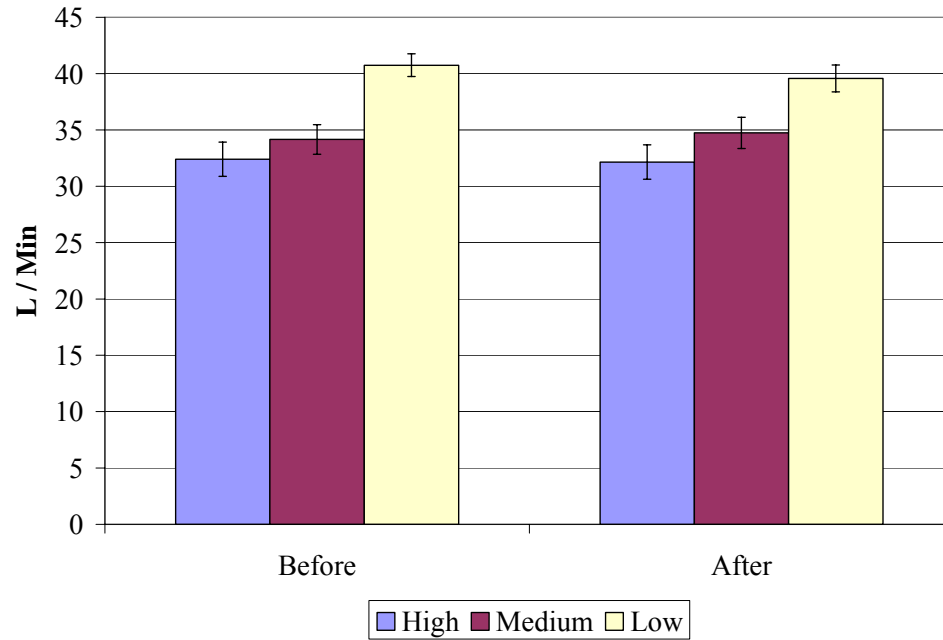


Figure 5-25. The peak expiratory flow rates in the blood donors, before and after blood loss.

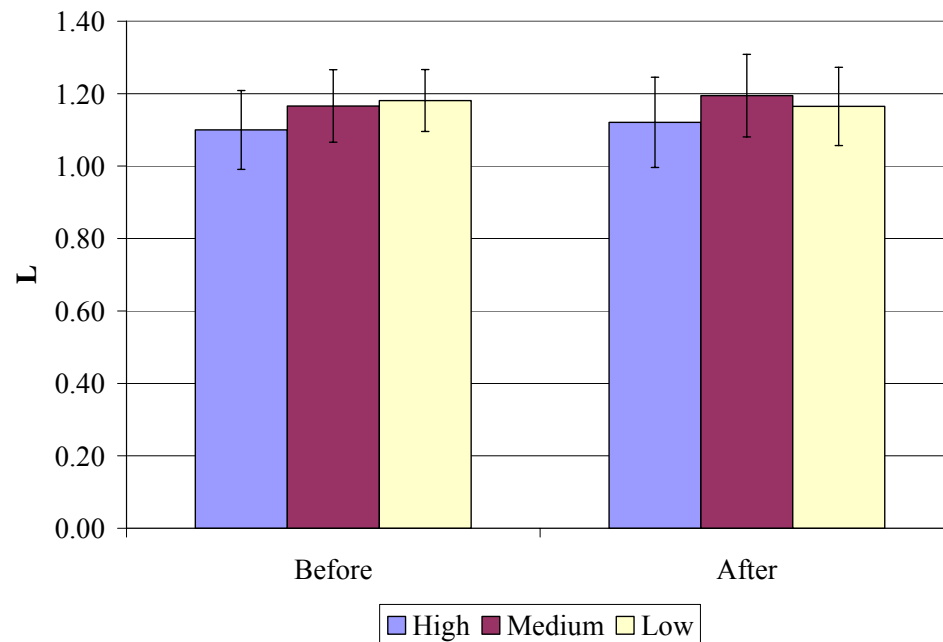


Figure 5-26. The respiratory volumes in the blood donors, before and after blood loss.

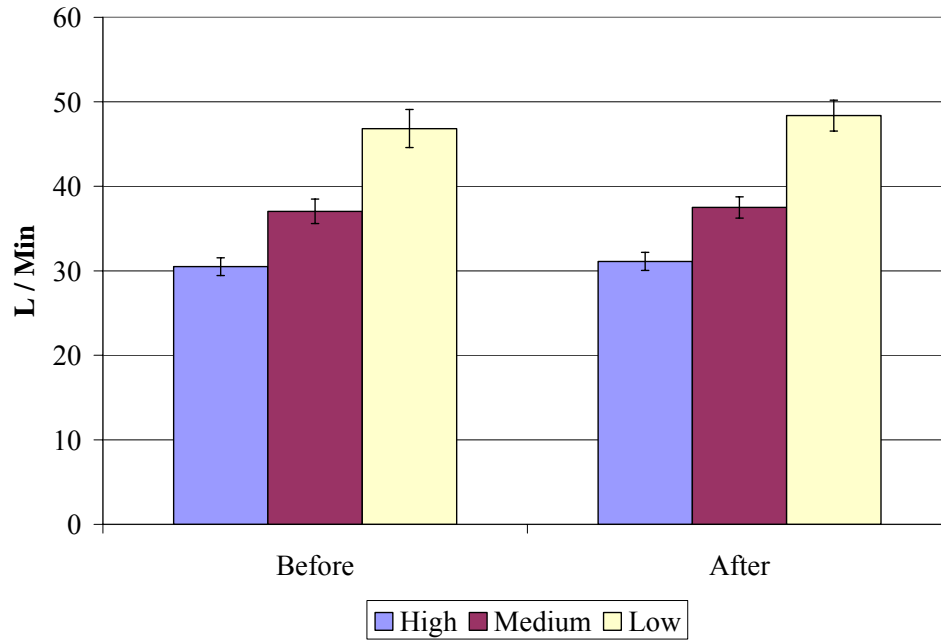


Figure 5-27. The peak inspiratory flow rates in the HD patients, before and after HD.

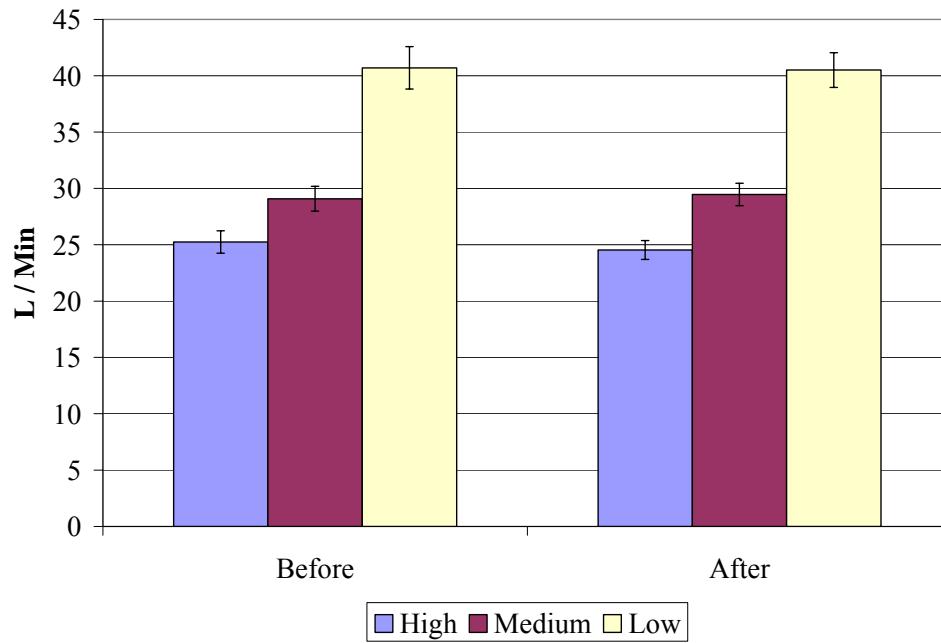


Figure 5-28. The peak expiratory flow rates in the HD patients, before and after HD.

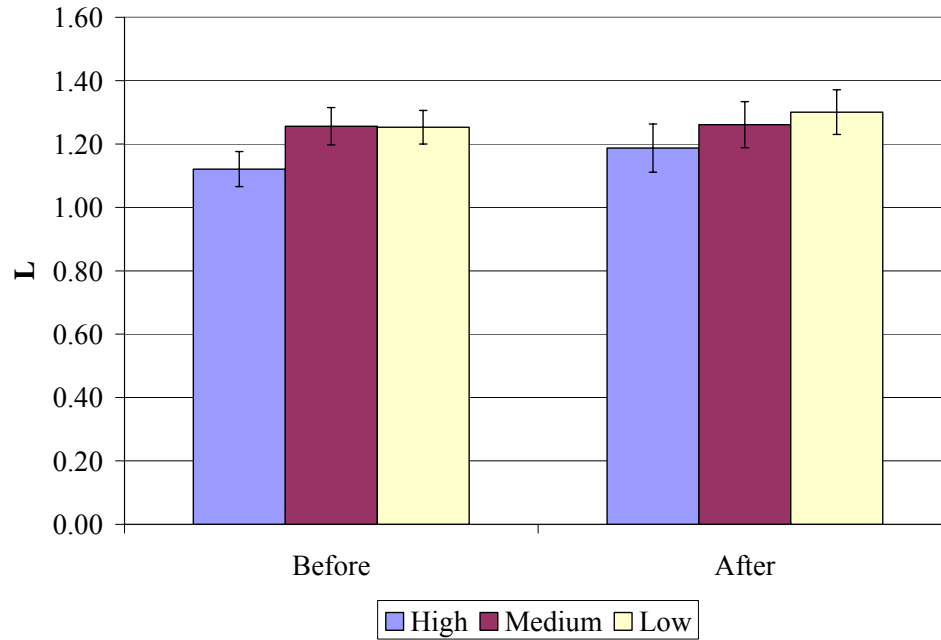


Figure 5-29. The respiratory volumes in the HD patients, before and after HD.

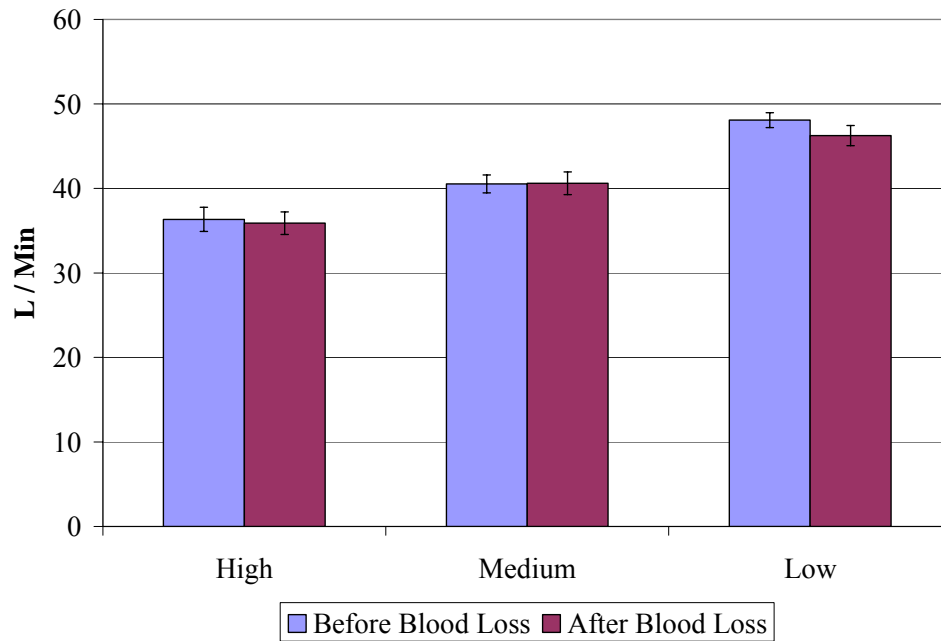


Figure 5-30. The peak inspiratory flow rates of the blood donors for all three levels of respiratory resistance.

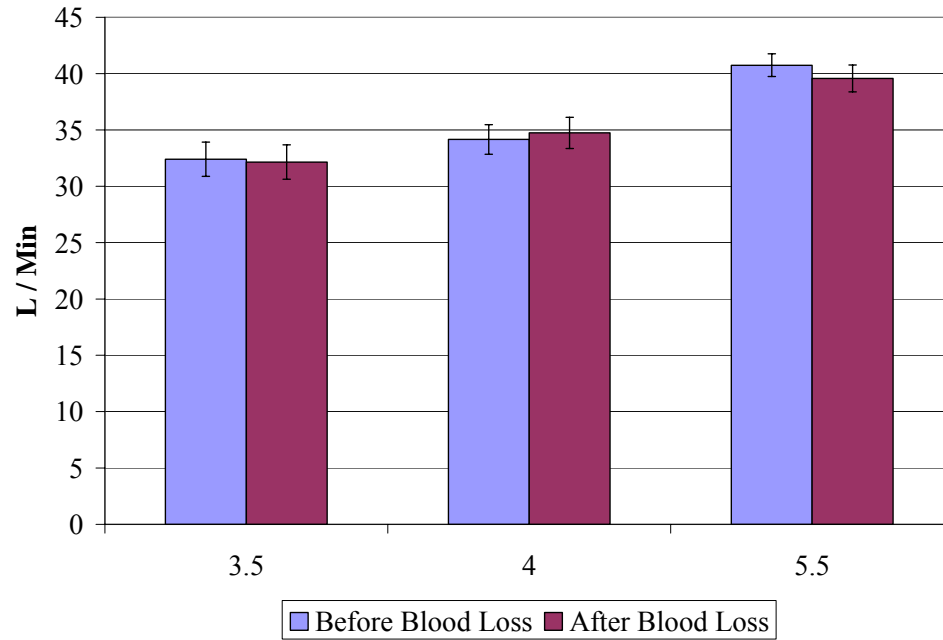


Figure 5-31. The peak expiratory flow rates of the blood donors for all three levels of respiratory resistance.

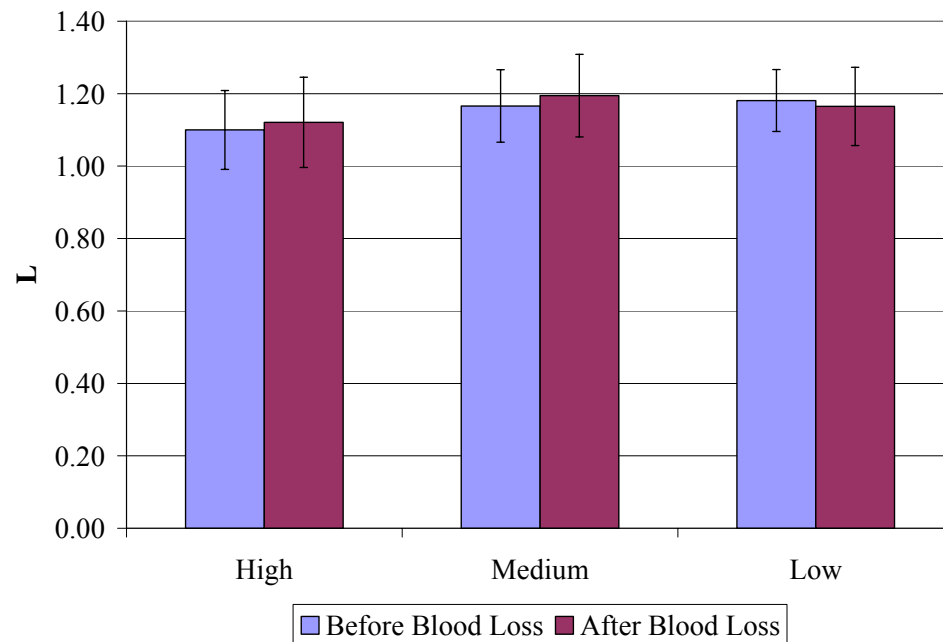


Figure 5-32. The respiratory volumes of the blood donors for all three levels of respiratory resistance.

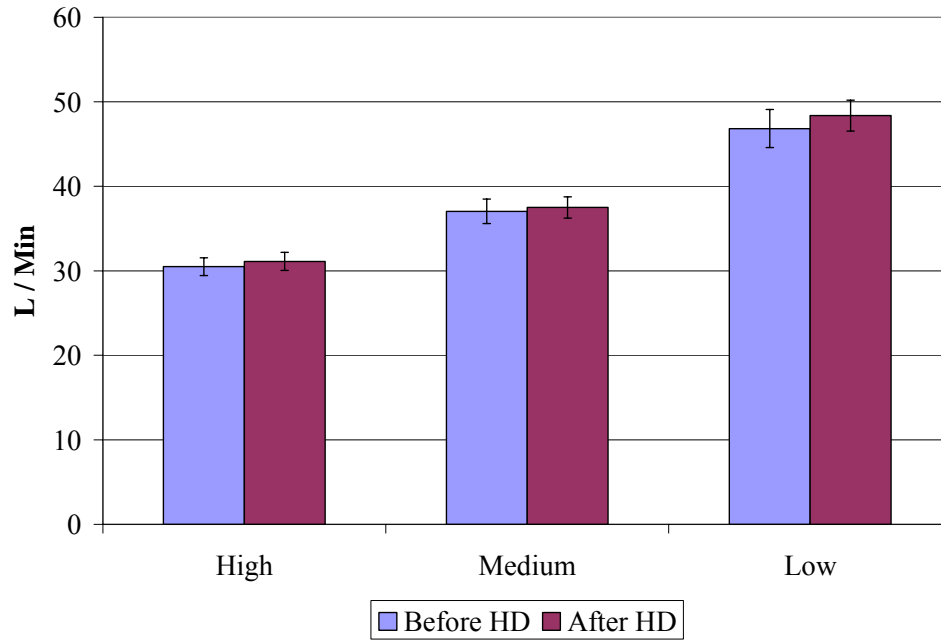


Figure 5-33. The peak inspiratory flow rates of the HD patients for all three levels of respiratory resistance.

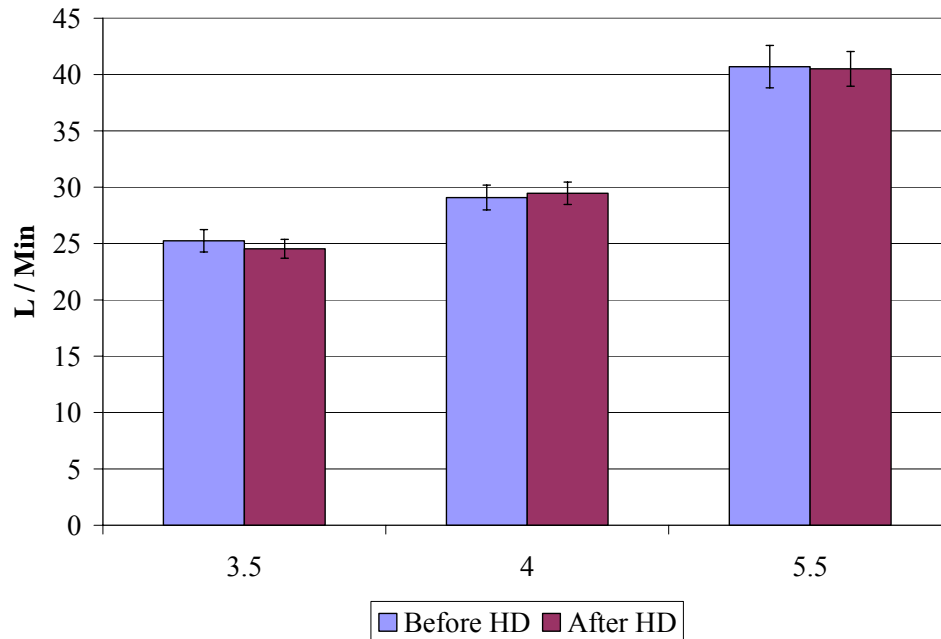


Figure 5-34. The peak expiratory flow rates of the HD patients for all three levels of respiratory resistance.

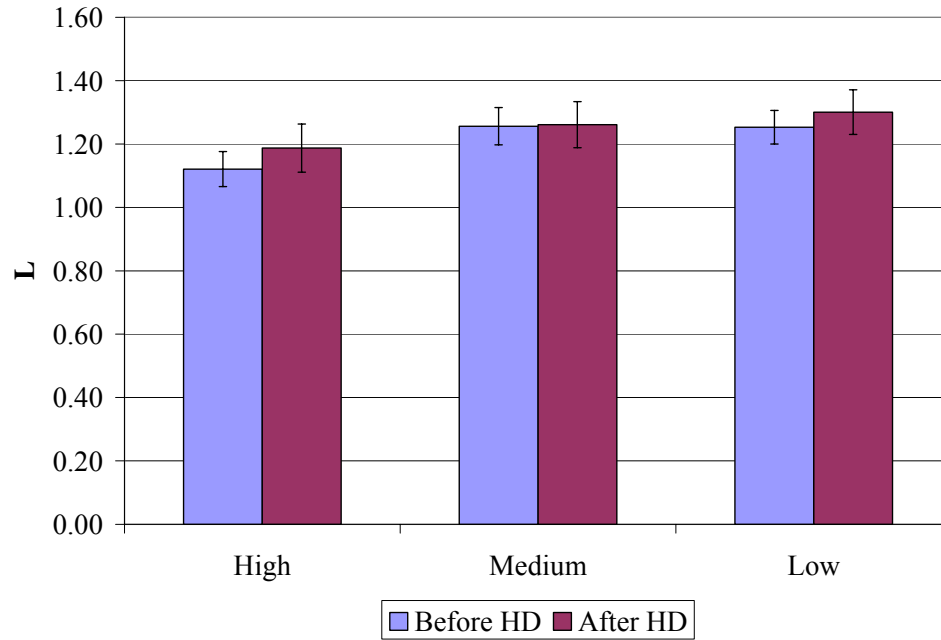


Figure 5-35. The respiratory volume of the HD patients for all three levels of respiratory resistance.

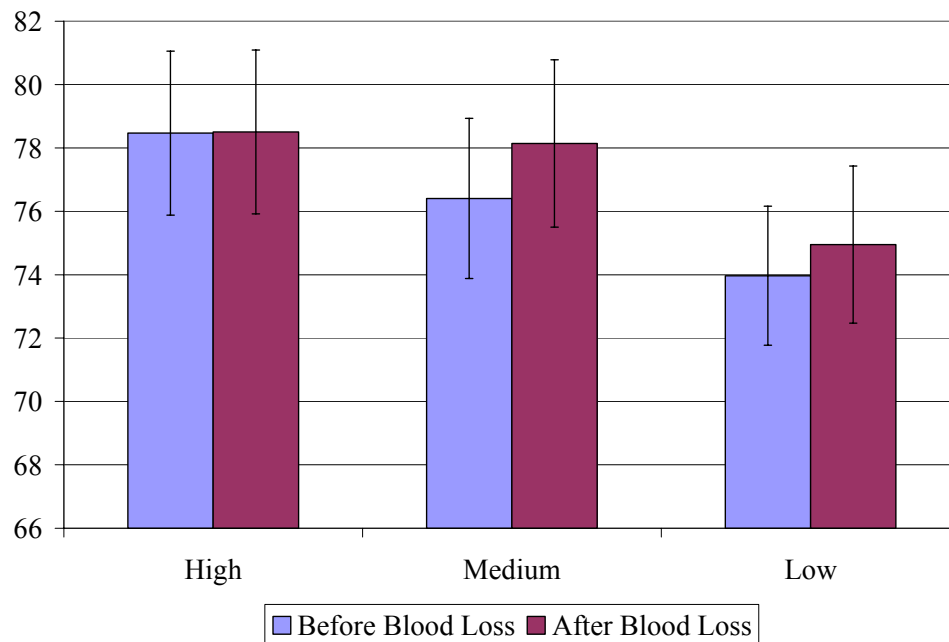


Figure 5-36. The pulse rate of the blood donors for all three levels of resistance.

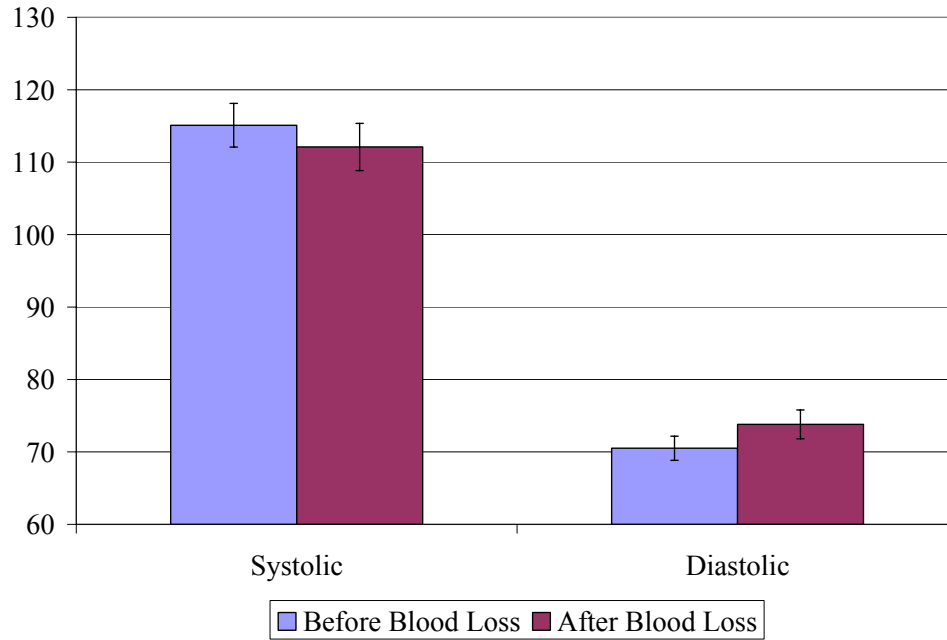


Figure 5-37. The seated blood pressure of the blood donors for all three levels of resistance.

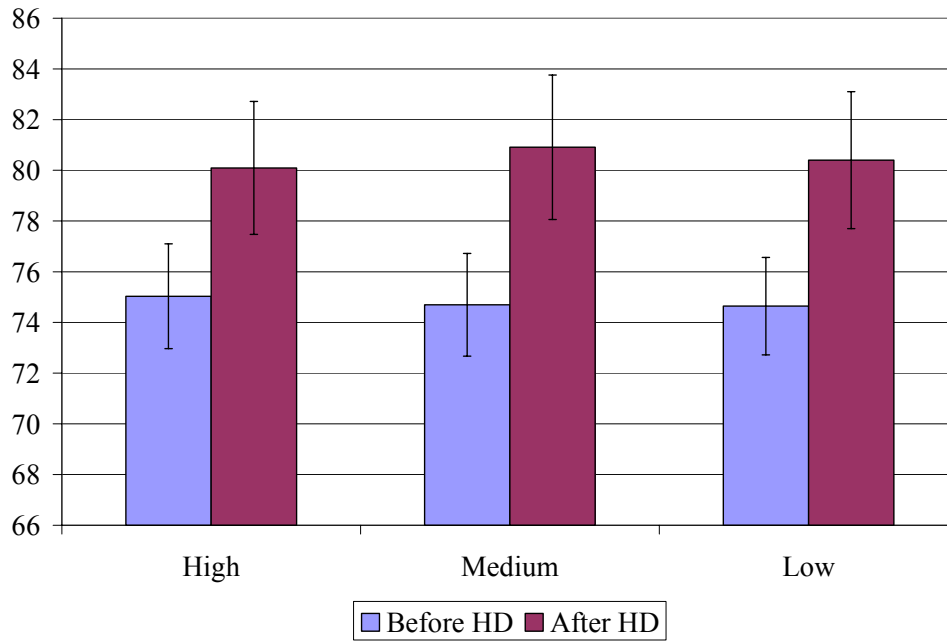


Figure 5-38. The pulse rate of the HD patients for all three levels of resistance.

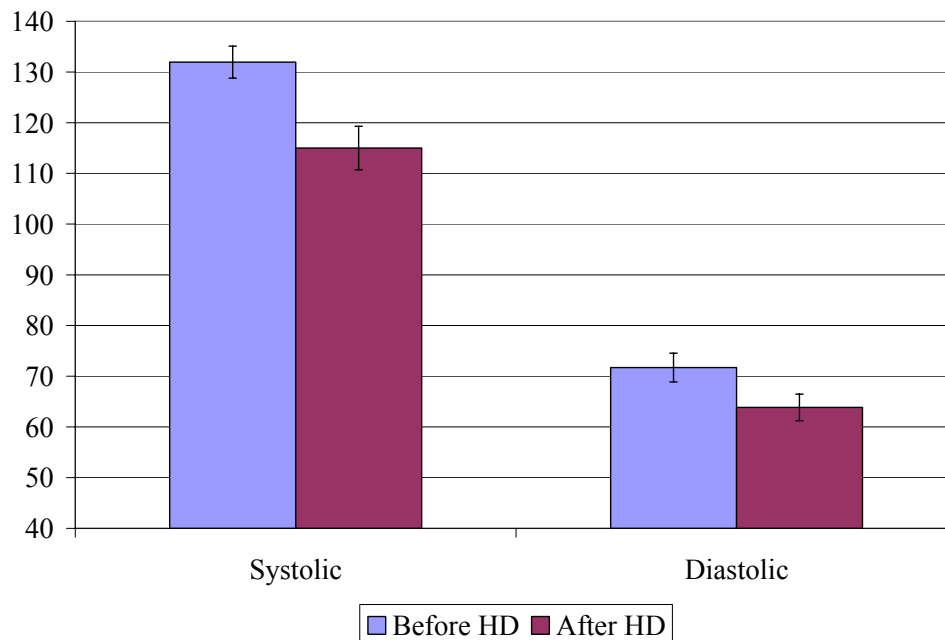


Figure 5-39. The seated blood pressure of the HD patients for all three levels of resistance.

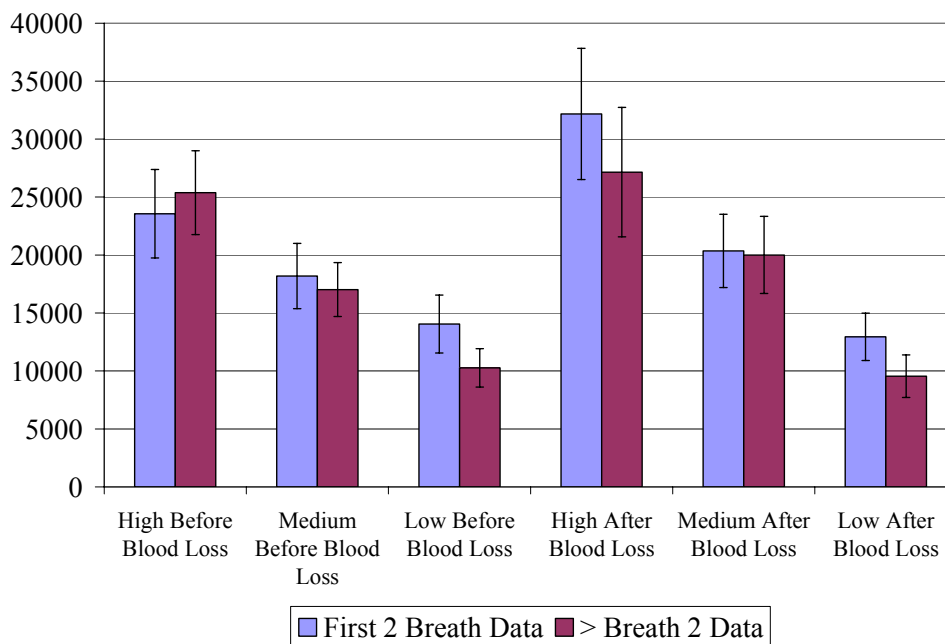


Figure 5-40. A comparison between the alar LFC Swings from the first two breaths and subsequent breaths in the blood donors, before and after blood loss.

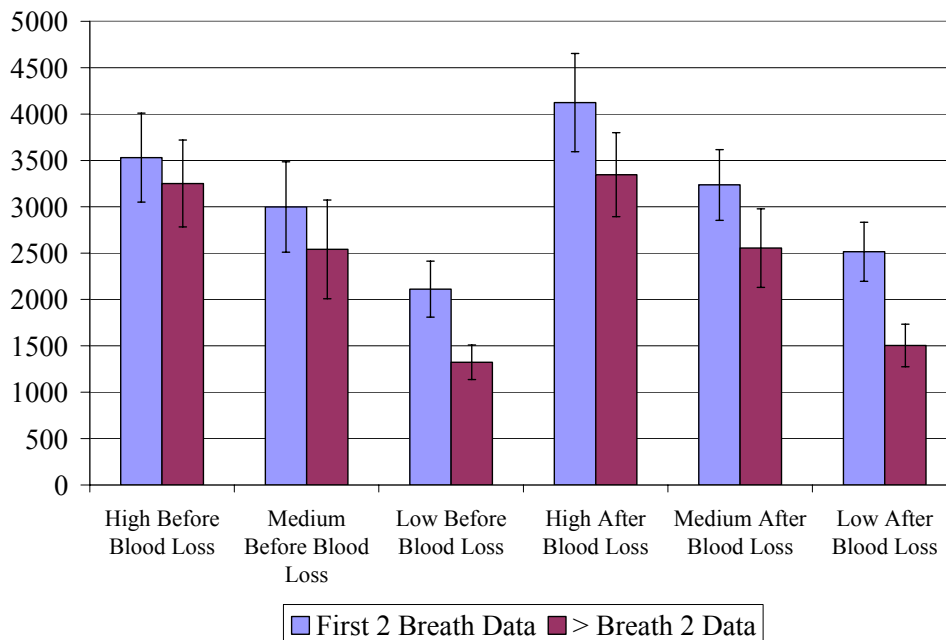


Figure 5-41. A comparison between the finger LFC Swings from the first two breaths and subsequent breaths in the blood donors, before and after blood loss.

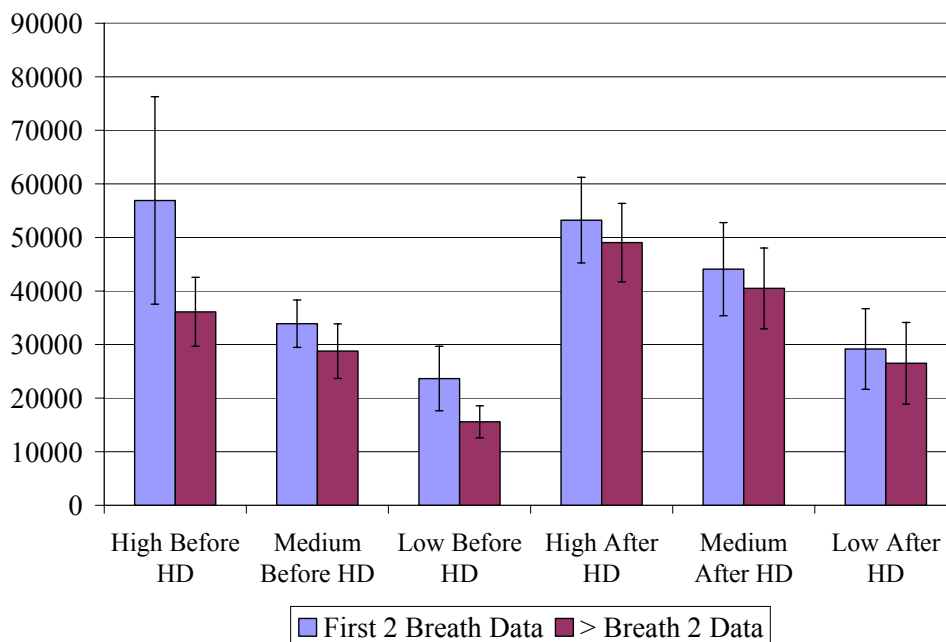


Figure 5-42. A comparison between the alar LFC Swings from the first two breaths and subsequent breaths in the HD patients, before and after HD.

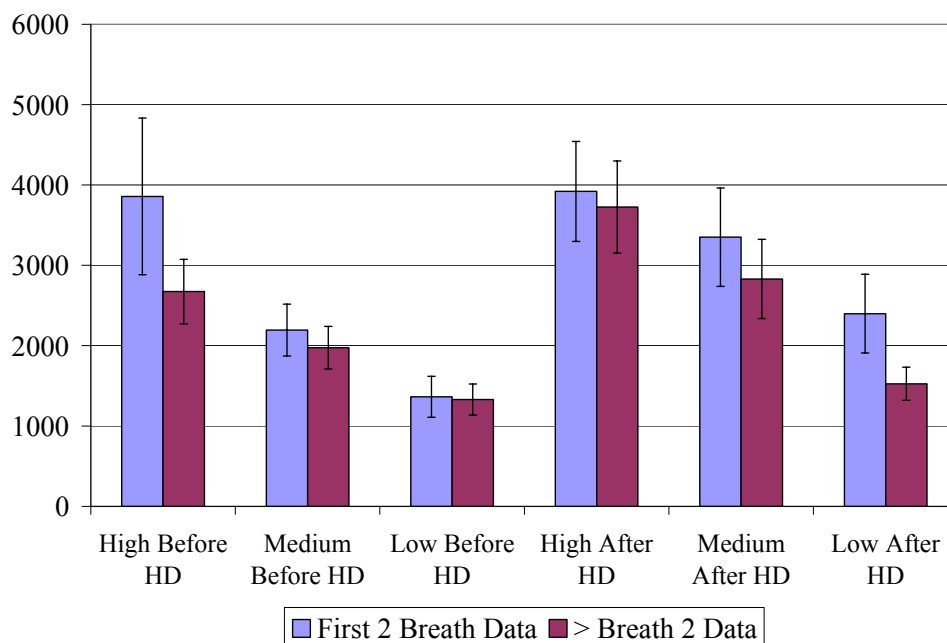


Figure 5-43. A comparison between the finger LFC Swings from the first two breaths and subsequent breaths in the HD patients, before and after HD.

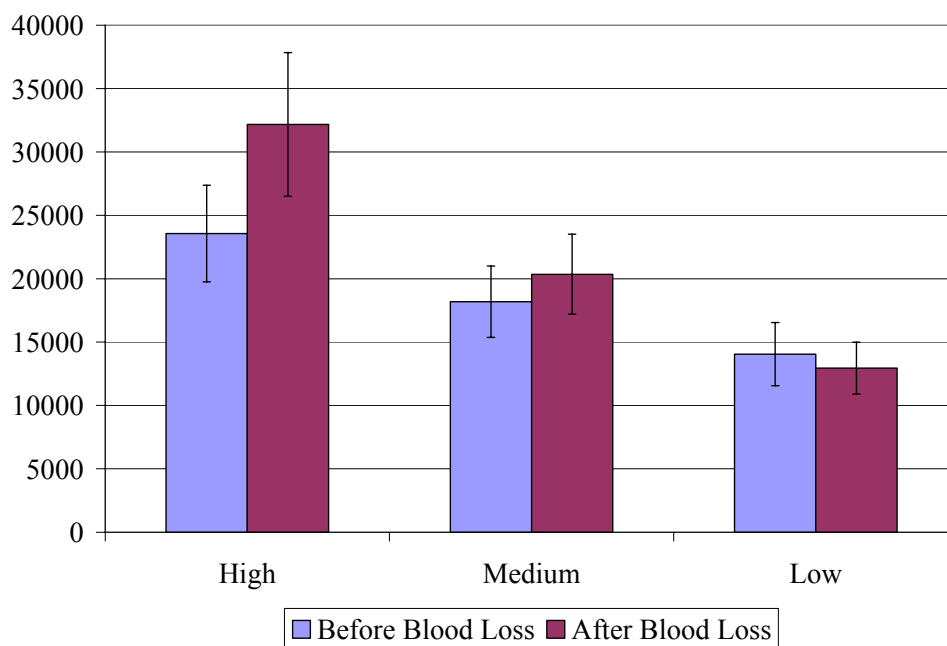


Figure 5-44. The alar LFC Swings from the first two breaths of the blood donors, before and after blood loss.

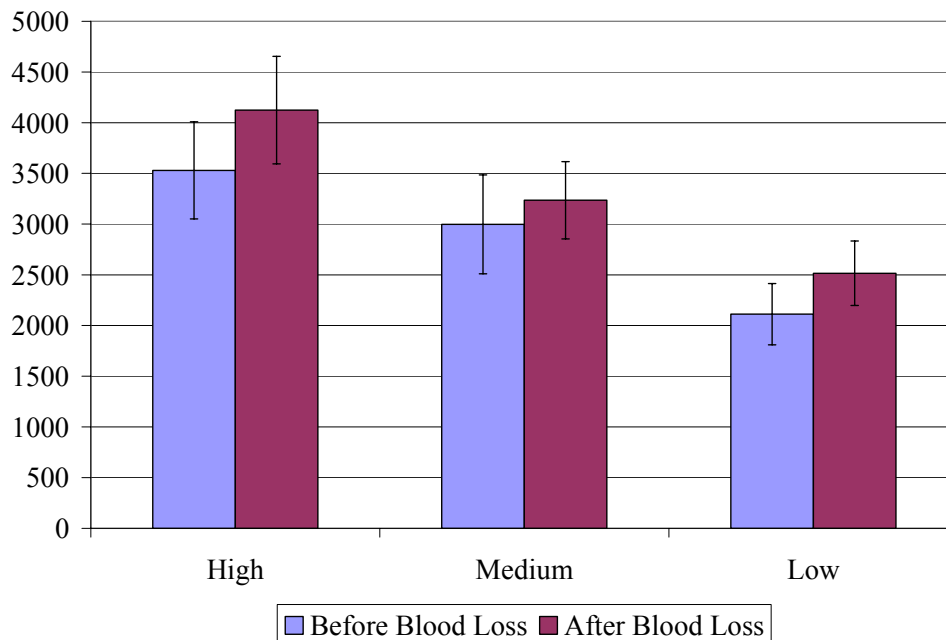


Figure 5-45. The finger LFC Swings from the first two breaths of the blood donors, before and after blood loss.

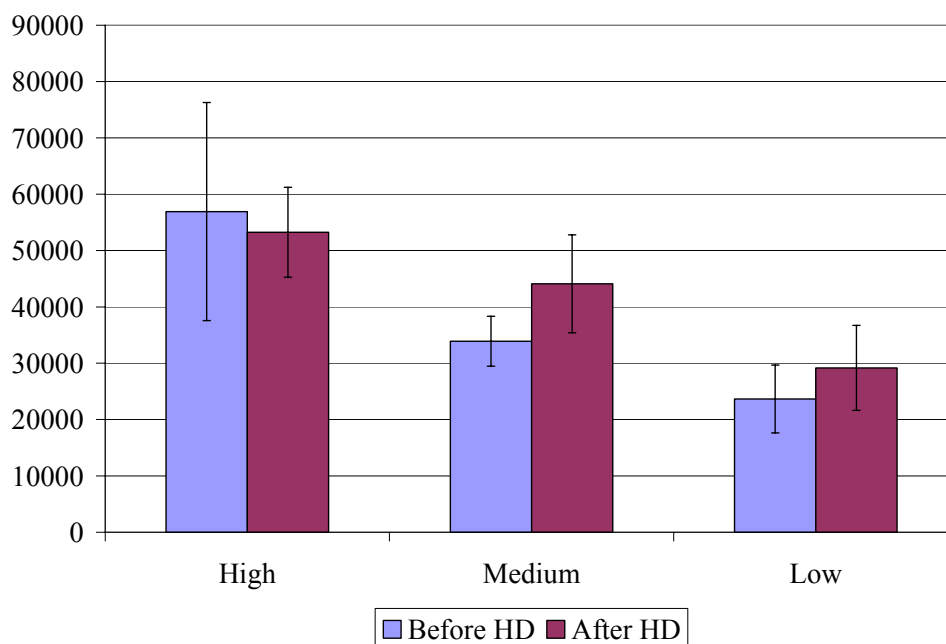


Figure 5-46. The alar LFC Swings from the first two breaths of the HD patients, before and after HD.

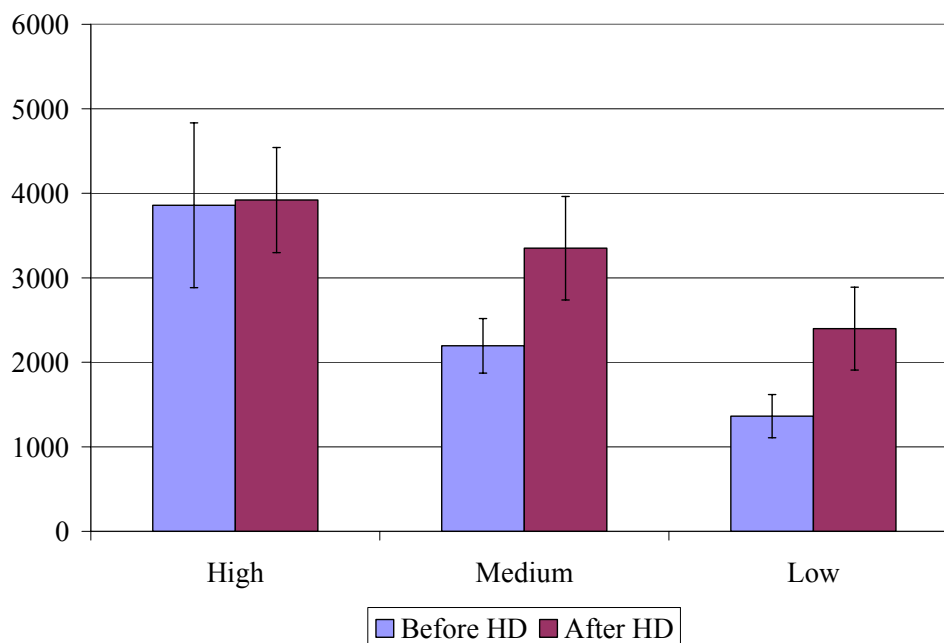


Figure 5-47. The finger LFC Swings from the first two breaths of the HD patients, before and after HD.

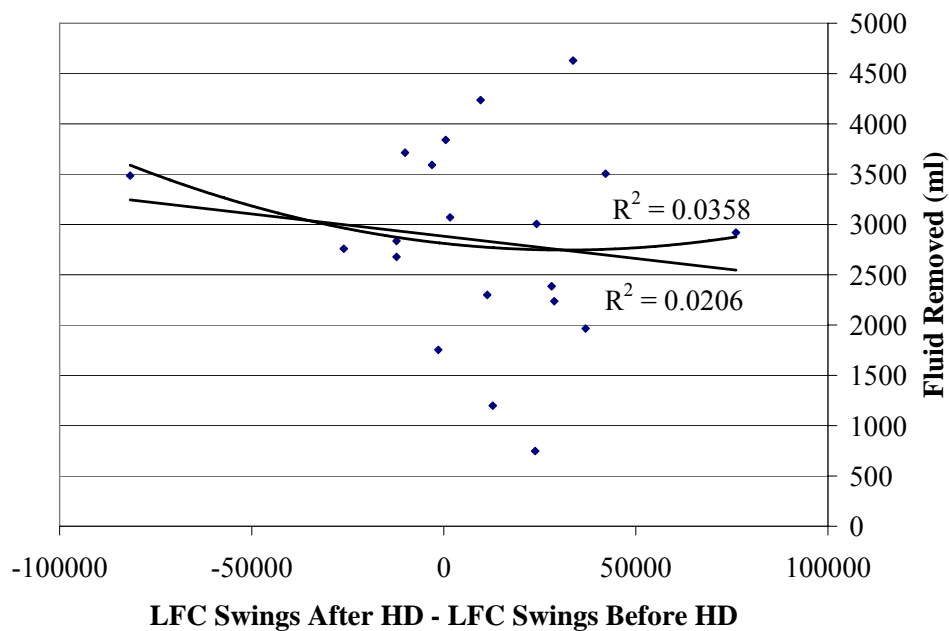


Figure 5-48. Ultrafiltrate removed vs alar LFC Swings in the HD patients for the high resistance level.

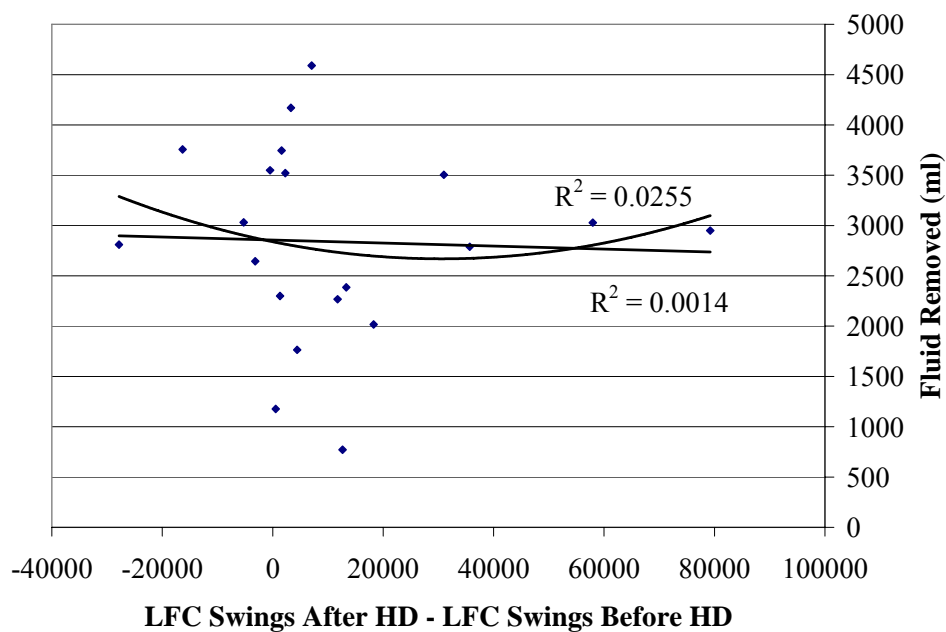


Figure 5-49. Ultrafiltrate removed vs alar LFC Swings in the HD patients for the medium resistance level.

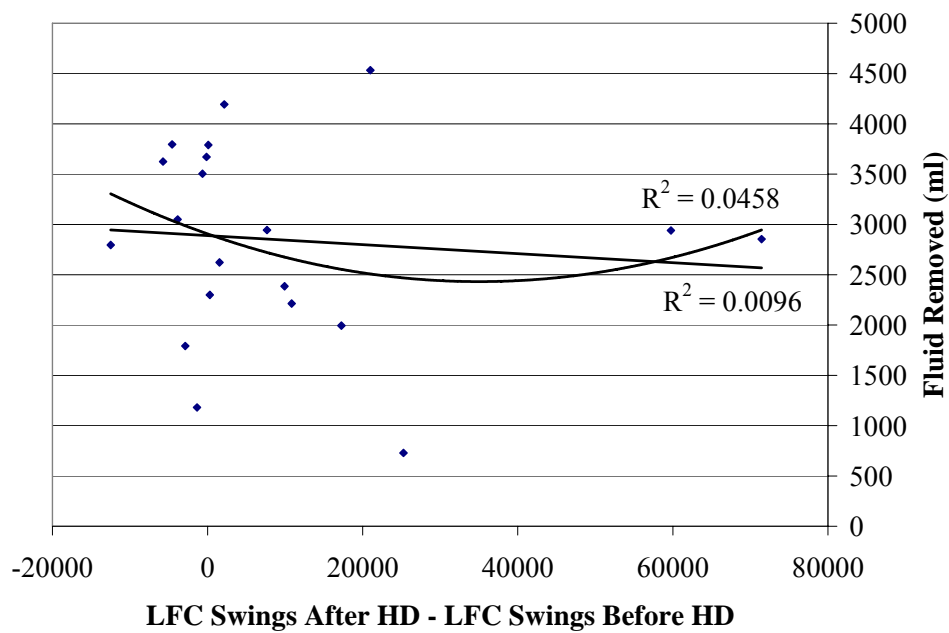


Figure 5-50. Ultrafiltrate removed vs alar LFC Swings in the HD patients for the low resistance level.

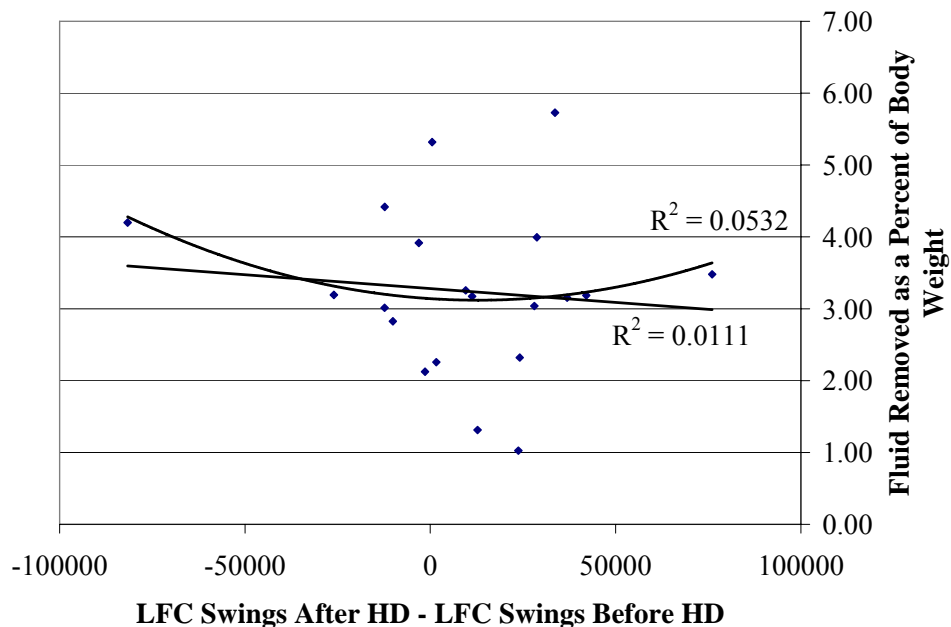


Figure 5-51. Ultrafiltrate removed as a percent of body weight vs alar LFC Swings in the HD patients for the high resistance level.

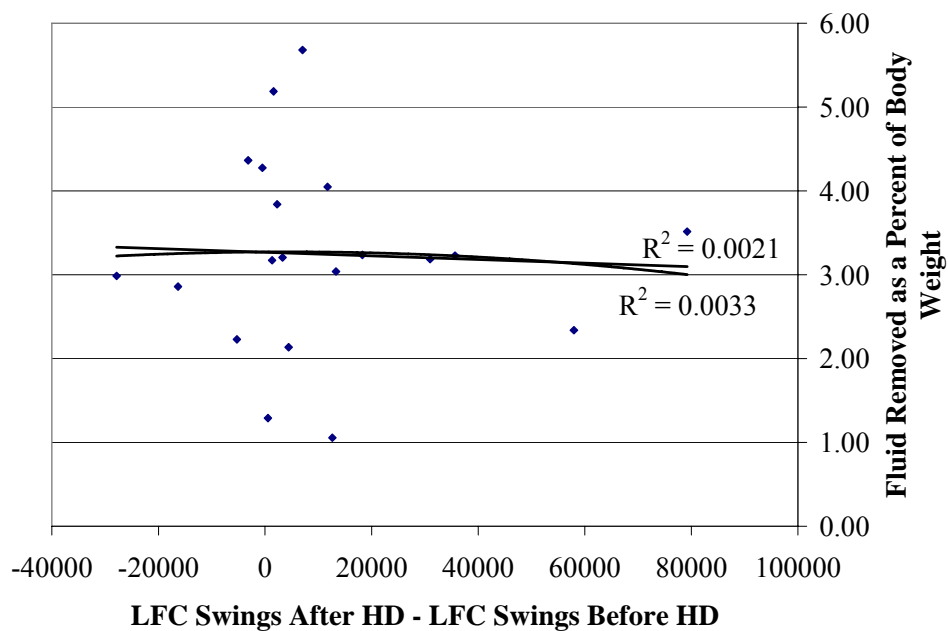


Figure 5-52. Ultrafiltrate removed as a percent of body weight vs alar LFC Swings in the HD patients for the medium resistance level.

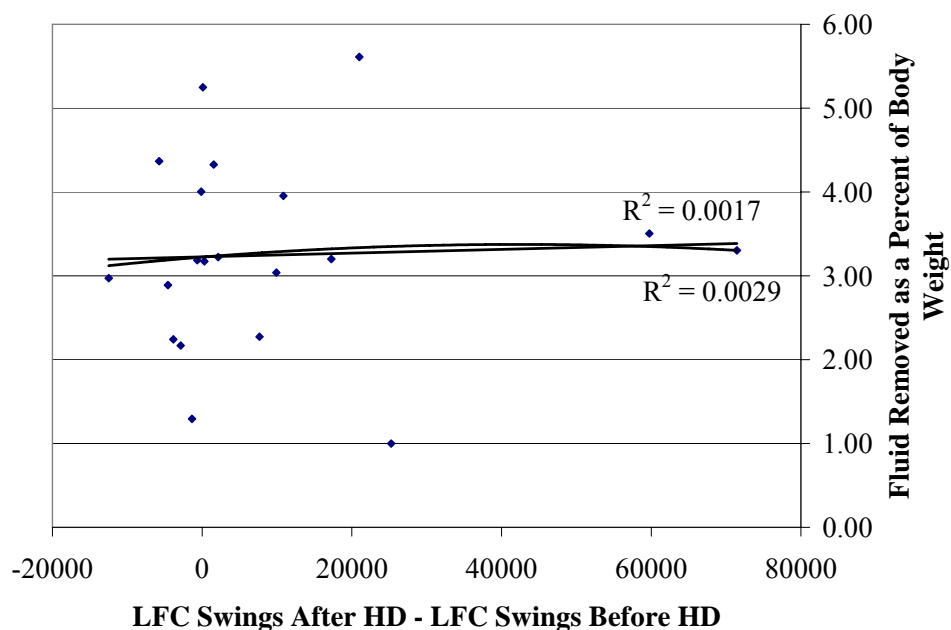


Figure 5-53. Ultrafiltrate removed as a percent of body weight vs alar LFC Swings in the HD patients for the low resistance level.

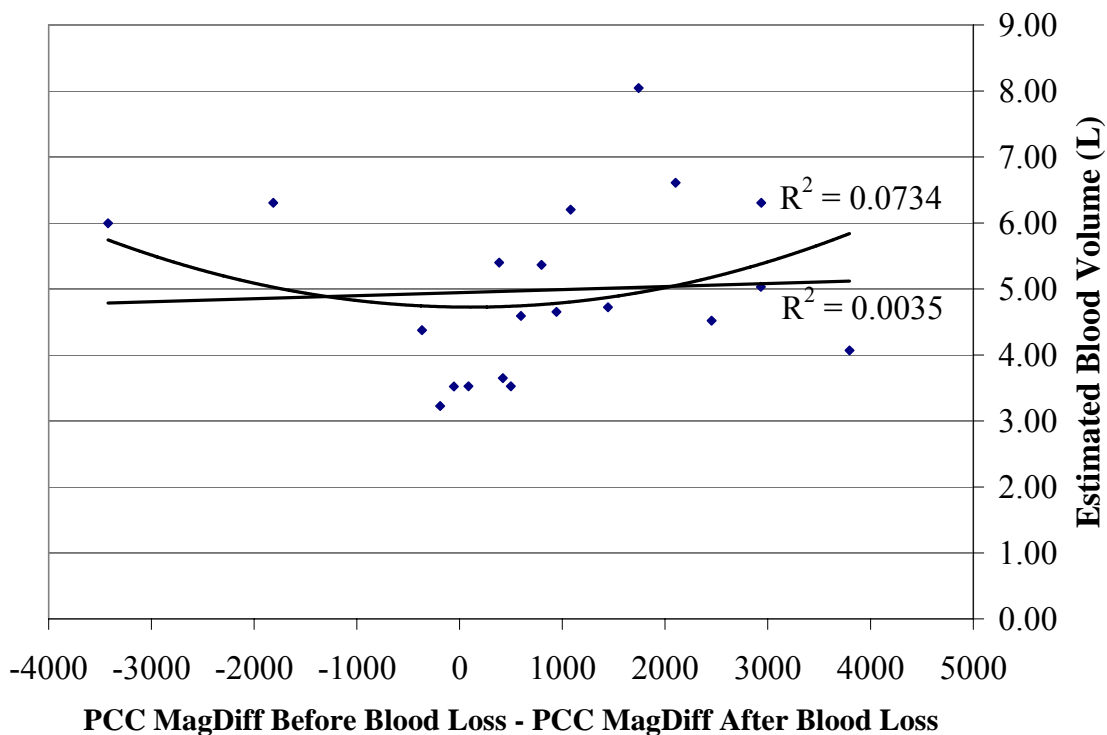


Figure 5-54. Estimated blood volume vs alar PCC MagDiff in the blood donors for the low resistance level.

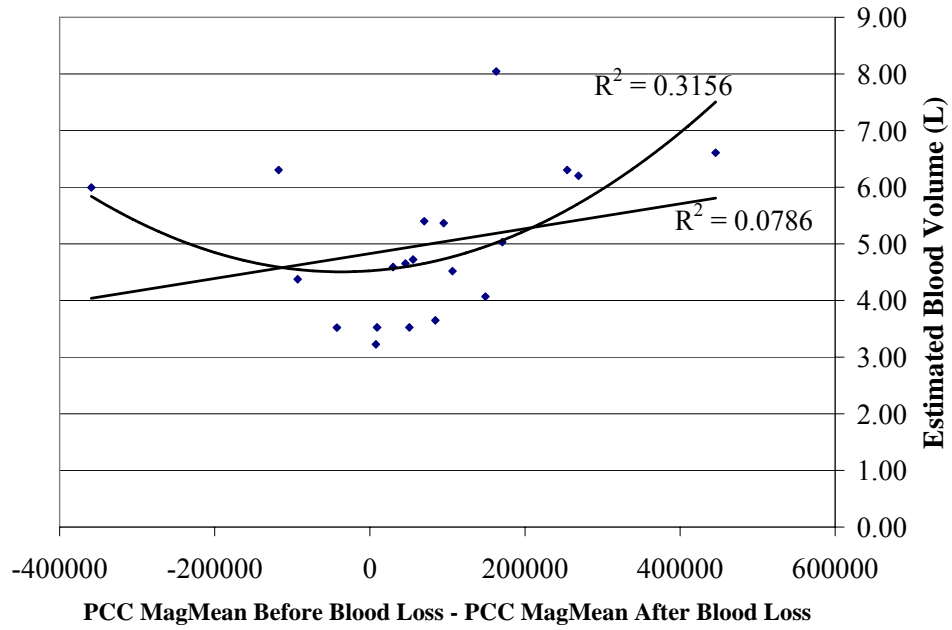


Figure 5-55. Estimated blood volume vs alar PCC MagMean in the blood donors for the low resistance level.

CHAPTER 6
CLINICAL SIGNIFICANCE AND INDIVIDUAL SUBJECT ANALYSIS

Statistical and Clinical Significance

Statistical significance is affected by the sample size, intersubject variability, and the presence of outliers. It does not imply clinical relevance. Various parameters, both physiologic and nonphysiologic, affect the photoplethysmograph (PPG). When the PPG is divided into the low frequency component (LCF) and pulsatile cardiac component (PCC), the physiologic parameters affecting both are easily explored.

The two main contributors to the PCC are the stroke volume and arterial compliance. Factors affecting stroke volume include preload, afterload, and contractility. Factors affecting the preload include venous return, mitral insufficiency, mitral stenosis, aortic insufficiency, fluid volume, medications, posture, and intrathoracic pressure (Topol et al. 2002). Factors affecting the afterload include aortic valve stenosis, peripheral constriction, hypertension, polycythemia, medications, vasoconstriction due to temperature, and intrathoracic pressure. Factors affecting contractility include medications, sympathetic tone, hypercalcemia, hypoxia, hypercapnia, and heart disease. Factors affecting arterial compliance include age, hypertension, sympathetic tone, medications, impedance by venous blood or edema, and temperature.

The LFC represents venous blood; hence anything affecting the movement of venous blood affects the LFC. These factors include blood pressure, gravity, valves, the skeletal muscle pump, respiratory pump, sympathetic tone, venous blood volume, and venous compliance.

Nonphysiologic factors affecting the LFC and PCC include artifact caused by subject or probe movement, excessive light interference and 60 Hz interference. For each individual subject, most these factors were controlled and did not change.

The PPG data obtained from the finger is very prone to confounding variables. The finger PPG is sensitive to the positioning of the hand relative to the heart. Slight positional adjustments of the hand may result in large compartmental shifting of pooled blood, affecting the LFC and PCC. Additionally, the hands are particularly sensitive to the affects of ambient temperature and local blood flow is moderated accordingly. These variables were not controlled in this study. Even though several statistical analyses showed significance in the finger comparisons, individual subject finger analyses were not performed due to the possible presence of additional confounding variables that were not controlled for and can not be identified. Additionally, it is suspected that central sites will be the future of PPG monitoring; hence the alar was the focus of this analysis. Finally, the individual finger data was excluded for the sake of brevity.

Individual Analysis

Hypothesis 1

The LFC Swings differed statistically across the three levels of resistance. This indicates that the LFC could potentially be used to detect major airway resistance changes in a variety of patient populations. The data for each individual subject for each population were explored for trends.

Of the factors affecting the LFC, only changes in the intrathoracic pressure caused by the respiratory pump varied in this study. Since this comparison was made for each subject individually, and the position of the subject was constant during the breathing

study, blood pressure, gravity caused by position, venous valves, the skeletal muscle pump, sympathetic tone and venous compliance were all constant.

First, individual data for the three resistance levels were compared for trends in all blood donors and HD patients. The intersubject variability was high in the alar LFC Swings of the blood donors and HD patients. Possible causes of this variability include thickness of the alar, pigmentation of skin, and light emitting diode (LED) power of the pulse oximeter probe. Subjects with a thin alar, or those who were not darkly pigmented, required a power of <50 for proper functionality of the LED. Other subjects required the maximum LED power of 254. Additionally, the placement of the alar probe affects the baseline amount of light striking the photodiode (PD), affecting the LFC. To eliminate these variables, the alar probes were secured with adhesive tape. Assuming each probe was in the same position for the duration of each breathing study, these variables would be controlled for in each individual subject. Intersubject variability, however, would still be high. Changes in the positioning of the probe causes changes in the LED power, hence the LED power was monitored. Any shifting in the alar probe not causing LED power change was deemed insignificant.

Overall, the alar LFC Swings decreased with decreasing resistance. In subject 9, the LFC Swings for the low level of resistance were greater than the medium level of resistance (Figure 6-1). Of the 40 total comparisons, there were 11 instances of unexpected results in the blood donors (Figure 6-2) and in the HD patients (Figure 6-3).

In HD patient 13, the alar LFC Swings behaved opposite to what was expected following HD and as expected before HD. Also, of the 40 total subjects from both

populations, only three had alar LFC Swings that behaved unexpectedly both before and after fluid loss.

To understand why certain subjects behaved differently from the majority of the others, several follow-up analyses were conducted. First, the inspiratory and expiratory flow rates were analyzed for trends (Figure 6-4). The relationship between the peak respiratory flow rates and volumes and the LFC Swings for each individual subject was explored. The alar LFC Swings of blood donor subject 9 behaved differently from the other nine subjects (Figure 6-1). The peak inspiratory flow was most likely not the cause (Figure 6-4). In several of the individual breathing studies the flow rates and volumes were consistent and in others they differed. The reasons for the unusual LFC Swing data in subject 13 and in all other subjects whose data behaved differently were not caused by variations in the respiratory flow rates or volumes.

Each breathing study lasted only several minutes, yet in several cases the LED power of the alar probe changed, indicating a shift of the alar probe. Of the 80 total analyses, the LED power changed during a breathing study in 18 of them. Of the 18, only six occurred in subjects whose LFC Swing data behaved inconsistently. Of the 22 breathing studies whose data was inconsistent, the LED power changed in six of them. Based on these results it is unlikely that changes in the LED power affected the LFC Swings. It does affect the baseline light striking the photodetector but does not change the low frequency change in light striking the photodetector caused by the respiratory resistance.

In summary, the differences in the three levels of resistance were statistically significant. Of the 80 individual analyses, 72% of the results were expected, with the

LFC Swings decreasing as resistance decreased. This indicates that on a per-subject basis, the LFC Swings can be used to detect major changes in respiratory resistance with corresponding changes in intrathoracic pressure. In 28% of the individual studies, the LFC Swings in at least one of the resistance levels did not decrease with decreasing resistance. The reasons for these individual variations are unclear but do not seem to be caused by changes in respiratory flow or volumes, or changes in LED power. Although these individual aberrations did not affect the statistical significance of the populations, they do create the need for follow-up studies to identify their cause when considering the development of a clinical device.

Hypothesis 2

The intrathoracic pressure changes, as estimated by Equation 3-3, did not statistically correlate with the LFC Swings. The intersubject variability was the main reason for this lack of relationship. The high resistance LFC Swings in some subjects was approximately equal to the low resistance LFC Swings in other subjects. While each individual subject may have behaved as expected, the variability between subjects caused a failure to show an overall relationship.

For each subject, the before and after fluid loss states were analyzed separately. For this analysis the individual breath data was not averaged. This resulted in approximately ten breaths of data for each resistance level, both before and after fluid loss. A plot of the first blood donor is shown (Figure 6-5). Each data point represents the LFC Swing of an individual breath. There are three groups of data points present, each group representing a different resistance level. There was nearly a significant relationship. This analysis was performed for the 20 blood donors and 20 HD patients both before and after fluid loss. The results are presented (Tables 6-1 and 6-2) where the

numbers represent the number of analyses that fell within that range of R^2 values. In the blood donors and HD patients, approximately half resulted in R^2 values $< .5$ with very few being $> .8$.

The LFC Swing analysis presented is not sensitive enough to reproducibly correlate with the estimated intrathoracic pressure changes per breath as estimated by the Equation 3-3. This is possibly due to the inapplicability of the equation in human subjects. Future studies should measure esophageal pressure, an estimate of intrathoracic pressure, and compare these measurements to LFC Swings in different patient populations.

Hypothesis 3

The LFC Swings increased significantly in the HD patients and did not change in the blood donors. Since this comparison occurred between breathing studies that took place several hours apart, the following factors may have affected the LFC: blood pressure, sympathetic tone, and venous blood volume. Also, due to the extended duration, the alar probe is likely to have shifted. For these comparisons, the resistance levels being compared were the same, hence the intrathoracic pressure and respiratory pump were kept constant.

To investigate the potential clinical utility of the alar LFC Swings for determining fluid loss in individual subjects, an analysis on a per-subject, descriptive basis in the HD patients was conducted. The alar LFC Swings before HD were compared the alar LFC Swings after HD, for each level of resistance, for each subject. A sample plot is shown (Figure 6-6).

Following HD, for the high resistance level, the alar LFC Swings of 11 of the subjects increased, five decreased, and four did not change. For the medium resistance

level, the alar LFC Swings increased in nine, decreased in two and did not change in nine. For the low level of resistance the alar LFC Swings increased in eight, decreased in three, and did not change in nine. Additionally, the following trends were identified:

- The alar LFC Swings of subject 13 were considerably larger than all other subjects for all resistance levels, yet the finger LFC Swings were smaller than most other subjects.
- Also in subject 13, the alar LFC Swings decreased after HD at the highest resistance level and increased after HD at the medium and low resistance levels.
- Subjects 6 and 17 had alar LFC Swings that decreased following HD through all three resistance levels.
- Subject 16 had a very large increase in LFC Swings following HD in all three resistance levels.
- Seven of the 20 subjects had alar LFC Swings that increased after HD across all three resistance levels.

The peak inspiratory and expiratory flow rates were compared before and after HD. No differences were found for most subjects for all resistance levels. In subjects 1 and 20, the peak inspiratory flow rates before HD were greater than after HD, for all three resistance levels. The expiratory flow rate was also smaller after HD in subject 20, across all levels of resistance. No obvious relationship existed between inspiratory or expiratory flow and alar LFC Swings as the LFC Swings of subjects 1 and 20 did not behave inconsistent with the other subjects.

Next, the total respiratory volumes were analyzed. In subject 8, the respiratory volume decreased following HD, while in subject 20 it increased. In all other subjects the respiratory volumes were consistent before and after HD. The respiratory volume did not have a consistent affect on the LFC Swings in the HD patients.

The volume of fluid removed during HD varied greatly between subjects. No direct relationship existed between the volume of fluid removed and the magnitude of the LFC Swings. This relationship was further explored on an individual subject basis for trends. The subjects with the largest percentage of fluid removed were 12, and 15. Those with the least percentage of fluid removed were 7 and 9. This does not explain any of the trends found in the LFC Swings.

Following HD, systolic and diastolic blood pressures were analyzed for each subject individually. The systolic blood pressure decreased by at least 10 mmHg in 14 of the 20 subjects. The systolic blood pressure increased by at least 10 mmHg in subjects 1 and 13. The diastolic blood pressure decreased by at least 10 mmHg in nine of the subjects and increased by more than 10 mmHg in subject 4. The systolic blood pressure increased in subject 13, who also had LFC Swings that behaved inconsistent with other subjects. The systolic pressure also increased in subject 1, whose LFC Swings behaved as expected. There were no clear trends between changes in blood pressure and changes in the LFC.

The PCC MagDiff and PCC MagMean were analyzed for trends and for a relationship to the LFC Swings. These were plotted for each HD patient individually. There were no statistical differences before and after HD in either of these variables. In most individual subjects the PCC MagDiff did not change following HD. Subjects 3, 13 and 16 increased while subject 18 decreased after HD.

Unlike the PCC MagDiff, the PCC MagMean of many of the subjects did change following HD but many increased while many others decreased, resulting in no statistical

differences overall. Seven of the 20 subjects increased, six decreased and seven had very little or no change.

Hemodialysis subject 13 had alar LFC Swings considerably larger than the other subjects. Additionally the LFC Swings increased following HD, as expected, for the low and medium resistance levels but decreased at the high resistance level. There was no apparent cause for this finding as the respiratory flow rates and volumes did not differ. Subject 13 was one of only two subjects to have systolic blood pressure increase by at least 10 mmHg. Additionally, the PCC MagDiff increased in subject 13. Subject 13 was an African-American, 58 year-old male, weighing 190 kg. A review of the medications taken by subject 13 did not reveal any possible reasons for these findings.

To fully explore the LFC Swings relationship to all other variables, a multiple variable linear regression analysis was performed and the results are presented (Table 6-3). Percentage of fluid removed is the total volume of fluid removed divided by total pre-HD body weight. All variables ending with “difference” indicate values after HD minus values before HD. A multiple variable linear regression analyzes each independent variable for its relationship to the dependent variable—in this case the alar LFC Swings at the high resistance level. In the linear model, the significance indicates how closely these two variables are linearly related, independent of the effects of the other variables. A significance level of $<.05$ is considered significant. As suspected, none of these variables were significantly related to the alar LFC Swings. The results for the medium and low resistance levels were similar.

The 20 HD patients were taking a total of 97 unique medications with the average subject taking nearly ten. Of the 97 medications, 46 of them were taken by only one

subject. All subjects except 11, 13 and 20 take at least one medication unique to themselves. Many different medications within the same class are often prescribed, explaining this finding. For example, only subject 5 was taking atenolol however other subjects were taking metoprolol. Due to the number of different drugs taken by the HD patients, attributing specific LFC changes to specific drugs is virtually impossible. Interesting to note, however, is that subject 13, is one of the few subjects not taking a drug prescribed only to him.

Finally, the LED power was reviewed and analyzed for changes. Due to the duration of the HD sessions, the LED power of the alar probe changed in virtually all subjects. The LED power increased in several of the subjects and decreased in several other subjects. In subject 13, the LED power only changed from 76 before HD to 86 after HD. No trends could be identified as specific causes for the LFC Swing changes.

In summary, there were statistical differences between the alar LFC Swings of the HD patients, before and after HD. The individual subject analysis revealed many interesting findings but the reasons for these findings were elusive. The alar LFC Swings increased in approximately 50% of the subjects so individual clinical monitoring of HD patients for fluid loss requires follow up studies to fully understand the reasons why the alar LFC swings changed the way they did.

Hypotheses 4 and 5

Hypotheses 4 and 5 explored the effects of fluid loss on the PCC of the PPG. In blood donors, the alar PCC MagDiff and PCC MagMean both decreased after blood loss whereas in the HD patients they did not change. This is in contrast to the LFC Swings, which increased in HD patients and not in blood donors. Individual subject analyses for

the PCC MagDiff and PCC MagMean of the blood donors were performed (Figures 6-8 and 6-9).

The alar PCC MagDiff decreased significantly after blood loss. Individually, the PCC MagDiff decreased in 14 of the subjects. The alar PCC MagMean decreased significantly after blood loss and decreased in 14 subjects as well. As expected, the two PCC variables mirrored each other very well. Subjects 5, 8 and 14 were the most interesting. The PCC variables both increased after blood loss in subjects 5 and 14. In subject 8 the PCC variables had unusually large values, but decreased, as expected.

Several variables contributed to changes in the PCC following fluid loss, including venous return, fluid volume, vasoconstriction due to temperature, intrathoracic pressure, sympathetic tone, and impedance by venous blood or edema. Vasoconstriction due to temperature and sympathetic tone mainly affect the PPG from the finger and should not affect the PPG from the alar. Intrathoracic pressure is constant since the comparison of the PCC variables is between the same resistance level. The main factors contributing to the changes in the PCC should therefore be venous return and venous impedance, both affected by total blood volume, which also directly affects the PCC.

The PCC variables decreased in most blood donors, indicating their potential utility for monitoring blood loss. In several subjects, however, the PCC variables either increased or did not change.

The peak inspiratory and peak expiratory flow rates were evaluated before and after blood loss (Figure 6-10). The peak expiratory flow rates were nearly identical. In all subjects, the flow rates before and after blood loss were within 10 L/min of each other with most being within 5 L/min. Subjects 5, 8 and 14 do not show any trends that could

explain their unusual findings. Subject 14 did have inspiratory and expiratory after blood loss greater than before blood loss, however other subjects without unusual findings did as well.

Next, the total respiratory volumes were analyzed for all 20 blood donors (Figure 6-11). In subject 14, the respiratory flow rates and volumes increased following blood loss, potentially explaining the reason for the inconsistent findings in the PCC variables.

During blood donation approximately 500 ccs of whole blood was removed from all donors, regardless of weight. The option for “double red blood cells” was available and two of the blood donors chose this option. During double donation approximately 360 cc’s of packed red blood cells was removed with approximately 500 cc’s of saline plus all plasma returned to the subject. Subjects 1 and 11 underwent a double donation procedure, and while they each lost double red blood cells, they actually experienced a slight net gain in total fluid. Both of these subjects had a decrease in PCC variables following this donation procedure and both had either no change or a slight increase in the LFC Swings.

Subjects 1 and 11 had the largest percentage of red blood cells removed due to the double donation. Subjects 5, 8 and 14 had smaller than average percentage of blood removed so the interesting findings associated with these three subjects are not attributable to the volume of blood lost.

The pulse rate affects the PCC variable calculations in several ways. When heart rate increases, the stroke volume decreases to maintain a constant cardiac output. In the blood donors subjects it was shown that the pulse rate did not change statistically across all subjects. An individual subject analysis was performed to analyze trends.

The blood donor average pulse rate before and after blood loss is shown (Figure 6-13). The pulse rate was stable in all subjects with only subjects 4 and 18 experiencing a pulse rate increase of 10 and 12 beats per minute, respectively. The systolic and diastolic blood pressures were very similar. Only subjects 6, 9, 16 and 20 had a decrease in systolic blood pressure of greater than 10 mmHg and only subject 1 had an increase in diastolic blood pressure greater than 10 mmHg with no subjects having a greater than 10 mmHg drop in diastolic blood pressure following blood loss. It is not likely that pulse rate variation or changes in blood pressure attributed to PCC variable variation.

The LFC Swings of the blood donors did not change statistically following blood loss. The LFC Swings of the individual subjects were explored for trends (Figure 6-14). The high and medium resistance levels show very similar results, while at the low resistance, several subjects experienced a decrease in alar LFC Swings following blood loss. Subjects 5 and 14 both had PCC variables that increased following blood loss and the alar LFC Swings of these two subjects also increased. Additionally, subject 8 had very large PCC variables and also had very large LFC Swings. While the fact that the LFC Swings behaved in a fashion similar to the PCC variables does not attribute causality it does solidify trends and supports physiologic believability.

A multiple variable linear regression analysis was then performed for the PCC MagDiff and the PCC MagMean variables (Table 6-4). Percent red blood cells removed is the total estimated blood volume divided by the volume of red blood cells removed. All variables ending with “difference” indicate values after blood loss minus values before blood loss. A multiple variable linear regression analyzes each independent variable for its relationship to the dependent variable—in this case the alar PCC MagDiff.

In the linear model, the significance indicates how closely these two variables are linearly related, independent of the effects of the other variables. A significance level of $<.05$ is generally considered significant. As suspected from the descriptive analyses presented above, none of the variables were significantly related to the PCC MagDiff, however the alar LFC Swings at the high resistance level showed the best overall relationship as indicated by the smallest significance value.

The alar LFC Swings at the medium level of resistance were significantly related to the alar PCC MagMean while at the high level of resistance the alar LFC Swings were trending towards significance. This indicates a near linear relationship between the difference in alar LFC Swings and difference in alar PCC MagMean. Most blood donors experienced no change in alar LFC Swings and a decrease in the PCC MagMean following blood loss. In several subjects, however, both variables increased, partially explaining this relationship. The reasons why the physiology of these subjects was different from the remaining subjects can not be determined.

Lastly, the LED power was explored for changes before and after blood loss. Of the 20 blood donors, nine had LED power after blood loss slightly different from before blood loss. Several of the subjects had an increase in LED power and several had a decrease. The most likely cause of the change in LED power is slight shifting of the probe during blood donation. There appears to be no relationship between the LED power and the PCC variables.

In summary there were statistical differences between the alar PCC variables of the blood donors before and after blood loss. The individual subject analysis revealed many interesting findings but the reasons for these findings were elusive. The PCC

variables decreased in approximately 70% of the subjects, so individual clinical monitoring of whole blood loss is a possibility.

Table 6-1. The R^2 values for the regression analysis between estimated intrathoracic pressure changes and alar LFC Swings for the blood donors.

R^2	Linear	Secondary
< 0.3	11	7
0.3 – 0.5	11	10
0.5 – 0.8	15	19
> 0.8	3	4

Table 6-2. The R^2 values for the regression analysis between estimated intrathoracic pressure changes and alar LFC Swings for the HD patients.

R^2	Linear	Secondary
< .3	12	10
.3 - .5	10	10
.5 - .8	17	18
> .8	1	2

Table 6-3. Multiple variable regression analysis for the alar LFC Swings during high resistance for the HD patients.

Variable	Significance
Height	0.785
Weight	0.881
Age	0.767
Fluid Removed	0.694
Percent Fluid Removed	0.791
Systolic Pressure Difference	0.443
Diastolic Pressure Difference	0.688
Pulse Rate Difference	0.541
Inspiratory Flow Difference	0.693
Expiratory Flow Difference	0.973
Respiratory Volume Difference	0.303
PCC MagDiff Difference	0.978
PCC MagMean Difference	0.492

Table 6-4. Multiple variable linear regression analysis for the alar PCC MagDiff for the blood donors.

Variable	Significance
Height	0.702
Weight	0.643
Age	0.817
Total Estimated Blood Volume	0.611
Red Blood Cells Removed	0.761
Percent Red Blood Cells Removed	0.709
Systolic Pressure Difference	0.920
Diastolic Pressure Difference	0.728
Pulse Rate Difference	0.803
Inspiratory Flow Rate Difference	0.801
Expiratory Flow Rate Difference	0.599
Volume Difference	0.489
Alar LFC Swings Difference High Resistance	0.273
Alar LFC Swings Difference Medium Resistance	
Resistance	0.382
Alar LFC Swings Difference Low Resistance	0.965

Table 6-5. Multiple variable linear regression analysis for the alar PCC MagMean for the blood donors.

Variable	Significance
Height	0.985
Weight	0.994
Age	0.953
Total Estimated Blood Volume	0.580
Red Blood Cells Removed	0.227
Percent Red Blood Cells Removed	0.191
Systolic Pressure Difference	0.863
Diastolic Pressure Difference	0.225
Pulse Rate Difference	0.449
Inspiratory Flow Rate Difference	0.708
Expiratory Flow Rate Difference	0.443
Volume Difference	0.172
Alar LFC Swings Difference High Resistance	0.101
Alar LFC Swings Difference Medium Resistance	
Resistance	0.032
Alar LFC Swings Difference Low Resistance	0.799

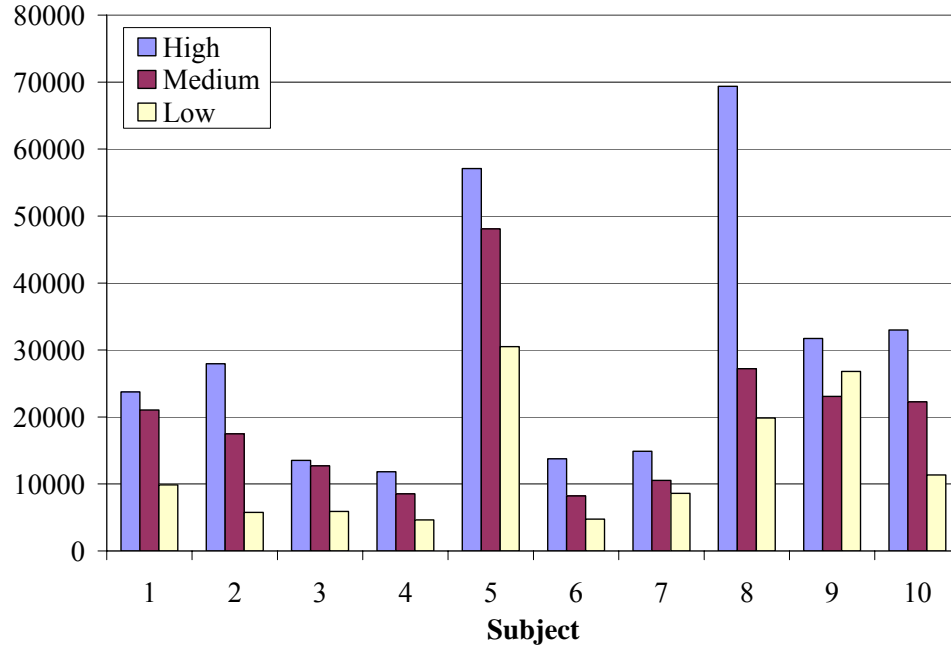


Figure 6-1. The alar LFC Swings for all three resistance levels for the first ten blood donors, before blood loss.

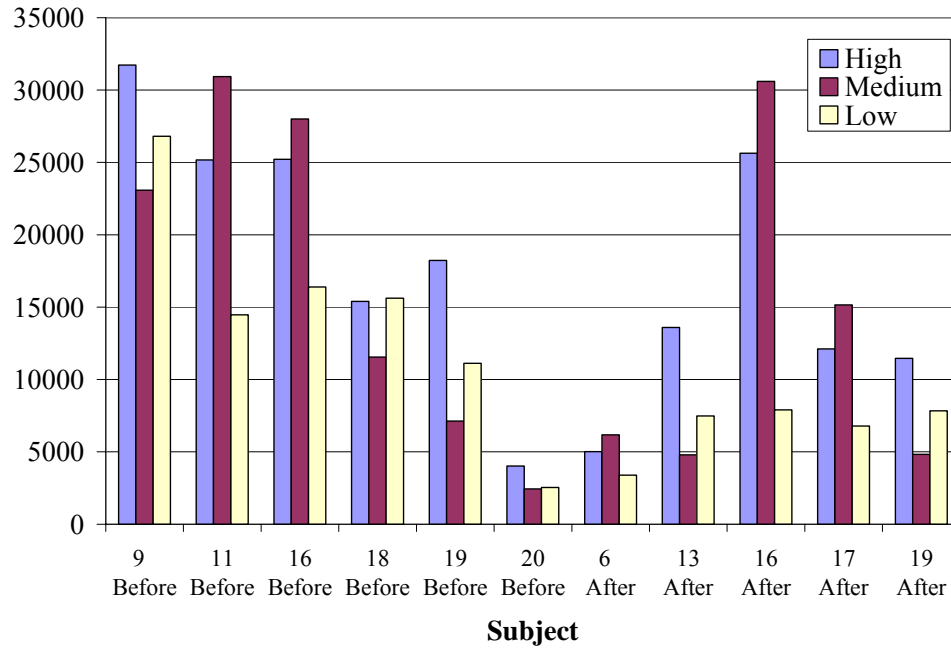


Figure 6-2. The unexpected alar LFC Swings for all three resistance levels for the blood donors, both before and after blood loss.

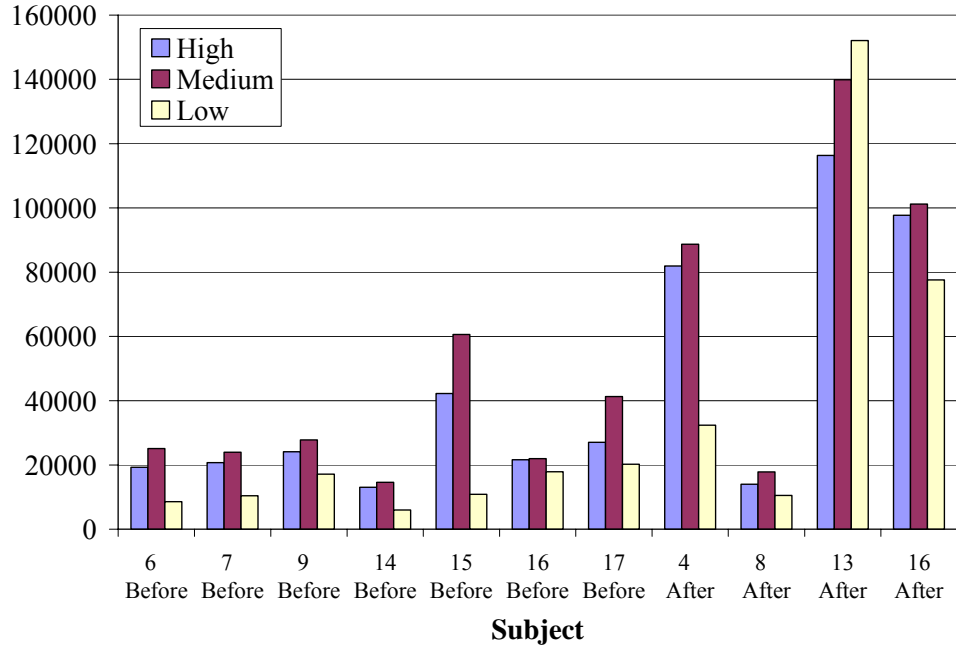


Figure 6-3. The unexpected alar LFC Swings for all three resistance levels for the HD patients, both before and after HD.

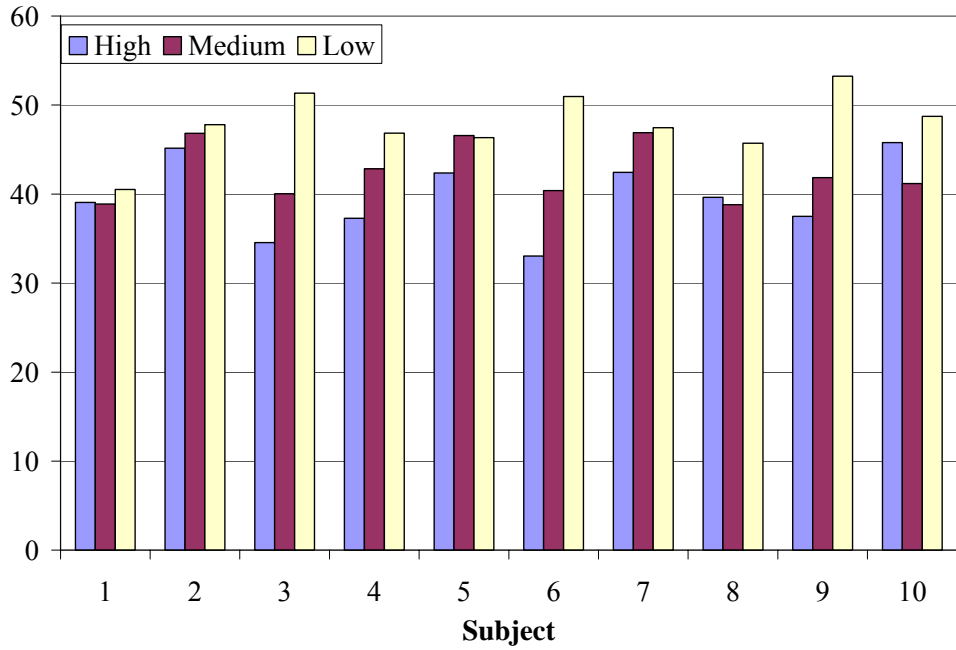


Figure 6-4. The peak inspiratory flow rates for all three levels of resistance for the blood donors, before blood loss.

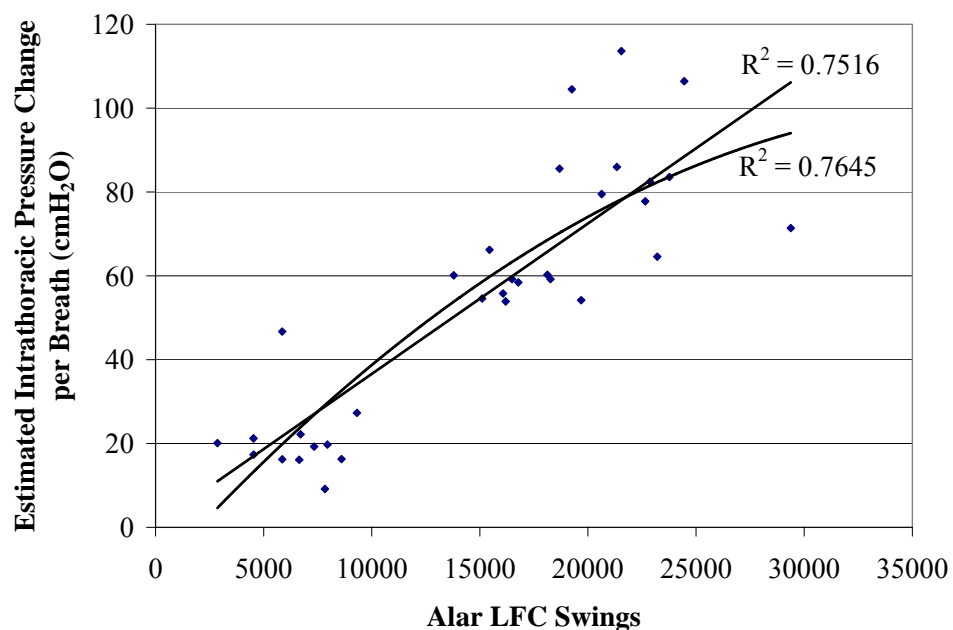


Figure 6-5. Estimated intrathoracic pressure changes per breath vs alar LFC Swings in blood donor subject 1, after blood loss.

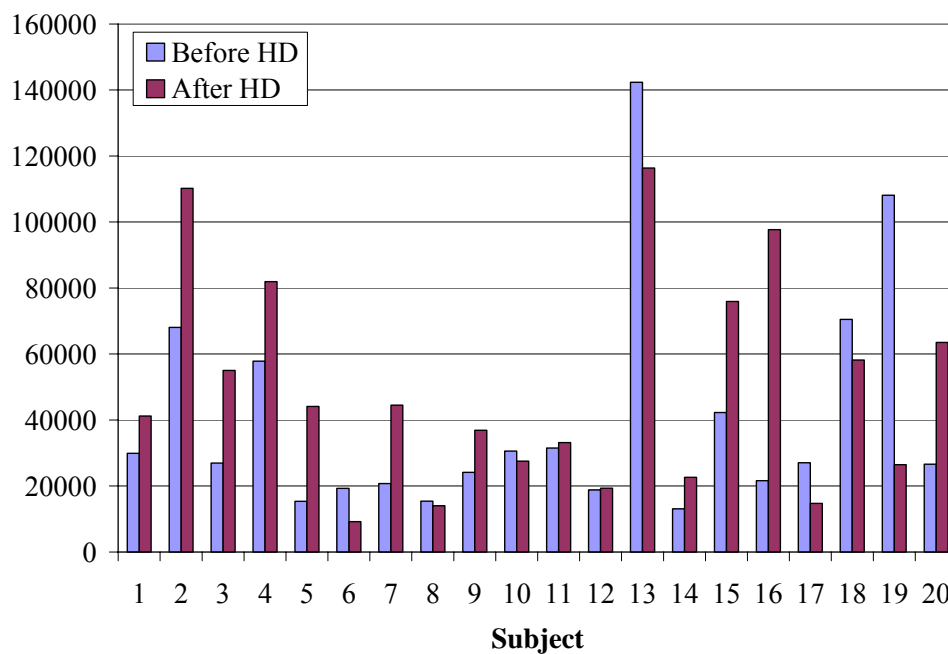


Figure 6-6. The alar LFC Swings for the HD patients, both before and after HD.

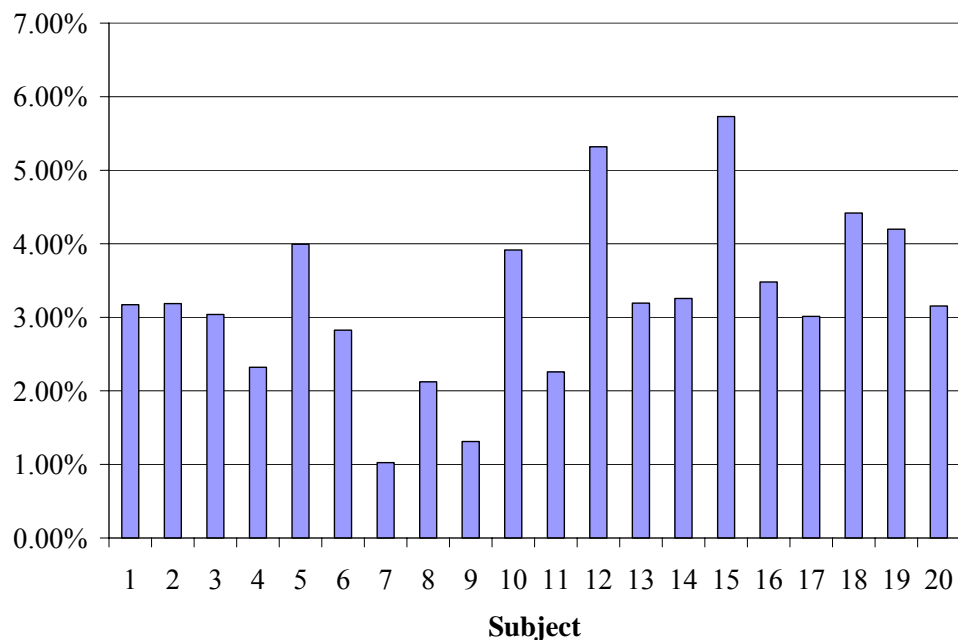


Figure 6-7. Fluid removed as a percent of body weight in the HD patients.

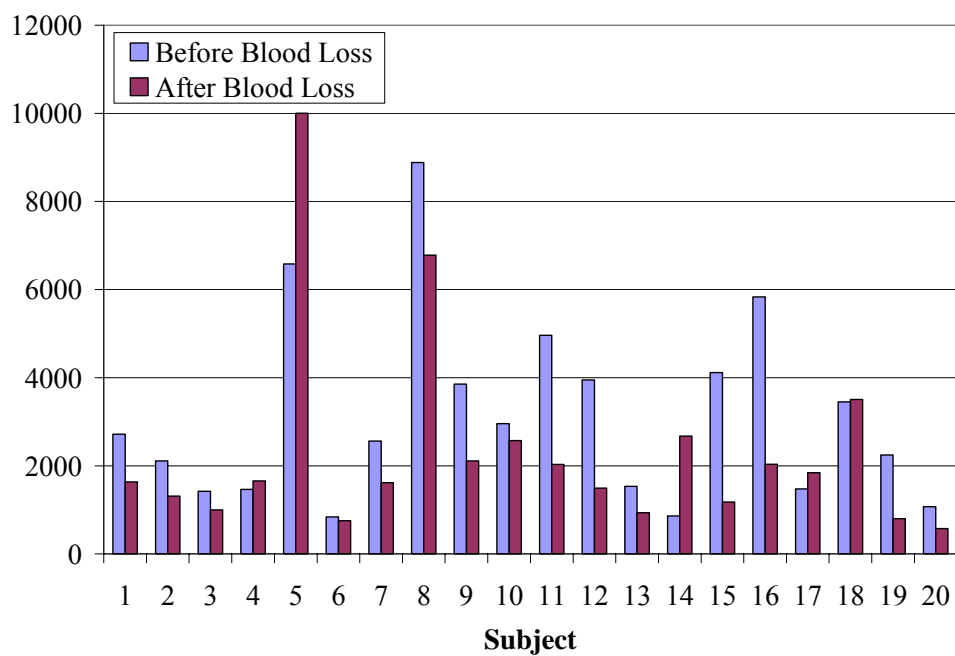


Figure 6-8. The alar PCC MagDiff for the blood donors, both before and after blood loss.

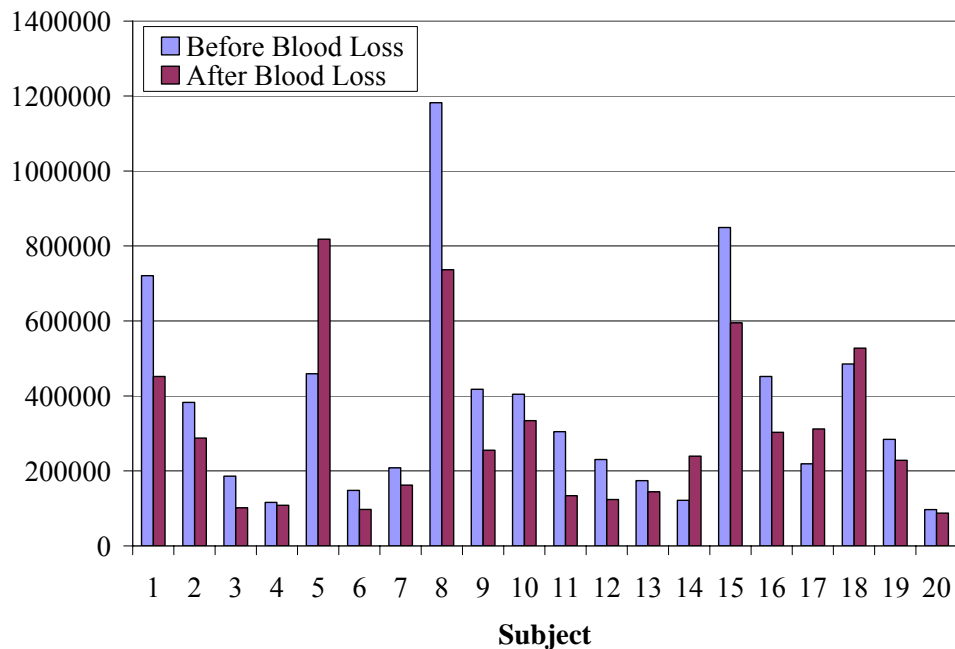


Figure 6-9. The alar PCC MagMean for the blood donors, both before and after blood loss.

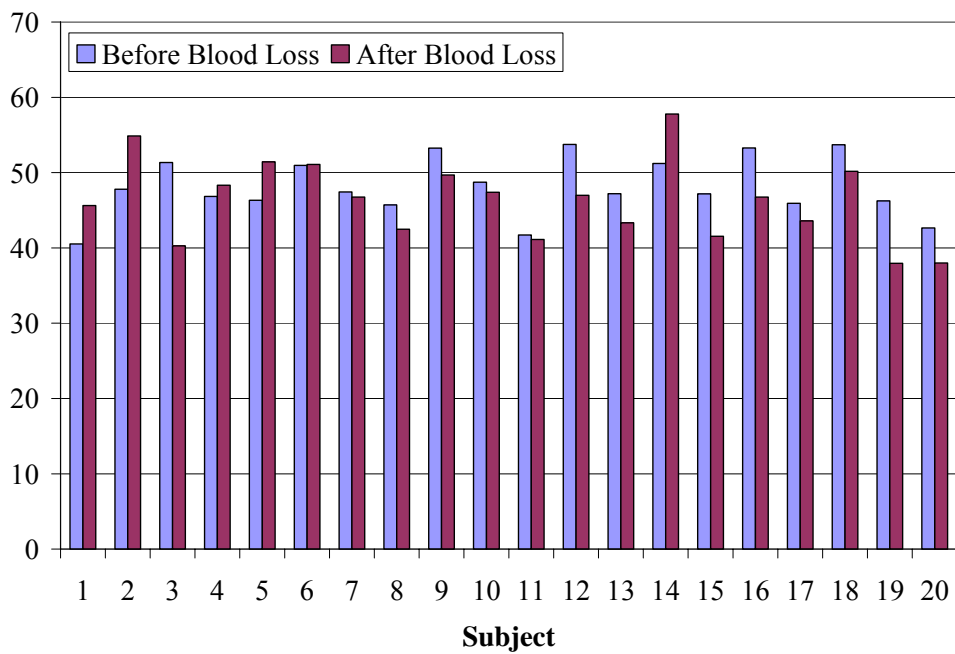


Figure 6-10. The peak inspiratory flow rate for the blood donors, both before and after blood loss.

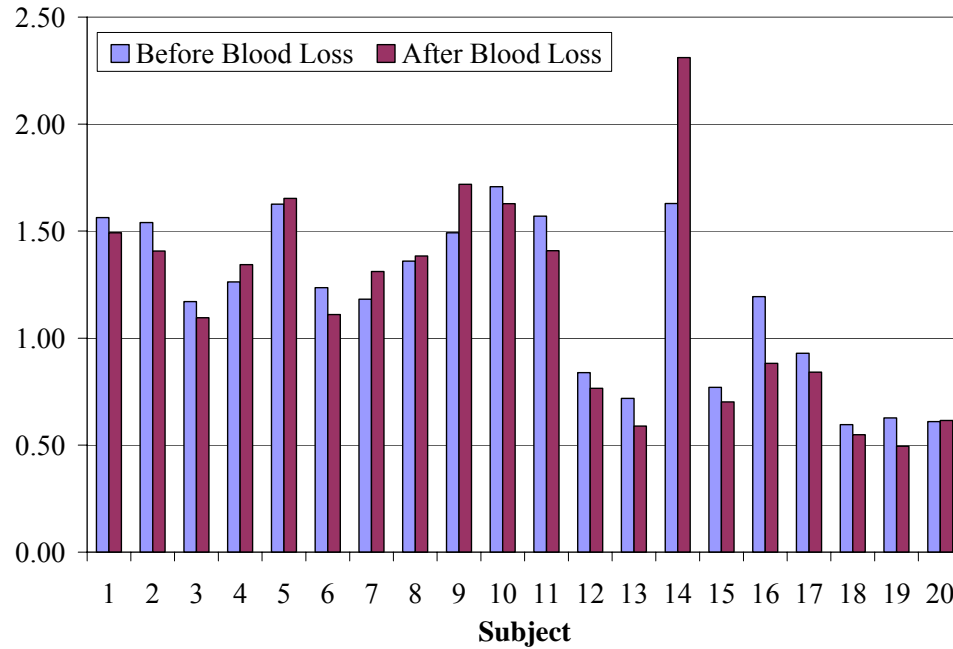


Figure 6-11. The total respiratory volume for the blood donors, both before and after blood loss.

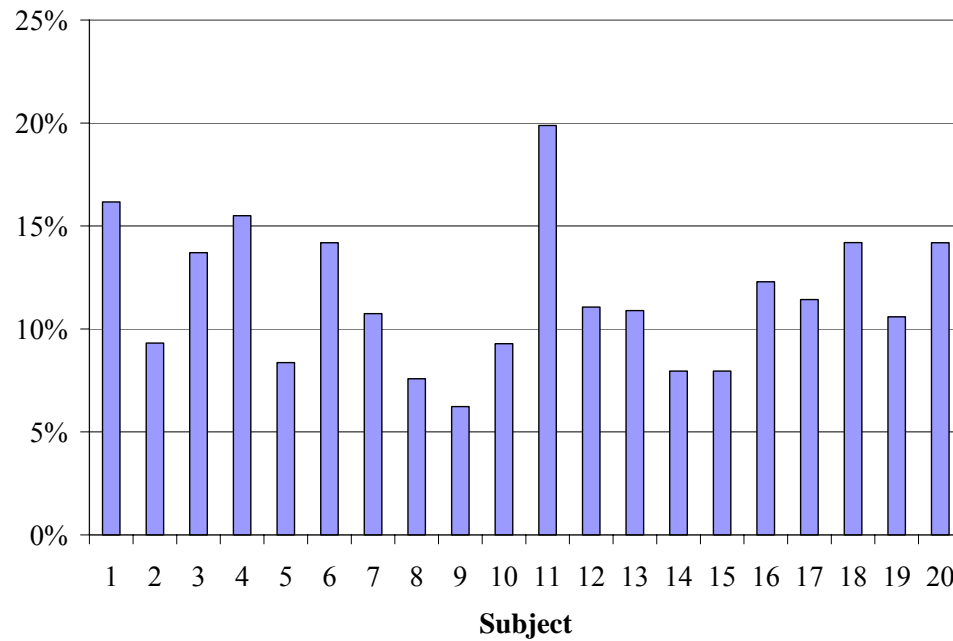


Figure 6-12. The approximate percentage of red blood cells removed in the blood donors.

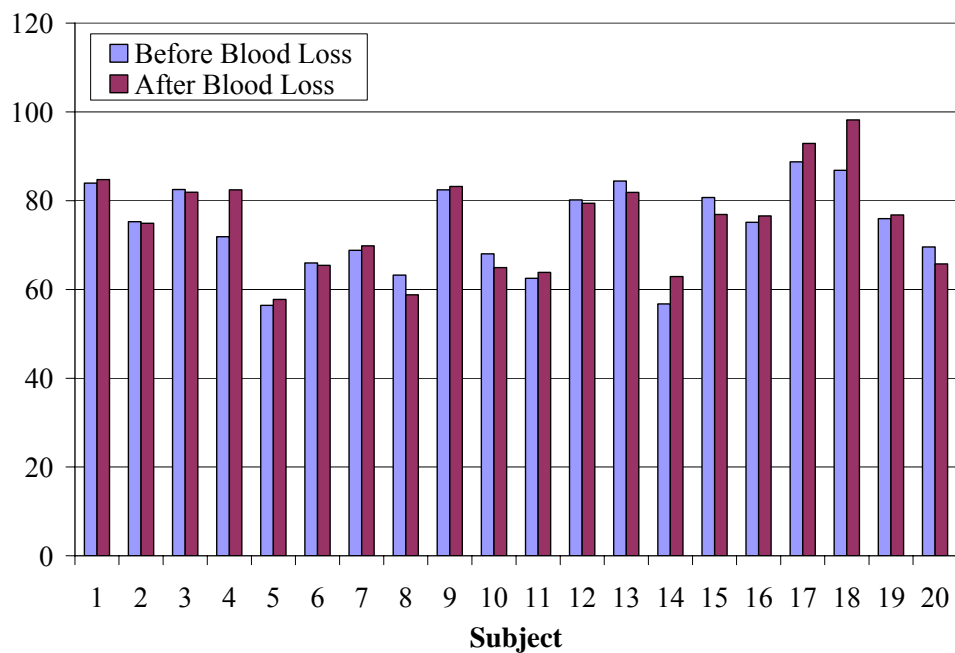


Figure 6-13. The pulse rate of the blood donors, both before and after blood loss.

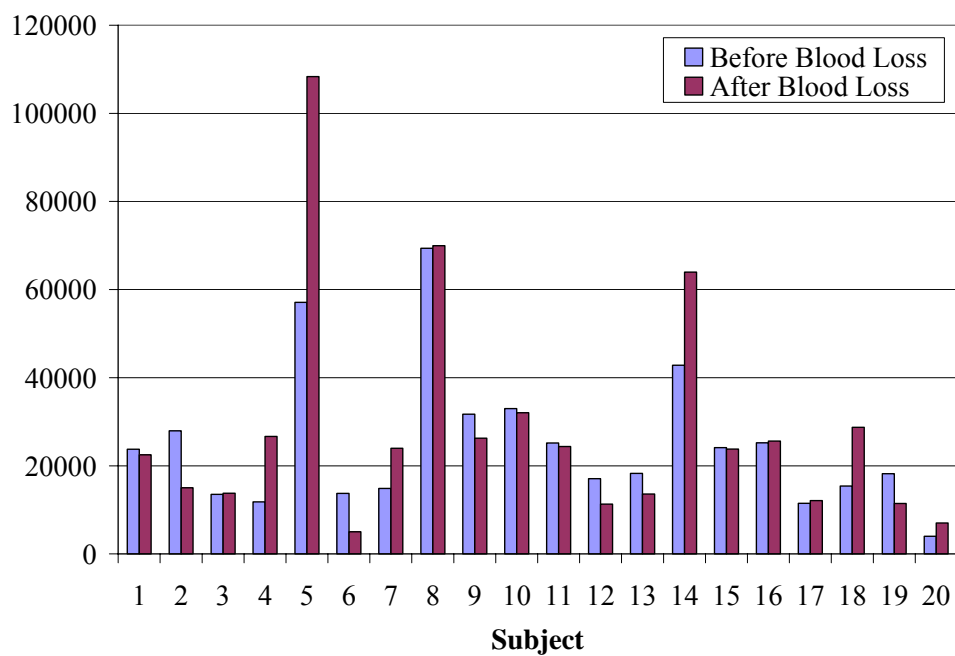


Figure 6-14. The alar LFC Swings for the blood donors, both before and after blood loss.

CHAPTER 7 CONCLUSIONS

Summary of Conclusions

Hypothesis 1 explored the ability of the low frequency component (LFC) Swings to detect changes in airway resistance in several different populations. Statistically significant differences were found across all populations. Individually, 72% of the subjects experienced changes in the LFC corresponding to the changes in airway resistance, indicating the potential for individual patient monitoring.

Hypothesis 2, which was an extension of hypothesis 1, explored the sensitivity of the LFC Swings for predicting intrathoracic pressure changes, as estimated by an experimentally derived equation. No statistically significant relationship was found between the estimated intrathoracic pressure change per breath and the LFC Swings. Most individual subjects had a borderline significant relationship with R^2 values between 0.5 and 0.8 with several being >0.8 . Since Equation 3-3 was developed to estimate pressure drop across endotracheal tubes and does not take human variability into account, it is possible that the equation may be the reason for the lack of relationship.

Hypotheses 3, 4 and 5 each explored various measures of the photoplethysmograph (PPG) to detect either whole blood loss during blood donation or ultrafiltrate loss during hemodialysis (HD). The HD patients had a statistically significant increase in LFC Swings following HD and the blood donors had a statistically significant decrease in pulsatile cardiac component (PCC) MagDiff and PCC MagMean

following blood loss. This important difference indicates the potential for the PPG to be used to differentiate between whole blood loss and fluid loss.

Individually, approximately 50% of the HD subjects experienced an increase in LFC Swings following HD and 72% of the blood donor subjects had a decrease in the PCC variables following blood loss.

Clinical Relevance and Future Studies

Clinical Goal 1

The first broad clinical goal was to show that the PPG could be used to detect changes in airway resistance and be used to estimate intrathoracic pressure changes. Clinical uses include, but are not limited to, noninvasive diagnosis of severity of asthma and detecting obstructive sleep apnea (OSA) and an estimating its severity.

The statistical and clinical results of hypothesis 1 indicate that it is possible to use the LFC to detect major airway resistance changes in a variety of populations. For the first broad clinical goal, asthmatic subjects are one of the target clinical populations of interest.

The current standard of care for the monitoring of asthma includes monitoring pulmonary function with spirometry and peak flow measurements (NAEPP 1997). There is no standard for direct measurement of airway resistance. Identification of new noninvasive measures of airway resistance for determining asthma severity is an active area of research. Asthma severity is dictated by airway resistance, which is proportional to the intrathoracic pressure changes with respiration. If the PPG derived noninvasively from a pulse oximeter could reliably measure intrathoracic pressure changes, it may also be an indicator of airway resistance and hence asthma severity.

If the LFC derived noninvasively from the PPG of an alar pulse oximeter probe could differentiate major changes in airway resistance, it could either replace or supplement the more traditional spirometry measures for the diagnosis and monitoring of the severity of asthma. Asthmatic patients would first establish the LFC Swings for normal, baseline breathing. They would then breathe through a series of endotracheal (ET) tubes, creating resistance. Flow rates and volumes would be monitored and controlled. The LFC Swings for each of these levels of resistance would be calculated to establish the LFC Swings for that individual subject through the full range of airway resistances. Whenever airway obstruction needed to be estimated, the LFC Swings could be measured and compared to these established baseline values. Additionally, the severity of an attack could be estimated using the LFC Swings as an indicator of major airway obstruction.

LFC measurements currently have some limitations and would require validation before meeting these clinical expectations. First, the alar probe placement and its affect on the magnitude of the LFC Swings would need to be fully understood. In our study, the alar probe was left in place for the duration of the comparisons. Removing and replacing the probe hours, days, or even weeks apart may affect the LFC measurements. As previously discussed, the exact placement of the probe on the alar affects the overall LFC value, reflecting baseline light striking the photodiode (PD), but should not affect the LFC Swings, which measure the shifting of venous blood.

A future study should explore the relationship between the alar probe placement position and the magnitude of the LFC Swings. A very simple study design could be as follows: recruit healthy volunteers to perform the breathing study previously outlined

(Chapter 4) while being monitored with an alar pulse oximeter probe. Move the alar probe on the same nostril and repeat the breathing study. Have them come back one week and one month later for repeated breathing studies. The LFC Swings should not differ if the probe placement does not affect the LFC Swings.

When comparing LFC measures from the same individual several days or weeks apart would be important to eliminate other confounding variables. Other possible variables affecting the LFC could include time of day, autonomic activation, position of subject, state of hydration, etc. In addition to evaluating the effect of the probe placement on the alar, these other confounding variables should be evaluated independently and understood.

The LFC Swings did not correlate with the intrathoracic pressure changes, as estimated by equation 3-3. It is important to understand if the LFC could potentially be a sensitive enough measure to predict precise levels of airway obstruction and intrathoracic pressure changes. A future study should monitor a variety of subjects with esophageal balloons to estimate intrathoracic pressure changes. Similar breathing studies should then create a variety of intrathoracic pressure changes. The relationship between the LFC Swings and the intrathoracic pressure changes should then be evaluated. Other analyses of the LFC should be performed and other measures of the LFC may have a closer relationship to the intrathoracic pressure than the LFC Swings, defined in our study.

The results presented (Chapters 5 and 6) show promise for the use of the LFC to monitor airway obstruction and asthma severity. The lack of relationship between the LFC Swings and the estimated intrathoracic pressure coupled with the lack of

understanding of many other variables that potentially affect the LFC necessitate the need for follow-up studies to verify the feasibility of monitoring asthma severity with the PPG.

The second clinical population of interest includes OSA syndrome patients including snoring, upper airway resistance syndrome (UARS) and OSA. Snoring is a respiratory noise generated from the upper airway during sleep that may occur during inspiration or expiration. A decrease in tone of the upper airway muscles results in constriction of the oropharynx and results in snoring. There is no standard measure of snoring and it is often quantitated using a microphone and sound meter (Collop 2005). UARS describes patients experiencing excessive daytime somnolence caused by repetitive instances of increasingly negative intrathoracic pressure associated with upper airway flow limitation. A noninvasive, simpler method to accurately measure respiratory effort by measuring intrathoracic pressure changes would make diagnosis of UARS more practical. Finally, OSA is a repetitive, partial or complete obstruction of the upper airway during sleep, and is the most severe of the OSA syndromes. A more accurate indicator of OSA severity is needed and is an active area of research.

The gold standard for diagnosing OSA remains the attended, overnight level I polysomnogram (Pang and Terris 2006). Unfortunately, limited resources, including limited number of recording beds, high cost, long waiting lists, and labor requirements prevent diagnosis in a large portion of the population. Screening questionnaires and devices have also been developed. The ideal screening device should be cheap, readily accessible, easily used with minimal instructions, have no risks or side effects to the patient and be safe and accurate (Pang and Terris 2006).

The LFC Swings from an alar pulse oximeter probe could either be used as a supplemental measure with the standard overnight PSG or used in place of the PSG entirely. The alar probe could be placed on the patient before going to sleep. While sleeping, prior to the obstructive events occurring, the baseline LFC Swings could be measured. The LFC Swings should then increase dramatically when the obstructive events occur. To normalize the degree of obstruction, the patient could complete a similar breathing study, as outlined above, and the LFC Swings created by these levels of resistance could act as the control values for that subject.

Since the LFC Swings would be measured continuously in one night, the other confounding variables, including probe placement, time of day, etc would be eliminated. Comparing the degree of overnight obstruction to a baseline breathing study or comparing them to values obtained from monitoring from prior nights would require a full understanding of the variables discussed in the asthma section. For simple comparisons to the nighttime baseline, pilot studies should take place. Patients should be monitored with a full PSG, including an esophageal balloon, while being monitored with an alar probe. The LFC Swings should be compared to the esophageal pressure values and the other standard measures of obstruction severity. It would also be important to understand the effects of shifting during sleep and sympathetic activation during dreams.

Using the LFC Swings from a centrally placed pulse oximeter probe to detect major airway resistance changes in individual asthma subjects or during sleep in OSA subjects is not too far away. To precisely estimate the exact degree of severity would require several more key studies to determine feasibility.

Clinical Goal 2

The gold standard for monitoring volume status in critically ill patients is pulmonary artery wedge pressure, or in its absence, central venous pressure. Other means include heart rate, blood pressure, effects of mechanical ventilation on arterial blood pressure and urine output. To explore the feasibility of using the PPG to detect changes in fluid volume, two patient populations who lost a measurable amount of fluid were explored.

The results of hypotheses 3, 4, and 5 indicate that it may be possible to use various measures of the PPG to monitor clear fluid loss and whole blood loss and possibly distinguish the difference between the two. Significant changes in the LFC Swings of the HD patients were found following a physiologically significant fluid loss. Following this fluid loss, however, there were no changes in the PCC variables, which was initially unexpected. The blood donors did not lose a physiologically significant amount of whole blood, evidenced by lack of change in blood pressure and pulse rate following blood loss. The blood donors, did, however, experience a decrease in PCC variables following blood loss. The contrasting results of the HD patients and blood donors have important clinical implications. We hypothesize that the PPG differences between the blood donors and HD patients is attributed to the volume and type of fluid lost by each group.

The LFC represents changes in venous capacitance. Hemodialysis patients lost a physiologically significant volume of fluid, evidenced by the increase in heart rate and decrease in blood pressure. This fluid loss affected the venous capacitance and was reflected in the LFC swings. Blood donors lost a physiologically insignificant volume of blood resulting in no affect on venous capacitance and no change in the LFC swings.

The PCC is a measure of arterial blood flow. The PCC variables decreased significantly in the blood donors. This was caused by the volume of red blood cells lost during blood loss. The PPG is derived from the infrared (IR) light striking the PD. The amount of the IR light striking the PD is mainly influenced by its absorption by the oxygenated hemoglobin found in the red blood cells of arterial blood. This theory is further supported by the lack of change in the PCC variables found in the HD patients, who lost no red blood cells. While the stroke volume and cardiac output may have both decreased following HD, the PCC variables did not change, as the total number of red blood cells present remained constant.

Under some circumstances, the PCC amplitude may not purely reflect stroke volume, as previously reported (Murray and Foster 1996), but may more closely reflect the total number of red blood cells passing by the PD. If the stroke volume is cut in half yet the concentration of red blood cells doubles, the PCC may not change. This hypothesis deserves further elaboration. No previous research has explored the differences between whole blood and ultrafiltrate fluid loss and how they affect the PPG. These represent quite different causes of intravascular volume reduction and may allow further insight into the PPG signal.

The differences in the LFC swings between the blood donor subjects and the HD patients may also be caused by the differences in the compensatory mechanisms of the populations. The smooth muscles in the veins control the capacitance of the venous system. A variety of conditions inhibit the ability of this smooth muscle to appropriately moderate capacitance by impairing sympathetic/parasympathetic activation. Since the blood donors represent a generally healthy population, it is assumed that these

mechanisms are intact. The HD patients, on the other hand, are chronically ill and may have an impaired ability to adequately moderate venous capacitance. The differences in the LFC swings of the two populations may reflect the differences in the ability to compensate for fluid loss. Further studies are needed to determine if the PPG can detect these impairments.

It may be possible to use various measures of the PPG to differentiate ultrafiltrate (or other causes of acellular fluid losses, such as diarrhea) and whole blood loss. This may be valuable during monitoring of a wide variety of patients. It may also be possible to detect impairment of physiologic compensation to fluid loss. With the alar probes, motion artifact is generally minimal. Additionally, since the monitoring took place over several hours, each patient acted as their own control over discrete monitoring periods. Additional studies are needed to verify the above claims.

The main clinical population who could stand to benefit from a device used to monitor whole blood or fluid loss is critically ill patients, who are receiving positive pressure ventilation. The extent of the fluctuations caused by positive pressure ventilation depend on central blood volume (Murray and Foster 1996). The PPG could be incorporated into the ventilator and the LFC and PCC variables measured in real time. The duration of the breaths would be known from the ventilator and used in the calculations. If the subject being monitored experienced a sudden loss of fluid or blood, the LFC Swings would increase or the PCC variables would decrease. An alarm threshold can be set. If the increase or decrease is greater than a certain preset amount, an alarm could sound alerting the nurse or physician to investigate possible fluid or blood volume changes.

Since critically ill subjects are generally motionless, movement artifact and positional changes are generally avoided. Additionally, since the monitoring would take place over several hours, each patient would act as their own control for each individual monitoring period. Additional studies are needed to verify the possibility of a device such as this. First, the effect of positive pressure ventilation is different from the effects of breathing through resistance. It would be important to fully understand the effects of positive pressure ventilation on the PPG. Pilot studies should invasively monitor the fluid status of critically ill subjects and compare these measures to the LFC and PCC measures defined in our study.

The PPG derived from a pulse oximeter is a noninvasive window into various physiologic parameters. The centrally derived PPG has many advantages over the more traditional peripheral PPG and will become the standard for PPG monitoring. With these studies as a foundation for future studies to build upon, many new clinical uses for the PPG will surface. Monitoring the severity of asthma and OSA, and detecting blood and fluid loss in critically ill subjects is just the tip of the iceberg of the clinical possibilities of the PPG.

LIST OF REFERENCES

- Al-Ali, A., Diab, M., Kiani, M., Kopotic, R. and Tobler, D. Stereo Pulse Oximeter. United States Patent Number 6,334,065. 2001.
- Al-Ali, A., Diab, M., Kiani, M., Kopotic, R. and Tobler, D. Stereo Pulse Oximeter. United States Patent Number 6,898,452. 2005.
- Allen, T., Peng, M., Chen, K., Huang, T., Chang, C and Fang, H. Prediction of Blood Volume and Adiposity in Man From Body Weight and Cube of Height. *Metabolism*. 1956; 5(3):328-45.
- Aoyagi, T. Pulse Oximetry: Its Invention, Theory and Future. *Journal of Anesthesia*. 2003; 17:259-266.
- Awad, A., Stout, R., Ghobashy, M., Rezkanna, H., Simverman, D and Shelley, K. Analysis of the Ear Pulse Oximeter Waveform. *Journal of Clinical Monitoring and Computing*. In Press, 2006.
- Banner, M., Blanch, P. and Kirby, R. Imposed Work of Breathing and Methods of Triggering a Demand-Flow, Continuous Positive Airway Pressure System. *Critical Care Medicine*. 1993; 21(2):183-90.
- Barleben, A., Muller, E., Wilke, A. and Vogel J. Lung Function Diagnosis Using Multi-Frequency Oscillometry with Reference to Lung Volume. *Pneumologie*. 1990; 44:950-4.
- Basile, C. Should Relative Blood Volume Changes be Routinely Measured During the HD Session? *Nephrology HD Transplant*. 2001; 16:10-2.
- Bhattacharya, J., Kanjilal, P. and Muralidhar, V. Analysis and Characterization of the Photo-Plethysmographic Signal. *IEEE Transactions on Biomedical Engineering*. 2001; 48(1):5-11.
- Boon D., van Montfrans, G., Koopman, M., Krediet, R. and Bos, W. Blood Pressure Response to Uncomplicated HD: The Importance of Changes in Stroke Volume. *Nephron Clinical Practice*. 2004; 96:c82-7.
- Bortolotto, L., Blacher, J., Kondo, T., Takazawa, K. and Safar, M. Assessment of Vascular Aging and Atherosclerosis in Hypertensive Subjects: Second Derivative of Photoplethysmogram Versus Pulse Wave Velocity. *American Journal of Hypertension*. 2000; 13:165-71.

- Chakravarti, I., Laha, R. and Roy, J. Handbook of Methods of Applied Statistics, Volume I, John Wiley and Sons. 1967:392-394.
- Chowienczyk, P., Kelly, R., MacCallum, H., Millasseau, S., Andersson, T., Gosling, R., Ritter, J. and Anggard, E. Photoplethysmographic assessment of pulse wave reflection: blunted response to endothelium-dependent beta2-adrenergic vasodilation in type II diabetes mellitus. *Journal of the American College of Cardiology*. 1999; 34(7):2007-14.
- Cogswell, J. Forced Oscillation Technique for Determination of Resistance to Breathing in Children. *Archives of Disease in Childhood*. 1973;48:259-66.
- Collop, N. Obstructive Sleep Apnea Syndromes. *Seminars in Respiratory and Critical Care Medicine*. 2005; 26(1):13-24.
- Converse, R., Jacobsen, T., Jost, C., Toto, R., Grayburn, P., Obregon, T., Fouad-Tarazi, F. and Victor, R. Paradoxical Withdrawal of Reflex Vasoconstriction as a Cause of HD-Induced Hypotension. *Journal of Clinical Investigation*. 1992; 90:1657-65.
- Convertino, V., Ratliff, D., Ryan, K., Doerr, D., Ludwig, D., Muniz, G., Britton, D., Clah, S., Fernald, K., Ruiz, A., Lurie, K. and Idris, A. Hemodynamics Associated with Breathing Through an Inspiratory Impedance Threshold Device in Human Volunteers. *Critical Care Medicine*. 2004; 32(9):S381-6.
- Coriat, P., Vrillon, M., Perel, A., Baron, J., Le Bret, F., Saada, M. and Viars, P. A Comparison of Systolic Pressure Variations and Echocardiographic Estimates of End-Diastolic Left Ventricular Size in Patients After Aortic Surgery. *Anesthesia and Analgesia*. 1994; 78:46-53.
- Cucchiara, R. and Messick, J. The Failure of Nasal Plethysmography to Estimate Cerebral Blood Flow During Carotid Occlusion. *Anesthesiology*. 1981;55(5):585-6.
- Daugirdas, J. Pathophysiology of HD Hypotension: An Update. *American Journal of Kidney Disease*. 2001; 38:S11-S17.
- Daul, A., Wang, X., Michel, M. and Brodde, O. Arterial Hypotension in Chronic Hemodialyzed Patients. *Kidney International*. 1987; 32:728-35.
- Dekker, J. Apparatus and Method for Monitoring Respiration with a Pulse Oximeter. United States Patent Number 6,709,402. 2004.
- Donauer, J. and Bohler, J. Rationale for the Use of Blood Volume and Temperature Control Devices during HD. *Kidney and Blood Pressure Research*. 2003; 26:82-9.

- Dubois, A., Botelho, S. and Comroe, J. A New Method for Measuring Airway Resistance in Man Using a Body Plethysmograph: Values in Normal Subjects and in Patients with Respiratory Disease. *Journal of Clinical Investigation*. 1956a; 35:327-35.
- Dubois, A., Brody, A., Lewis, D. and Burgess, B. Oscillation Mechanics of Lungs and Chest in Man. *Journal of Applied Physiology*. 1956b; 8:587-94.
- Ducharme, F. and Davis, G. Measurement of Respiratory Resistance in the Emergency Department: Feasibility in Young Children with Acute Asthma. *Chest*. 1997; 11:1519-25.
- Ducharme, F. and Davis, G. Respiratory Resistance in the Emergency Department: A Reproducible and Responsive Measure of Asthma Severity. *Chest*. 1998; 113:1566-72.
- Duiverman, E., Clement, J., van de Woestijne, K., Neijens, H., van den Bergh A. and Kerrebijn K. Forced Oscillation Technique: Reference Values for Resistance and Reactance Over a Frequency Spectrum of 2-26 Hz in Healthy Children Aged 2.3-12.5 Years. *Bulletin of European Physiopathology of Respiration*. 21:171-8.
- Esforzado, A., Cases, A., Bono, I., Gaya, B., Calls, G. and Rivera, F. Autonomic Nervous System and Adrenergic Receptors in Chronic Hypotensive HD Patients. *Nephrology HD Transplant*. 1997; 12:939-44.
- Ezri, T., Lurie, S., Konichezky, A. and Soroker, D. Pulse Oximetry from the Nasal Septum. *Journal of Clinical Anesthesia*. 1991; 3:447-50.
- Fichter, J., Wilkens, J. and Fabel, H. Oscillatory Measurement of Airway Resistance with the Custo Vit in Comparison with Oscillaire and Whole Body Plethysmography. *Pneumologie*. 1989; 43:382-6.
- Foo, J., and Wilson, S. Estimation of Breathing Interval from the Photoplethysmographic Signals in Children. *Physiological Measurements*. 2005; 26(6):1049-58.
- Frey, B. and Butt, W. Pulse Oximetry for Assessment of Pulsus Paradoxus: A Clinical Study in Children. *Intensive Care Medicine*. 1998; 24:242-6.
- Goldie, E. Device for Continuous Indication of Oxygen Satuaration of Circulating Blood in Man. *Journal of Scientific Instrumentation*. 1942; 19:23-25.
- Goldman, J., Petterson, M., Kopotic, R. and Barker S. Masimo Signal Extraction in Pulse Oximetry. *Journal of Clinical Monitoring and Computing*. 2000; 16:475-83.
- Goodman, J. Physiological Signal Monitoring System. United States Patent Number 6,616,613. 2003.

- Grace, R. Pulse Oximetry: Gold Standard or False Sense of Security? *The Medical Journal of Australia*. 1994; 160(10):638-44.
- Groveman, J., Cohen, D. and Dillon, J. Rhinoplethysmography: Pulse Monitoring at the Nasal Septum. *Anesthesia and Analgesia*. 1966; 45(1):63-8.
- Guilleminault, C., Stoohs, R., Clerk, A., Cetel, M. and Maistros, P. A Cause of Daytime Sleepiness: The Upper Airway Resistance Syndrome. *Chest*. 1993; 104:781-7.
- Guttmann, J., Kessler, V., Mols, G., Hentsche, I R., Haberthur, C. and Geiger K. Continuous Calculation of Intratracheal Pressure in the Presence of Pediatric Endotracheal Tubes. *Critical Care Medicine*, 28(4) 1018-26, 2000.
- Haba-Rubio, J., Darbellay, G., Herrmann, F., Frey, J., Fernandes, A., Vesin, J., Thiran, J. and Tschopp, J. Obstructive Sleep Apnea Syndrome: Effect of Respiratory Events and Arousal on Pulse Wave Amplitude Measured in NREM Sleep. *Sleep and Breathing*. 2005; 9:73-81.
- Hadjikoumi, I., Hassan, A. and Milner, A. Effects of Respiratory Timing and Cheek Support on Resistance Measurements, Before and After Bronchodilation in Asthmatic Children Using the Interrupter Technique. *Pediatric Pulmonology*. 2003; 36:495-501.
- Hartert, T., Wheeler, A. and Sheller, J. Use of Pulse Oximetry to Recognize Severity of Airflow Obstruction in Obstructive Airway Disease: Correlation to Pulsus Paradoxus. *Chest*. 1999; 115:475-81.
- Heitmiller, E. and Wetzel, R. Hemodynamic Monitoring: Considerations in Pediatric Critical Care. In: Rogers, M. (ed). *Textbook of Pediatric Intensive Care*. Williams and Wilkins, Baltimore, 1996; 609.
- Hertzman A. Photoelectric Plethysmography of the Fingers and Toes in Man. *Proceedings of the Society of Experimental Biology and Medicine*. 1937a; 37:529.
- Hertzman A. Photoelectric Plethysmography of the Nasal Septum in Man. *Proceedings of the Society of Experimental Biology and Medicine*. 1937b; 37:290.
- Hoffstein, V. Is Snoring Dangerous to Your Health? *Sleep*. 1996; 506-16.
- Hoppe-Seyley, F. Uber die chemischen und optischen Eigenschaffen des Blutfarbstoffs. *Archives of Pathological Anatomy and Physiology*. 1864; 29:233-51.
- Hu, F., Willet, W., Manson, J., Colditz, G., Rimm, E., Speizer, F., Hennekens, C. and Stampfer, M. Snoring and Risk of Cardiovascular Disease in Women. *Journal of the American College of Cardiology*. 2000; 35:308-13.

- Ishibe, S. and Peixoto, A. Methods of Assessment of Volume Status and Intercompartmental Fluid Shifts in HD Patients: Implications in Clinical Practice. *Seminars in HD*. 2004; 17(1):37-43.
- Johansson, A. Neural Network for Photoplethysmographic Respiratory Rate Monitoring. *Medical and Biological Engineering & Computing*. 2003; 41:424-8.
- Jost, C., Agarwal, R., Khair-el-Din, T., Grayburn, P., Victor, R. and Henrich, W. Effects of Cooler Temperature Dialysate on Hemodynamic Stability in 'Problem' HD Patients. *Kidney International*. 1993; 44:606-12.
- Jubran, A. Pulse Oximetry. *Critical Care*. 1999; 3:R11-R17.
- Kato, R., Sato, J., Iuchi, T. and Higuchi, Y. Quantitative Determination of Arterial Wall Mechanics with Pulse Oximetric Finger Plethysmography. *Journal of Anesthesia*. 1999; 13:197-204.
- Katz, J., Kraemer, R. and Gjerde, G. Inspiratory Work and Airway Pressure with Continuous Positive Airway Delivery Systems. *Chest*. 1988; 88:519-26.
- Kersh, E., Kronfield, S., Unger, A., Popper, R., Cantor, S. and Cohn, K. Autonomic Insufficiency in Uremia as a Cause of HD-Induced Hypotension. *New England Journal of Medicine*. 1974; 290:650-3.
- Kiani, M. Noninvasive Hypovolemia Monitor. United States Patent Application 20060058691. 2006.
- Kooi, E., Schokker, S., van der Molen, T. and Duiverman, E. Airway Resistance Measurements in Pre-School Children with Asthmatic Symptoms: The Interruptor Technique. *Respiratory Medicine*. 2006; Epub Ahead of Print.
- Kooman, J., Gladziwa, U., Bocker, G., van Bortel, L., van Hooff, J. and Leunissen, K. Role of the Venous System in Hemodynamics During Ultrafiltration and Bicarbonate HD. *Kidney International*. 1992; 42:718-26.
- Koomans, H., Geers, A. and Mees, E. Plasma Volume Recovery After Ultrafiltration in Patients with Chronic Renal Failure. *Kidney International*. 1984; 26:848-54.
- Krepel, H., Nette, R., Akcahuseyin, E., Weimar, W. and Zietse, R. Variability of Relative Blood Volume During HD. *Nephrology HD Transplant*. 2000; 15:673-9.
- Lawless, S. Crying Wolf: False Alarms in a Pediatric Intensive Care Unit. *Critical Care Medicine*. 1994; 22:981-5.
- Leonard, P., Beattie, T., Addison, P. and Watson, J. Standard Pulse Oximeters can be used to Monitor Respiratory Rate. *Emergency Medical Journal*. 2003; 20(6):524-5.

- Leonard, P., Grubb, N., Addison, P., Clifton, D. and Watson, J. An Algorithm for the Detection of Individual Breaths from the Pulse Oximeter Waveform. *Journal of Clinical Monitoring and Computing*. 2004; 18:309-12.
- Leonard, P., Douglas, J., Grubb, N., Clifton, D., Addison, P. and Watson, J. A Fully Automated Algorithm for the Determination of Respiratory Rate from the Photoplethysmogram. *Journal of Clinical Monitoring and Computing*. 2006; 20(1):33-6.
- Leunissen, K., Kooman, J., van der Sande, F and van Kuijk, W. Hypotension and Ultrafiltration Physiology in HD. *Blood Purification*. 2000; 18:251-4.
- Leypoldt, J., Cheung, A., Steuer, R., Harris, D and Conis, J. Determination of Circulating Blood Volume by Continuously Monitoring Hematocrit During HD. *Journal of the American Society of Nephrology*. 1995; 6:214-9.
- Lilley, J., Golden, J. and Stone, R. Adrenergic Regulation of Blood Pressure in Chronic Renal Failure. *Journal of Clinical Investigation*. 1976; 57:1190-1200.
- Lilliefors, H. On the Kolmogorov-Smirnov test for normality with mean and variance unknown. *Journal of the American Statistical Association*. 1967; 64:399-402.
- Lurie, K., Voelckel, W., Plaisance, P., Zielinski, T., McKnite, S., Kor, D., Sugiyama, A. and Sukhum, P. Use of an Inspiratory Impedance Threshold Valve During Cardiopulmonary Resuscitation. *Resuscitation*. 2000a; 44:219-30.
- Lurie, K., Zielinski, T., McKnite, S. and Sukhum, P. Improving the Efficiency of Cardiopulmonary Resuscitation with an Inspiratory Impedance Threshold Valve. *Critical Care Medicine*. 2000b; 28:N207-9.
- Lurie, K., Zielinski, T., Voelckel, W., McKnite, S. and Plaisance, P. Augmentation of Ventricular Preload During Treatment of Cardiovascular Collapse and Cardiac Arrest. *Critical Care Medicine*. 2002a; 30:S162-5.
- Lurie, K., Zielinski, T., McKnite, S., Aufderheide, T. and Voelckel, W. Use of an Inspiratory Impedance Valve Improves Neurologically Intact Survival in a Porcine Model of Ventricular Fibrillation. *Circulation*. 2002; 105:124-9.
- Maggiore, Q., Pizzarelli, F., Zoccali, C., Sisca, S., Nicolo, F. and Parlongo, S. Effect of Extracorporeal Blood Cooling on Dialytic Arterial Hypotension. *Proceedings of the European HD Transplant Association*. 1981; 18:597-602.
- Middleton, P. and Henry, J. Pulse Oximetry: Evolution and Directions. *International Journal of Clinical Practice*, 2000; 54(7):438-44.
- Millasseau, S., Kelly, R., Ritter, J. and Chowienczyk, P. Determination of Age-Related Increases in Large Artery Stiffness by Digital Pulse Contour Analysis. *Clinical Science*. 2002; 103:371-77.

- Millasseau, S., Kelly, R., Ritter, J. and Chowienczyk, P. The Vascular Impact of Aging and Vasoactive Drugs: Comparison of Two Digital Volume Pulse Measurements. *American Journal of Hypertension*. 2003; 16:467-72.
- Millikan, G., Papenheimer, J. and Rawson A. Continuous Measurement of Oxygen Saturation in Man. *American Journal of Physiology*. 1941; 133:390.
- Miro, A. and Pinsky, M. Cardiopulmonary Interactions. In: Fuhrmann, B. and Zimmerman, J. (eds). *Pediatric Critical Care*. Mosby, St Louis, 1992; 256.
- Mitra, S., Chamney, P., Greenwood, R. and Farrington, K. Linear Decay of Relative Blood Volume During Ultrafiltration Predicts Hemodynamic Instability. *American Journal of Kidney Disease*. 2002; 40:556-65.
- Moller, J., Johannessen, N., Espersen, K., Ravlo, O., Pedersen, B., Jensen, P., Rasmussen, N., Rasmussen, L., Pedersen, T. and Cooper J. Randomized Evaluation of Pulse Oximetry in 20,802 Patients: 1. Design, Demography, Pulse Oximetry Failure Rate and Overall Complication Rate. *Anesthesiology*. 1993; 78:436-44.
- Morgan, B., Crawford, E and Guntheroth, W. The Hemodynamic Effects of Changes in Blood Volume During Intermittent Positive Pressure Ventilation. *Anesthesiology*. 1969; 30:297-305.
- Murray, W. and Foster, A. The Peripheral Pulse Wave: Information Overlooked. *Journal of Clinical Monitoring*. 1996; 12:365-77.
- National Asthma Education and Prevention Program (NAEPP). Expert Panel Report: Guidelines for the Diagnosis and Management of Asthma. National Institutes of Health pub no. 91-3642. 1991, Bethesda, MD.
- National Asthma Education and Prevention Program (NAEPP). Expert Panel Report: Guidelines for the Diagnosis and Management of Asthma. National Institutes of Health pub no. 97-4051. 1997, Bethesda, MD.
- Nilsson, L., Johansson, A. and Kalman, S. Monitoring of Respiratory Rate in Postoperative Care Using a New Photoplethysmographic Technique. *Journal of Clinical Monitoring and Computing*. 2000; 16:309-15.
- Nilsson, L., Johansson, A. and Kalman, S. Respiratory Variations in the Reflection Mode Photoplethysmographic Signal. Relationships to Peripheral Venous Pressure. *Medical and Biological Engineering & Computing*. 2003; 41:149-54.
- Nilsson, L., Johansson, A. and Kalman, S. Respiration can be Monitored by Photoplethysmography with High Sensitivity and Specificity Regardless of Anaesthesia and Ventilatory Mode. *Acta Anaesthesiologica Scandinavica*. 2005; 49:1157-62.

- Oates, J. and Martin, D. Method and Apparatus for Non-Invasive Monitoring of Respiratory Parameters in Sleep Disordered Breathing. International Patent Number WO 2006/037184. 2006.
- O'Leary, R., Landon, M., and Benumof, J, Buccal Pulse Oximeter is More Accurate than Finger Pulse Oximeter in Measuring Oxygen Saturation. *Anesthesia and Analgesia*. 1992; 75:495-8.
- Officer, T., Pellegrino, R., Brusasco, V. and Rodarte, J. Measurement of Pulmonary Resistance and Dynamic Compliance with Airway Obstruction. *Journal of Applied Physiology*. 1998; 85(5):1982-8
- Pagani, J., Villa, M., Calcagnini, G., Alterio, A., Ambrosia, R., Censi, F and Ronchetti, R. Pulse Transit Time as a Measure of Inspiratory Effort in Children. *Chest*. 2003; 124(4):1487-93.
- Pang, K. and Terris, D. Screening for Obstructive Sleep Apnea: An Evidence-Based Analysis. *American Journal of Otolaryngology*. 2006; 27:112-8.
- Partridge, B. Use of Pulse Oximetry as a Noninvasive Indicator of Intravascular Volume Status. *Journal of Clinical Monitoring*. 1987; 3:263-268.
- Patil, S., Punjabi, N., Schneider, H, O'Donnell, C., Smith, P. and Schwartz, A. A Simplified Method for Measuring Critical Pressures During Sleep in the Clinical Setting. *American Journal of Respiratory Critical Care Medicine*. 2004; 170:86-93.
- Perel, A., Pizov, R. and Cotev, S. Systolic Blood Pressure Variation is a Sensitive Indicator of Hypovolemia in Ventilated Dogs Subjected to Graded Hemorrhage. *Anesthesiology*. 1987; 67(4):498-502.
- Perutz, M. The Haemoglobin Molecule. *Proceedings of the Royal Society of London* 1969; B173:113-40.
- Pfenninger, J. Akute Obstruktion der oberen Atemwege: Epiglottis und Krupp-Syndrom. *Padiatr Fortbildk Praxis*. 1985; 59:121-31.
- Pinsky, M. and Summer, W. Cardiac Augmentation by Phasic High Intra-Thoracic Pressure Support in Man. *Chest*. 1983; 84:370-5.
- Pizov, R., Ya'ar, Y. and Perel, A. A Systolic Pressure Variation is Greater During Hemorrhage than During Sodium Nitroprusside Induced Hypotension in Ventilated Dogs. *Anesthesia and Analgesia*. 1988; 67:170-4.
- Reich, D., Timcenko, A., Bodian, C., Kraidin, J., Hofman, J., DePerio, M., Konstadt, S., Kurki, T. and Eisenkraft, J. Predictors of Pulse Oximetry Data Failure. *Anesthesiology*. 1996; 84:859-64.

- Rooke, G., Schwid, H. and Shapira, Y. The Effect of Graded Hemorrhage and Intravascular Volume Replacement on Systolic Pressure Variation in Humans During Mechanical and Spontaneous Ventilation. *Anesthesia and Analgesia*. 1995; 80:925-32.
- Rouby, J., Rottembourg, J., Durande, J., Basset, J. and Legrain, M. Importance of the Plasma Refilling Rate in the Genesis of Hypovolemic Hypotension During Regular HD and Controlled Sequential Ultrafiltration-HD. *Proceedings of the European HD and Transplant Association*. 1978; 15:239-44.
- Runciman, W., Webb, R., Barker, L. and Currie, M. The Australian Incident Monitoring Study: The Pulse Oximeter: Applications and Limitations: An Analysis of 2000 Incident Reports. *Anesthesia and Intensive Care*. 1993; 21:543-550.
- Shamir, M., Eidelman, L.A., Floman, Y., Kaplan, L and Pizov, R. Pulse Oximetry Plethysmographic Waveform During Changes in Blood Volume. *British Journal of Anaesthesia*. 1999; 2:178-81.
- Shelley, K., Silverman, D., Shelley, A. and Stout, R. Method of Assessing Blood Volume Using Photoelectric Plethysmography. International Patent Number 2004/080300. 2004.
- Sherman, R. Intradialytic Hypotension: An Overview of Recent, Unresolved and Overlooked Issues. *Seminars in Hemodialysis*. 2002; 15(3):141-3.
- Simm, F. Polyfrequent Oscillometry Measurement of Airway Resistance Including the Associated Phase Angle. *Pneumologie*. 1989; 43:382-6.
- Solyman, L., Landser, F. and Duiverman, E. Measurement of Resistance with the Forced Oscillation Technique. *European Respiratory Journal*. 1989; 2:150s-3s.
- SPSS Base 14.0 Users Guide. 2005, SPSS Inc., Chicago, IL.
- Stojceva-Taneva, O., Masin, G., Polenakovic, M., Stojcev, S and Stojkovski, L. Autonomic Nervous System Dysfunction and Volume Non-Responsive Hypotension in HD Patients. *American Journal of Nephrology*. 1991; 11:123-6.
- Stokes, G. On the Reduction Oxygenation of the Colouring Matter of the Blood. *Philosophical Magazine*. 1864; 28:391.
- Tonelli, M., Astephen, P., Andreou, P., Beed, S., Lundigran, P. and Jindal K. Blood Volume Monitoring in Intermittent HD for Acute Renal Failure. *Kidney International*. 2002; 62:1075-80.
- Topol, E., Califf, R., Isner, J., Prystowsky, E., Swain, J., Thomas, J., Thompson, P., Young, J. and Nissen, S. *Textbook of Cardiovascular Medicine*. 2002, Lippincott Williams & Wilkins.

- Trivedi, N., Ghouri, A., Shah, N., Lai, E. and Barker S. Effects of Motion, Ambient Light and Hypoperfusion on Pulse Oximeter Function. *Journal of Clinical Anesthesia*. 1997; 9:179-183.
- Van der Sande, F., Kooman, J., Konings, C. and Leunissen, K. Thermal Effects and Blood Pressure Response During Postdilution Hemodiafiltration and HD: The Effect of Amount of Replacement Fluid and Dialysate Temperature. *Journal of the American Society of Nephrology*. 2001; 12:1916-20.
- van Oostrom, J. and Melker, R. Comparative Testing of Pulse Oximeter Probes. *Anesthesia and Analgesia*. 2004; 98:1354-8.
- Von Neergaard, K. and Wirz, K. Die Messung des Stromungswiderstande in dem Atemwegen des menschen, Insbesondere bei Asthma und Emphysema. *Z Klin Med*. 1927; 105:51-82.
- Wallin, C., Rossi, P., Jacobson, S and Leksell, L. Central Blood Volume, Atrial Natiuretic Peptide and Intermittent HD. *Scandinavian Journal of Urology and Nephrology*. 2004; 38:78-84.
- Welch, P. The Use of Fast Fourier Transform for the Estimation of Power Spectra: A Method Based on Time Averaging Over Short, Modified Periodograms. *IEEE Transactions on Audio Electroacoustics*. 1967; 15:70-3.
- Wilcoxon, F. Individual comparisons by ranking methods. *Biometrics*. 1945; 1:80-83.).
- Wood, E. and Geraei, J. Photoelectric Determination of Arterial Saturation in Man. *Journal of Laboratory and Clinical Medicine*. 1949; 34:387-401.
- Young, T., Peppard, P. and Gottlieb, D. Epidemiology of Obstructive Sleep Apnea: A Population Health Perspective. *American Journal of Respiratory Critical Care Medicine*. 2002; 165:1217-39.

BIOGRAPHICAL SKETCH

Brian Scott Fuehrlein was born in 1977 and is originally from Oceanside, NY. He graduated with honors from the University of Central Florida (Orlando) in 2000 with a Bachelor of Science degree in industrial engineering. He was awarded the university-wide most outstanding thesis and was the class of 2000 graduating industrial engineering senior of the year. In 2001, Brian enrolled in the M.D./Ph.D. program at the University of Florida and was named a University of Florida Alumni Fellow. Brian has completed 2 years of medical school and passed the first step of the United States Medical Licensing Exam. Under the guidance of Richard J. Melker, Brian graduated with his Ph.D. in Biomedical Engineering in 2006 and will return to complete the final 2 years of medical school. Brian is married to Dianna Fuehrlein and together, they have a dog, T-Bone.